Clinical presentation and genetic characterisation of mitochondrial disease in Kuwait

Ahmad A Alahmad

BSc, MSc

Supervisors:

Professor Robert W. Taylor

Professor Robert McFarland

This thesis is submitted for the degree of

Doctor of Philosophy

Wellcome Centre for Mitochondrial Research,

Translational and Clinical Research Institute,

Newcastle University

August 2020

Abstract

Mitochondrial disorders are a group of clinically heterogenous conditions affecting multiple systems with a prevalence that is estimated to affect 1 in 4,300 individuals. Mitochondrial function is under the control of both the mitochondrial and nuclear genomes which encode >1200 mitochondrial proteins. Manifold biochemical pathways and possible gene targets contribute to the highly variable genotype-phenotype correlations observed in mitochondrial patients, posing distinct challenges in reaching a genetic diagnosis. Whole Exome Sequencing (WES) is a gene agnostic approach that has been hugely powerful in diagnosing mitochondrial disease patients and broadening the genotypic spectrum of disease. Mitochondrial genetic disease is largely understudied in Kuwait where levels of consanguinity reach 50% in the community. Studying the genetics and aetiology of mitochondrial disorders in Kuwait presents huge potential in identifying novel Mendelian causes of disease.

I custom-designed mitochondrial disease criteria to evaluate and recruit patients suspected of mitochondrial disease in Kuwait. WES led to the diagnosis of 14 out of 22 recruited families: 8 families harboured variants in known mitochondrial disease genes (*SLC19A3*, *PDHX*, *SURF1*, *MPC1*, *TTC19*, *NDUFA13*, *NDUFB9* and *RRM2B*), 2 harboured variants in a novel mitochondrial disease gene (*LETM1*), and 4 were diagnosed with phenocopies of mitochondrial disease (*RNASEH2C*, *TREX1*, *VPS13B* and *ATP8A2*). Functional validation of novel variant pathogenicity was performed in patient fibroblasts from 4 families. Functional validation was also carried out on additional mitochondrial patients from Newcastle and external collaborators (*COX15*, *TTC19*, *NDUFAF3* and *NDUFC2*). Complexome profiling helped characterise the effect of *NDUFC2* variants (a novel candidate gene) on Complex I assembly while a controlled lentiviral rescue experiment partially recovered protein expression and validated variant pathogenicity.

My work highlights the potential of employing WES to identify novel causes of disease in understudied consanguineous populations and emphasises the importance of establishing functional pipelines alongside the genetic studies in the Kuwait Medical Genetics Centre.

Acknowledgment

During the past 4 years as a PhD student, many individuals have supported me through my journey, and I want to take this opportunity to extend my gratitude to them.

First and foremost, I want to begin by thanking Professors Robert W Taylor and Robert McFarland for allowing me the opportunity to study under their esteemed supervision. Their guidance and patience as mentors have encouraged me to take on this challenge and I am grateful for their time.

I want to thank the Government of the State of Kuwait for funding and supporting my PhD studies. I want to thank my wife Dr Fajer Almutawa and our son Sami for their patience, support and love during my time as a PhD student. We have made many memories during our time together in Newcastle upon Tyne. I want to thank my family and friends for their continued support throughout my time away from Kuwait.

I want to thank Dr Buthaina Albash for her efforts in reviewing potential patients to recruit for my PhD research and for her guidance during the review process. I want to thank Dr Ahmad Alaqeel for his enthusiastic efforts in finding potential patients to recruit and more importantly for his efforts in acquiring patient skin biopsies which have greatly contributed to the depth of my research. I want to thank my clinical and laboratory colleagues at the Kuwait Medical Genetics Centre for their help in recruiting potential patients and facilitating the acquiring of DNA samples. I want to thank Dr Laila Bastaki, the Head of the Kuwait Medical Genetics Centre for her support during my studies and for allowing me access to the facilities and samples. I want to thank referring clinicians who knowing referred patients to my cohort by providing all the information we required in efforts to strengthen my study, including Dr Dina Ramadan and Dr Asmaa Altawari.

I want to thank Dr Kyle Thompson and Dr Angela Pyle for their time, guidance advice while acquiring new skills in the lab. I want to thank the staff at the NHS Highly Specialised Mitochondrial Diagnostic Services for their support and I want to thank the bioinformaticians Dr Helen Griffin, Dr Angela Pyle and Dr Fiona Robertson for processing the whole exome sequencing data for analysis.

Regarding the large collaboration study, I undertook during my studies, I want to thank Professor Robert W Taylor for his guidance throughout the project, thank Dr Kyle

Thompson for his advice and guidance, and thank Dr Langping He for her analysis of enzyme activity in the patients' cells. I want to thank Dr Seham Alameer, Dr Fahad Al Hakami and Dr Abeer Almehdar, collaborators at King Saud bin Abdulaziz University for Health Sciences in Jeddah, Kingdom of Saudi Arabia, for referring their patient for our study. I want to thank Dr Alessia Nasca, Dr Andrea Legati, Dr Eleonora Lamantea, Dr Menuela Spagnolo and Prof Danielle Ghezzi, collaborators at the Fondazione IRCCS Istituto Neurologico Carlo Besta in Milan, Italy, for referring their patient and contributing towards the project with their information and facilities. I want to thank Dr Juliana Heidler, Dr Jana Meisterknecht and Prof Ilka Wittig, collaborators at Goethe-Universität in Frankfurt, Germany, for their contribution towards our study especially with their complexome profiling analysis of the patient cell lines.

Lastly, I want to thank everyone at the Wellcome Centre for Mitochondrial Research for providing the friendly environment to thrive together and grow with each other. I have really enjoyed my time in the lab and have made many friends. I wish everyone all the best in the future.

Publications arising from my work during my PhD studies

Vona, B., Maroofian, R., Bellacchio, E., Najafi, M., Thompson, K., **Alahmad, A.**, He, L., Ahangari, N., Rad, A., Shahrokhzadeh, S., Bahena, P., Mittag, F., Traub, F., Movaffagh, J., Amiri, N., Doosti, M., Boostani, R., Shirzadeh, E., Haaf, T., et al. (2018) Expanding the clinical phenotype of IARS2-related mitochondrial disease. *BMC Medical Genetics*. 19 (1), 196.

Saoura, M., Powell, C.A., Kopajtich, R., **Alahmad, A.**, AL-Balool, H.H., Albash, B., Alfadhel, M., Alston, C.L., Bertini, E., Bonnen, P.E., Bratkovic, D., Carrozzo, R., Donati, M.A., Nottia, M.D., Ghezzi, D., Goldstein, A., Haan, E., Horvath, R., Hughes, J., et al. (2019) Mutations in ELAC2 associated with hypertrophic cardiomyopathy impair mitochondrial tRNA 3′-end processing. *Human Mutation*. 40 (10), 1731–1748.

Alahmad, A., Muhammad, H., Pyle, A., Albash, B., McFarland, R. & Taylor, R. (2019) Mitochondrial disorders in the Arab Middle East population: the impact of next generation sequencing on the genetic diagnosis. *Journal of Biochemical and Clinical Genetics*. 54–64.

Alahmad, A., Nasca, A., Heidler, J., Thompson, K., Oláhová, M., Legati, A., Lamantea, E., Meisterknecht, J., Spagnolo, M., He, L., Alameer, S., Hakami, F., Almehdar, A., Ardissone, A., Alston, C.L., McFarland, R., Wittig, I., Ghezzi, D. and Taylor, R.W. (2020) 'Bi-allelic pathogenic variants in NDUFC2 cause early-onset Leigh syndrome and stalled biogenesis of complex I', *EMBO Molecular Medicine*, 12(11), p. e12619.

Table of Contents

Abstract 2

Acknowledgment 3

Publications arising from my work during my PhD studies 5

Table of Contents 6

Table of Figures 15

Table of Tables 18

Abbreviations 19

Chapter 1. Introduction 30

1.1 Mitochondria 30

1.1.1 Structure 30

1.1.2 Mitochondrial dynamics 31

1.1.2.1 Fusion 31

1.1.2.2 Fission 32

1.1.3 ER-mitochondrial interactions 34

1.1.4 The mitochondrial genome 35

1.1.5 Mitochondrial genetics 38

1.1.6 Nuclear encoded mitochondrial components 39

1.1.7 Replication of mtDNA 40

1.1.7.1 Strand displacement replication 40

1.1.7.2 Ribonucleotides Incorporated Through Out the Lagging Strand (RITOLS) replication 40

1.1.7.3 Strand coupled replication 41

1.1.8 mtDNA gene expression 42

1.1.8.1 Transcription initiation 42

1.1.8.2 Transcription elongation 42

1.1.8.3 Transcription termination 42

1.1.8.4 Transcript processing and maturation 43

1.1.8.5 Mitoribosome structure 45

1.1.8.6 Translation 46

1.1.9 Mitochondrial protein import 48

1.1.9.1 Matrix proteins 49

1.1.9.2 Outer membrane transmembrane proteins 49

1.1.9.3 Inner membrane transmembrane proteins 49

1.1.9.4 Intermembrane space proteins 50

1.2 Mitochondrial functions 52
1.2.1 Metabolic pathways 52
1.2.2 OXPHOS complexes 54
1.2.2.1 Complex I – NADH:ubiquinone oxidoreductase 54
1.2.2.2 Complex II - Succinate:ubiquinone oxidoreductase 55
1.2.2.3 Coenzyme Q10 56
1.2.2.4 Complex III – Ubiquinol:cytochrome c reductase 56
1.2.2.5 Cytochrome c 58
1.2.2.6 Complex IV – Cytochrome c oxidase 58
1.2.2.7 Complex V – ATP synthase 59
1.2.2.8 Supercomplexes/Respirasomes 61
1.2.2.9 Reactive Oxygen Species production 61
1.2.3 Other mitochondrial functions 62
1.2.3.1 Apoptosis 62
1.2.3.2 Mitochondrial Autophagy (Mitophagy) 62
1.2.3.3 Calcium Homeostasis 63
1.2.3.4 Iron-Sulphur and Heme Cluster Biogenesis 63
1.3 Mitochondrial disorders 64
1.3.1 Clinical features of mitochondrial disease 64
1.3.2 Biochemical investigations and findings in mitochondrial disease 66
1.3.2.1 Biomarkers of mitochondrial disease 66
1.3.2.2 BN-PAGE and SDS-PAGE 66
1.3.2.3 Biochemical OXPHOS and respiratory oxygen consumption assays 67
1.3.3 Histological/histochemical and immunohistochemical investigation techniques and findings in mitochondrial disease 67
1.3.3.1 H&E histological stain and modified trichrome Gomori histological stains 69
1.3.3.2 Cytochrome c oxidase and succinate:ubiquinone oxidoreductase histochemical assay 69
1.3.3.3 Quadruple Immunofluorescence 69
1.3.4 Causes of mitochondrial disease 70
1.3.4.1 mtDNA associated mitochondrial disorders 70
1.3.4.2 nDNA associated mitochondrial disorders 70
1.3.4.3 Complex multigenic mitochondrial disease 71
1.3.4.4 Genotype-phenotype correlation. 71
1.3.5 Genetic studies of mitochondrial disease 72
1.3.5.1 Classification of called variants 73
1.4 Kuwait and the Middle East 73
1.4.1 Population and ancestry 73
1.4.2 Consanguinity 74

1.4.3 Diagnosis of Mitochondrial disease in Kuwait 74
1.4.4 Research in the Middle Eastern Arab population 75
1.4.5 Impact of NGS on the discovery of novel candidate genes in the Middle East 75
1.4.6 Founder mutations in the Middle Eastern population 77
1.4.7 Preventable mitochondrial disease in the Middle East 79
1.4.8 Treatment of mitochondrial diseases in the Middle East 79

1.5 Aims 80

Chapter 2. Materials and Methods 81

2.1 Materials 81
2.1.1 Equipment 81
2.1.1.1 General laboratory 81
2.1.1.2 Genetic analysis 81
2.1.1.3 Cell culture 82
2.1.1.4 Western blotting 82
2.1.1.5 BN-PAGE 82
2.1.2 Consumables 82
2.1.3 Chemicals and reagents 83
2.1.3.1 General reagents 83
2.1.3.2 Polymerase chain reaction (PCR) reagents 84
2.1.3.3 Sanger sequencing reagents 84
2.1.3.4 Tissue culture reagents 84
2.1.3.5 Agarose gel electrophoresis reagents 85
2.1.3.6 SDS-PAGE and Western blot reagents 85
2.1.3.7 BN-PAGE reagents 85
2.1.3.8 Vector cloning reagents 86
2.1.3.9 Lentiviral transduction reagents 86
2.1.4 Solutions 87
2.1.4.1 PCR amplification 87
2.1.4.2 Agarose gel electrophoresis 87
2.1.4.3 Tissue culture 87
2.1.4.4 Western blotting 88
2.1.4.5 BN-PAGE 89
2.1.5 Software 90

2.2 Methods 91
2.2.1 Recruitment of patients 91
2.2.2 Ethical guidelines 91
2.2.3 Extraction of DNA samples from recruited patients and families 91
2.2.4 Control fibroblast cell lines 91
2.2.5 Whole exome sequencing 92

2.2.6 *In silico* analysis of candidate gene variants 93
2.2.7 Oligodeoxynucleotide primers for PCR 93
2.2.8 Custom primer design 93
2.2.9 Polymerase chain reaction (PCR) 94
2.2.10 Gradient PCR for primer optimisation 95
2.2.11 Agarose gel electrophoresis 95
2.2.12 Sanger sequencing 96
2.2.13 Ethanol precipitation of DNA 97
2.2.14 DNA sequencing 97
2.2.15 Acquiring patient fibroblast cell lines from skin biopsies 97
2.2.16 Establishing primary cell lines from skin biopsies 98
2.2.17 Culturing of fibroblasts 98
2.2.18 Subculturing of fibroblasts 98
2.2.19 Harvesting of cells 98
2.2.20 Freezing of cells 98
2.2.21 Western blotting 99
2.2.21.1 Preparation of cell lysates for protein analysis 99
2.2.21.2 Bradford assay 99
2.2.21.3 Assessment of steady-state protein levels by western blotting 99
2.2.22 Blue Native-PAGE 100
2.2.22.1 Enrichment of mitochondria 100
2.2.22.2 Solubilisation of enriched mitochondria 101
2.2.22.3 BCA protein assay 101
2.2.22.4 Assessment of OXPHOS complex assembly using BN-PAGE 102
2.2.23 Immunoblotting 102
2.2.24 Analysis of respiratory chain complex activity 102

Chapter 3. Identification of a paediatric patient cohort in Kuwait with suspected mitochondrial disease 104

3.1 Introduction 104

3.2 Aims 105

3.3 Methods 106

3.3.1 Selection of patients suspected of mitochondrial disease in Kuwait for study cohort 108
3.3.1.1 Paediatric metabolic specialist review 108
3.3.1.2 Mitochondrial Disease Criteria Scoring 108

3.4 Results 114

3.4.1 Clinical reports of recruited patients 114
3.4.1.1 Family 1 114
3.4.1.2 Family 2 115

3.4.1.3 Family 3 116
3.4.1.4 Family 4 117
3.4.1.5 Family 5 119
3.4.1.6 Family 6 120
3.4.1.7 Family 7 121
3.4.1.8 Family 8 123
3.4.1.9 Family 9 124
3.4.1.10 Family 10 126
3.4.1.11 Family 11 126
3.4.1.12 Family 12: 127
3.4.1.13 Family 13 128
3.4.1.14 Family 14 129
3.4.1.15 Family 15 131
3.4.1.16 Family 16 131
3.4.1.17 Family 17 132
3.4.1.18 Family 18 132
3.4.1.19 Family 19 134
3.4.1.20 Family 20 134
3.4.1.21 Family 21 135
3.4.1.22 Family 22 135

3.5 Summary of recruited families and cases 136

3.6 Discussion 143

Chapter 4. Whole exome sequencing of paediatric patients from Kuwait suspected of mitochondrial disease 146

4.1 Introduction 146

4.2 Aims 148

4.3 Methods 149

4.3.1 Whole exome sequencing 149
4.3.2 In silico analysis of candidate gene variants 149
4.3.3 Sanger Sequencing 149
4.3.4 Filtration of variants called in WES 149
4.3.4.1 Rare or novel homozygous variants 149
4.3.4.2 Mitochondrial proteins 150
4.3.4.3 'In silico' predictions of pathogenicity 150
4.3.4.4 Modifications to the prioritisation scheme 150

4.4 Results 152

4.4.1 Average coverage and depth of utilised WES kits and platforms 152

4.4.2 LETM1 152
4.4.2.1 Family 1 152
4.4.2.2 Family 6 155
4.4.3 Family 8 158
4.4.4 Family 5 159
4.4.5 Family 7 161
4.4.6 Family 2 163
4.4.7 Family 4 165
4.4.8 Family 10 167
4.4.9 Family 9 168
4.4.10 Family 3 170
4.4.11 Family 11 172
4.4.12 Family 12 174
4.4.13 Family 13 176
4.4.14 Family 14 177
4.4.15 Undiagnosed cases 179
4.4.15.1 Family 16 179
4.5 Summary of findings 179
4.5.1 Variants in patients from consanguineous unions 179
4.5.2 Rate of candidate variants identified 179
4.6 Discussion 183
4.6.1 Mitochondrial disease diagnoses 183
4.6.1.1 LETM1 183
4.6.1.2 NDUFA13 185
4.6.1.3 MPC1 187
4.6.1.4 TTC19 188
4.6.1.5 SLC19A3 188
4.6.1.6 SURF1 190
4.6.1.7 RRM2B 190
4.6.1.8 NDUFB9 191
4.6.1.9 PDHX 192
4.6.2 Non-mitochondrial diagnoses 193
4.6.2.1 RNASEH2C 193
4.6.2.2 TREX1 193
4.6.2.3 VPS13B 194
4.6.2.4 ATP8A2 195
4.7 Summary 196
4.8 Conclusion 197

Chapter 5. The functional validation of genetic variants identified by whole exome sequencing 199

5.1 Introduction 199

5.2 Aims 202

5.3 Methods 205

5.3.1 Recruitment of Patients 205
5.3.2 Acquiring patient fibroblast cell lines from skin biopsies 205
5.3.3 Establishing primary cell lines from skin biopsies 205
5.3.4 Cell culture 205
5.3.5 Cell lysing in preparation for protein steady-state analysis using western blotting 205
5.3.6 Assessment of protein steady-state levels using western blotting 205
5.3.7 Enrichment of mitochondria 206
5.3.8 Solubilisation of enriched mitochondria 206
5.3.9 Assessment of OXPHOS complex assembly using BN-PAGE 206
5.3.10 Analysis of respiratory chain complex activity 206

5.4 Results 207

5.4.1 Clinical summaries of investigated patients 207
5.4.1.1 Patient 23 207
5.4.1.2 Patients 24-I and 24-II 209
5.4.1.3 Patient 25 212
5.4.2 Functional analysis results 213
5.4.2.1 NDUFA13 213
5.4.2.2 COX15 213
5.4.2.3 NDUFAF3 216
5.4.2.4 TTC19 217
5.4.2.5 MPC1 219
5.4.2.6 TREX1 220

5.5 Discussion 221

5.5.1 NDUFA13 221
5.5.2 COX15 222
5.5.3 NDUFAF3 222
5.5.4 TTC19 223
5.5.5 MPC1 223
5.5.6 TREX1 224

5.6 Summary 225

5.7 Final discussion 227

Chapter 6. *NDUFC2* mutations are a novel cause of Complex I deficiency in Leigh syndrome patients. 230

6.1 Introduction 230

6.2 Aims 231

6.3 Methods 233

6.3.1 Patient consent 233

6.3.2 Next-generation sequencing 233

6.3.2.1 Patient A-1 233

6.3.2.2 Patient B 233

6.3.3 Sanger Sequencing 233

6.3.4 RNA transcript levels 234

6.3.5 Cell culture 234

6.3.6 Oxygen consumption 234

6.3.7 Respiratory chain enzyme activities 235

6.3.8 Blue native PAGE and in gel activity stains 235

6.3.9 Western blotting & blue native-PAGE 235

6.3.10 Complexome profiling 235

6.3.11 Lentiviral rescue 236

6.4 Results 238

6.4.1 Clinical presentations of patients 238

6.4.1.1 Family A 238

6.4.1.2 Family B 241

6.4.2 Genetic investigations 242

6.4.2.1 Family A 242

6.4.2.2 Family B 242

6.4.3 Assessment of NDUFC2 mRNA gene expression in patients' fibroblasts 245

6.4.4 Assessment of respiratory chain enzyme activity in patients' tissue and cell lines 245

6.4.5 Steady-state protein levels of complex I subunits in patient cell lines 247

6.4.6 Complex I assembly in patient cell lines 247

6.4.7 Doxycycline inducible lentiviral rescue experiment 250

6.4.7.1 Optimisation of doxycycline dosage by assessing steady-state protein levels of NDUFC2 and other complex I subunits in transduced patient cell lines 250

6.4.7.2 Assessment of Complex I assembly in induced patient cell lines 252

6.4.8 Complexome profiling of patient fibroblast cell lines 253

6.5 Discussion 257

Chapter 7. General discussion 262

7.1 The role of patient recruitment on the diagnostic rate 262

7.2 Limitations of recruiting candidate cases from Kuwait 263

7.3 WES as a first-tier genetic analysis technique 264

7.4 Functional validation of segregated variants 265

7.5 *LETM1* is a novel mitochondrial disease gene 265

7.6 GeneMatcher facilitated the *NDUFC2* collaboration 265

7.7 Future approaches to diagnosing mitochondrial disease patients 266

7.8 Future work 267

7.9 Concluding remarks 268

Appendix 269

References 275

Table of Figures

Figure 1.1 Mitochondrial structures and membranes. 31
Figure 1.2 Mitochondrial Fusion and fission 33
Figure 1.3 The mitochondrial genome 37
Figure 1.4 Mitochondrial genome heteroplasmy 39
Figure 1.5 mtDNA replication models 41
Figure 1.6 Transcription of the mitochondrial genome 45
Figure 1.7 Translation of mitochondrial mRNA 47
Figure 1.8 Import pathways of nuclear encoded mitochondrial proteins 51
Figure 1.9 Metabolic pathways in the mitochondria 53
Figure 1.10 NADH:ubiquinone oxidoreductase 55
Figure 1.11 Succinate:ubiquinone oxidoreductase 56
Figure 1.12 Ubiquinol:cytochrome c reductase 57
Figure 1.13 Cytochrome c oxidase 59
Figure 1.14 Structure of ATP synthase 60
Figure 1.15 OXPHOS Supercomplexes 61
Figure 1.16 Histological, histochemical, and immunohistochemical methods of analysing muscle tissue from a patient with a single large scale mtDNA deletion. 68
Figure 3.1 Map of Kuwait Governorates and locations of main hospitals that refer cases to KMGC in the Al-Sabah Health Region 107
Figure 3.2 Flowchart outlining filtration and selection scheme of patients suspected of mitochondrial disease in Kuwait for the study cohort 109
Figure 3.3 Mitochondrial disease criteria used to score presentations and investigation results of patients referred to the study. 110
Figure 3.4 Brain MRI neuroradiological images for Patient 2 116
Figure 3.5 Brain MRI neuroradiological image for Patient 4-III. 119
Figure 3.6 Brain MRI neuroradiological image for patient 7-I 122
Figure 3.7 Brain MRI radiological images of Patient 8 123
Figure 3.8 Brain MRI radiological findings in Patient 9 125
Figure 3.9 Brain MRI neuroradiological images for Patient 12 128
Figure 4.1 Genome regions targeted by different NGS techniques 147
Figure 4.2 Whole exome sequencing variant filtration flowchart 151

Figure 4.3 Segregation of *LETM1* deletion in Family 1.....154
Figure 4.4 Segregation of *LETM1* variant in Family 6. 156
Figure 4.5 Segregation of *NDUFA13* variant in Family 8 158
Figure 4.6 Segregation of *MPC1* variant in Family 5 160
Figure 4.7 Segregation of *TTC19* deletion in Family 7.....162
Figure 4.8 Segregation of novel missense *SLC19A3* variant in Family 2. 164
Figure 4.9 Segregation of *SURF1* deletion in Family 4. 166
Figure 4.10 Confirmation of missense *RRM2B* mutation in Patient 10. 167
Figure 4.11 Segregation of *NDUFB9* variant in Family 9 169
Figure 4.12 Segregation of *PDHX* truncating variant in Family 3.....171
Figure 4.13 Segregation of *RNASEH2C* variant in Family 11. 173
Figure 4.14 Segregation of *TREX1* variant in Family 12 175
Figure 4.15 Confirming identified VPS13B frameshift deletion in Patient 13 176
Figure 4.16 Segregation of *ATP8A2* variant in Family 14 178
Figure 5.1 An overview of workflow utilised in identifying variants and validating their pathogenicity in association with mitochondrial disease. 203
Figure 5.2 Locations and consequences of identified and previously reported COX15 variants. 208
Figure 5.3 Family pedigree of Patients 24-I and 24-II 210
Figure 5.4 Brain MRI Neuroradiological Images of Patient 24-I 211
Figure 5.5 Investigating NDUFA13 expression and Complex I assembly in Patient 8 fibroblasts 214
Figure 5.6 Steady-state analysis of OXPHOS subunits and complex assembly analysis of OXPHOS complexes in Patient 23.....215
Figure 5.7 Investigating protein steady-state in Patient 25 216
Figure 5.8 Investigating TTC19 expression and Complex III assembly in fibroblasts of TTC19 patients 218
Figure 5.9 Investigating protein steady-state in Family 5 219
Figure 5.10 Investigating protein steady-state in Patient 12 220
Figure 6.1 Complex I subunits and factors categorised based on association with disease. 232
Figure 6.2 Neuroimaging of Patient A-1 239
Figure 6.3 Neuroimaging of Patient A-2.....240
Figure 6.4 Neuroimaging of Patient B 241

Figure 6.5 Identification and segregation of *NDUFC2* deletion in Family A 243
Figure 6.6 Identification and segregation of *NDUFC2* missense variant in Family B. 244
Figure 6.7 NDUFC2 mRNA transcript levels in *NDUFC2* patients' fibroblasts 245
Figure 6.8 Analysis of respiratory chain complex activities in NDUFC2 patients' fibroblasts..... 246
Figure 6.9 Western blot analysis of complex I subunits in *NDUFC2* patient fibroblasts. 248
Figure 6.10 Assessment of OXPHOS complex assembly in *NDUFC2* patients' fibroblasts using BN-PAGE. 248
Figure 6.11 Assessment of assembly of complex I containing supercomplexes in Patient B..... 249
Figure 6.12 Assessing the effect of lentiviral transduction of wild-type NDUFC2 cDNA on steady-state complex I subunit levels in patient cell lines. 251
Figure 6.13 Assessing the effect of lentiviral transduction of wild-type NDUFC2 cDNA on complex I assembly in patient cell lines 252
Figure 6.14 Complexome profiling of fibroblasts from patients A-1 and B confirm complex I deficiency..... 254
Figure 6.15 Complexome Profiling of Fibroblasts from Patients A-1 and B confirm deficiency in supercomplex formation. 255
Figure 6.16 Complexome Profiling of Fibroblasts from Patient B demonstrate modular assembly of complex I. 256
Figure 6.17 Molecular consequences of defects in NDUFC2 on complex I 259

Table of Tables

Table 1.1 Diagnosis and novel candidate gene discoveries in studies that utilised NGS to investigate patient cohorts in the Middle East 76
Table 2.1 PCR protocol for DNA amplification 95
Table 2.2 PCR protocol for Cycle Sequencing 96
Table 2.3 Polyacrylamide gel casting reagents and solutions 100
Table 3.1 Table of clinical presentations in patients recruited for the study 137
Table 3.2 Table of investigation results of patients recruited for the study 139
Table 3.3 Table of neuroradiological findings in patients recruited for the study 141
Table 4.1 Phenotypes of *LETM1* patients 157
Table 4.2 Summary of variants identified using WES in recruited patients showing in silico predictions of pathogenicity in missense mutations 181
Table 5.1 Summary of functional results in patient fibroblasts 226

Abbreviations

aaRS	Aminoacyl tRNA synthetase
aaRS2	Mitochondrial aminoacyl tRNA synthetase
aCGH	Array comparative genomic hybridisation
ACMG	American College of Medical Genetics
ACTH	Adrenocorticotropic hormone
ADP	Adenosine Diphosphate
AGS	Aicardi Goutières Syndrome
AHE	Alaskan Husky Encephalopathy
AIF	Apoptosis inducing factor
ALT	Alanine aminotransferase
APS	Ammonium Persulphate
ARMS-PCR	Amplification-Refractory Mutation System-PCR
ASD	Arterial septic defect
AST	Aspartate aminotransferase
ATG	Autophagy related genes
ATP	Adenosine triphosphate
BAM	Binary Alignment/Map
BCA	Bicinchoninic Acid
BCL-2	B-cell lymphoma-2
BN-PAGE	Blue native polyacrylamide gel electrophoresis
BNGE	Blue Native Gel Electrophoresis
BSA	Bovine Serum Albumin

BTRBGD	Biotin thiamine responsive basal ganglia disease
BWA	Burrows-Wheeler Alignment
CAMRQ4	Cerebellar ataxia, mental retardation and dysequilibrium syndrome 4
CBC	Complete blood count
cDNA	Complementary DNA
CE	C-terminal Extension
CGH	Comparative genomic hybridisation
CI	Complex I / NADH:ubiquinone oxidoreductase
CIA	Cytosolic Iron-sulphur protein Assembly
CII	Complex II / Succinate:ubiquinone oxidoreductase
CIII	Complex III / Ubiquinol:cytochrome c oxidoreductase
CIV	Complex IV / Cytochrome c oxidase
CK	Creatine kinase
CNS	Central nervous system
CNV	Copy number variant
CoQ10	Coenzyme Q10 / Ubiquinone / Ubiquinol
COX	Cytochrome c oxidase / Complex IV
COX/SDH	Cytochrome c oxidase and succinate:ubiquinone oxidoreductase
CPEO	Congenital progressive external ophthalmoplegia
CRISPR	Clustered regularly interspaced short palindromic repeats
Cryo-EM	Cryo electron microscopy
CS	Citrate synthase
CSF	Cerebrospinal fluid
CT	Computed topography

CTD	C-terminal domain
CV	Complex V / ATP synthase
Cyt-c	Cytochrome c
D-loop	Displacement loop
DDM	Dodecyl maltoside
DMEM	Dulbecco's Modified Eagle Media
DMSO	Dimethyl Sulphoxide
DNA	Deoxyribonucleic acid
dNTP	Deoxyribonucleotide Triphosphate
DRP1	Dynamin GTPase encoded by DNM1L
DTR	Deep tandem repeat
E3BP	Pyruvate dehydrogenase E3 binding protein
EARS2	Glutamyl0tRNA synthetase
ECG	Electrocardiogram
ECHO	Echocardiogram
ECL	Electrochemiluminescence
EEG	Electroencephalogram
EM	Electron microscopy
EMG	Electromyogram
EndoG	Endonuclease G
ER	Endoplasmic reticulum
ETC	Electron transport chain
ETS	Electron transport system
ExoFAP	Exonuclease I/FastAP thermosensitive Alkaline Phosphatase

FAD	Flavin Adenine Dinucleotide
FASTKD2	Fas-activated serine threonine kinase domain 2 protein
FBS	Foetal Bovine Serum
FCCP	Carbonyl cyanide-4-phenylhydrazone
FGF-21	Fibroblast growth factor 21
Fis1	Fission 1
FISH	Fluorescent *in situ* hybridisation
FLAIR	Fluid attenuated inversion recovery
FMN	Flavin mononucleotide
GARS	Glycyl-tRNA synthetase
GatCAB	Glutamyl-tRNAGln aminotransferase protein complex
GDF-15	Growth differentiation factor 15
GDP	Guanosine diphosphate
GGT	Gamma-glutamyl transferase
GI	Gastrointestinal
gnomAD	Genome aggregation database
GORD	Gastrointestinal oesophageal reflux disease
GOSH	Great Ormond Street Hospital
GTP	Guanosine triphosphate
GTPase	Guanosine triphosphatase
H&E	Haematoxylin and eosin
HEK	Human embryonic kidney cells
HRP	Horseradish peroxidase
HSP1	mtDNA Heavy strand transcription promoter site 1

HSP2	mtDNA Heavy strand transcription promoter site 2
HTRA2	HtrA Serine Peptidase 2
iBAQ	Intensity based absolute quantification
IEM	Inborn errors of metabolism
IMM	Mitochondrial inner membrane
IMS	Inter membrane space
INF2	Inverted Formin 2
IP3R	Inositol 1,4,5 triphosphate receptor
IPMDS	International Paediatric Mitochondrial Disease Scale
IRCCS	Istituto di Ricovero e Cura a Carattere Scientifico (IRCCS: Scientific Institute for Research, Hospitalization and Healthcare)
ISC	Iron-Sulphur cluster
IUGR	Intrauterine growth retardation
KARS	Lysyl-tRNA synthetase
KMGC	Kuwait Medical Genetics Centre
KSS	Kearns-Sayre Syndrome
L-OPA1	Long OPA1
LHON	Leber Hereditary Optic Neuropathy
LRPPRC	Leucine rich pentatricopeptide repeat containing protein
LS	Leigh syndrome
LSP	mtDNA Light strand transcription initiation site
MAF	Minor allele frequency
MAM	Mitochondria-associated ER membranes
MCIA	Mitochondrial complex I assembly complex
mCU	mitochondrial calcium uniporter

MDC	Mitochondrial disease criteria
MDDS	Mitochondrial DNA depletion syndrome
MELAS	Mitochondrial encephalopathy lactic acidosis and stroke like episodes
MEM	Minimal Essential Media
MERRF	Myoclonic epilepsy and ragger red fibres
Mff	Mitochondrial fission factor
Mfn1	Mitofusin 1
Mfn2	Mitofusin 2
MFRN1	Mitoferrin 1
MFRN2	Mitoferrin 2
MIA	Mitochondrial IMS import and assembly
MiD49	Mitochondrial dynamics protein 49 kDa
MiD51	Mitochondrial dynamics protein 51 kDa
MLPA	Multiplex Ligation-dependent Probe Amplification
MnSOD	Mitochondrial superoxide dismutase
MPC	Mitochondrial pyruvate carrier
MPP	Mitochondrial processing peptidase
MRG	Mitochondrial RNA granules
MRI	Magnetic resonance imaging
mRNA	Messenger RNA
MRP	Mitochondrial ribosomal proteins
MRS	Magnetic resonance spectrometry
MSF	Mitochondrial import stimulation factor
mt-mRNA	Mitochondrial messenger RNA

mt-rRNA	Mitochondrial ribosomal RNA
mt-tRNA	Mitochondrial transcription RNA
mtDNA	Mitochondrial DNA / mitochondrial genome
mtEFG1	Mitochondrial elongation factor G1
mtEFG2	Mitochondrial elongation factor G2
mtEFTs	Mitochondrial elongation factor Ts
mtEFTu	Mitochondrial elongation factor Tu
MTFMT	Mitochondrial methionyl-tRNA formyltransferase
mtHsp70	Mitochondrial 70kDa heat shock protein
mtLSU	39S Large mitoribosomal subunit
mtPAP	Mitochondrial Poly(A) Polymerase
mtRF1a	Mitochondrial release factor 1a
mtRNA	Mitochondrial RNA
mtRRF	mitochondrial recycling factor
mtSSB	Mitochondrial single strand binding proteins
mtSSU	28S Small mitoribosomal subunit
NAD	Nicotinamide Adenine Dinucleotide
NAFLD	Non-alcoholic fatty acid liver disease
NARP	Neuropathy ataxia and retinitis pigmentosa
NCR	Non-coding region
nDNA	Nuclear DNA / nuclear genome
NGS	Next-generation sequencing
NHS	National Health Service
NICU	Neonatal intensive care unit

NLRP3	NOD-like receptor protein 3
NMDAS	Newcastle Mitochondrial Disease Adult Scale
NPMDS	Newcastle Paediatric Mitochondrial Disease Scale
O_H	mtDNA Origin of replication on light strand
O_L	mtDNA Origin of replication on light strand
OMM	Mitochondrial outer membrane
OPA1	Mitochondrial Dynamin Like GTPase
OSCP	Oligomycin sensitive conferring protein
OXPHOS	Oxidative phosphorylation
PACI	Public Authority for Civil Information in Kuwait
Parkin	Parkinson juvenile disease protein 2
PCR	Polymerase chain reaction
PDH	Pyruvate Dehydrogenase
PDHc	Pyruvate Dehydrogenase complex
PEO	Progressive External Ophthalmoplegia
PGC1α	Peroxisome proliferator-activated receptor gamma coactivator 1-alpha / (Mitochondrial transcription activator)
Pi	Inorganic phosphate
Pink1	PTEN inducible putative kinase
PMSF	Phenylmethylsulphonyl fluoride
PNPase	Polynucleotide Phosphorylase
POLG	Polymerase gamma
POLG1	Mitochondrial DNA polymerase 1
POLG2	Mitochondrial DNA polymerase 2
POLRMT	Mitochondrial RNA polymerase

PTEN	Phosphatase and tensin homolog
PVDF	Polyvinylidene fluoride
Q	Ubiquinone
QH2	Ubiquinol
qPCR	Quantitative Polymerase chain reaction
qRT-PCR	Quantitative real-time PCR
RCC	Respiratory chain complex
RFLP	Restricted Fragment Length Polymorphism
RMND3	Regulator of mitochondrial dynamics 3
RNA	Ribonucleic acid
ROS	Reactive oxygen species
ROX	Residual oxygen consumption
RP	Retinitis Pigmentosa
RRF	Ragged red fibres
RRM2B	Ribonucleotide Reductase subunit M2B
rRNA	Ribosomal RNA
RVCL	Retinal vasculopathy with cerebral leukodystrophy
S-OPA1	Short OPA1
SAM	Sequence Alignment/Map
SAM	Sorting and assembly machinery
SCAD	Short-chain acyl CoA dehydrogenase
SCAF1	Supercomplex assembly factor 1
SDH	Succinate:ubiquinone oxidoreductase / Complex II
SDS	Sodium Dodecyl Sulphate

SDS-PAGE	Sodium dodecyl sulphate polyacrylamide gel electrophoresis
siRNA	Small interfering RNA
SIRT1	Mitochondrial deacetylase
SLIRP	Stem-loop interacting RNA-binding protein
SMAC/DIABLO	Second Mitochondria-derived Activator of Caspases/ Direct IAP [inhibitor of apoptosis]
SNHL	Sensorineural hearing loss
SNP	Single nucleotide polymorphism
SOD	Superoxide dismutase
Spire1C	Mitochondrial-bound actin-nucleating Spire protein
TAE	Tris-Acetate-EDTA
TALEN	Transcription activator-like effector nuclease
TBS-T	Tris-Buffered Saline and Tween-20
TCA	tricarboxylic acid
TEFM	Mitochondrial transcription elongation factor
TEM	Transmission electron microscopy
TEMED	N, N, N', N'- Tetramethylethylenediamine
TFAM	Mitochondrial transcription Factor A
TFB1M	Mitochondrial transcription Factor B1
TFB2M	Mitochondrial transcription Factor B2
TGF-β	Transforming-growth factor β
TIM	Mitochondrial translocase of the inner membrane
TNFR	Tumour necrosis factor receptor
TOM	Mitochondrial translocase of the outer membrane
TPP	Thiamine pyrophosphate

tRNA	Transcription RNA
TRNT1	tRNA nucleotidyl transferase 1
TSH	Thyroid stimulating hormone
TTP	Thiamine Triphosphate
TWINKLE	Mitochondrial DNA helicase
UCSC	University of California Santa Cruz
VAMP	Vesicle-associated membrane proteins
VAPB	VAMP associated protein B
VAPC	VAMP associated protein C
VDAC	Voltage-dependent anion channel / porin
VEP	Variant effect predictor
VSD	Ventricular septal defect
VUS	Variant of uncertain significance
WB	Western blot
WES	Whole exome sequencing
WGS	Whole genome sequencing
WHS	Wolf Hirschhorn Syndrome

Chapter 1. Introduction

1.1 Mitochondria

Mitochondria are dynamic double-membraned cellular organelles, ubiquitous to all nucleated cells, that carry out many cellular metabolic processes including the Kreb's cycle, fatty acid oxidation and oxidative phosphorylation (OXPHOS) (Nunnari and Suomalainen, 2012). In addition, mitochondria play a major role in calcium homeostasis, autophagy, apoptosis, and heme and iron-sulphur cluster biosynthesis (Contreras *et al.*, 2010; Glick *et al.*, 2010; Stehling *et al.*, 2014; Vakifahmetoglu-Norberg *et al.*, 2017).

Mitochondria were first described by Kölliker (1856), but Richard Altmann (1894) studied their structure and function describing them as "elementary organisms" resembling bacteria, sustaining metabolic and genetic functions, and he named them "bioblasts" (meaning "life germs") in the process (Dahl and Thorburn, 2001; O'Rourke, 2010). However, the term "mitochondria" (meaning "thread granules") was coined by Carl Benda in 1898 (Reid and Leech, 1980) (Reid and Leech, 1980). Mitochondria are hypothesised to have originated from alpha-proteobacteria that were incorporated into eukaryote precursor cells via endosymbiosis; prokaryotes (the eukaryotic precursor cells) engulfed mitochondrial proteobacteria giving rise to the modern eukaryotic cells (Gray *et al.*, 1999; Lane and Martin, 2010).

1.1.1 Structure

A mitochondrion is a double membraned organelle with an outer membrane (OMM) separating the mitochondrial intermembrane space (IMS) from the cell's cytoplasm and an inner membrane (IMM) separating the space it encloses called the "matrix" from the IMS (**Figure 1.1**). The electron transport chain (ETC) complexes, along with adenosine triphosphate (ATP) synthase, are transmembrane proteins that reside within the IMM. To increase its surface area, the IMM forms numerous folds called cristae. The OMM possesses a number of transmembrane proteins that passively or actively transport ions and cofactors; an example is the voltage-dependent anion channel protein (VDAC) that allows the passive diffusion of certain molecules and ions through the OMM (Marchi *et al.*, 2014).

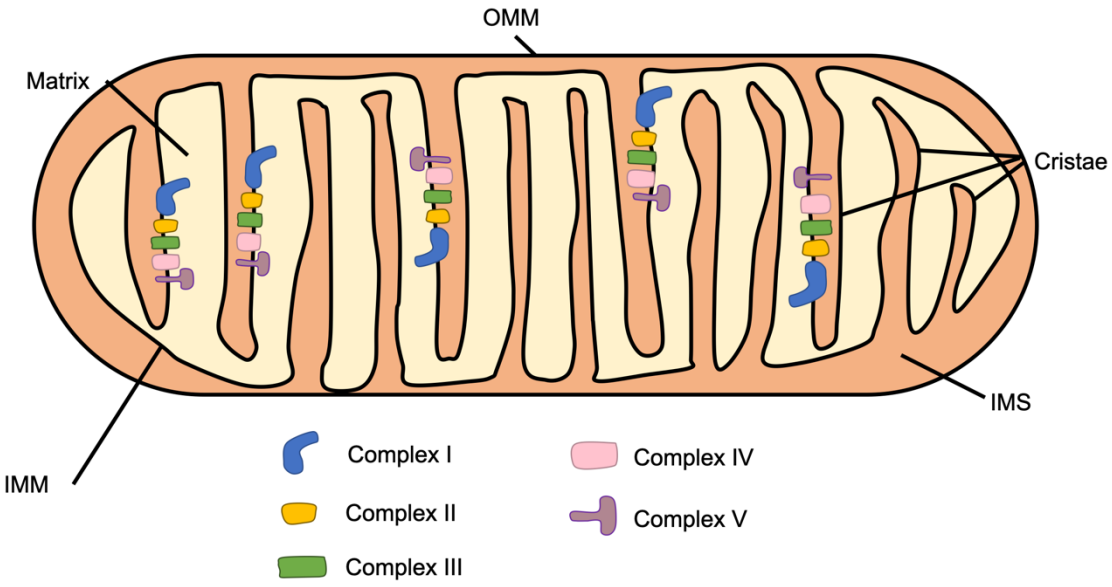

Figure 1.1 Mitochondrial structures and membranes.

The structure of the mitochondrial membranes and compartments. The matrix (yellow space) is the compartment enclosed by the mitochondrial inner membrane (IMM), while the mitochondrial intermembrane space (IMS, orange space) is the compartment located between the mitochondrial outer membrane (OMM) and the IMM. The OXPHOS complexes are depicted in the mitochondrial cristae.

1.1.2 Mitochondrial dynamics

Mitochondria are dynamic organelles that constantly fuse and divide allowing mitochondrial distribution to adapt to surrounding conditions during cell growth, division and differentiation (van der Bliek *et al.*, 2013; Ni *et al.*, 2015). This process of fission and fusion is directed by the dynamin family of large guanosine triphosphatases (GTPases) found in the cytosol. The processes of fission and fusion will be outlined below.

1.1.2.1 Fusion

Fusion of the OMM is mediated by members of the dynamin superfamily of GTPase proteins such as OMM-bound mitofusins Mfn1 and Mfn2 while IMM fusion is mediated by IMM bound OPA1 (Antonny *et al.*, 2016; Giacomello *et al.*, 2020). Upon binding GTP, mitofusins extend their structure from the outer membrane and interact with mitofusins on opposing mitochondria. GTP hydrolysis causes conformational changes in mitofusins reducing the distance between membranes while the release of GDP results in

the fusion of the opposing OMMs (Chen *et al.*, 2003). Both mitofusins Mfn1 and Mfn2 participate in OMM fusion through homomeric or heteromeric interactions.

OMM fusion usually is accompanied by the fusion of the IMM (van der Bliek et al., 2013). The alternative splicing of the IMM fusion mediating *OPA1* gene results in the production of 8 isoforms of OPA1 protein; 3 cleavage sites along the polypeptide allow for further processing by peptidases such as OMA1 and Yme1L leading to the formation of the IMM-bound long-OPA1 (L-OPA1) and the IMS form short-OPA1 (S-OPA1) which has a similar structure to Drp1 (another member of the dynamin superfamily of GTPases that is encoded by *DNM1L*) (**Figure 1.2**) (Smirnova *et al.*, 2001; Lee and Yoon, 2016). Knockouts of the OMA1 and Yme1L allow for the accumulation of L-OPA1 which did not affect fusion suggesting it plays a central role in IMM fusion; the expression of S-OPA1 in these knock out cells induced mitochondrial fission without influencing fusion suggesting both forms of OPA1 balance the process of IMM fission and fusion (Anand *et al.*, 2014).

1.1.2.2 Fission

During the process of fission, Drp1 binds to the receptors mitochondrial fission factor (Mff), fission 1 (Fis1), mitochondrial dynamics proteins of 49 kDa and 51 kDa (MiD49 and MiD51) anchored to the OMM between the mitochondria and the endoplasmic reticulum (ER) where the ER tubule wraps around the mitochondrial tubule (Ni *et al.*, 2015). At this ER-mitochondrial interface, Spire1C, a mitochondrial-bound actin-nucleating Spire protein, induces the polymerisation of actin by the ER-associated actin modulator inverted formin 2 (INF2) where Drp1 binds to its receptors leading to the initial constriction of the mitochondrial tubule (Manor *et al.*, 2015). Drp1 then forms a ring around the mitochondria and its GTPase activity further constricts the ring leading to mitochondrial fission. Mff triggers GTPase activity of Drp1 leading to mitochondrial fission while MiD51 inhibits the GTPase activity suggesting a regulatory role between these receptors during fission (Osellame *et al.*, 2016).

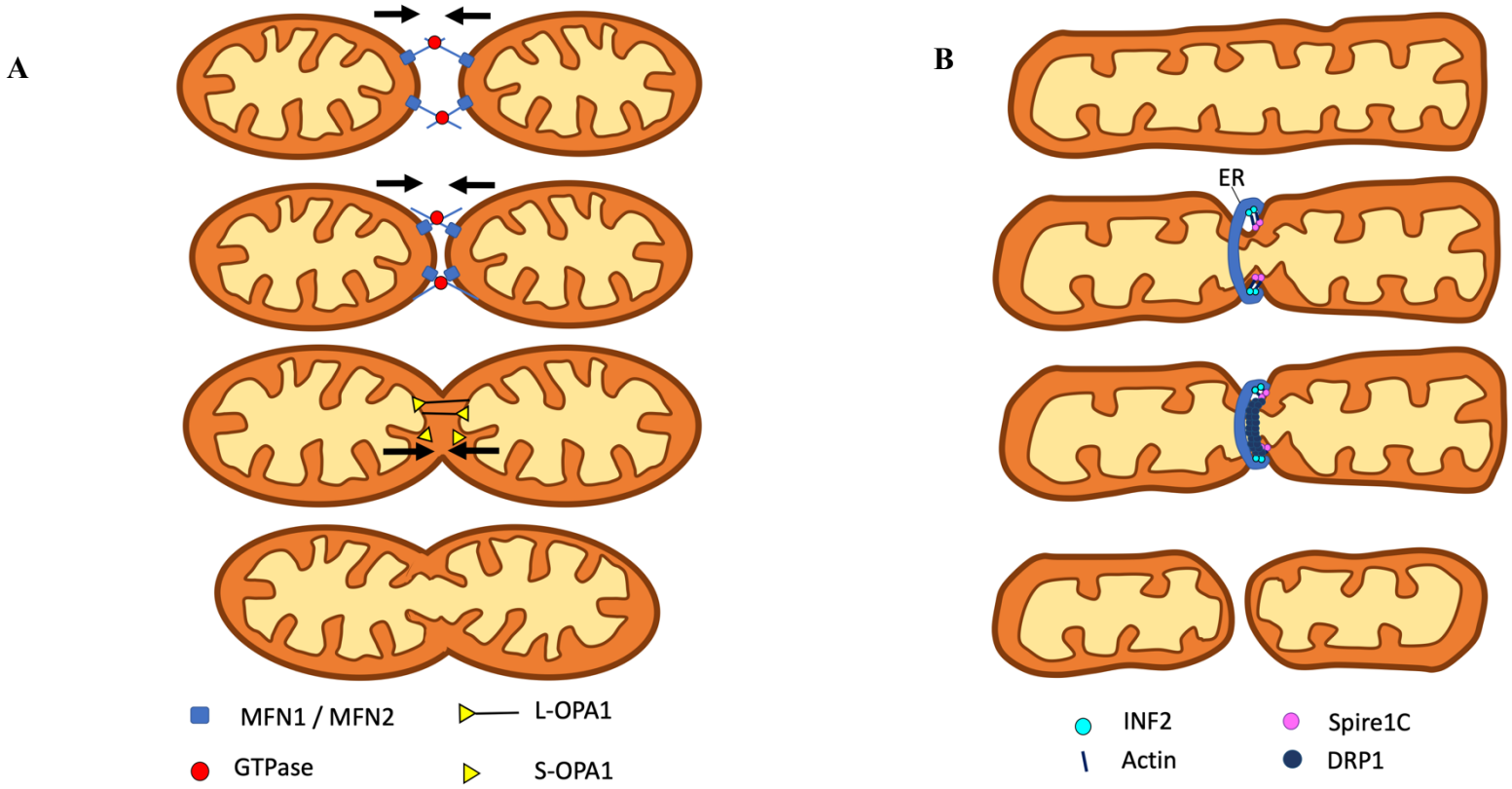

Figure 1.2 Mitochondrial Fusion and fission

A Fusion of the OMM it facilitated by the dynamin proteins MFN1 and MFN2 binding and GTPase activity pulls the membranes together to fuse. Fusion of the IMM is mediated by L-OPA1 that bind to opposing IMMs and fuse the membranes together.
B Mitochondrial fission initially involves the wrapping of the ER around a segment of mitochondria where MAMs (including Spire1C) bind the mitochondria to the ER and recruit DRP1 to form a ring. Subsequent to the formation of the ring, DRP1 constrict resulting in the formation of 2 separate mitochondria.

1.1.3 ER-mitochondrial interactions

The interaction between the ER and OMM takes place at points of contact named mitochondria-associated ER membranes (MAMs) (Patergnani *et al.*, 2011). These junctions are linked to pathways facilitating and regulating mitochondrial fission, calcium homeostasis, autophagy and inflammation. During fission, MAMs contain ER-bound INF2 which plays a crucial role in facilitating the formation of the DRP1 ring (Marchi *et al.*, 2014). These MAMs are points where mitochondrial fission takes place as a result of DRP1 ring formation and constriction (Friedman *et al.*, 2011).

In addition to its involvement in mitochondrial fission, there are other ER interactions with the mitochondria that are important for such diverse functions as calcium homeostasis, autophagy and inflammation. With regards to calcium homeostasis, the ER functions as a calcium storage and releases these ions, via the ER bound transmembrane protein inositol 1,4,5-trophosphate receptor (IP3R) at MAMs, for the mitochondria to take up (Marchi *et al.*, 2018). There is evidence showing that IP3R bind to the OMM transmembrane protein VDAC facilitating the efficient transfer of calcium from the ER to the mitochondria. Calcium overload in the mitochondria results in apoptotic signalling (Marchi *et al.*, 2018).

Autophagy is the process of degrading cellular components and organelle due to damage or cellular starvation by forming autophagosome vesicles that fuse with lysosomes to form autophagolysosomes resulting in the digestion of the cellular components within (Glick *et al.*, 2010). Autophagy induced by starvation triggers non-selective degradation of organelles such as the ER and mitochondria. Autophagy related genes (ATG) that localise in the cytosol and ER migrate to MAMs indicating importance of these junctions in autophogasome formation (Axe et al., 2011). ER-bound vesicle-associated membrane proteins (VAMP) associated proteins B and C (VAPB and VAPC) and OMM transmembrane protein Regulator of mitochondrial dynamics 3 (RMND3) were discovered to tether the organelles and their dissociation stimulated the formation of autophagosomes (Gomez-Suaga *et al.*, 2017).

In the inflammatory pathway, NOD-like receptor protein 3 (NLRP3) is an inflammasome that is activated by reactive oxygen species (ROS) (Zhou *et al.*, 2011). As signal molecules, ROS do not travel long distances before they trigger a signal or are neutralised by superoxide dismutases (SODs). Therefore, NLRP3 which initially localises in the ER

is released into MAMs where ROS levels are more representative of mitochondrial oxidative stress levels.

1.1.4 The mitochondrial genome

Mitochondria have multiple copies of their own genome which is the only inheritable extra-nuclear DNA. The human mitochondrial DNA (mtDNA) molecule is a circular genome comprising 16,569 bp (**Figure 1.3**) (Anderson *et al.*, 1981). The mitochondrial genome encodes 37 genes that are fundamental to mitochondrial function including 2 rRNAs, 22 tRNAs and 13 polypeptides, which are all essential subunits of the OXPHOS complexes I, III, IV and ATP Synthase (complex V) (Anderson *et al.*, 1981). These protein subunits are synthesised by the mitochondrial protein synthesis components. The strands of the mtDNA are assigned as heavy strand (H-strand) and light strand (L-strand) due to differences in buoyant densities in denaturing caesium chloride gradients based on their guanine and thymine content (Kasamatsu and Vinograd, 1974; Anderson *et al.*, 1981). The H-strand codes for 14 tRNAs, 12 polypeptides, and 2 rRNAs along with the two sites for transcription initiation HSP1 and HSP2 and the origin of L-strand replication O_L. The L-strand codes for 8 tRNAs, 1 polypeptide, the transcription initiation site LSP and the origin of H-strand replication O_H. Genes in the mitochondrial genome lack introns and some genes overlap such as the genes coding for complex I subunits ND4 and ND4L (*MT-ND4* and *MT-ND4L*) as well as complex V subunits ATPase 6 and ATPase 8 (*MT-ATP6* and *MT-ATP8*).

The displacement loop (D-loop) is a non-coding region (NCR) of mtDNA that incorporates a third DNA strand, homologous to the H-strand, named 7S DNA (Walberg and Clayton, 1981). This region is flanked by genes coding for tRNAs phenylalanine and proline and contained within it are the transcription promoters for the H-strand and L-strand (HSP1, HSP2 and LSP) and the origin of H-strand replication site O_H. Another NCR is located at the origin of L-strand replication site O_L that is flanked by 5 tRNAs.

Nucleated cells may contain high copy numbers of mtDNA packed into nucleoids ranging from hundreds to thousands per cell (Grady *et al.*, 2018). Mitochondrial transcription factor A (TFAM) is a member of the high-mobility group proteins and is a DNA packaging component that binds to mtDNA within nucleoids and is present in large numbers to cover the length of the genome and it acts as transcription initiation factor (Alam *et al.*, 2003; Kolesnikov, 2016). Other proteins identified in nucleoids are proteins

that play role in mtDNA transcription and replication such the mitochondrial transcription activator peroxisome proliferator-activated receptor gamma coactivator 1-alpha (PGC1α), the deactylase SIRT1, DNA helicase (Twinkle), mitochondrial single strand binding proteins (mtSSBs), mitochondrial RNA polymerase (POLRMT), and mitochondrial DNA polymerases POLG1 and POLG2 (Kolesnikov, 2016).

In evolutionary terms, the reduction of mtDNA to its current size was due either to the loss of unnecessary proteobacterial function genes (such as those expressing proteins for cell wall synthesis), the availability of gene homologs in the nuclear genome (nDNA) providing substitute proteins to those in mtDNA such as genes expressing ribosomal proteins that duplicate and target mitochondrial translation (Mollier *et al.*, 2002), or the unilateral transfer of genes from mtDNA to nDNA (Adams and Palmer, 2003). Fragments of the human mtDNA (mitochondrial pseudogenes) were located in different regions and chromosomes of the human nDNA providing evidence supporting the hypothesis of unilateral gene transfer from mtDNA to nDNA as a major evolutionary step leading to the formation of complex eukaryotic cells (Mourier *et al.*, 2001; Hazkani-Covo *et al.*, 2003).

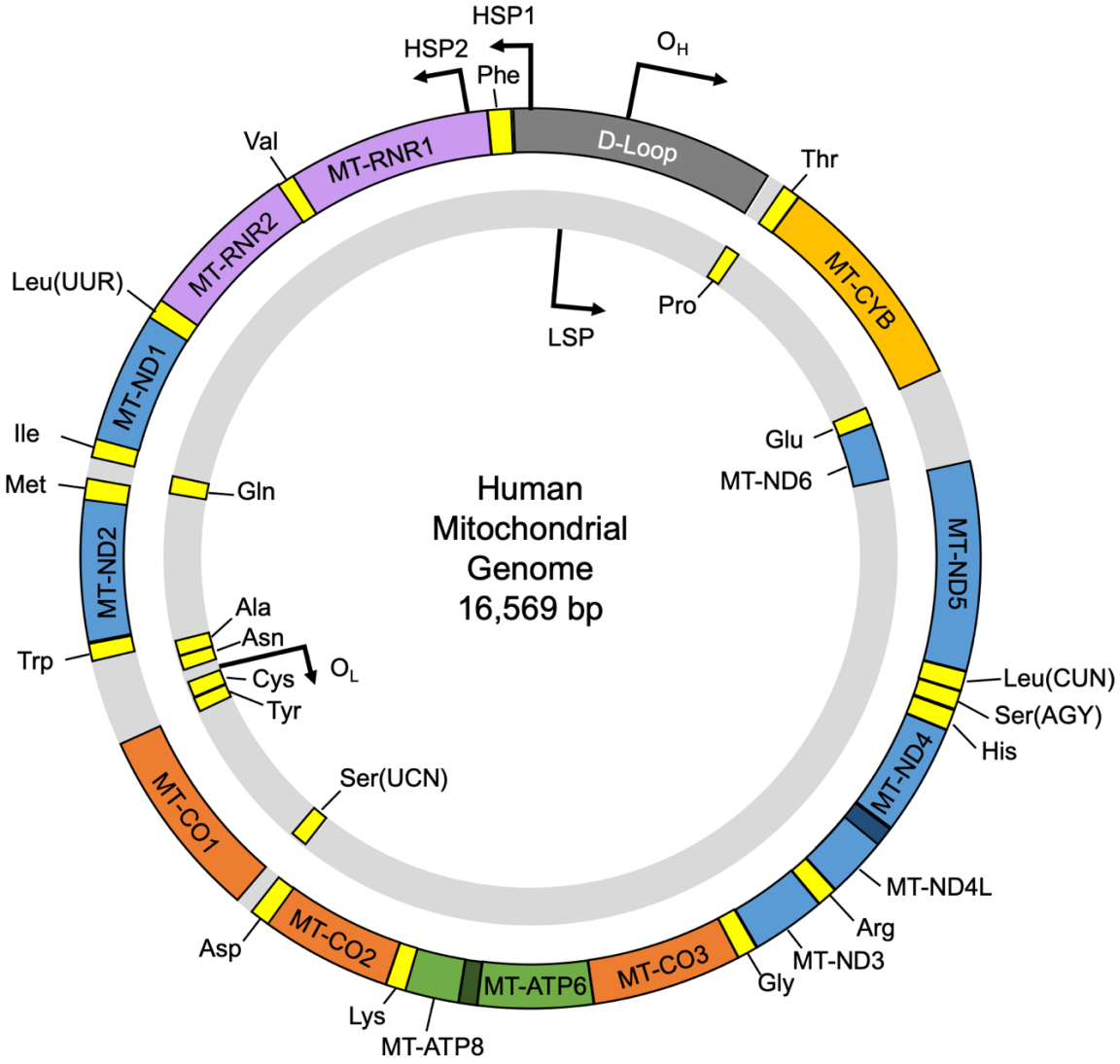

Figure 1.3 The mitochondrial genome

A diagram highlighting the genes in the mitochondrial genome, the mitochondrial tRNAs (neon yellow) and rRNAs (purple) required for mitochondrial gene translation. Genes coding for complex I core subunits are in blue, cytochrome b (a complex III subunit) is in dark yellow, complex IV subunits are in orange, and complex V subunits are in green. The D-loop (grey) is the region that anchors the mitochondrial genome to the IMM. Genes on the heavy strand are depicted on the outer circle while the light strand is depicted in the smaller inner circle. Also highlighted are the transcription promoters (HSP1, HSP2, and LSP) and the origins of replication (O_H and O_L) on both strands.

1.1.5 Mitochondrial genetics

Mitochondrial DNA associates with proteins forming nucleoprotein structures called nucleoids which are anchored to the inner mitochondrial membrane (Bogenhagen, 2012). These nucleoids are in close proximity to the mitochondrial respiratory chain which produces reactive oxygen species creating a hostile environment that may make mtDNA prone to develop mutations (Chinnery *et al.*, 2000). Proteins associated with mtDNA in nucleoids do not protect mtDNA as efficiently compared to the histone protection of nDNA, which may also contribute to the frequency of accumulated mtDNA mutations (Kolesnikov, 2016). The presence of mtDNA mutations at varying levels is termed "heteroplasmy" where a mixture of wild-type and mutant mitochondrial genomes co-exist within a single individual or cell; whereas when all mtDNA copies are identical, this is termed "homoplasmy" (**Figure 1.4**).

The mitochondrial genome is inherited maternally due to the high abundance of maternal mitochondria in the oocyte compared to the low number of mitochondria in the sperm during fertilisation (Hutchison *et al.*, 1974). Moreover, mechanisms of paternal mtDNA degradation were discovered further supporting uniparental inheritance (Sato and Sato, 2013; Yu *et al.*, 2017).

Maternally inherited mtDNA has repeatedly shown varying levels of mtDNA heteroplasmy in offspring; this variation is hypothesised to be the result of a "bottleneck" effect where a selection of mitochondria harbouring certain levels of heteroplasmy are transmitted to offspring (Chinnery *et al.*, 2000; Friedman and Nunnari, 2014). Within a single individual, different tissues may harbour different levels of heteroplasmy due to asymmetric distribution of mitochondria during mitosis leading to a variation in affected organs amongst patients with similar mtDNA mutations. The threshold effect is a key factor in the presentation of mitochondrial disorders resulting from mtDNA mutations as the level of mutant heteroplasmy needs to exceed a certain threshold level (usually 60% and above) (Holt *et al.*, 1990; Rossignol *et al.*, 2003). When mutant heteroplasmy levels exceed this threshold level, this results in a significant defect in mitochondrial or respiratory function leading to symptoms developing in these tissues. For example, patients harbouring 2 different mutations affecting the same nucleotide mt.8993T>C and mt.8993>G in *MT-ATP6* exhibited different threshold levels; patients with the mt.8993T>C mutation presented clinically when exceeding the threshold of 80%

heteroplasmy level, while patients with the mt.8993T>G mutation presented clinically at heteroplasmy levels below 60% (White *et al.*, 1999).

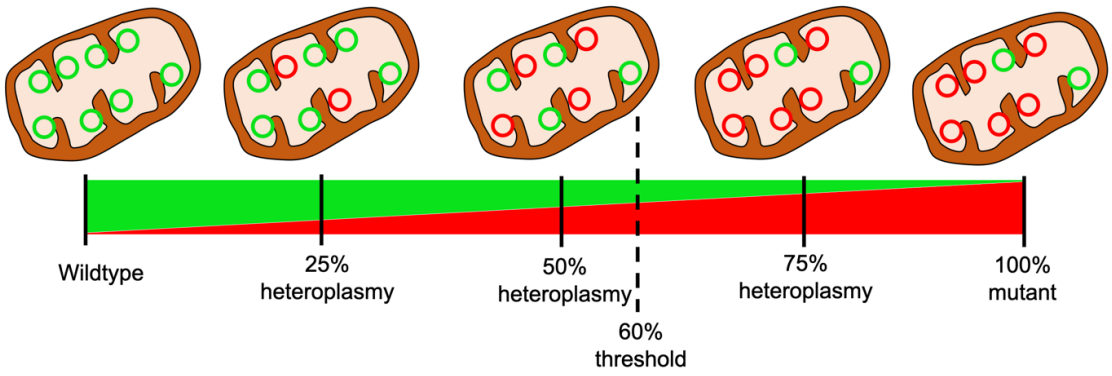

Figure 1.4 Mitochondrial genome heteroplasmy

A representation of DNA heteroplasmy in the presence of variants within the number of mitochondrial genomes. Wild-type mtDNA genomes (green) and mutant mtDNA genomes (red) can both be present in the same mitochondria. The higher the number of mutant mtDNA, the higher the level of heteroplasmy. The 60% threshold is highlighted with a dashed line to demonstrate the estimated level where variant heteroplasmy is associated disease.

1.1.6 Nuclear encoded mitochondrial components

Mitochondrial function is reliant on genes encoded in both the mitochondrial and nuclear genomes. Nuclear DNA encodes the vast majority of OXPHOS subunits, including the whole of complex II, alongside other genes that regulate OXPHOS and mitochondrial functions (>1,400 genes) (Lopez *et al.*, 2000; Calvo *et al.*, 2006). The MitoCarta2.0 inventory (https://www.broadinstitute.org/scientific-community/science/programs/metabolic-disease-program/publications/mitocarta/mitocarta-in-0) lists 1158 genes encoding proteins involved in pathways that take place within the mitochondria (Pagliarini *et al.*, 2008; Calvo *et al.*, 2016). These genes include the 13 mtDNA genes encoding OXPHOS components, but all of the remaining mitochondrial respiratory chain subunits and accessory subunits, the mitochondrial ribosomal (mitoribosome) subunits and RNA polymerases requires for mtDNA gene expression, DNA polymerases necessary for

mtDNA replication and many other proteins required for mitochondrial maintenance are encoded by the nuclear genome.

1.1.7 Replication of mtDNA

Three different models of mtDNA replication have been described in the literature (**Figure 1.5**) (McKinney and Oliveira, 2013). All three models of replication initiate at the H-strand O_H where the replicative mtDNA helicase TWINKLE binds and unwinds the dsDNA forming a replication fork where polymerase γ (POLG) binds and commences mtDNA replication in the 5' to 3' direction (Holt and Reyes, 2012; McKinney and Oliveira, 2013). Binding of mtSSB to the lagging strand protects it from degradation by nucleases.

POLG is a heterotrimeric protein comprised of a single POLG-α subunit that carries out all the catalytic activities and two POLG-β subunits that regulate POLG-α activity enhancing the speed of DNA replication 100-fold (Ciesielski *et al.*, 2016). The POLG-α subunit contains domains that facilitate 5' to 3' DNA synthesis, 3' to 5' exonuclease activity to repair error during replication, and 5' deoxyribophosphate lyase activity also required for repair mechanisms.

1.1.7.1 Strand displacement replication

The first model is the strand displacement replication model where replication initiates unilaterally from the origin of the H-strand` replication O_H (McKinney and Oliveira, 2013). When replication reaches two-thirds of the way around the mtDNA, the origin of L-strand replication O_L is exposed; mitochondrial RNA polymerase (POLRMT) binds to O_L and synthesises a 25nt primer allowing the binding of POLG and the initiation of L-strand replication in the opposite direction (Robberson *et al.*, 1972; Fusté *et al.*, 2010). This results in the formation of 2 copies of the mtDNA which are then segregated.

1.1.7.2 Ribonucleotides Incorporated Through Out the Lagging Strand (RITOLS) replication

The second model theorises that after replication initiates at the O_H origin of replication site, RNA is incorporated on to the lagging strand forming RNA:DNA hybrids that protect against nuclease cleavage (Yang *et al.*, 2002; Yasukawa *et al.*, 2006). The mechanism of RNA binding is not yet known but suggestions of primase activity and the binding of processed gene transcripts have been raised (Reyes *et al.*, 2013) . When the O_L origin of

replication site is exposed, replication initiates in the opposite direct in a similar fashion to the strand displacement replication model. The mechanism of RNA removal or conversion to DNA remains unknown although RNase H activity is suggested to play a role in the process (Holt and Reyes, 2012; Ciesielski *et al.*, 2016; Zinovkina, 2019).

1.1.7.3 Strand coupled replication

A third model was proposed after experiments with mtDNA depletion following exposure to ethidium bromide demonstrated that other sites of replication initiation were discovered on the lagging strand in the region coding for cytochrome *b* and complex I subunits ND5 and ND6 (Holt *et al.*, 2000; Bowmaker *et al.*, 2003). This resulted in the simultaneous replication of both the H-strand and L-strand. Though this mechanism of replication is assumed to be a secondary form of replication, evidence of extensive use of this model of replication in chicken suggests species specific replication models (McKinney and Oliveira, 2013; Ciesielski *et al.*, 2016).

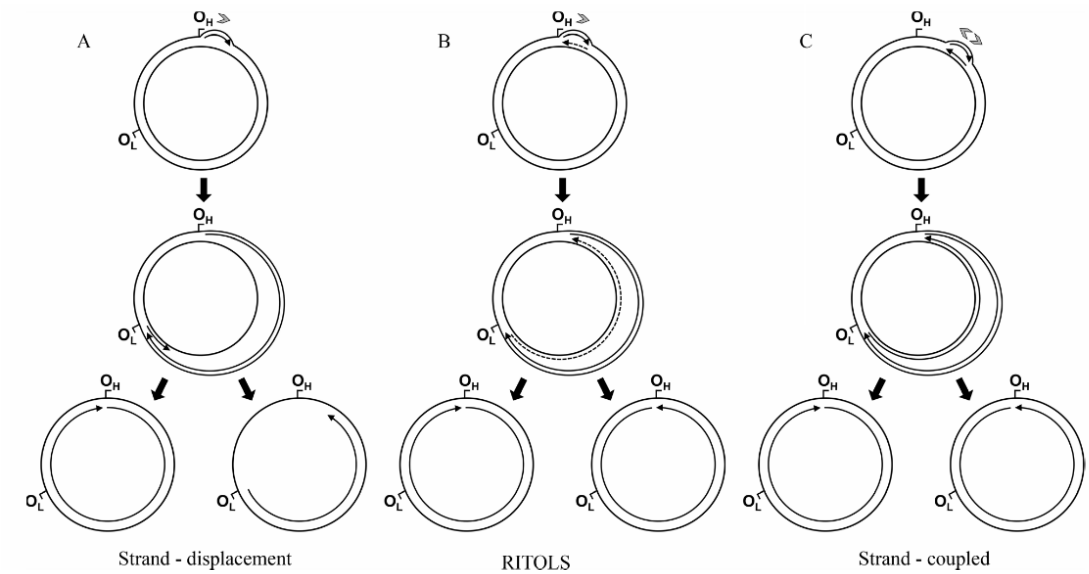

Figure 1.5 mtDNA replication models

A visual presentation of the 3 models of mtDNA replication described in ***Section 1.1.7***. (McKinney and Oliveira, 2013).

1.1.8 mtDNA gene expression

1.1.8.1 Transcription initiation

Gene expression of mtDNA starts at transcription initiation sites (Montoya *et al.*, 1982). TFAM binds to the promoter regions for H-strand transcription (HSP1 and HSP2) and L-strand transcription (LSP), both located in the D-loop, and recruits the transcription complex heterodimer comprised of POLRMT and the mitochondrial transcription factor B2 (TFB2M) (Asin-Cayuela and Gustafsson, 2007). TFAM is hypothesised to cause a conformational change in mtDNA in order to recruit the transcription complex.

1.1.8.2 Transcription elongation

The transition from transcription initiation to elongation occurs when the transcription initiation factors TFAM and TFB2M are released from the transcription complex and the transcription elongation factor (TEFM) binds to POLRMT forming the transcription elongation (antitermination) complex (Minczuk *et al.*, 2011). TEFM has been shown to play an important role in stabilising the synthesis and release of nascent RNA and facilitates the transcription of almost the whole mitochondrial genome by preventing the formation of secondary structures in the RNA during synthesis (Posse *et al.*, 2015; Hillen *et al.*, 2018). The transcription complex synthesises mtRNAs until transcription is terminated by one of a few uncovered and hypothesised termination mechanisms detailed below.

1.1.8.3 Transcription termination

The known termination mechanism involves mitochondrial transcription termination factor 1 MTERF1 that binds to the 3' end of the tRNA $Leu^{(UUR)}$ gene (*MT-TL1*) where is triggers termination upon interaction with the transcription complex (Kruse *et al.*, 1989; Asin-Cayuela and Gustafsson, 2007). This termination site is linked with the transcription of mt-rRNAs where transcription initiates at HSP in the D-loop. This termination mechanism could result in a higher transcription rate of mt-rRNAs relative to other mtRNAs which has been observed in mitochondria (Roberti *et al.*, 2009). The other known mechanism is the formation of a hairpin structure in newly synthesised mtRNA that interacts with the transcription complex resulting in the release of the transcription complex; this was observed in bacteriophages (Byrnes and Garcia-Diaz, 2014). In human mitochondria however, a suggested G-quadraplex formation in newly synthesised

mtRNA might be a possible mechanism of transcription termination (Wanrooij *et al.*, 2010).

1.1.8.4 Transcript processing and maturation

The result of mtDNA transcription are long polycistronic mtRNA molecules that require processing into respective mitochondrial tRNA (mt-tRNA), mitochondrial rRNA (mt-rRNA), and protein coding mitochondrial mRNA (mt-mRNA) sequences (**Figure 1.6**) (Sanchez *et al.*, 2011; D'Souza and Minczuk, 2018). These newly transcribed polycistronic mtRNAs colocalise into foci called mitochondrial RNA granules (MRG) where they are processed before their release into the mitochondrial matrix (Iborra *et al.*, 2004; Jourdain *et al.*, 2016). In the MRGs, the mitochondrial tRNA punctuation model dictates that mtRNA are processed by RNase P and ELAC2 endonucleases at specific junctions between mtDNA genes resulting in the cleavage of these sites and the formation of individual mtRNA transcripts (Ojala *et al.*, 1981). Post-cleavage, the transcripts are further modified.

Transcripts of mt-mRNA are polyadenylated by mitochondrial Poly(A) polymerase (mtPAP) (excluding the ND6 transcript) (Slomovic *et al.*, 2005). Leucine rich pentatricopeptide repeat containing protein (LRPPRC) and stem-loop interacting RNA-binding protein (SLIRP) interact to form a complex that maintains and stabilises these polyadenylated mt-mRNA transcripts (Sasarman *et al.*, 2010; Ruzzenente *et al.*, 2012).

Transcripts of mt-tRNA are extensively modified and a CCA trinucleotide is added to its 3' end by tRNA nucleotidyl transferase 1 (TRNT1) before the binding of its corresponding amino acid (Chen *et al.*, 1992; Nagaike *et al.*, 2001). Thereafter, various positional modifications to the mt-tRNAs are carried out by an array of enzymes such as ABH1 and NSUN3 (Haag *et al.*, 2016), MTO1 and GTPBP3 (Asano *et al.*, 2018), MTU1 (Wu *et al.*, 2016b), TRIT1 (Yarham *et al.*, 2014), TRMT5 (Powell *et al.*, 2015), and PUS1 (Patton *et al.*, 2005). The removal of poly(A) tails from the 3’ end of mt-tRNAs is performed by the 3’-5’ exonuclease PDE12 (2’ phosphodiesterase) (Pearce *et al.*, 2017).

After all the modifications have taken place, the mt-tRNAs need to be charged with their cognate amino acids. This is carried about by aminoacyl-tRNA synthetases (aaRS) of which most are unique to mitochondria (aaRS2) (Sissler *et al.*, 2017). However, some are shared with the cytoplasmic pathways such as Glycyl-tRNA synthetase (GARS) (Chihara *et al.*, 2007) and Lysyl-tRNA synthetase (KARS) (Tolkunova *et al.*, 2000). Interestingly,

the charging of mt-tRNA^{Gln} takes place indirectly via the mitochondrial glutamyl-tRNA synthetase (EARS2) by charging it with a glutamate amino acid forming Glu-mt-tRNA^{Gln}, and then the glutamate is transamidated into Gln-mt-tRNA^{Gln} by the glutamyl-tRNA^{Gln} amidotransferase protein complex (GatCAB) (Nagao *et al.*, 2009; Echevarría *et al.*, 2014).

The mitochondrial 12S rRNA and 16S rRNAs transcripts undergo nucleotide modifications at several residues before their incorporation into the 28S small mitochondrial ribosomal subunit and 39S large mitochondrial ribosomal subunit respectively; these subunits bind to form the 55S mitoribosome (O'Brien, 1971; Gerber *et al.*, 2017). These modifications are carried out by methyltransferases; NSUN4 and mitochondrial transcription factor 1B (TFB1M) modify 12S rRNA and TRMT61B, MRM1, MRM2, and MRM3 modify 16S rRNA while RPUSD4 carries out pseudouridylation of 16S rRNA (Metodiev *et al.*, 2009; Lee *et al.*, 2013; Metodiev *et al.*, 2014; Rorbach *et al.*, 2014; Bar-Yaacov *et al.*, 2016; Zaganelli *et al.*, 2017). The fas-activated serine threonine kinase domain 2 protein (FASTKD2) plays an essential role in the stability of the 16S rRNA and it plays a role in the assembly of the large ribosomal subunit (Antonicka and Shoubridge, 2015; Popow *et al.*, 2015). Finally, the degradation of mtRNA is mediated by a complex formed by 2 proteins, polynucleotide phosphorylase (PNPase) and helicase hSUV3 (Borowski *et al.*, 2013).

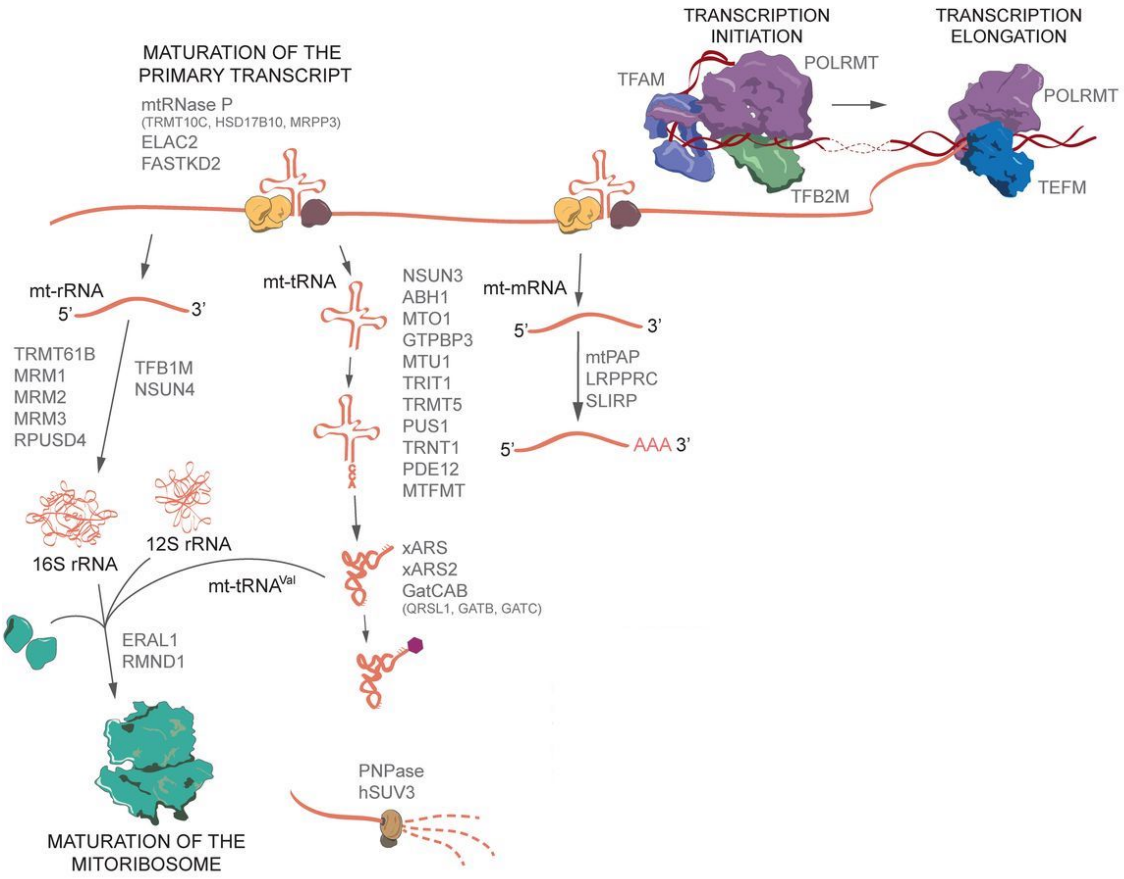

Figure 1.6 Transcription of the mitochondrial genome

A flow diagram outlining the various stages of mtDNA transcription, processing, and role in mitochondrial translation. The pathways and highlighted proteins involved are described in detail in ***Section 1.1.8***. The transcription initiation pathway is described in ***Section 1.1.8.1***, the transcription elongation pathway is described in ***Section 1.1.8.2***, and the transcript processing and maturation pathway is described in ***Section 1.1.8.4***. (Adapted from (D'Souza and Minczuk, 2018)).

1.1.8.5 Mitoribosome structure

The human mitoribosome is a 55S RNA-protein complex that is comprised of a 39S large subunit (mtLSU), a 28S small subunit (mtSSU), and 3 mtRNA molecules: the 16S rRNA, 12S RNA and mt-tRNA^{Val} (Amunts *et al.*, 2015). By utilising cryo electron microscopy (cryo-EM), studies have determined that the mtLSU is comprised of 48 mitochondrial ribosomal protein subunits (MRPs) of which 21 are specific to mitochondria, and the mtSSU is comprised of 30 MRPs of which 14 are specific to mitochondria (Brown *et al.*, 2014; Amunts *et al.*, 2015). In contrast to bacterial ribosomes, mammalian mitoribosomes

have a lower RNA:protein ratio where RNAs were replaced by 36 proteins specific to the mitoribosome (Greber *et al.*, 2015; D'Souza and Minczuk, 2018). The assembly of the mitoribosome involves non-ribosomal proteins that act as assembly factors; these proteins include RNA modification enzymes, RNA chaperones, guanosine triphosphatases, DEAD-box RNA helicases, and kinases (Dennerlein *et al.*, 2010; De Silva *et al.*, 2013; Janer *et al.*, 2015; Kim and Barrientos, 2018; Maiti *et al.*, 2018; Fontanesi *et al.*, 2020).

1.1.8.6 Translation

The translation process can be broken down into 3 steps; initiation, elongation and termination (Figure 1.7) (Smits *et al.*, 2010). Proteins required for this process to be carried out including translation factors for the sequential steps, MRPs, and mt-tRNA synthetases are all nuclear encoded. Prior to the initiation of translation, mitochondrial methionyl-tRNA formyltransferase (MTFMT) formylate a portion of the met-tRNA^{Met} in the mitochondria to form N-formylmethionine-tRNA^{Met} (fMet-tRNA^{Met}) which is used to initiate translation (Tucker *et al.*, 2011). Mitochondrial translation factor mtIF3 binds to mtSSU and prepares for the initiation of mt-mRNA translation (Koc and Spremulli, 2002). The initial formylated methionyl-tRNA binds to the mt-mRNA transcript with the assistance of GTP bound mitochondrial translation initiation factor 2 (mtIF2). This facilitates the release of mtIF3 while GTP hydrolysis on mtIF2 triggers its release and the mtLSU binds to the initiation complex forming the mitoribosome. The elongation of the polypeptide follows with the binding of the elongation factor Tu (mtEFTu) complex containing aminoacylated tRNA and GTP (Cai *et al.*, 2000). Upon the complex's entry into the acceptor (A) site and the verification of codon-anticodon pairing, GTP hydrolysis releases the mtEFTu·GDP component of the complex. The mtEFTu·GDP is converted back to mtEFTu·GTP by the nucleotide exchange protein elongation factor Ts (mtEFTs) allowing for the formation of a new bond with a new aminoacylated tRNA. The peptide chain residues are translocated from the acceptor (A) and Peptide (P) sites to the P and Exit (E) sites by GTP hydrolysis of the elongation factor G1 (mtEFG1)·GTP resulting in the release of the tRNA bound to the peptide residue in the E site allowing a new elongation step to commence (Bhargava *et al.*, 2004). Translation terminates when the mitochondrial release factor 1a (mtRF1a)·GTP recognises the stop codon, binds to the A site and catalyses the release of the newly formed polypeptide using GTP hydrolysis and dissociates from the mitoribosome (Soleimanpour-Lichaei *et al.*, 2007). The dissociation of the mitoribosome into its subunits is catalysed by mitochondrial recycling factor

(mtRRF) and elongation factor G2 (mtEFG2)·GTP (Rorbach *et al.*, 2008; Tsuboi *et al.*, 2009).

It is key to note that mt-mRNA transcripts utilise a modified codon system than that used by nuclear mRNA transcripts. Compared to cytosolic translation, in mitochondrial translation AUA codes for an initiation methionine instead of isoleucine, AGG and AGG code for stop codons instead of arginine, and UGA codes for tryptophan instead of a stop codon (Anderson *et al.*, 1981).

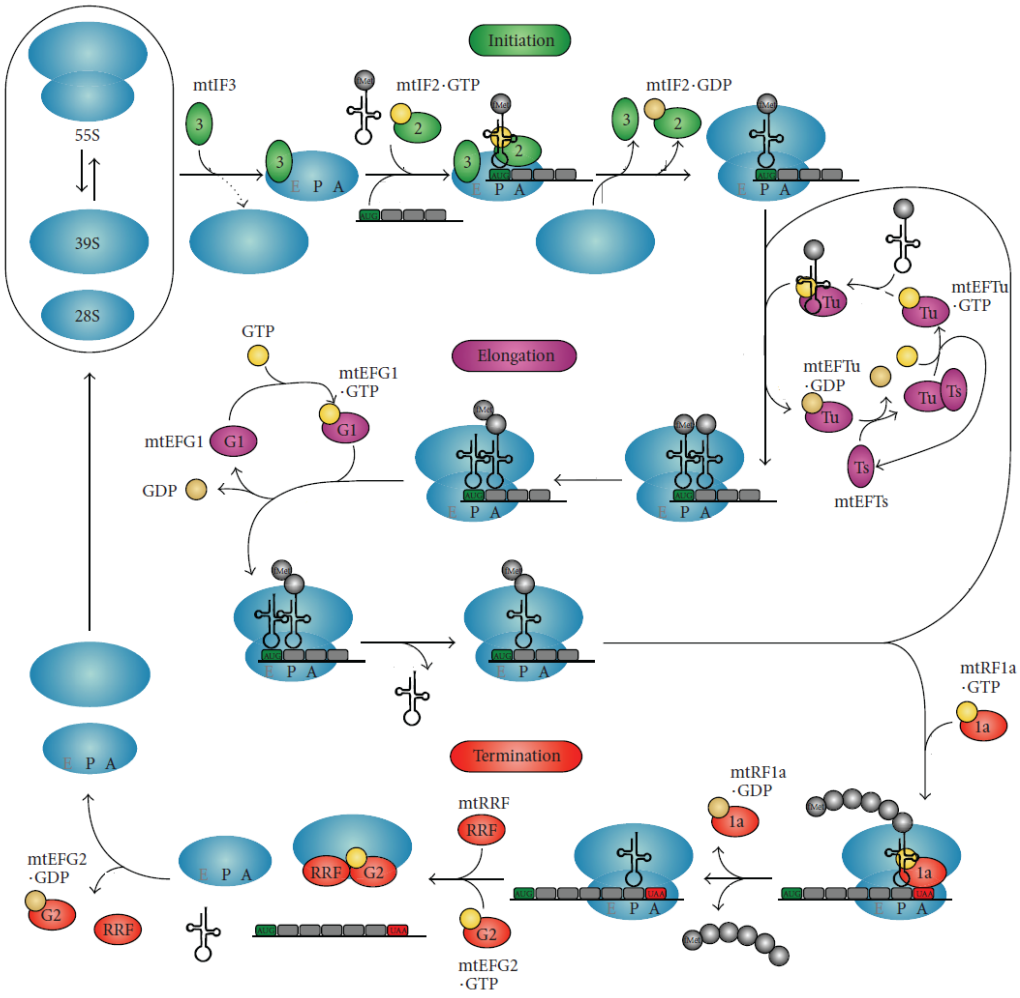

Figure 1.7 Translation of mitochondrial mRNA

Pathway outlining the translation of mt-mRNA in the mitochondria. Molecule abbreviations are referenced in ***Section 1.1.8.6***. (Smits *et al.*, 2010).

1.1.9 Mitochondrial protein import

Since most of the mitochondrial proteome is encoded by nDNA and synthesised in the cytosol, protein import mechanisms are essential to ensure the translocation of these proteins to their destination in the mitochondria. The mitochondrial double membrane houses import machinery that imports mitochondrial proteins from the cytosol to the mitochondria via a number of pathways. It is important to note that the majority of research on mitochondrial protein import has been performed in yeast (Kang *et al.*, 2018).

Incoming proteins initially interact with the translocases of the outer membrane (TOM) complex. It consists of receptor subunits Tom20 and Tom22 that form a subcomplex that recognises cleavable N-terminus presequences; the Tom70 receptor subunit that recognises hydrophobic internal targeting sequences; the general import pore Tom40 which is a transmembrane beta-barrel channel; and the small proteins Tom5, Tom6 and Tom7 that modulate the binding of the receptor subunits to Tom40 (Alconada *et al.*, 1995; Pfanner *et al.*, 1996; Dietmeier *et al.*, 1997). The Tom70 receptor initiates the importation of the precursor protein through an ATP-dependent pathway while the Tom20-Tom22 receptor subcomplex does not.

The mitochondrial import stimulation factor (MSF) and the heat shock protein Hsp70 are important cytoplasmic chaperones that recognise signal sequences on newly synthesised mitochondrial precursor proteins (preproteins), maintain the protein in an unfolded state and guide them to the Tom-Tim complexes for importation into the mitochondrial matrix (Mihara and Omura, 1996). The MSF directs protein import by interacting with the Tom70 receptor subunit and an ATP-dependent step transfers the preprotein to the Tom22-Tom20 receptor subcomplex before translocation through the OMM; MSF directs the import of mitochondrial preproteins in the presence or absence of a signal sequence such as the case with importing the OMM transmembrane protein VDAC (Pfanner and Meijer, 1997). The Hsp70 chaperone guides preproteins to the Tom22-Tom20 receptor subcomplex in a non-ATP-dependent pathway.

Preproteins are generally processed through one of 4 main pathways depending on the intended destination of the protein (**Figure 1.8**) (Wiedemann and Pfanner, 2017).

1.1.9.1 Matrix proteins

Preproteins destined to be localised in the mitochondrial matrix pass through the translocase of the inner membrane (TIM) complex TIM23 (Neupert and Herrmann, 2007). The complex is comprised of nine subunits of which 4 are membrane sectors (Tim50, Tim23, Tim22, and Tim17) and 5 are import motors (Tim44, Tim16, Tim14, mtHsp70 and Mge1). Mitochondrial 70 kDa heat shock protein (mtHsp70) is a chaperone localised in the matrix that binds to Tim44 with the assistance of the co-chaperone Mge1; the mtHsp70-Tim44 subcomplex directs preprotein translocation by binding to the imported polypeptide and pulling the preprotein through while maintaining it in an unfolded state on either side of the mitochondrial double membranes (Schneider *et al.*, 1996; Pfanner and Meijer, 1997). The mtHsp70 is then released from Tim44 and a new mtHsp70 binds to continue the process of protein translocation. The mitochondrial processing peptidase (MPP) cleaves off the N-terminal presequence after the protein is released into the matrix (Gakh *et al.*, 2002). The membrane potential across the IMM is a necessary driving force in mitochondrial protein translocation but is not driven exclusively by the proton motive force since the amino terminal of the preprotein is positively charged and the matrix contains the negatively charged side of the membrane potential (Martin *et al.*, 1991).

1.1.9.2 Outer membrane transmembrane proteins

Preproteins destined to form OMM beta-barrel transmembrane proteins contain a sequence motif recognised by the small Tim9-Tim10 chaperone complex that escort the protein to the sorting and assembly machinery (SAM) where they are inserted into the OMM (Höhr *et al.*, 2015). SAM is comprised of the 3 core subunits Sam50, Sam37 and Sam35. Sam50 forms a beta-barrel and its N-terminus contains the polypeptide transport-associated domain while the Sam35 and Sam37 subunits both face the cytosolic side of the OMM where Sam35 is a beta-signal receptor and Sam37 stabilises the SAM complex while assisting in the release of newly formed beta-barrel proteins.

Some outer membrane preproteins containing only a single transmembrane domain are inserted into the OMM by the mitochondrial import complex (MIM) (Straub *et al.*, 2016).

1.1.9.3 Inner membrane transmembrane proteins

Preproteins destined to localise to the IMM can be processed through 3 possible pathways (Höhr *et al.*, 2015). The first is by inserting the protein into the IMM by the TIM22

complex which inserts proteins with multiple transmembrane domains. The second pathway inserts proteins with single membrane spanning domains into the IMM through the stop of protein translocation midway through the TIM23 complex followed by the insertion into the IMM. The final pathway involves the complete importing of the preprotein into the matrix where it is then inserted into the IMM via the oxidase assembly protein Oxa1.

1.1.9.4 Intermembrane space proteins

Preproteins destined to localisation in the IMS are processed in various possible pathways. One possible pathway takes place after translocation through the TOM complex where the mitochondrial IMS import and assembly (MIA) machinery (which is anchored to the IMM) reacts with the protein to form disulphide bonds via its core component Mia40 (Straub *et al.*, 2016). Some IMM embedded proteins are bipartite proteins that have a cleavage site on the domain extending into the IMS; cleaving that site leads to the release of that polypeptide into the IMS (Höhr *et al.*, 2015).

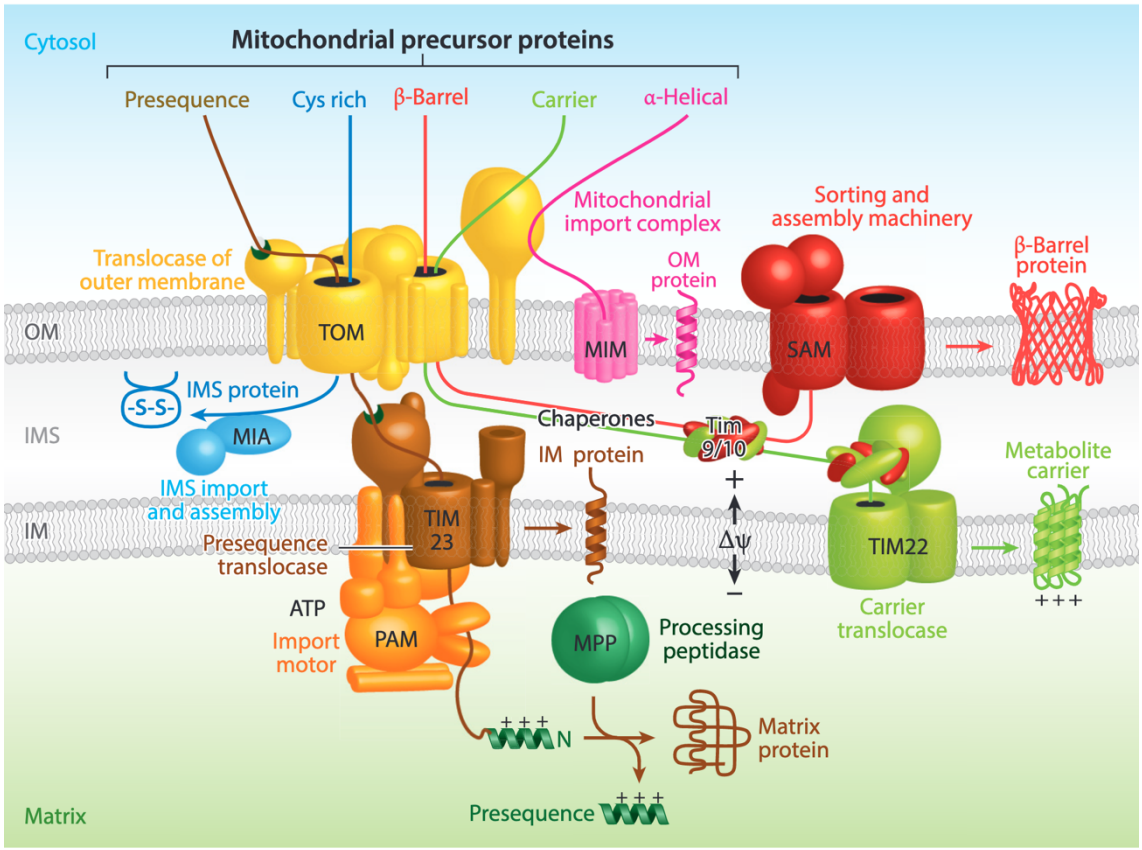

Figure 1.8 Import pathways of nuclear encoded mitochondrial proteins

The 4 main pathways of mitochondrial protein import are highlighted in this diagram:
Mitochondrial matrix proteins (brown pathway) are recognised by the mitochondrial targeting sequence (presequence) and imported through the Tom-Tim complexes into the mitochondrial matrix where MPP finally cleaves the presequence.
OMM proteins destined to be beta-barrel proteins (red pathway) are imported through the TOM complex and guided by the Tim9-Tim10 chaperone complex to the SAM complex which insert it into the OMM. Some OMM proteins are inserted into by the MIM complex (pink pathway).
Proteins destined to be IMM proteins (green pathway) are imported through the TOM complex and guided by the Tim9-Tim10 chaperone complex to the TIM22 complex which insert it into the IMM.
IMS proteins (blue pathway) are imported through the TOM complex and guided by the MIA machinery and released into the IMS.
(Wiedemann and Pfanner, 2017)

1.2 Mitochondrial functions

1.2.1 Metabolic pathways

Mitochondria house metabolic pathways that reduce Nicotinamide Adenine Dinucleotide (NAD) and Flavin Adenine Dinucleotide (FAD) that donate their electrons to the ETC. This results in the pumping of protons from the matrix across the IMM into the IMS maintaining a proton gradient that it utilised by complex V to generate the cell's energy currency, ATP (**Figure 1.9**).

Glycolysis takes place in the cytosol resulting in the generation of pyruvate which is imported into the mitochondrial matrix via membrane channels mitochondria pyruvate carriers MPC1 and MPC2 (Bricker *et al.*, 2012). The pyruvate dehydrogenase complex (PDHc) converts pyruvate to acetyl-CoA. Three subunits (E1, E2 and E3) bind to form the PDHc which is regulated by a pair of phosphatases and a group of kinases that activate and inactivate PDHc respectively (Patel *et al.*, 2014). Regulation is governed by a feedback loop that inactivates PDHc in the presence of high levels of acetyl-CoA and activates it in the presence of high levels of pyruvate.

In the mitochondrial matrix, the tricarboxylic acid cycle (TCA cycle) utilises acetyl-CoA to generate NADH and $FADH_2$ which donate their electrons to the inner membrane bound ETC complexes (Martínez-Reyes and Chandel, 2020). The matrix also houses the proteins responsible for fatty acid oxidation which breaks down fats into multiple acetyl-CoA metabolites (Houten *et al.*, 2016).

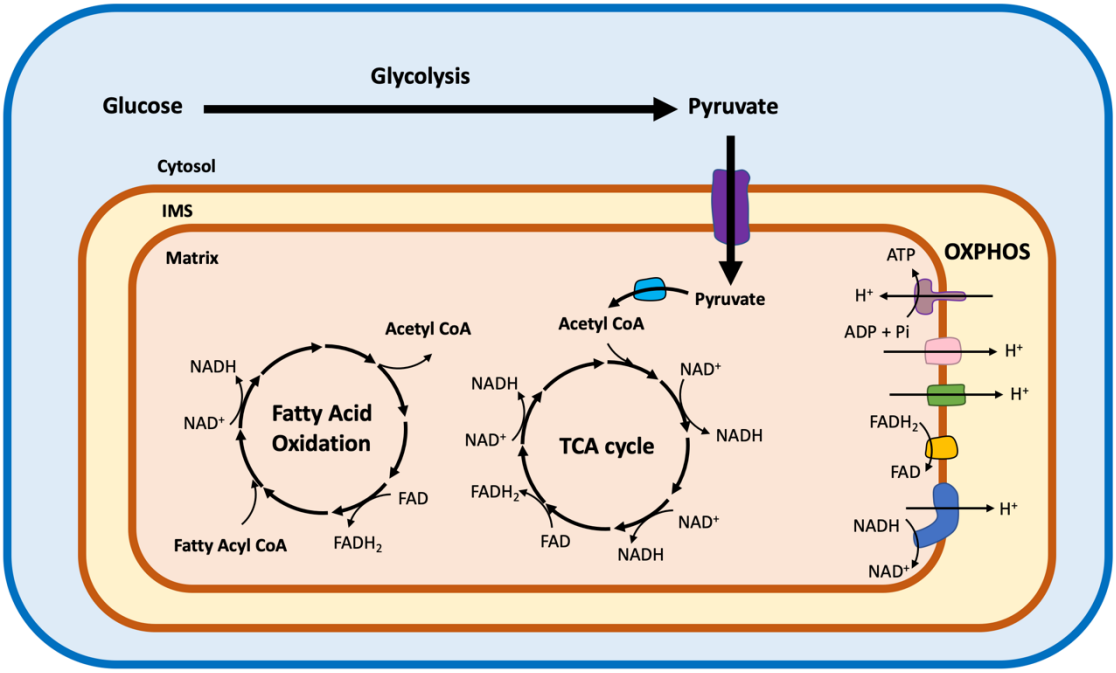

Figure 1.9 Metabolic pathways in the mitochondria

A scheme illustrating the conversion of glucose into pyruvate which is imported into the mitochondrial and converted into Acetyl CoA via pyruvate dehydrogenase (blue molecule. Fatty acids (Fatty Acyl CoA) are broken down to Acetyl CoA within the mitochondrial matrix. Acetyl CoA enters the tricarboxylic acid cycle (TCA cycle) that results in the reduction of NAD^+ to NADH and FAD into $FADH_2$; these reduction reactions also take place in the fatty acid oxidation cycle. Reduced NADH and $FADH_2$ transfer their electron to the OXPHOS complexes I and II and the maintained proton gradient across the IMM drives the production of ATP synthesis via ATP synthase (Complex V).

1.2.2 OXPHOS complexes

1.2.2.1 Complex I – NADH:ubiquinone oxidoreductase

Mammalian NADH:ubiquinone oxidoreductase (Complex I), the largest of the respiratory chain complexes, plays a crucial role in the respiratory chain by maintaining the proton gradient across the mitochondrial inner membrane; it couples the transfer of 2 electrons from NADH through its subunits to ubiquinone (CoQ10) with the translocation of four protons from the mitochondrial matrix to the mitochondrial intermembrane space (Agip *et al.*, 2018).

The complex I multimeric protein is comprised of 44 different subunits encoded by both nuclear and mitochondrial genomes (Carroll *et al.*, 2006; Balsa *et al.*, 2012). Fourteen of the subunits are core conserved subunits which the mitochondrial genome encodes seven hydrophobic of these core subunits; the remaining subunits are encoded by the nuclear genome including hydrophilic subunits housing all the redox driving groups, one flavin mononucleotide (FMN) and eight iron-sulphur clusters (Vinothkumar *et al.*, 2014; Wirth *et al.*, 2016). The 30 accessory subunits play important roles in iron-sulphur cluster cofactor binding and protein assembly and stability. 13 assembly factors required for complex I assembly are also encoded in the nuclear genome (Sánchez-Caballero *et al.*, 2016).

Electrons are transferred from reduced NADH to the FMN cofactor bound to ND1 (one of mitochondrial encoded core subunits) where it is then passed through 7 iron sulphur clusters and finally to a ubiquinone binding site where CoQ10 (Q) is reduced to ubiquinol (QH_2) (**Figure 1.10**) (Friedrich, 2014). The conformational change at the ubiquinone binding site induces an electrostatic pulse that stimulates the translocation of protons through 3 mitochondrial-encoded antiporter subunits (ND2, ND4, and ND5) in addition to a fourth pathway found between subunits ND2 and ND4L (Wirth *et al.*, 2016). The overall reaction that takes place in complex I is as follows:

$$\mathbf{NADH + Q + 5H^{+}_{matrix} \rightarrow NAD^{+} + QH_2 + 4\ H^{+}_{IMS}}$$

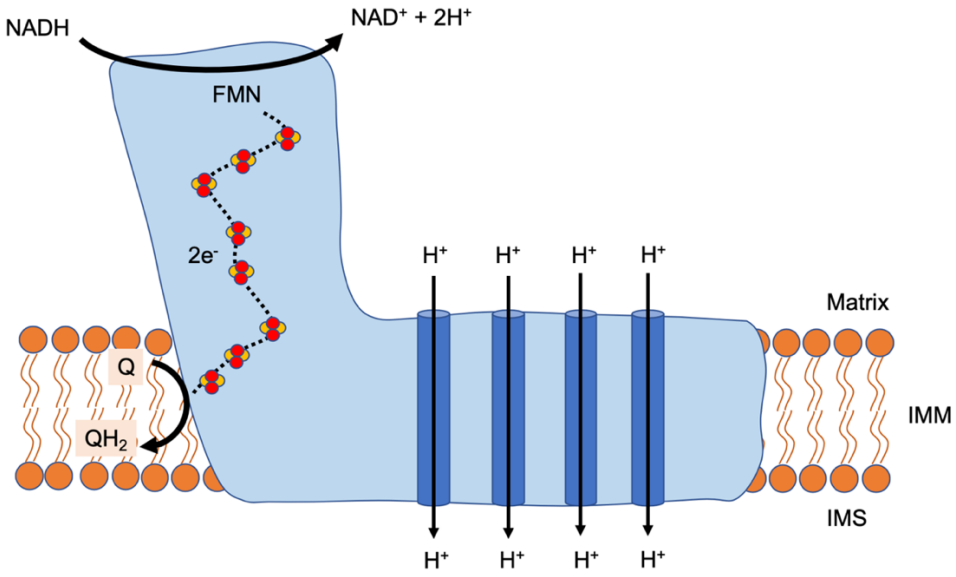

Figure 1.10 NADH:ubiquinone oxidoreductase

Structural representation of NADH:ubiquinone oxidoreductase highlighting the electron transport pathway through complex I. FMN catalyses the oxidation of NADH to NAD then the acquired electrons travel through a chain of iron-sulphur clusters (red and yellow) and finally reduce a ubiquinone molecule (Q) to ubiquinol (QH_2). The transport of electrons results in a conformational change in the membrane domain of the complex resulting in the active transport of protons from the matrix into the IMS. IMM: mitochondrial inner membrane; IMS: mitochondrial intermembrane space.

1.2.2.2 Complex II - Succinate:ubiquinone oxidoreductase

Succinate:ubiquinone oxidoreductase (Complex II) is an oligomer comprised of 4 nuclear encoded subunits (SDHA, SDHB. SDHC and SDHD) and 4 identified assembly factors (SDHAF1, SDHAF2, SDHAF3 and SDHAF4) are required for its assembly (**Figure 1.11**) (Rutter *et al.*, 2010; Bezawork-Geleta *et al.*, 2017). Complex II is the only ETC complex that plays an additional metabolic role in mitochondria; it catalyses the oxidation of succinate to fumarate in the Kreb's cycle pathway reducing a covalently attached FAD to its reduced form which is then oxidised and its pair of electrons are passed through a chain of iron-sulphur clusters within it ending up in one of two ubiquinone binding sites (Cecchini, 2003). The overall reaction that takes place in complex II is as follows:

$$\textbf{Succinate} + \textbf{Q} \rightarrow \textbf{Fumarate} + \textbf{QH}_2$$

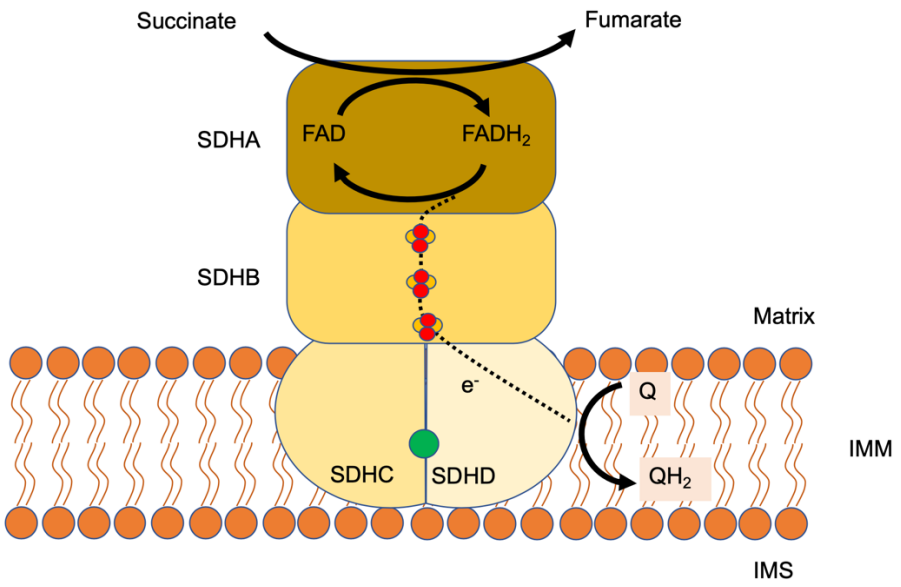

Figure 1.11 Succinate:ubiquinone oxidoreductase

Structural representation of Succinate:ubiquinone oxidoreductase highlighting the passage of electrons through complex II. Electrons from succinate reduce FAD to FADH2 and then pass through a series of iron-sulphur clusters and finally reduce ubiquinone (Q) to ubiquinol (QH_2). A heme molecule (green) is found as part of the SDHC and SDHD structure but no clear molecular pathway has been deduced thus far.

1.2.2.3 Coenzyme Q10

In humans, CoQ10 is a benzoquinone ring with a polyisoprenoid side chain containing 10 isoprene units (CoQ10) that resides within the inner mitochondrial membrane (Alcazar-Fabra *et al.*, 2016). Synthesis of CoQ10 takes place in the inner mitochondrial membrane through the mevalonate pathway and the benzoquinone ring is later modified by a series of reactions (Bentinger *et al.*, 2010). CoQ10 is an electron carrier that receives electrons from a number of sources most notably complex I and complex II of the mitochondrial respiratory chain and transfers them to complex III. The full reduction of CoQ10 requires 2 electrons, but upon stepwise reduction with a single electron, an intermediate semiquinone is formed that contains a free radical (Crofts *et al.*, 2017).

1.2.2.4 Complex III – Ubiquinol:cytochrome c reductase

Ubiquinol:cytochrome *c* oxidoreductase (Complex III) is a transmembrane protein embedded in the mitochondrial inner membrane. It is a multiheteromeric protein composed of 11 subunits which all but one subunit are encoded in the nuclear genome;

the assembled complex forms a dimer which is the final functioning protein complex (Fernández-Vizarra and Zeviani, 2015). Redox cofactors are bound to 3 of these subunits; the function of the remaining 8 subunits is still being investigated. Six nuclear encoded assembly factors are required for the construction of complex III.

In the Q cycle, complex III receives electrons from reduced CoQ10 (QH_2) which it initially gained from complex I or complex II. Complex III transfers 2 electrons through its redox cofactors to cytochrome *c* (Cyt-c), which is also found in the IMS (**Figure 1.12**) (Trumpower and Gennis, 1994; Berry *et al.*, 2000). This process is coupled with the pumping of protons from the matrix to the IMS to maintain the proton gradient utilised by complex V to produce ATP. The overall reaction that takes place in complex III is as follows:

$$\mathbf{2QH_2 + Q + 2\ Cyt\ c_{oxidised} + 2H^+_{matrix} \rightarrow 2Q + QH_2 + 2\ Cyt\ c_{reduced} + 4H^+_{IMS}}$$

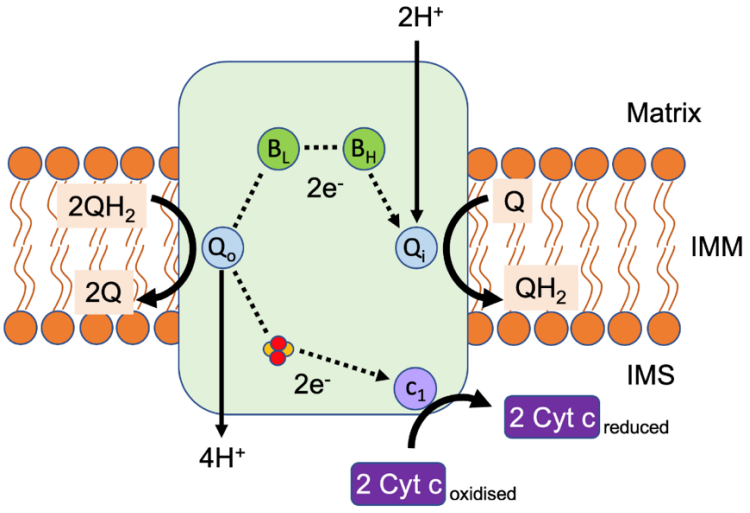

Figure 1.12 Ubiquinol:cytochrome c reductase

Structural representation of ubiquinol:cytochrome *c* reductase highlighting the passage of electrons through complex III. At the quinone-binding site Q_o site, 2 ubiquinol are oxidised to ubiquinone and the electrons then pass through 2 pathways that are part of the Q-cycle. The first pathway shows the passage of electrons through an iron-sulphur cluster to cytochrome c_1 (c_1) which in turn reduces cytochrome *c* (Cyt c). The other pathway shows the passage of electrons through 2 heme molecules, heme B_L (B_L) and Heme B_H (B_H), to the other quinone-binding site Q_i site where ubiquinol is regenerated by reducing ubiquinone. The overall rection results in the translocation of protons from the matrix to the IMS.

1.2.2.5 Cytochrome c

Cytochrome *c* (Cyt-c) is mitochondrial protein containing the iron cofactor heme c that localises in the IMS (Ow *et al.*, 2008). It plays an important role in electron transport since its major role is the transfer of electron from complex III to complex IV of the mitochondrial respiratory chain (Chertkova *et al.*, 2017). However, it also plays an important role in apoptosis via its release into the cytoplasm due to a death signalling cascade that results in the activation of caspases and the formation of apoptosomes (Goldstein *et al.*, 2000).

1.2.2.6 Complex IV – Cytochrome c oxidase

Cytochrome *c* oxidase (Complex IV) is the terminal transmembrane protein in the ETC where electrons are transferred to the terminal electron acceptor, oxygen, to form water (Michel *et al.*, 1998). The protein complex is composed of 13 subunits; the 3 core catalytic subunits – MTCO1, MTCO2, and MTCO3 – are encoded by mtDNA and the remaining 10 subunits are encoded in nDNA (Kadenbach and Hüttemann, 2015). Complex IV assembly requires over 20 nuclear encoded accessory factors and additional ancillary proteins play an important role in the incorporation of cofactors including 3 copper ions, 2 heme moieties, and magnesium, sodium and zinc ions (Carr and Winge, 2003). Complex IV is an oligomeric protein that can also form a dimer with itself forming a larger complex (Carr and Winge, 2003).

Complex IV couples the transfer of electrons from Cyt-c to molecular oxygen with the translocation of protons from the matrix into the IMS with a ratio of 1 proton translocated for every electron transferred to the terminal electron acceptor oxygen (**Figure 1.13**). The overall reaction that takes place in complex IV is as follows:

$$\mathbf{4\ Cyt\ }c_{\mathbf{reduced}}\mathbf{ + 8H^{+}_{matrix} + O_2 \rightarrow 4\ Cyt\ }c_{\mathbf{oxidised}}\mathbf{ + 2H_2O + 4H^{+}_{IMS}}$$

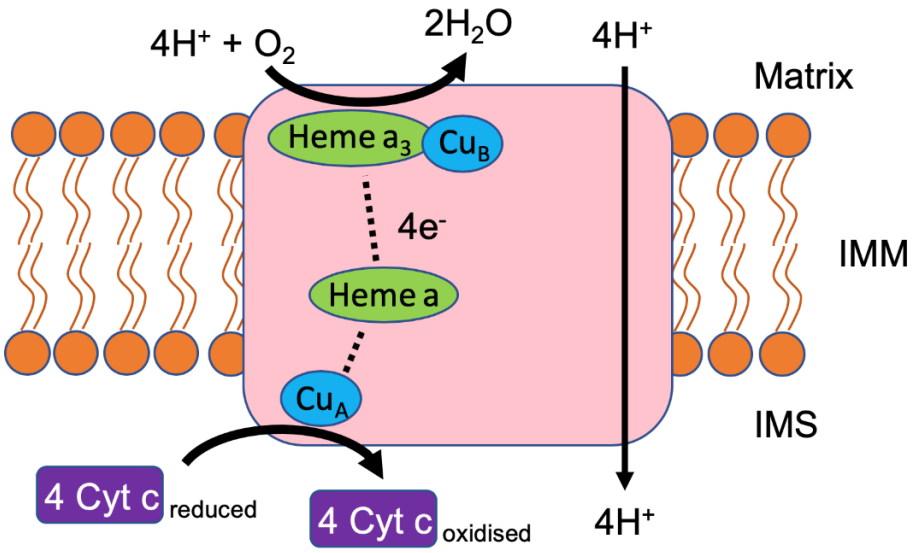

Figure 1.13 Cytochrome c oxidase

Structural representation of cytochrome *c* oxidase highlighting the passage of electrons through complex IV. Copper centre Cu_A catalyses the oxidation of cytochrome *c*, then the electrons pass through Heme a to a Heme a_3/Cu_B centre that catalyses the reduction of oxygen (O_2) into water (H_2O).

1.2.2.7 Complex V – ATP synthase

ATP synthase (complex V) is a transmembrane protein that localised in the IMM that utilises the proton motive force, generated and maintained by the ETC, to bind inorganic phosphate (Pi) to adenosine diphosphate (ADP) and forming ATP. The protein consists of 2 sectors; the F_O sector that is embedded within the IMM and the F_1 sector that protrudes out of the IMM into the matrix (**Figure 1.14**). The F_O sector is comprised of a c-ring subunit that is formed by 8 copies of the c subunit, a stalk formed by a single copy of subunits a, b, d, F6 and an oligomycin sensitive-conferring protein (OSCP) bound to the end of the stalk (Jonckheere *et al.*, 2012). Subunits e, f, g and A6L are membrane proteins associated with the F_0 sector. The F_1 sector is formed of 3 copies of α and β subunits wrapped around a central stalk comprised of the subunits γ, δ and ε. Subunits a and A6L are encoded in the mitochondrial genes *ATP6* and *ATP8* respectively while the rest of the subunits are nuclear encoded. The assembly of the F_1 sector requires the ATP synthase assembly factors 1 and 2 (ATPAF1 and ATPAF2), and the assembly of the complex as a whole requires the presence of transmembrane protein 70 (TMEM70)

(Cizkova *et al.*, 2008). Complex V utilises the proton motive force to drive the rotation of the γ subunit resulting in conformational changes in the α and β subunits that have ADP and Pi bound to them. The conformational changes result in the formation and release of 3 ATPs per full rotation.

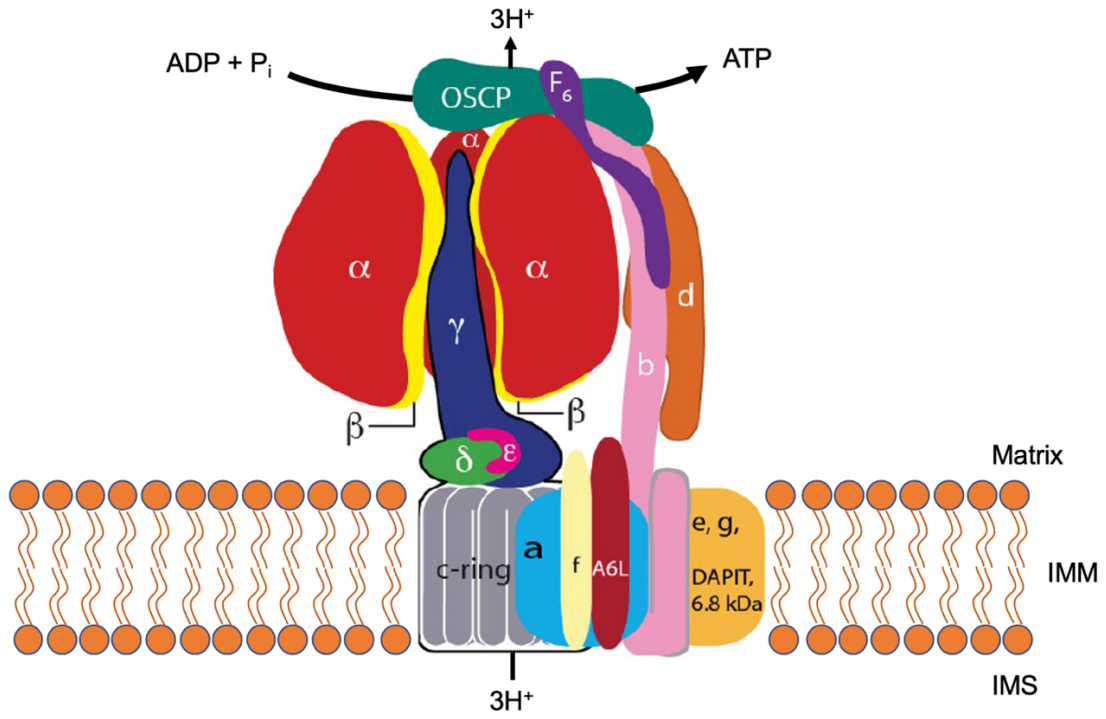

Figure 1.14 Structure of ATP synthase

Structural composition of ATP synthase and a summarized depiction of the reaction that utilized the proton gradient in the synthesis of ATP (Adapted from Neupane et al., 2019).

1.2.2.8 Supercomplexes/Respirasomes

Complexes I, III and IV can bind together within the IMM to form supercomplexes or respirasomes that consist of a single complex I heteromer, a complex III dimer and a complex IV heteromer (**Figure 1.15**) (Cogliati *et al.*, 2016). Supernumerary and accessory subunits of these complexes participate in the formation of bonds between the complexes (Wu *et al.*, 2016a). In addition, the replacement of certain subunits of these respiratory chain complexes participate in the binding between complexes such as the substitution of complex IV subunit COX7A2 with the supercomplex assembly factor 1 (SCAF1) resulting in the formation of the III2+IV supercomplex (Wu *et al.*, 2016a). SCAF1 is also known as COX7A2L due to the similarities between it and the complex IV subunit.

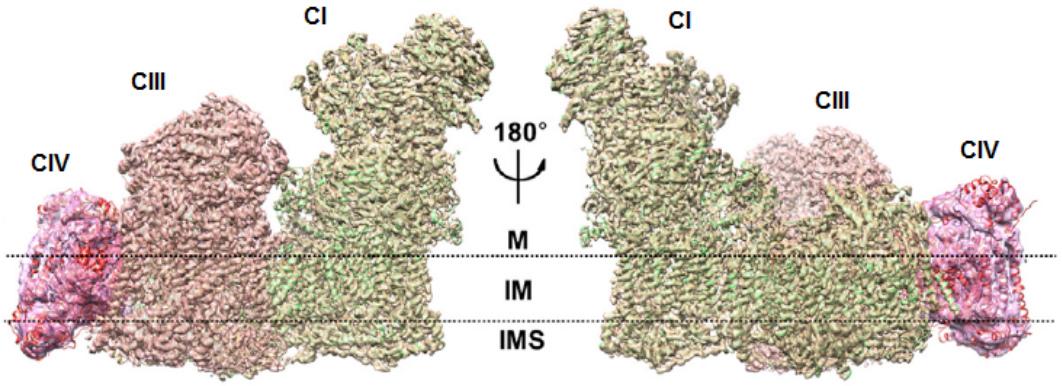

Figure 1.15 OXPHOS Supercomplexes

Configuration of OXPHOS complexes CI, CIII and CIV within the structure of a respirasome. (Adapted from (Wu *et al.*, 2016a))

1.2.2.9 Reactive Oxygen Species production

Reactive oxygen species (ROS) are a group of oxygen-based molecules carrying electron radicals as a product of the redox reactions that take place in the mitochondrial respiratory chain (Ray *et al.*, 2012). These molecules cause oxidative damage to DNA and cellular structures such as proteins by reacting with sulphur containing residues such as cysteine and altering the structure of the protein. The cell expresses ROS neutralising proteins such as superoxide dismutase (SOD) and a mitochondrial specific superoxide dismutase

(MnSOD) to reduce the rate of such damaging reactions (Murphy, 2009). ROS also play a role in cellular signalling mediating apoptosis, autophagy, inflammatory responses and mitochondrial dynamics (Bolisetty and Jaimes, 2013).

1.2.3 Other mitochondrial functions

1.2.3.1 Apoptosis

Apoptosis is the process of programmed cell death that is initiated by two main pathways, an intrinsic and an extrinsic pathway, in addition to a third known pathway (Ashe and Berry, 2003; Elmore, 2007). The extrinsic pathway involves the tumour necrosis factor receptor (TNFR) superfamily of proteins, which are plasma membrane proteins, initiating a reaction cascade leading to apoptosis. The intrinsic pathway involves the mitochondrial bound B-cell lymphoma-2 (BCL-2) family of proteins that regulate apoptosis via inhibition and induction pathways. Apoptosis is triggered by signals such as oxidative stress, Ca^{2+} concentration overload, ER stress and DNA damage resulting in the release of apoptosis promoting factors from the IMS to the cytosol (Martinou, 1999; Vakifahmetoglu-Norberg *et al.*, 2017). Death-promoting factors include Cyt-c, AIF (Apoptosis-Inducing Factor) EndoG (Endonuclease G), SMAC/DIABLO (Second Mitochondria-derived Activator of Caspases/ Direct IAP [inhibitor of apoptosis]) Binding mitochondrial protein) and HTRA2 (HtrA Serine Peptidase 2). Their release into the cytosol triggers a cascade reaction leading to the activation of caspases (a family of proteases) while AIF and EndoG translocate via independent pathways to the nucleus and induce DNA fragmentation and chromatin condensation hence leading to apoptosis (Elmore, 2007; Kilbride and Prehn, 2013; Vakifahmetoglu-Norberg *et al.*, 2017).

1.2.3.2 Mitochondrial Autophagy (Mitophagy)

Mitochondrial autophagy (mitophagy) degrades damaged mitochondria to maintain a functioning mitochondrial network and reduce the effects of oxidative stress caused by ROS and reduce the rate of apoptosis which is also triggered by mitochondrial dysfunction due to stress and damage (Grosso *et al.*, 2017). PTEN -inducible putative kinase 1 (Pink1) is continuously imported into the matrix and digested by mitochondrial proteases; but upon membrane depolarisation Pink1 is not imported and degraded resulting in its accumulation at the OMM (Saito and Sadoshima, 2015). Pink1 recruits and phosphorylates MFN2 which in turn binds a (Parkin) resulting in a cascade reaction

triggering the mitophagy process leading to the degradation of the depolarised mitochondria.

1.2.3.3 Calcium Homeostasis

Calcium handling is crucial for the regulation of cellular metabolism, signalling cell proliferation and initiating apoptotic cascades (Contreras *et al.*, 2010). The fluctuation in calcium concentration is influenced by the activity of calcium channelling transmembrane proteins found in the plasma membrane and membranes of cell organelles including mitochondria. Low calcium concentrations in the mitochondria lead to a reduction of ATP synthesis while a surge in calcium concentration in the matrix opens the mitochondrial permeability transition pore resulting in the release of apoptosis inducing factors and therefore cell death (Contreras *et al.*, 2010; Shao *et al.*, 2016). Calcium uptake, which is driven by the membrane potential, is mediated by mitochondrial calcium uniporter (mCU) and its homologs along with Ca^{2+}/H^{+} antiporters and numerous other calcium channels (Duchen, 2000).

1.2.3.4 Iron-Sulphur and Heme Cluster Biogenesis

Iron-sulphur clusters (ISC) are protein cofactors that play important roles in the mitochondrial, cytosolic and nuclear protein activity such as electron transport, reaction catalysis, sulphur activation, iron homeostasis, and nuclear protein activity including DNA synthesis, repair and telomere maintenance (Stehling and Lill, 2013; Stehling *et al.*, 2014).

ISC biosynthesis takes place in the mitochondrial matrix and involves approximately 30 proteins found both in the mitochondria and the cytosol (Stehling and Lill, 2013). The ISC assembly machinery involves 17 proteins (Stehling *et al.*, 2014). Ferrous iron is initially imported into the mitochondria via a proton motive force driven mechanism involving the mitochondrial solute carriers mitoferrin 1 and 2 (MFRN1 and MFRN2) (Stehling *et al.*, 2014). Cysteine desulphurase (Nfs1-Isd11) catalyses the transformation of cysteine to alanine and retains the sulphate. Frataxin (Yfh) acts as a in iron donor, since free iron is not found in the cell, donating it iron to the cysteine desulphurase complex (Lill, 2009). An electron is donated to the process by a reaction involving ferridoxin reductase (Arh1) and ferridoxin (Yah1) leading to the formation of a [2Fe-2S] cluster on the scaffold protein Isu1. The newly formed iron-sulphur cluster is released from the scaffold and is chaperoned by a number of proteins including the gluteradoxin GLRX5

to either its apoprotein destination or exported into the cytosol via the Atm1 (an ABC transported) to be incorporated into cytosolic proteins through the Cytosolic Iron-sulphur protein Assembly (CIA) machinery (Stehling and Lill, 2013). In the mitochondria, Fe-S clusters are inserted into their target proteins by the assembly proteins Isa1, Isa2 and Iba57 converting the target protein from an apoprotein to a holoprotein (Lill, 2009). These 3 proteins (ISCA1, ISCA2 and IBA57) play a critical role in the maturation of [4Fe-4S] clusters (Sheftel *et al.*, 2012).

Heme is another iron containing protein cofactor that catalyses redox reaction and acts as an electron carrier in iron incorporating proteins such as haemoglobin, myoglobin and cytochromes (Ajioka *et al.*, 2006). Heme consists of an iron molecule surrounded by 4 pyrroles (tetrapyrrole); Ferrachelatase catalyses the insertion of a ferrous iron molecule into the tetrapyrrole containing molecule protoporphyrin IX resulting in the formation of the heme cofactor. The pathway of heme biosynthesis involves proteins localised in both the mitochondrial compartments and cytosol where the synthesis process initiates in the mitochondria, progresses in the cytosol and finally returns to the mitochondria where the formation of heme is completed (Hamza and Dailey, 2012).

1.3 Mitochondrial disorders

As discussed throughout this introduction, mitochondria play a role in many important cellular functions and there are hundreds of nuclear genes involved in these functions, including the expression of the mtDNA encoded subunits, the import of mitochondrial bound proteins, apoptosis, and iron-sulphur and heme cluster biosynthesis. As a consequence, the term mitochondrial disorder is an umbrella term for many different pathologies of mitochondrial dysfunction with high morbidity and mortality that present with a wide array of symptoms affecting multiple systems (Stenton and Prokisch, 2020; Thompson *et al.*, 2020a).

1.3.1 Clinical features of mitochondrial disease

Clinical syndromes that were later categorised as mitochondrial disorders have been described since the 1800s. Theodore Leber described patients with visual loss as a consequence of optic nerve involvement (Leber, 1871; Yu-Wai-Man *et al.*, 2002); Denis Leigh described patients with "subacute necrotizing encephalopathy" who presented with neurodegenerative and ophthalmological symptoms with the possible involvement of the heart, liver, kidneys or gastrointestinal tract (Leigh, 1951); and Kearns and Sayre detailed

patients with chronic progressive external ophthalmoplegia (CPEO), retinitis pigmentosa (RP), and cardiomyopathy frequently accompanied by small stature, progressive weakness of facial, pharyngeal and peripheral muscles, deafness, abnormal Electroencephalogram (EEG) and increased proteins in the cerebrospinal fluid (CSF) (Kearns and Sayre, 1958; Kearns, 1965). These phenotypes were named Leber Hereditary Optic Neuropathy (LHON), Leigh syndrome (LS) and Kearns-Sayre syndrome (KSS) respectively. Myoclonic epilepsy with ragged red fibres (MERRF) and mitochondrial encephalopathy, lactic acidosis and stroke-like episodes (MELAS) are two other clinical syndromes that were described as mitochondrial disorders (Fukuhara *et al.*, 1980; Pavlakis *et al.*, 1984). Many other syndromes with various symptoms were later added to the collective list of mitochondrial disorders.

The prevalence of mitochondrial disorders is estimated to be at least 6.2/100,000 for paediatric cases and adult mitochondrial cases are more than 1/4,300 (Chinnery *et al.*, 2000; Skladal *et al.*, 2003; Schaefer *et al.*, 2004; Gorman *et al.*, 2015).

Mitochondrial disorders are heterogeneous in their clinical presentations meaning a single deleterious mutation can lead to varying symptoms even among siblings harbouring the same variant. Disease might present with a single organ affected or it might be multi-systemic in its presentation. Mitochondrial disorders can result in symptoms affecting the ophthalmologic system resulting in CPEO, RP, nystagmus, ptosis, or visual acuity; or it can affect the auditory system leading to hearing impairment or loss (Gorman *et al.*, 2016). Most notably, neurological and brain symptoms can develop in patients resulting in a variety of symptoms including delay in psychomotor development, stroke-like episodes, seizures, myoclonus, ataxia, and encephalopathy with MRI and CT scan findings that include lesions and hyperintense signals in the brain along with abnormal EEG. Muscle fatigue and weakness are also prominent phenotypes of mitochondrial disorders that could present as hypotonia, ataxia or dysphagia among other presentations (Munnich *et al.*, 1996). Cardiac symptoms have been observed in mitochondrial disorder patients with left ventricular hypertrophy as a key finding in an echocardiogram (Meyers *et al.*, 2013).

1.3.2 Biochemical investigations and findings in mitochondrial disease

1.3.2.1 Biomarkers of mitochondrial disease

Certain metabolites involved in mitochondrial pathways are biomarkers that can be measured to help determine if mitochondrial disease is suspected in a patient (Boenzi and Diodato, 2018). Due to the absence of a reliable single biomarker to suggest mitochondrial disease, various biomarker findings are considered by physicians during this process . For example, elevated lactate levels in the blood and CSF are indicators of metabolic stress suggesting mitochondrial dysfunction (Robinson, 2006). Brain magnetic resonance spectrometry (MRS) might find elevated levels of lactate and lactate/creatine ratios in the brain also(Lunsing *et al.*, 2017). Accompanying some hypotonic symptoms might be elevated levels of creatine kinase (CK). Other biomarkers measured in association with mitochondrial disease include serum pyruvate levels, serum and urinary amino acids, urinary organic acids, and acylcarnitines (Shaham *et al.*, 2010; Boenzi and Diodato, 2018).

Fibroblast growth factor 21 (FGF-21) is a hormone that regulates metabolism and increased serum levels have been observed in obese individuals (Dushay *et al.*, 2010), in individuals who ingest fructose (Dushay *et al.*, 2015), in patients with non-fatty acid liver disease (NAFLD) (Li *et al.*, 2010), and in mitochondrial patients with muscle involvement (Davis *et al.*, 2013; Fisher and Maratos-Flier, 2016). Growth differentiation factor 15 (GDF-15) is a member of the transforming-growth factor β (TGF-β) superfamily and elevated serum levels have been reported in patients with cardiac disease (Hagström *et al.*, 2017), renal disease (Nair *et al.*, 2017), and prostate cancer (Li et al., 2015). In addition, GDF-15 has shown high specificity and sensitivity in patients with mitochondrial disease (Yatsuga *et al.*, 2015). Together, FGF-21 and GDF-15 have been shown to help differentiate patients with mitochondrial myopathy from other myopathies (Lehtonen *et al.*, 2016). FGF-21 and GDF-15 have both been shown to be potential biomarkers of mitochondrial disease but caution is necessary regarding other influencing factors (Scholle *et al.*, 2018).

1.3.2.2 BN-PAGE and SDS-PAGE

Sodium dodecyl sulphate polyacrylamide gel electrophoresis (SDS-PAGE) and blue native polyacrylamide gel electrophoresis (BN-PAGE) are two methods of detecting protein levels in tissue (Schägger, 2006; Wittig *et al.*, 2006).

Proteins extracted from biopsy and established cell lines are run on a polyacrylamide gel and then labelled by specific antibodies; comparison between control and patient protein levels can help determine any reduction or overexpression of proteins in the tissue. BN-PAGE keeps and detects protein complexes in their tertiary form while SDS-PAGE detects individual complex subunits. These results only give an indication of any overall differences in protein expression at the tissue level.

1.3.2.3 Biochemical OXPHOS and respiratory oxygen consumption assays

Mitochondrial function can be analysed in muscle biopsy samples using biochemical assays that assess the function of individual OXPHOS complexes (Frazier *et al.*, 2020). This assay can be performed on homogenised muscle samples or isolated mitochondria from cultured patient fibroblast cell lines and therefore only presents an overall picture of OXPHOS defects at the tissue level rather than at the cellular level. An alternative method to assess for mitochondrial OXPHOS complex deficiencies is measuring the rate of oxygen consumption using high-resolution respirometry in patient cell lines or permeabilised tissue samples (Pesta and Gnaiger, 2011; Germain *et al.*, 2019). In addition, OXPHOS deficiencies can also be determined in patient tissue homogenates and isolated mitochondria by microscale oxygraphy using the Seahorse Extracellular Flux Analyser (Invernizzi *et al.*, 2012).

1.3.3 Histological/histochemical and immunohistochemical investigation techniques and findings in mitochondrial disease

Levels of heteroplasmy vary amongst cells due to asymmetric distribution of mitochondria during mitosis. This could result in different levels of OXPHOS protein function amongst a group of cells. This mosaic pattern of OXPHOS defect could indicate a difference in heteroplasmy levels, as opposed to a more uniform pattern due to nDNA mutations associated with complex IV assembly (Pronicki *et al.*, 2008; Roos *et al.*, 2019). The following assays describe methods of analysing patient tissue and cell lines to detect any overall protein expression differences or functional defects in OXPHOS complexes I-IV at the tissue level in addition to identifying specific cells with RRF, functional defects in complexes II and IV, or protein expression variation in complexes I and IV (**Figure 1.16**) (Alston *et al.*, 2017).

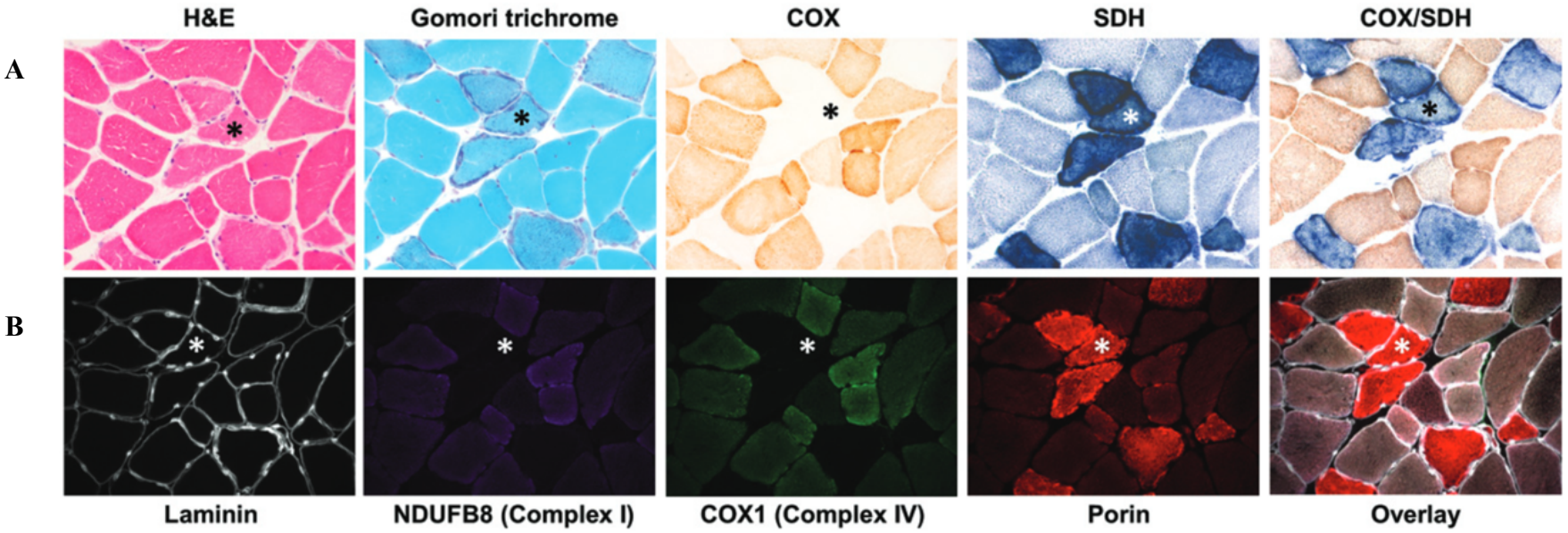

Figure 1.16 Histological, histochemical, and immunohistochemical methods of analysing muscle tissue from a patient with a single large scale mtDNA deletion.

A Histological analysis with H&E staining was used to assess muscle morphology and modified Gomori trichrome staining was used to look for RRFs as seen around highlighted muscle fibre (*). Histochemical reactions in separate COX and SDH and sequential COX/SDH staining identify muscle fibres that are deficient in complex IV activity as seen in the highlighted muscle fibre (*).
B The quadruple immunofluorescence assay uses antibodies to quantify the levels of complex I (NDUFB8), complex IV (COX1), cell size (laminin) and mitochondrial mass (porin). The highlighted muscle fibre (*) has a clear complex I and IV deficiency and has an accumulation of mitochondria is observed (Alston *et al.*, 2017).

1.3.3.1 H&E histological stain and modified trichrome Gomori histological stains

Haematoxylin and eosin (H&E) stain the nucleic acids and proteins respectively enabling the differentiation between the nucleus and the cytosol (Fischer *et al.*, 2008). Modified Gomori trichrome stains muscle fibres blue and mitochondria red. Intense red staining outlining blue stained fibres, termed ragged-red fibres (RRF), indicates the accumulation of mitochondria as a result OXPHOS complex deficiency (Olson *et al.*, 1972; Egger *et al.*, 1981; Moraes *et al.*, 1992). RRFs may be present in a mosaic pattern among muscle cells due to varying levels of heteroplasmy in the cells leading to mosaic OXPHOS deficiency. Subsequent assays can help indicate which of the OXPHOS complexes is affected.

1.3.3.2 Cytochrome c oxidase and succinate:ubiquinone oxidoreductase histochemical assay

Cytochrome *c* oxidase and succinate:ubiquinone oxidoreductase (COX/SDH) histochemical staining is applied to biopsy sections and provides a visual presentation of respiratory activity in complex IV (COX) and the fully nuclear encoded complex II (SDH) (Old and Johnson, 1989; Sciacco and Bonilla, 1996). The sequential application of these stains assists in pointing out any complex deficient cells, indicating the presence of a mitochondrial defect within these cells, and suggesting which genome the causative variant could be located in. Complex II deficiency indicates the presence of a variant in the nuclear genome since all its subunits and assembly factors are exclusively nuclear encoded.

In comparison to the biochemical assay, this method can detect mosaic OXPHOS deficiencies at the cellular level while the biochemical assay only provides an overview of OXPHOS protein deficiency within the tissue.

1.3.3.3 Quadruple Immunofluorescence

A recently developed technique applies immunofluorescent labelling to detect complex I and IV expression levels in biopsy samples at the cellular level. This method utilises antibodies that target complex I and complex IV subunits, and porin (VDAC) to detect the abundance of complexes I and IV and determine the mitochondrial mass (Grünewald *et al.*, 2014). An antibody targeting the basement membrane protein laminin is used to outline muscle cells in muscle biopsy samples while a tyrosine hydroxylase targeting

label is used to highlight neuron cells in brain biopsy samples (Grünewald *et al.*, 2014; Rocha *et al.*, 2015). This helps determine cell borders to ensure accurate detection of any mosaic complex deficiencies.

1.3.4 Causes of mitochondrial disease

1.3.4.1 mtDNA associated mitochondrial disorders

Mutations in mtDNA have been studied intensively and certain groups of symptoms have been linked to mutations within certain genes (Lloyd and McGeehan, 2013). MELAS is commonly associated with a mutation in the gene encoding mitochondrial tRNA leucine (*MT-TL1*) at the nucleotide position 3243, m.3243A>G in mt-tRNA$^{Leu(UUR)}$ (Goto *et al.*, 1990). However, clinical heterogeneity has been observed in patients harbouring m.3243A>G as it has been associated with an array of clinical presentations such as hearing impairment, diabetes and gastro-intestinal disturbance, and research suggests that nuclear factors could be influencing clinical presentation in patients (Nesbitt *et al.*, 2013; Pickett *et al.*, 2018). The heteroplasmy level of the m.3243A>G is a factor that affects the disease burden in patients; heteroplasmy levels of m.3243A>G measured vary depending on the different patient samples with heteroplasmy levels gradually decreasing with age in blood samples compared to muscle and urine samples (Grady *et al.*, 2018). Moreover, 80% of MELAS cases have been associated with m.3243A>G while the remaining 20% have been associated with other mtDNA mutations (Schon *et al.*, 2012; Gorman *et al.*, 2016).

MERRF is largely associated with a mutation in the gene encoding mitochondrial tRNA lysine (*MT-TK*) at the nucleotide position 8344, m.8344A>G in mt-tRNA^{Lys} (Yoneda *et al.*, 1990). However, more than 10 other mtDNA point mutations and mtDNA rearrangements and deletions have also been associated with MERRF (Lorenzoni *et al.*, 2014). Other mitochondrial syndromes such as LHON, Pearson syndrome and KSS have been associated with various mtDNA mutations such as point mutations, large scale deletions, and rearrangements. These mtDNA mutations are either maternally inherited as described in ***Section 1.1.5*** or can be sporadic de novo mutations.

1.3.4.2 nDNA associated mitochondrial disorders

So far, 1,145 genes related to mitochondrial function are nDNA encoded which raises a challenge in locating causal mutations if mutations in the 37 mtDNA genes are excluded. Mutations in over 300 nuclear genes have been associated with mitochondrial disorders

so far (Stenton and Prokisch, 2020; Thompson *et al.*, 2020a). NGS has facilitated the identification and verification of variants in many genes related to mitochondrial function (Frazier *et al.*, 2019; Stenton and Prokisch, 2020; Thompson *et al.*, 2020a). I will discuss the application in further detail in **Chapter 4**.

Patient cell lines are crucial in confirming the pathogenicity of a novel variant by performing rescue experiments by assessing the effect on protein function and expression (Haack *et al.*, 2012; Alston *et al.*, 2016a; Danhauser *et al.*, 2016). Many studies also perform complementation experiments and yeast models of the genotyped mutations to help determine whether a variant is pathogenic (Bricker *et al.*, 2012; Haack *et al.*, 2012; Haack *et al.*, 2013; Lieber *et al.*, 2013; Bianciardi *et al.*, 2016; Thompson *et al.*, 2016; Sommerville *et al.*, 2017). Novel variants are frequently associated with certain phenotypes but studies with larger cohorts that are genotyped with the same variant or variants in the same gene present a more accurate frequency of phenotypes among cases (Sommerville *et al.*, 2017; Repp *et al.*, 2018; Saoura *et al.*, 2019). More detailed description of these approaches is outlined later in **Chapter 5**. Alternatively, a cumulative retrospective comparison of reported cases with new cases also helps expand the clinical phenotypes associated with the reported gene variants (Kropach *et al.*, 2017; Habibzadeh *et al.*, 2019).

1.3.4.3 Complex multigenic mitochondrial disease

Clinical heterogeneity of mitochondrial disease phenotypes in patients with the m.3243A>G mutation is a puzzling challenge to investigate. Evidence of nuclear modifiers have been suggested to play a role in the observed variety of phenotypes in these patients and can be associated with certain phenotypes (Pickett *et al.*, 2018; Boggan *et al.*, 2019).

1.3.4.4 Genotype-phenotype correlation.

Mitochondrial disorders often show a weak genotype-phenotype correlation, but some mutations and symptoms show a high genotype-phenotype correlation. An example of these are *AGK*, *GTPBP3*, *MTO1* and *ELAC2* gene mutations are highly associated with cardiomyopathy (Mayr *et al.*, 2012; Lightowlers *et al.*, 2015; Saoura *et al.*, 2019). On the other hand, a low genotype-phenotype correlation is observed in LS patients due to the various mutations identified in more than 85 genes present in both mtDNA and nDNA encoding the numerous OXPHOS complex subunits and different mitochondrial

functions (Lake *et al.*, 2019). Further complicating and weakening the genotype-phenotype correlation in LS patients are alternative phenotypes reported in patients that are genotyped with mutations in genes associated with LS (Rahman *et al.*, 2017). This poses as a challenge that need to be overcome while genetically investigating mitochondrial disease patients.

1.3.5 Genetic studies of mitochondrial disease

Mitochondrial disorders were first associated with mtDNA mutations due to evident maternal inheritance of the disorder. However, the absence of mtDNA mutations in addition to evidence of autosomal or X-linked inheritance of the disorder in patients led to the investigation of nDNA mutations (Stenton and Prokisch, 2020).

Targeted gene sequencing was the method used to diagnose mitochondrial disorders and OXPHOS activity results from patient muscle biopsies helped narrow down which mitochondrial protein complex or enzyme to sequence based on findings; this resulted in the discovery of many mitochondrial disease genes (Frazier *et al.*, 2019). This targeted method requires biopsy samples, which are painful for patients especially from paediatric cases. Upon the introduction of next-generation sequencing (NGS) techniques, the field shifted from using targeted sequencing methods to gene agnostic approaches such as whole exome sequencing (WES) where the protein coding regions of all genes are sequenced, or whole genome sequencing (WGS) which includes sequencing of non-coding regions. Moreover, NGS studies can be performed to look for possible causative variants before acquiring any biopsy samples. Due to price reduction for utilising this high-throughput technique, WES became more affordable and cost effective and many patients have been analysed leading to a better understanding of the genotype-phenotype relationship of mitochondrial disorders (Calvo and Mootha, 2010; Wadapurkar and Vyas, 2018). Recent cohort studies investigating mitochondrial disorders employed WES and not only resulted in the discovery of novel mutations in genes already associated with mitochondrial disorder but discovered novel genes associated with mitochondrial disorders (Haack *et al.*, 2010; Haack *et al.*, 2012; Lieber *et al.*, 2013; Yang *et al.*, 2013; Taylor *et al.*, 2014; Wortmann *et al.*, 2015). The results of these investigations will be discussed in more detail in **Chapter 4**.

1.3.5.1 Classification of called variants

Called variants identified in genetic studies are classified using criteria published by the American College of Medical Genetics and Genomics (ACMG) (Richards *et al.*, 2015). The criteria take into consideration the frequency of the identified variant in the genetic databases; *in silico* predictions of pathogenicity by available tools; availability of functional studies related to the variant; segregation of variant within the family; location of the variant in relation to previously identified variants; and the patient's phenotype relative to previously reported cases. This classification system is useful as a universal tool and it categorises variants into 5 distinct groups: "pathogenic", "likely pathogenic", "uncertain significance", "likely benign", and "benign". With the help of these criteria, called variants can be categorised using available data and updated depending on the availability of more recent supporting evidence.

However, ethical issues are raised when the method of genome sequencing identifies variants that are not related to the diagnosis of the investigated patient. Interpretation of "incidental findings" that are associated with other diseases or risk factors pose an ethical question of whether to report it to the patient or not (Holm et al., 2017). More importantly, the interpretation of such findings (especially "pathogenic" and "likely pathogenic" variants) may increase the harm of false-positive results that are reported back to patients as they may not be accurate findings based on the method of sequencing used. Therefore, extreme care and discretion need to be practiced in such scenarios.

1.4 Kuwait and the Middle East

1.4.1 Population and ancestry

The Central Bureau of Statistics in Kuwait estimated the population of Kuwait in 2018 was 4.2 million (Central Bureau of Statistics, 2018). Approximately 1.35 million of the population are Kuwaiti nationals comprising about 30% of the total population. The Kuwaiti population can be divided into 3 genetics subgroups of different ancestries (Alsmadi *et al.*, 2013). The first subgroup is of Persian ancestry with genetic analysis showing European and West Asian origins; the second subgroup is of Saudi tribe ancestry with a genetic analysis showing a high level of Arabian ancestry; and the third subgroup is of Bedouin (tent-dwellers) ancestry with a distinct genetic mixture of Arabian and African origin. Ancestral markers including those of French Basque and the Brahui and

Kalash tribes from Pakistan were found in the genotyped Kuwaiti cohort (Alsmadi *et al.*, 2013).

1.4.2 Consanguinity

Consanguinity, defined as union between second cousins or closer, and the practice of endogamy are major factors affecting clinical genetics (Tadmouri *et al.*, 2009). Consanguineous marriages are common practice in many parts of the world with preference estimated in at least 20% of the global population with more than 8.5% of children worldwide having consanguineous parents (Modell and Darr, 2002). Consanguinity rates reaching and exceeding 50% are reported in many Arab countries with rates of first cousin marriages exceeding 20% (Tadmouri *et al.*, 2009). Prevalence of inherited disorders among consanguineous populations is often higher than in non-consanguineous populations (Skladal *et al.*, 2003; Shawky *et al.*, 2013). This has been observed in Kuwait where levels of consanguinity exceeding 50% have been reported (Al-Awadi *et al.*, 1985; Radovanovic *et al.*, 1999; Tadmouri *et al.*, 2009; Al-Kandari and Crews, 2011).

1.4.3 Diagnosis of Mitochondrial disease in Kuwait

Mitochondrial disorders have been reported in Kuwait with phenotypes including Leigh syndrome in 3 affected siblings with consanguineous parents (Abdul-Rasoul *et al.*, 2002); lactic acidosis and developmental delay associated with PDH deficiency in 4 patients from 2 consanguineous families (Ramadan *et al.*, 2004); ethylmalonic encephalopathy in 2 cases, both from 2 consanguineous first cousin marriages, both presented with developmental delay, hypotonia, lactic acidosis and encephalopathy with one patient exhibiting complex IV deficiency in a muscle biopsy (Heberle *et al.*, 2006); another ethylmalonic encephalopathy case, whose parents are consanguineous double first cousins, was also reported that presented with developmental delay, myoclonic epilepsy, hypotonia, elevated lactate and encephalopathy (Ismail *et al.*, 2009); and LHON in a large family with consanguineous grandparents (Behbehani *et al.*, 2014). No genetic analyses were reported for the 3 siblings with reported Leigh syndrome, however patients from the 2 consanguineous families with reported PDHc deficiency were reported homozygous for novel nonsense mutations in the *PDHX* gene, one of the pair of ethylmalonic encephalopathy patients was homozygous for a novel single nucleotide deletion in the *ETHE1* gene causing a frameshift leading to early termination of translation, and the final

ethylmalonic encephalopathy was homozygous for exon 4 deletion in the *ETHE1* gene. Furthermore, two coinherited mtDNA mutations were identified in the large family with LHON but the presence of consanguinity did not necessarily rule out maternal inheritance as a possible mode of inheritance. With the high rate of consanguinity in Kuwait and its surrounding regions, diseases can seem like autosomal dominant with varied penetrance if thorough family history is not taken. Therefore, mtDNA inheritance cannot be ruled out.

In Kuwait, mitochondrial disease patients are primarily investigated based on available clinical data and mtDNA is sequenced for mutations using DNA extracted from blood. Due to the lack of expertise in Kuwait, no muscle biopsies are obtained from patients compared to how mitochondrial disease patients are assessed in specialised centres around the world. This requirement in diagnosing mitochondrial disease is only obtained if patients travel abroad to the United Kingdom or the United States for specialist advice and diagnosis. There are no clear indicators that muscle biopsies will be acquired in Kuwait soon.

1.4.4 Research in the Middle Eastern Arab population

Genetic disorders in the Middle Eastern Arabs were investigated using linkage analysis, candidate gene analysis, and contemporary DNA (cDNA) sequencing prior the introduction of NGS. This resulted in the identification of novel candidate gene associated with mitochondrial function (*TK2*, *PDHB*, *SLC19A3*, and *SLC25A22*) (Saada *et al.*, 2001; Brown *et al.*, 2004; Molinari *et al.*, 2005; Zeng *et al.*, 2005). In addition, novel pathogenic variants in Middle Eastern Arabs were identified in established mitochondrial disease genes (*PDHX*, *ETHE1*, *MPV17*, and *SLC25A20*) (Al Aqeel *et al.*, 2003; Ramadan *et al.*, 2004; Heberle *et al.*, 2006; Spinazzola *et al.*, 2008).

1.4.5 Impact of NGS on the discovery of novel candidate genes in the Middle East

Upon the introduction of NGS, a number of patient cohorts from the Middle East were investigated for suspected genetic disorders (Ben-Rebeh *et al.*, 2012; Dixon-Salazar *et al.*, 2012; Shamseldin *et al.*, 2012; Alazami *et al.*, 2015; Yavarna *et al.*, 2015; Alfares *et al.*, 2017; Anazi *et al.*, 2017; Monies *et al.*, 2017; Maddirevula *et al.*, 2019). These studies involved over 2,000 families (mostly consanguineous) and led to the successful diagnosis of more than half the investigated families and the discovery of more than 170 novel candidate genes associated with genetic disease (**Table 1.1**) (Alahmad *et al.*, 2019). More

recently, studies utilising NGS have identified novel candidate genes associated with mitochondrial function while investigating Middle Eastern families (*MFF*, *FBXL4*, *ELAC2*, *PET100*, *ISCA2*, *PMPCA*, *SLC39A8*, *SLC25A42*, *YME1L1*, *MIPEP*, *MICU2*, *COX5A*, *COQ5*, and *NUDT2*) (Shamseldin *et al.*, 2012; Haack *et al.*, 2013; Lim *et al.*, 2014; Al-Hassnan *et al.*, 2015; Boycott *et al.*, 2015; Jobling *et al.*, 2015; Eldomery *et al.*, 2016; Hartmann *et al.*, 2016; Shamseldin *et al.*, 2016; Baertling *et al.*, 2017a; Shamseldin *et al.*, 2017; Malicdan *et al.*, 2018; Yavuz *et al.*, 2018).

Table 1.1 Diagnosis and novel candidate gene discoveries in studies that utilised NGS to investigate patient cohorts in the Middle East

Reference	**Families**	**Diagnosed**	**Novel candidate genes**
Shamseldin et al., 2012	10 families	10 families	2 novel candidate genes
Ben-Rebeh et al., 2012	34 families	34 families	0
Dixon-Salazar et al., 2012	118 families	32 families (37 %)	22 novel candidate gene (19% of cohort)
Alazmi et al., 2015	143 families	104 families (73%)	69 novel candidate genes
Yavarna et al., 2015	149 probands	89 families (60%)	7 novel candidate genes (5% of cohort)
Anazi et al., 2016	337 families	196 families (58%)	3 novel candidate genes
Alfares et al., 2017	454 probands	22 probands (5%)	0
Monies et al., 2017	1000 families	340 families (34%)	75 novel candidate genes reported
Total	***2245 families***	***1027 families***	***178 novel candidate genes***

(Alahmad et al., 2019)

1.4.6 Founder mutations in the Middle Eastern population

Founder mutations in novel mitochondrial disease genes such as *PET100*, *ISCA2*, *PMPCA*, and *NUDT2* were identified in unrelated families when investigated as part of their respective cohorts (**Table 1.2**) (Lim *et al.*, 2014; Al-Hassnan *et al.*, 2015; Jobling *et al.*, 2015; Yavuz *et al.*, 2018). For example, a cohort of five unrelated consanguineous families were investigated leukodystrophy and neurological regression using NGS and all patients were homozygous for a founder mutation identified in the novel mitochondrial disease gene *ISCA2* (p.Glu77Ser) which codes for a protein that plays a critical role in the maturation of [4Fe-4S] clusters (Sheftel *et al.*, 2012; Al-Hassnan *et al.*, 2015). Functional study on fibroblast cell line of an *ISCA2* patient who was homozygous for the founder mutation revealed defects in multiple OXPHOS complexes in addition to defects in the α-ketoglutarate dehydrogenase and pyruvate dehydrogenase complexes when compared to controls and therefore validated the mutation's pathogenicity (Lebigot *et al.*, 2017). Patients from nine more consanguineous Saudi families who were investigated for infantile onset leukodystrophy were genotyped with the same *ISCA2* founder mutation using WES and targeted mutation sequencing (Alfadhel *et al.*, 2018).

Other novel variants identified in mitochondrial disease genes were established as founder mutations in the Middle East after further investigations (*SLC39A8*, *SLC19A3*, *ELAC2*, *FARS2*, *SLC25A42*, and *MICU*) (Alfadhel, 2017; Riley *et al.*, 2017; Shinwari *et al.*, 2017; Almannai *et al.*, 2018a; Almannai *et al.*, 2018b; Musa *et al.*, 2018). The founder mutation in *ELAC2* (which codes for mitochondrial RNase Z, a protein responsible for the endonucleolytic cleavage at the 3' termini of mt-tRNA transcripts in mitochondria) was first identified in a cohort of patients investigated for infantile cardiomyopathy where functional studies on patient fibroblasts revealed defects in OXPHOS subunits and showed an accumulation of unprocessed mt-tRNA transcripts compared to controls (Brzezniak *et al.*, 2011; Haack *et al.*, 2013). The founder mutation was later identified in 19 unrelated consanguineous Middle Eastern families that were investigated for infantile cardiomyopathy (Shinwari *et al.*, 2017; Saoura *et al.*, 2019). So far, more than 10 founder mutations in mitochondrial disease genes have been reported.

Table 1.2 List of founder mutations and common mitochondrial disease diagnoses reported in the Middle Eastern population, observed phenotypes, and therapeutic treatments.

Gene	Protein	Variants	Observed phenotypes/ syndromes; key findings	Treatment
ECHS1	Enol-CoA Hydratase, Short chain 1	27 variants reported.	Elevated 3MGA; lactic acidosis; apnoeic episodes MRI: Basal ganglia lesions, cerebral and cerebellar atrophy; MRS lactate peak	N/A
ELAC2	Mitochondrial RNase Z	Founder mutation: c.460T>C p.Phe154Leu	Hypertrophic cardiomyopathy, elevated lactate, multiple OXPHOS defects	N/A
ETHE1	Persulphide Dioxygenase	34 variants reported. 2 variants exclusively reported in Arabs: c.505+1G>T; p. exon 4 skipping And genetic deletion of exon 4	Ethylmalonic encephalopathy, ethylmalonic aciduria, elevated C4 and C5 acylcarnitines (*SCAD* patients have higher C4 and C5 acylcarnitine levels)	Metronidazole, N-acetylcysteine
FARS2	Mitochondrial Phenylalanyl-tRNA Synthetase	Founder mutation: c.431A>G p.Tyr144Cys	2 phenotypes: 1. Early-onset epileptic encephalopathy 2. Late-onset spastic paraplegia	N/A
ISCA2	Iron-Sulphur Cluster Assembly protein 2	Founder mutation: c.229G>A p.Glu77Ser	MRI: leukodystrophy, spinal cord involvement Variable clinical phenotype	N/A
MICU1	Mitochondrial Calcium Uniporter 1	Founder mutation: c.553C>T p.Gln185*	Elevated liver transaminase, elevated creatine kinase, normal lactate	N/A
SLC19A3	Mitochondrial Thiamine Transporter 2	Founder mutation: c.1264A>G p.Thr422Ala	3 phenotypes: 1. Early-infantile Leigh-like syndrome. 2. Childhood biotin-thiamine responsive basal ganglia disease. 3. Adult Wernicke's-like encephalopathy	Biotin, thiamine
SLC25A42	Mitochondrial CoA Transporter	Founder mutation: c.871A>G p.Asn291Asp	Variable clinical phenotype MRI: iron deposits in globus pallidus and substantia nigra	N/A
SERAC1	Serine Active Site containing 1	42 variants reported.	2 phenotypes: 1. Hypotonia with progressive spasticity, dystonia, hearing loss, elevated 3MGA 2. Complicated hereditary spastic paraplegia Key finding: MRI: "putaminal eye"	N/A

(Alahmad et al., 2019)

1.4.7 Preventable mitochondrial disease in the Middle East

One of the earliest reported neurological presentations that mimicked mitochondrial diseases in the Middle East is Biotin-Thiamine responsive Basal Ganglia Disease (BTRBGD) (Ozand *et al.*, 1998). Patients from 8 consanguineous Arab families had varying neurological presentations but a consistent MRI finding of basal ganglia lesions was reported in all patients. Supplementation of biotin was identified as an effective treatment for the neurological presentations in the patients. Linkage analysis studies and targeted candidate gene sequencing identified mutations in *SLC19A3* which codes for a plasma membrane protein that functions as a thiamine transporter (Zeng *et al.*, 2005). One of the identified *SLC19A3* mutations was identified in patients from 13 unrelated consanguineous Saudi families and was established as a founder mutation (Alfadhel *et al.*, 2013).

With regards to genotype-phenotype correlation, 3 major phenotypic presentations have been associated with *SLC19A3* mutations: early-onset Leigh-like syndrome, childhood biotin-thiamine responsive basal ganglia disease, and adult Wernicke's-like encephalopathy (Alfadhel and Tabarki, 2018). MRI findings of basal ganglia lesions are reported in all the aforementioned presentations in addition to patients with Leigh syndrome which is associated with over 85 genes resulting in a weak genotype-phenotype correlation (Lake et al., 2019). It is key to point out that patients diagnosed with early-onset Leigh syndrome due to an *SLC19A3* mutation were less responsive to the biotin supplementation and had high rates of early mortality (Alfadhel, 2017).

1.4.8 Treatment of mitochondrial diseases in the Middle East

So far, there are no curative treatments established for mitochondrial disease, however there are therapeutic approaches that help alleviate some symptoms caused by mitochondrial dysfunction (Lake *et al.*, 2016; Slone *et al.*, 2018). These include the enhancing of OXPHOS complex function using supplements such as the aforementioned biotin, antioxidants such as co-enzyme Q10, vitamins C and E, and also include substances that enhances mitochondrial biogenesis. For example, *SLC19A3* patients respond well to biotin supplementation, and clinical symptoms of *ETHE1* patients improve after treatment with metronidazole (a bactericide) and N-acetylcysteine (Ozand *et al.*, 1998; Viscomi *et al.*, 2010). Genetic counselling for families with confirmed

genetic disease can help reduce the chances of having affected offspring by opting for Preimplantation Genetic Diagnosis.

1.5 Aims

Throughout this introduction I have discussed the structure and various functions and roles of mitochondria as a cellular organelle, how these mitochondrial functions are controlled by proteins encoded in the mitochondria's own genome in addition to the nuclear genome and outlined how mitochondrial dysfunction has been associated with clinically heterogeneity in patients harbouring mutations in these genes. The diagnosis of mitochondrial disease has been challenging due to weak genotype-phenotype correlation reported in patients. I highlight the importance of NGS in recent years in the rapid diagnosis of Mendelian mitochondrial disease in patients and the rapid discovery of novel mitochondrial disease genes.

Specifically, my aims for this project were to recruit and select patients suspected of mitochondrial disease in the highly consanguineous population of Kuwait by evaluating the patients' suggestive mitochondrial disease phenotype, family history suggestive of Mendelian inheritance of disease, and the availability of a thorough clinical history of disease progression. With the assistance of clinical specialist in Kuwait and Newcastle, I developed modified mitochondrial disease criteria to score the probability of mitochondrial disease involvement in patients. Selective sequencing of mtDNA mutations in patients were mostly excluded prior to recruitment.

After recruitment, I used WES as a first-tier genetic analysis method in search of nDNA variants associated with mitochondrial function and disease. Upon the identification of candidate pathogenic variants, I genotyped patients' family members to confirm the segregation of the variant within the family. Dependant on the availability of tissue samples from patients, I validated the pathogenicity of novel variants in patients using functional analysis methods such as western blotting and BN-PAGE and reported my findings. My research finally utilised a range of functional investigation methods to investigate a novel mitochondrial disease gene, validated the pathogenicity of the identified variants, and investigated the molecular aetiology of disease in patient fibroblast cell lines.

Chapter 2. Materials and Methods

2.1 Materials

2.1.1 Equipment

2.1.1.1 General laboratory

Analogue Tube Roller	Thermo Scientific
Benchtop Centrifuge 5417R (Refrigerated)	Eppendorf
Benchtop Centrifuge 5418	Eppendorf
Benchtop Centrifuge 5804	Eppendorf
Dry Heat Block	Techne
Magnetic stir bars	Fisherbrand
Microcentrifuge, Technicomini	Griffin Education
pH Meter 3510	Jenway
Stirrer, Ceramic Plate U151	Stuart
Vortex Genie 2	Scientific Industries
Water Purification System, NANOpureII	Barnstead

2.1.1.2 Genetic analysis

Genetic Analyser, ABI 3130*xl*	Applied Biosystems
Electrophoresis Unit, HU10 Mini-Plus Horizontal Unit	Scie-Plas
NanoDrop Spectrophotometer, ND-1000	Thermo Scientific
UVP PCR Cabinet	FisherScientific
Thermal Cycler, Veriti 96 Well	Applied Biosystems

2.1.1.3 Cell culture

Aspiration System Vacusafe	Integra
Benchtop Centrifuge, Universal 32	Hettich
Class II Microbiological Safety Cabinet, BH-EN-2004	Faster
CO_2 Cell culture Incubator, MCO-18AIC	Panasonic
LED Microscope, Leica DM IL	Leica

2.1.1.4 Western blotting

Imaging System, ChemiDoc MP	Bio-Rad
Mini Trans-Blot Cell system	Bio-Rad
Mini-Protean Tetra Cell system	Bio-Rad
Orbital Shaker, SSL1	Stuart
Plate Reader, SpectraMax M5e Multimode	Molecular Devices

2.1.1.5 BN-PAGE

Motor Drive Homogeniser	Glas-Col
Teflon-Dounce homogeniser	Glas-Col
Ultracentrifuge, Optima MAX-XP	Beckman Coulter
XCell Surelock Mini-Cell Electrophoresis System	ThermoFisher Scientific

2.1.2 Consumables

96-Well PCR Plate, Semi-Skirted, Clear	StarLab
PCR tubes (200µl)	StarLab
Cellstar Aspirating Pipette	Greiner Bio-One
Cellstar Disposable Tubes (5ml, 10ml, 25ml)	Greiner Bio-One
Cellstar Falcon Tubes (50ml)	Greiner Bio-One

Chromatography Paper, 3mm	Whatman
DNeasy Blood and Tissue Kit	Qiagen
Flat-bottom 96 well plate	TTP
Immobilon-P PVDF membrane (0.45µm)	Merck
Microfuge tubes (0.6ml, 1.5ml, 2ml)	Starlab
Nunc-Cryotube Vials	Thermo-Scientific
Parafilm	M
Syringe Filter Unit, 0.22µm, polyethersulphone, 33mm gamma sterilised	Millex-GP
Syringes without Filters, 10 ml	Fisher Scientific
Syringes without Filters, 50 ml	Fisher Scientific
Ultracentrifuge glass tubes	Beckman Coulter
Universal tubes, 20ml	Starlab

2.1.3 Chemicals and reagents

2.1.3.1 General reagents

Bovine Serum Albumin (BSA)	Sigma-Aldrich
Dimethyl Sulphoxide (DMSO)	Sigma-Aldrich
Ethanol, 100%	Fisher Chemical
Glycerol	Sigma-Aldrich
Isopropanol	Sigma-Aldrich
Liquid Nitrogen	BOC
Methanol, 100%	Fisher Chemical
Phenylmethylsulphonyl fluoride (PMSF)	Roche

2.1.3.2 Polymerase chain reaction (PCR) reagents

Colourless GoTaq Reacting Buffer, 5X	Promega
Deoxyribonucleotide Triphosphate (dNTP) Mix, 2mM	Bioline
GoTaq G2 DNA Polymerase, 5U µl-1	Promega
Ambion™ Nuclease-free water	Invitrogen
Orange G powder	Sigma-Aldrich
Tris-Acetate-EDTA (TAE) Buffer	Formedium

2.1.3.3 Sanger sequencing reagents

Big Dye Terminator v3.1 Cycle Sequencing Kit	Applied Biosystems
Exonuclease I, 20U μl^{-1}	Thermo Scientific
FastAP, thermosensitive Alkaline Phosphatase, 1U μl^{-1}	Thermo Scientific
Hi-Di formamide	Applied Biosystems

2.1.3.4 Tissue culture reagents

Amphotericin (Fungizone)	Gibco	15290018
Dulbecco's Modified Eagle Medium	Gibco	41965039
Dulbecco's Phosphate buffered saline X1 (DPBS)	Gibco	14190250
Foetal Bovine Serum (FBS)	Gibco	16000044
Minimum Essential Media	Gibco	11095080
MEM Non-essential Amino Acid Solution (100X)	Sigma-Aldrich	11140035
MEM Vitamins	Gibco	11120037
Penicillin and Streptomycin Solution	Gibco	15070063
Sodium pyruvate	Gibco	11360070
TrypLE Express	Gibco	12605010
Uridine	Sigma-Aldrich	U3750

2.1.3.5 Agarose gel electrophoresis reagents

Agarose (Molecular Grade)	Bioline
1 kb DNA Ladder, 0.1 μg μl^{-1}	Promega
SYBR Safe DNA Gel Stain, 10,000X	Invitrogen

2.1.3.6 SDS-PAGE and Western blot reagents

Acrylamide/Bis-acrylamide, 30%, 29:1	Bio-Rad
Detection Reagents, Amersham ECL Prime Western Blotting	GE Healthcare
Blue Wide Range Protein Ladder	Cleaver Scientific
Dried Skimmed Milk Powder	Marvel
Glycine	Sigma-Aldrich
N, N, N', N'- Tetramethyl ethylenediamine (TEMED)	Sigma-Aldrich
Polysorbate 20 (Tween-20)	Acros Organics
Protein Assay Dye Reagent Concentrate	Bio-Rad
Sodium Dodecyl Sulphate (SDS)	Sigma-Aldrich
Trisma Base	Sigma-Aldrich

2.1.3.7 BN-PAGE reagents

Coomassie Blue	Thermo Scientific
D-Mannitol	Sigma-Aldrich
Dodecyl maltoside (DDM)	Sigma-Aldrich
Ethylene glycol-bis(β-aminoethyl)-N, N, N', N'- tetra acetic acid (EGTA)	Sigma-Aldrich
N-dodecyl-β-maltoside	Thermo Scientific
NativeMark™ Unstained Protein Standard	Invitrogen
NuPAGE™ Anode Buffer, Running Buffer (20X)	Invitrogen

NuPAGE™ Cathode Buffer (20X)	Invitrogen
NuPAGE™ Transfer Buffer (20X)	Invitrogen
NativePAGE™ 4-16%, Bis-1.0 mm, Mini Protein Gel, 10-well	Invitrogen
Pierce BCA Protein Assay Kit	ThermoFisher Scientific
Ponceau S	Sigma-Aldrich
NativePAGE™ sample buffer, 4X	Invitrogen

2.1.3.8 Vector cloning reagents

BamHI restriction enzyme	NEB
CutSmart buffer	NEB
EcoRI restriction enzyme	NEB
In-Fusion HD Enzyme Premix	TaKaRa Bio
pLVX-TetOne-Puro vector	TaKaRa Bio

2.1.3.9 Lentiviral transduction reagents

Foetal Bovine Serum, Dialysed	Gibco
Doxycycline	TaKaRa Bio
Lenti-X Packaging Single Shots	TaKaRa Bio
Polybrene	Sigma-Aldrich
Puromycin	Sigma-Aldrich

2.1.4 Solutions

2.1.4.1 PCR amplification

PCR master mix	1X GoTaq reaction buffer
	200μM dNTPs
	1.2μM mixture of forward and reverse primers
	0.8U GoTaq G2 polymerase
	Nuclease-free water

2.1.4.2 Agarose gel electrophoresis

DNA Loading Dye	50% Glycerol
	50% dH_2O
	Orange G (to colour)
	Store at toom temperature
ExoFAP	10U Exonuclease I
	1U FastAP
Tris-Acetate-EDTA (TAE) Buffer, 1X	Store at room temperature

2.1.4.3 Tissue culture

Growth Media	Dulbecco's Modified Eagle Media (DMEM) high glucose
	10% Foetal Bovine Serum (FBS)
	1X Non-essential amino acids
	1% penicillin/streptomycin
	50μg ml^{-1} Uridine
	Store at 4°C

Transport Media	Minimal Essential Media (MEM)
	10% FBS
	1mM Sodium pyruvate
	MEM Vitamins
	1X Non-essential amino acids
	1% penicillin/streptomycin
	2.5µg ml^{-1} Amphotericin B

2.1.4.4 Western blotting

Ammonium Persulphate (APS), (w/v) 10%	Store at -20°C
Bromophenol Blue 1% (w/v)	Store at -20°C
Cell Lysis Buffer	50mM Tris-HCl, pH 7.4
	130mM $NaCl_2$
	2mM $MgCl_2$
	1% Nonidet P-40
	1X EDTA protease inhibitor cocktail tablet
	1mM PMSF
	Store at -20°C
Running Buffer, 10X	192 mM Glycine
	25 mM Tris
	0.1% SDS
	Store at room temperature
Sample Dissociation Buffer	6.25mM Tris-HCl, pH 6.8
	2% SDS

	10% Glycerol 100mM DDT 0.01% Bromophenol blue Store at -20°C
Sodium Dodecyl Sulphate (SDS) (w/v) 10%	Store at room temperature
Transfer Buffer, 10X	192 mM Glycine 25 mM Tris 0.02% SDS 15% Methanol Store at room temperature
Tris-Buffered Saline and Tween-20 (TBS-T)	1X TBS 0.1% Tween-20 Store at room temperature
Tris-HCl, 0.5M, pH 6.8	Store at room temperature
Tris-HCl, 3.75M, pH 8.5	Store at room temperature

2.1.4.5 BN-PAGE

Acetic Acid (w/v) 8%	Store at room temperature
Bovine Serum Albumin, 10%	Store at -20°C
Coomassie Blue, 5%	Store at -20°C
Dodecyl maltoside (DDM), 2%	Store at -20°C
Homogenisation Buffer	600mM D-Mannitol 10mM Tris-HCl, pH 7.4 1mM EGTA

	0.1 BSA 1mM PMSF
Phenylmethylsulphonyl Fluoride (PMSF) 100mM	Store at -20°C
Solubilisation Buffer	1X protein sample buffer 2% DDM 10% Glycerol Store at -20°C
Transfer Buffer 1X	1X NativePAGE Transfer Buffer 10% Methanol

2.1.5 Software

Alamut	Interactive Biosoftware
FinchTV (Version 1.4.0)	Geospiza Incorporated
Image Lab (Version 6.1)	Bio-Rad
Mutation Surveyor	SoftGenetics
SoftMax Pro	Molecular Devices

2.2 Methods

2.2.1 Recruitment of patients

Patients were recruited from Kuwait via the Kuwait Medical Genetics Centre (KMGC). The recruitment of the patients was approved by the Ethical Committee at KMGC.

Some patients included in this study were recruited from the NHS Highly Specialised Service for Rare Mitochondrial Disorders in Newcastle upon Tyne, UK, from the King Saud bin Abdulaziz University for Health Sciences in Jeddah, Saudi Arabia, and from the Fondazione IRCCS Istituto Neurologico Carlo Besta in Milan, Italy. Clinical summaries, DNA samples, and fibroblasts were provided by the respective centres.

DNA from patients and their families and patient skin biopsy samples were sent to the NHS Highly Specialised Service for Rare Mitochondrial Disorders in Newcastle upon Tyne. DNA and fibroblast cell lines were obtained from the Mitochondrial Diagnostic Service Lab following submission of a tissue and DNA request form.

A detailed outline of the recruitment and selection process is described in **Chapter 3**.

2.2.2 Ethical guidelines

All procedures were approved and performed under the ethical guidelines of the NHS Highly Specialised Service for Rare Mitochondrial Disorders in Newcastle upon Tyne and with the Helsinki Declaration of 1975, as revised in 2013. Informed consent was obtained from patients and/or guardians for research purposes.

2.2.3 Extraction of DNA samples from recruited patients and families

DNA extraction from recruited patient and families was performed at KMGC by lab technicians. DNA was extracted from blood using the standard phenol-chloroform DNA extraction method and stored in -80°C freezer for future investigations.

2.2.4 Control fibroblast cell lines

Appropriate age-matched control fibroblasts were obtained from the NHS Highly Specialised Service for Rare Mitochondrial Disorders for research purposes. This comprised of 4 paediatric fibroblast cell lines and 2 adult fibroblast cell lines.

2.2.5 Whole exome sequencing

Whole exome sequencing was performed at the Newcastle Genomics Core Facility at Newcastle University led by Dr Jonathan Coxhead as follows: For patients from families 1-13 and families 15-17, coding regions were enriched with Nextera Rapid Exome Capture (Illumina) and sequenced with 100 bp paired-end reads on an Illumina NextSeq500 platform. An in-house bioinformatics pipeline was applied to the raw FASTQ files by Dr Helen Griffin, and Dr Angela Pyle using a high-performance computing cluster at Newcastle University. The pipeline utilises a Linux command line and Bash Shell scripts that is able to simultaneously run multiple exome analyses followed by the removal of duplicate reads using FastUniq (version 1.1) (Xu *et al.*, 2012). The Burrows-Wheeler Alignment tool (BWA, version 0.7.12) was utilised to align the raw sequence read to the human genome reference sequence (GChr38) resulting in the generation of an alignment file in Sequence Alignment/Map (SAM) (SAMtools version 0.1.19) format (Li and Durbin, 2009). SAM files contain the aligned genetic sequences and are converted to a Binary Alignment/Map (BAM) format and variants were detected using Freebayes (version 1.0.2) (Garrison and Marth, 2012).

Variants were functionally annotated by the ANNOVAR tool to highlight which genes the variants are located in, whether they are in a coding or non-coding regions (NCR) of the gene, which exon they fall in, and the affected amino acid (Wang *et al.*, 2010). The variants were annotated using the reference genome databases RefSeq, UCSC Genome Browser, and Ensembl Genes (Rosenbloom *et al.*, 2015; Aken *et al.*, 2016; O'Leary *et al.*, 2016). The variants were further annotated with allele frequencies reported in a number of exome databases including the genome aggregation database (gnomAD) (Lek *et al.*, 2016), National Heart, Lung and Blood Institute Exome Sequencing Project (NHLBI ESP) (Exome Variant Server), and 1000 genomes project (Genomes Project *et al.*, 2015).

For patients from family 14 and families 18-22, exome capture was acquired using the Twist capture kit, sequenced using the Illumina NovaSeq 6000 system in 100 bp reads. An in-house bioinformatics pipeline was applied to the raw FASTQ files by Dr Fiona Robertson using a high-performance computing cluster at Newcastle University.

The pipeline utilises a Linux command line that is able to simultaneously run multiple exome analyses followed by the removal of duplicate reads using Picard (version 1.130) (https://broadinstitute.github.io/picard/). The BWA tool (version 0.7.12) was utilised to

align the raw sequence read to the human genome reference sequence (GChr38) resulting in the generation of an alignment file in SAM format (Li and Durbin, 2009).

Genetic variants were detected using Varscan (version 2.4.3) ((Koboldt *et al.*, 2012) http://dkoboldt.github.io/varscan/) and functionally annotated by Ensembl Variant Effect Predictor (VEP, version 96) ((McLaren *et al.*, 2016) https://www.ensembl.org/info/docs/tools/vep/index.html) to highlight which genes the variants are located in, whether they are in a coding or NCR of the gene, which exon they fall in, and the affected amino acid. The variants were annotated using the reference genome databases RefSeq, UCSC Genome Browser, and Ensembl Genes (Rosenbloom *et al.*, 2015; Aken *et al.*, 2016; O'Leary *et al.*, 2016). The annotated variants of the various patients were compared using BEDtools (version 2.19.0) ((Quinlan and Hall, 2010) https://github.com/arq5x/bedtools2).

2.2.6 *In silico* analysis of candidate gene variants

In silico analysis of the effect of detected variants were performed using the protein prediction tools PROVEAN (Choi *et al.*, 2012; Choi and Chan, 2015), Polyphen-2 (Adzhubei *et al.*, 2010), SIFT (Ng and Henikoff, 2001; Kumar *et al.*, 2009) and CADD (Kircher *et al.*, 2014). In addition, 14 *in silico* protein damage predicting tools including the previously mentioned prediction tools were used to analyse the effects of the variant using a new website that summarises these predictions in a single report (Jiang *et al.*, 2017). The gnomAD version 2 database, a database compiling reported variants in the genomes and exomes of 141,456 clinically normal individuals, will be searched for the suspected WES variants to ensure its absence or presence at a very low minor allele frequency (MAF) and to exclude the presence of any homozygous individuals in the database (Lek *et al.*, 2016).

2.2.7 Oligodeoxynucleotide primers for PCR

Primers used for genetic studies were made available from the Mitochondrial Diagnostic Services Lab or were custom-designed and ordered from Integrated DNA Technologies. A full list of all primers used is provided in **Appendix A**.

2.2.8 Custom primer design

Exonic regions harbouring the identified variants of interest were targeted along with 200 bps flanking upstream (5') and downstream (3') using genomic sequences from the

UCSC genome browser website (Kent *et al.*, 2002). Custom-designed forward and reverse primers were generated using Primer3 (Koressaar and Remm, 2007). The generated primer sequences were checked for common single nucleotide polymorphisms (SNPs) using SNPCheck3 (https://genetools.org/SNPCheck/snpcheck.htm). Final primers were flanked by universal M13-derived sequences that preceded each primer: forward (5'- TGTAAAACGACGGCCAGT -3') and reverse (5'- CAGGAAACAGCTATGACC -3'). Primers were ordered from Integrated DNA Technologies and primers were prepared in aliquots of 10 μM stocks containing both the forward and reverse primers.

2.2.9 Polymerase chain reaction (PCR)

DNA was extracted from peripheral blood of patients and their family members using the phenol-chloroform DNA extraction method. The concentrations of DNA samples were measured using the NanoDrop Spectrophotometer (***Section 2.1.1.2***).

PCR amplification of the identified variants was performed by adding 1.0μl of the patients' DNA to 24.0μl of PCR master mix (see ***Section 2.1.4.1***) and subjected to the PCR reaction heating steps as outlined in **Table 2.1.**

Table 2.1 PCR protocol for DNA amplification

Step	*Temperature (°C)*	*Duration*	
Initiation	94	4 minutes	
Denaturation	94	45 seconds	
Annealing	62	45 seconds	30 cycles
Extension	72	45 seconds	
Final extension	72	5 minutes	
Hold	4	Indefinitely	

2.2.10 Gradient PCR for primer optimisation

All primers were initially tested on a control human genome using a PCR reaction with an annealing temperature of 62°C. Should the PCR not result in any specific amplified PCR product, a reaction programmed using a gradient of annealing temperatures (58°C , 60°C, 62°C, 64°C and 66°C) was utilised to determine which of these temperatures is optimal for DNA amplification with the used primers. Should the gradient programme not result in any amplification of DNA, the gradient PCR was repeated with the addition of 10% DMSO to each sample.

2.2.11 Agarose gel electrophoresis

To cast a 1% agarose electrophoresis gel, 1.0g of agarose was dissolved in 100ml of 1X TAE buffer and heated up in a microwave until the agarose dissolved. Once dissolved, the solution is allowed to cool down until it was warm to the touch and then 4µl of SYBR Safe DNA gel stain was added to the solution and then poured with an appropriate comb added to form wells and was left to solidify. The gel was then submerged in 1X TAE buffer and samples were loaded into the wells.

A ladder marker (1kb) was loaded into a well and DNA samples were loaded in neighbouring wells. DNA samples were loaded with equal amounts of DNA loading dye (4µl of PCR product with 4µl DNA Loading Dye). The agarose gel was subjected to

electrophoresis at 100V for 30 minutes at room temperature. The gel was imaged using the ChemiDoc MP to visualise DNA bands using the UV transilluminator setting according to manufacturer guidelines.

2.2.12 Sanger sequencing

PCR products were treated with ExoFAP to clean up the mixture prior to cycle sequencing. In a 96-well PCR plate, 5µl of PCR product were added in duplicate for each sample, and 1.5µl of ExoFAP were added to each PCR product. The plate was capped using an adhesive plastic sheet and the solution was mixed and briefly spun down in a centrifuge. The mixture was run in a PCR heating programme as follows: 37°C for 15 minutes then 80°C for 15 minutes, and concluding with a hold step at 4°C. This reaction neutralises any unbound dNTPs and PCR primers that might interfere with the cycle sequencing reaction.

To make up a 20µl cycle sequencing reaction mixture, the following components were added to the PCR product and ExoFAP mixtures: 7.5µl of nuclease free water, 3µl 5X BigDye v 3.1 sequencing buffer, 2µl BigDye v 3.1 ready reaction mix and 1µl of universal forward or reverse primer. The 96-well PCR plate was sealed with an adhesive sheet and the solution was mixed and briefly spun down in a centrifuge. The cycle sequencing reaction heating steps were as follows in **Table 2.2**:

Table 2.2 PCR protocol for Cycle Sequencing

Step	*Temperature (°C)*	*Duration*	
Initiation	96	1 minute	
Denaturation	96	10 seconds	
Annealing	50	5 seconds	35 cycles
Extension	60	4 minutes	
Hold	4	Indefinitely	

2.2.13 Ethanol precipitation of DNA

DNA from the cycle sequencing products were obtained by ethanol precipitation prior to sequencing. The seal on the 96-well PCR plate was removed and to each sample the following were added: 2µl of 125mM EDTA, 2µl of 3M sodium acetate solution, and 70µl of 100% ethanol. The plate was sealed and the inverted to mix the solutions in each well and left at room temperature for 15 minutes. The plate was then centrifuged at 2,000*g* for 30 minutes at room temperature. As soon as the spin was over, the plate seal was removed, and the supernatant was removed by inverting the plate on tissue paper and tapped gently. The plate was kept inverted and fresh tissue paper was placed under it and the plate was spun up to 100*g* to remove any excess solution in the wells. The wells were then washed with 70µl of 70% ethanol and the plate was sealed and spun at 1,650*g* for 15 minutes at room temperature. As soon as the spin was over, the plate seal was removed, and the supernatant was removed by inverting the plate on tissue paper and tapped gently. The plate was kept inverted and fresh tissue paper was placed under it and the plate was spun up to 100*g* to remove any excess solution in the wells. Thereafter, the plate was allowed to air dry and shielded from light for 10 minutes. The plate was sealed and kept in a freezer at -20°C until ready to sequence.

When ready for sequencing, 10µl Hi-Di formamide was added to each sample and the plate was heated to 95°C for 2 minutes and then placed on ice for 1 minute.

2.2.14 DNA sequencing

DNA samples in the 96-well PCR plate were sequencing using an ABI 3130*xl* Genetic Analyser with the help of colleagues at the Mitochondrial Diagnostic Service Lab. Completed DNA sequencing results were retrieved from the ABI 3130*xl* Genetic Analyser as .ab1 files showing an electropherogram of raw DNA base sequences. Mutation Surveyor (SoftGenetics) or FinchTV (Geospiza) software were used to analyse the sequencing files and determine the genotypes of controls, patients, and their families.

2.2.15 Acquiring patient fibroblast cell lines from skin biopsies

Surviving patients living in Kuwait with novel variants of interest had a skin biopsy obtained by Dr Ahmad Alaqeel, a clinical colleague at the KMGC, and stored in Transfer Media (see ***Section 2.4.1.2***) at ambient room temperature. The biopsy samples were sent

to the NHS Highly Specialised Service for Rare Mitochondrial Disorders in Newcastle upon Tyne, UK.

2.2.16 Establishing primary cell lines from skin biopsies

Dr Gavin Falkous (NHS Highly Specialised Service for Rare Mitochondrial Disorders, Newcastle upon Tyne) established the primary fibroblast cell line from the obtained patient skin biopsies by slicing the biopsy samples and placing them in T25 flasks. The samples were cultured in Growth Media (see ***Section 2.4.1.2***) at 37°C in 5% CO_2. The established fibroblast cell lines were split once they reached 80% confluency.

2.2.17 Culturing of fibroblasts

Skin fibroblasts were cultured in T75 flasks with Growth Media (see ***Section 2.4.1.2***) at 37°C in 5% CO_2.

2.2.18 Subculturing of fibroblasts

Fibroblasts were expanded until they reached 60-80% confluency. Upon reaching this confluency, culture media was removed and TrypLE Express was added (2 ml in a T75 flask) and the flask was incubated at 37°C for 5 minutes. The flasks were tapped gently for cells to detach and were checked under a microscope. Afterwards, 6 ml of culture media was added to the flask and the mixture was transferred to a 20 ml universal tube. The tube was centrifuged at 1,200 rpm (Hettich Universal-32 benchtop centrifuge) for 5 minutes. The supernatant was disposed of and the pellet was resuspended in 1 ml of culture media. To expand the cell line, the resulting cell suspension was split into 2-3 culture flasks by aliquoting 500 µl or 330 µl (respectively) into flasks containing culture media.

2.2.19 Harvesting of cells

The cell suspension resulting for the centrifugation step in the previous ***Section*** (***2.2.17***) is aliquoted into a 1.5ml tube and centrifuged at 3,000 rpm for 3 minutes at room temperature. The supernatant was removed, and the pellet was flash frozen in liquid nitrogen and stored in -80°C freezer.

2.2.20 Freezing of cells

The cell pellet resulting for the centrifugation step in the previous ***Section*** (***2.2.17***) was suspended in 0.5ml of FBS with 10% DMSO and placed in a CoolCell Cell Freezing

Container (Biocision) and placed in a -80°C freezer. After a minimum of 24 hours the tubes were transferred into a liquid nitrogen containing storage vessel.

2.2.21 Western blotting

2.2.21.1 Preparation of cell lysates for protein analysis

Fibroblasts from patients and controls were harvested and treated with Cell Lysis Buffer (see ***Section 2.1.4.3***) vortexed for 30 seconds and kept on ice for 3 minutes. The mixture was vortexed again for 30 seconds and then centrifuged at 8,000*g* for 5 minutes at 4°C. The supernatant was transferred to a new tube and flash frozen in liquid nitrogen and stored at -80°C. The protein concentration was estimated using the Bradford assay.

2.2.21.2 Bradford assay

The protein concentration of cell lysates was determined using a Bradford assay. BSA was used to produce a standard curve formed of known concentrations; these were duplicates of 0, 2, 5, 10, 15 and 20 mg ml^{-1} made up in a total volume of 800µl. Cell lysates were diluted using 1µl and 2µl of cell lysate in a final volume of 800µl with ddH_2O for each sample. 200µl of Protein Assay Dye Reagent Concentrate (Bio-Rad) was added to each sample before being vortexed and incubated for 5 minutes at room temperature. Afterwards, 200µl of each sample, starting with the standard curve, was loaded in duplicate into a flat-bottom 96-well plate. The plate was then read at 595nm using a SpectraMax M5e Multimode Plate Reader (Molecular Devices).

The concentrations of the cell lysates were then estimated by determining the average concentrations of the 1µl and 2µl duplicates for each sample using the standard curve generated by the SoftMax Pro software based on absorbance readings. These were then used averaged to estimate the concentrations of each cell lysate.

2.2.21.3 Assessment of steady-state protein levels by western blotting

A volume of cell lysate equating to 50µg of total protein was treated with Sample Dissociation Buffer (see ***Section 2.1.4.3***) and incubated at 37°C for 15 minutes and then loaded into a 12% acrylamide gel that was cast using the Mini-Protean Tetra Cell system prepared by casting a 12% Resolving Gel and then casting a 3.75% Stacking Gel (see **Table 2.3**) above it to load the cell lysate samples. The gel was placed in Running Buffer

(see ***Section 2.1.4.3***) and subjected to electrophoresis at 200V for approximately 50 minutes.

Table 2.3 Polyacrylamide gel casting reagents and solutions

	12% Resolving Gel	*3.75% Stacking Gel*
Acrylamide/Bis-acrylamide 30% 29:1	2ml	0.625ml
3.7M Tris HCl, pH 8.5	0.5ml	-
0.5M Tris HCl, pH 6.8	-	1.25ml
dH_2O	2.395ml	3.02ml
10% SDS	50µl	50µl
10%APS	5µl	5µl
TEMED	50µl	50µl

Reagents are listed in ***Section 2.1.3.6*** and solution mixtures are outlined in ***Section 2.1.4.3***

The proteins were transferred on to a Polyvinylidene fluoride (PVDF) membrane in by layering the PVDF membrane and acrylamide gel and laying them between 2 sheets of Whatman paper using the Mini Trans-Blot Cell system (Bio-Rad), placed in Transfer Buffer (see ***Section 2.4.1.3***) and run at 100V for 1 hour. The membrane was check for successful transfer of the marker ladder bands and was blocked in 5% skimmed milk in TBS-T buffer (see ***Section 2.1.4.3***) for 1 hour before immunoblotting (see ***Section 2.2.22***).

2.2.22 Blue Native-PAGE

2.2.22.1 Enrichment of mitochondria

Fibroblast cell lines cultured to 80% confluency in at least 2 T225 flasks were harvested. The harvested cells were suspended in Homogenisation Buffer (see ***Section 2.1.4.4***) and kept on ice. The suspension was homogenised using a Teflon-Dounce homogeniser (Glas-col) with 15 passes at 80 rpm at 4°C and then centrifuged at 400*g* for 10 minutes

at 4°C. The supernatant was collected, and the pallet was resuspended in homogenisation buffer and the homogenisation process was repeated a further 2 times and the resulting supernatants were also collected. The collected supernatant samples were centrifuged at 400*g* for 10 minutes at 4°C to remove any transferred debris and the supernatants were collected again. The collected supernatants were centrifuged at 11,000*g* for 10 minutes at 4°C and the supernatant was discarded. The pellet was resuspended in a homogenisation buffer lacking BSA and PMSF and flash frozen in liquid nitrogen and stored at -80°C.

2.2.22.2 Solubilisation of enriched mitochondria

Samples pellets were suspended in Solubilisation Buffer while on ice and mixed using a glass spatula and incubated for 30 minutes. The suspensions were transferred to glass ultra-centrifuge tubes and centrifuged using an ultra-centrifuge at 100,000 *g* for 15 minutes at 4°C. The supernatant was collected, and the protein concentration was estimated using the Pierce Bicinchoninic Acid (BCA) Protein Assay Kit.

2.2.22.3 BCA protein assay

The protein concentration on solubilised samples was determined using a BCA assay (Pierce). Bovine serum albumin (BSA) was used to produce a standard curve formed of known concentrations; these were 250, 125, 50, 25, 5 and 0 μg ml^{-1}. Concentrations were measured by diluting 1μl and 2μl of the solubilised samples in a total of 100μl ddH_2O for each sample. Samples were vortexed and 25μl of each sample was added in duplicates to a flat-bottom 96-well plate.

The BCA Assay mixture was prepared as follows: 50 parts Reagent A: 1 part Reagent B. 200μl of the BCA Assay mixture was added to each sample in the plate and then shaken and incubated for 30 minutes at 37°C. Afterwards, the plate was then read at 562nm using a SpectraMax M5e Multimode Plate Reader (Molecular Devices).

The protein concentrations of the solubilised samples were then estimated by determining the average concentrations of the 1μl and 2μl duplicates for each sample using the standard curve generated by the SoftMax Pro software based on absorbance readings. These were then used averaged to estimate the concentrations of each solubilised sample.

2.2.22.4 Assessment of OXPHOS complex assembly using BN-PAGE

OXPHOS complexes were assessed in enriched mitochondrial pellets solubilised with DDM by BN-PAGE in patient and control fibroblast cells. 15 μg of protein were mixed with 5 μl of 5% Coomassie Blue and run on precast NativePAGE™ 4-16%, Bis-Tris, mini protein gel and subjected to electrophoresis in 1X NuPAGE™ cathode buffer at 150 V for 30 minutes using the XCell Surelock Mini-Cell electrophoresis system. The cathode buffer was replaced with 1X NuPAGE™ anode buffer and run at 300 V for 3 hours.

The proteins were transferred on to a PVDF membrane in by layering the PVDF membrane and acrylamide gel and laying them between 2 sheets of Whatman paper using the Mini Trans-Blot Cell system (Bio-Rad), placed in 1X NuPAGE™ Transfer Buffer (see ***Section 2.4.1.4***) and run at 100V for 1 hour. The membrane was check for successful transfer of the marker ladder bands and was blocked in 5% skimmed milk in TBS-T buffer (see ***Section 2.1.4.3***) for 1 hour before immunoblotting (see ***Section 2.2.22***).

2.2.23 Immunoblotting

The PVDF membranes were incubated with a primary antibody of target protein (**Appendix B**) diluted as recommended in 5% milk in TBS-T and incubated at room temperature for 3 hours or at 4°C overnight. The primary antibody was then removed, and the membrane was washed with TBS-T 3 times for a period of 10 minutes each. The membrane was then incubated in the respective Horseradish peroxidase (HRP) conjugated secondary antibody (diluted as recommended in 5% milk in TBS-T) at room temperature for 1 hour. The secondary antibody was then removed, and the membrane was washed with TBS-T 3 times for a period of 10 minutes each. The membrane was then treated with Electrochemiluminescence (ECL) prime (GE Healthcare) using 1:1 mixture of the substrates for 5 minutes and bands were visualised on a ChemiDoc Imager MP (Bio Rad).

2.2.24 Analysis of respiratory chain complex activity

These studies were performed by Dr Langping He at the NHS Highly Specialised Service for Rare Mitochondrial Disorders in Newcastle upon Tyne, UK.

Mitochondrial respiratory chain enzyme activities were assayed spectrophotometrically as previously described in patient fibroblasts (Frazier *et al.*, 2020) and in muscle samples (Bugiani *et al.*, 2004). In summary, respiratory chain activities of complexes I-IV are

measured in enriched mitochondrial fractions through assays that either measure a decrease or increase in absorbance spectrophotometrically of the enzyme substrate or a linked substrate; all respiratory chain enzyme activities are normalised to the activity of citrate synthase (CS), a mitochondrial matrix enzyme of the TCA cycle and marker of mitochondrial content.

Chapter 3. Identification of a paediatric patient cohort in Kuwait with suspected mitochondrial disease

3.1 Introduction

Due to the clinical heterogeneity associated with mitochondrial disease, criteria have been developed to predict the likelihood of mitochondrial disease involvement in patients (Wolf and Smeitink, 2002; Morava *et al.*, 2006). These clinical diagnostic criteria take into account the clinical presentation and findings in a patient at a certain time, while other reports published by Joost *et al.* (2012) and Chi (2015) provide a detailed flowchart outlining how patients are investigated. Some diagnostic flowcharts try to avoid the need for a muscle biopsy when suspecting mitochondrial disease since a "genetics first" approach has become a more rapid and cost-effective method in recent years. However, many of the aforementioned criteria continue to include a section for histological and/or biochemical findings in muscle biopsies of patients which may support the suspicion of mitochondrial disease. Pathogenic variants and deletions in the mitochondrial genome have been associated with maternally-inherited mitochondrial disease, whereas variants in the nuclear genome follow Mendelian patterns of mitochondrial disease inheritance (autosomal, sex-linked, and *de novo*) (Stenton and Prokisch, 2020; Thompson *et al.*, 2020a). The "genetics first" approach, especially when using next generation sequencing methods can help avoid the need for a muscle biopsy to confirm suspicions of mitochondrial disease involvement (Raymond *et al.*, 2018). Should a patient not be diagnosed using this approach, the need for a muscle biopsy is justified for follow-up biochemical investigations and multi-omics approaches to reach a diagnosis.

Confirmed mitochondrial disease cases have been scored using scales that assess disease progression in patients: Newcastle Mitochondrial Disease Adult Scale (NMDAS) (Schaefer *et al.*, 2006), Newcastle Paediatric Mitochondrial Disease Scale (NPMDS) (Phoenix *et al.*, 2006) and International Paediatric Mitochondrial Disease Scale (IPMDS) (Koene *et al.*, 2016). These scales are useful in longitudinal studies and meticulously gather information repeatedly. However, these scales were not fit for this project as they were utilised on confirmed mitochondrial disease cases, while a primary aim of this study is to diagnose mitochondrial disease cases in Kuwait by initially reviewing and selecting highly suspected cases.

Kuwait's population of 4.2 million is comprised of 1.3 million Kuwaiti nationals and 3.1 million foreigners residing in Kuwait (Central Bureau of Statistics, 2018). Amongst the populations of Kuwait and other Arab country population, the practice of consanguinity and endogamy are common with rates exceeding 50% in some regions (Modell and Darr, 2002; Tadmouri *et al.*, 2009). The prevalence of inherited disorders in such populations with high rates of consanguinity is often higher than in non-consanguineous populations and has a major effect on the clinical genetics of the population (Skladal *et al.*, 2003; Shawky *et al.*, 2013).

Patients in Kuwait referred to the Kuwait Medical Genetics Centre (KMGC) from governorate and specialised hospitals were reviewed for recruitment to the study. KMGC primarily employs Sanger sequencing of mtDNA for suspected pathogenic mutations. However, diagnosis rates for mitochondrial disease were poor considering the population is highly consanguineous. We required a process to evaluate and prioritise cases based on ranked suspicion of mitochondrial disease involvement to include in the study. This would help exclude cases presenting with phenocopies of mitochondrial disease.

For recruitment of cases to the study, we required criteria that scored the presentation and findings of patients at the time of assessment and review. I opted to develop criteria that took into account the available and gathered clinical data of patients and helped assess whether they are suspected of having mitochondrial disease. Depending on the scores and time of recruitment, cases were recruited to the study over the period of two and a half years and were prioritised for unbiased genetic testing using WES.

Upon the identification of likely pathogenic variants in the recruited patients, a segregation study confirmed the variant segregated within the family pedigree. Skin biopsies were acquired from patients when possible and functional studies using Western blotting and Blue Native-PAGE to assess the effect of the identified variants on protein expression and OXPHOS complex assembly when suspected.

3.2 Aims

The aim of this chapter is to outline the scheme used to recruit cases suspected of mitochondrial disease involvement to the study. This includes a flowchart of how patients were reviewed by experts and a description of a mitochondrial disease criteria used to score patients. This is followed by descriptions of clinical presentations and investigational findings in patients suspected of mitochondrial disease and recruited for

the study. Limitations of the recruitment process and findings that strongly support suspicion of mitochondrial disease involvement are discussed in addition to advantages of the recruitment process

3.3 Methods

Kuwait is divided into six governorates: The Capital, Hawalli, Al Farwaniya, Mubarak Al-Kabeer, Al Ahmadi and Al Jahra governorates. Five major government hospitals serve these governates and the Al-Sabah Health Region houses multiple specialised hospitals where patients from the major hospitals are referred to for specialised care and follow-up. KMGC is one of these specialised medical centres and is located adjacent to the Maternity Hospital in the Al-Sabah Health Region (**Figure 3.1**).

The governorates have Health Centres providing General Physician Clinics that serve every residential area. When necessary, these clinics refer patients to specialists based at the major Governorate Hospitals or the Al-Sabah Health Region to provide specialised care and follow-up. Alternatively, patients admitted to the Intensive Care Units of the major hospitals are also seen by (and referred to) the appropriate specialists based at the hospital.

Patients suspected of genetic disorders are referred to the KMGC for genetic investigation and diagnosis. Clinicians specialised in genetic disorders review referred patients with the benefit of referral notes which chart the course of disease with a summarised clinical history, previously requested test results, and imaging reports. A detailed family pedigree is drawn, and required tests, scans and genetic analyses are requested based on the suspected genetic disorder.

Cytogenetic karyotyping and Fluorescent *in situ* hybridisation (FISH) protocols are run by two separate laboratories at KMGC to identify any chromosomal aneuploidies or deletions. The molecular genetics laboratory uses various genetic analysis techniques such as Restricted Fragment Length Polymorphism (RFLP), Amplification-Refractory Mutation System (ARMS)-PCR, Quantitative-PCR (qPCR), Multiplex Ligation-dependent Probe Amplification (MLPA), and Sanger sequencing to genotype point mutations, indels or large deletions in genes associated with known genetic disorders. Sanger sequencing of mtDNA is performed for patients suspected of mitochondrial disease to search for mutations in disease associated genes; no nDNA mutations associated with mitochondrial disorders are genotyped or targeted at KMGC. In some

genetically undiagnosed cases, patient DNA samples are sent to commercial companies (e.g., CentoGene, CGC and GeneDx) that provide genetics analysis services such as WES in an attempt to obtain a diagnosis.

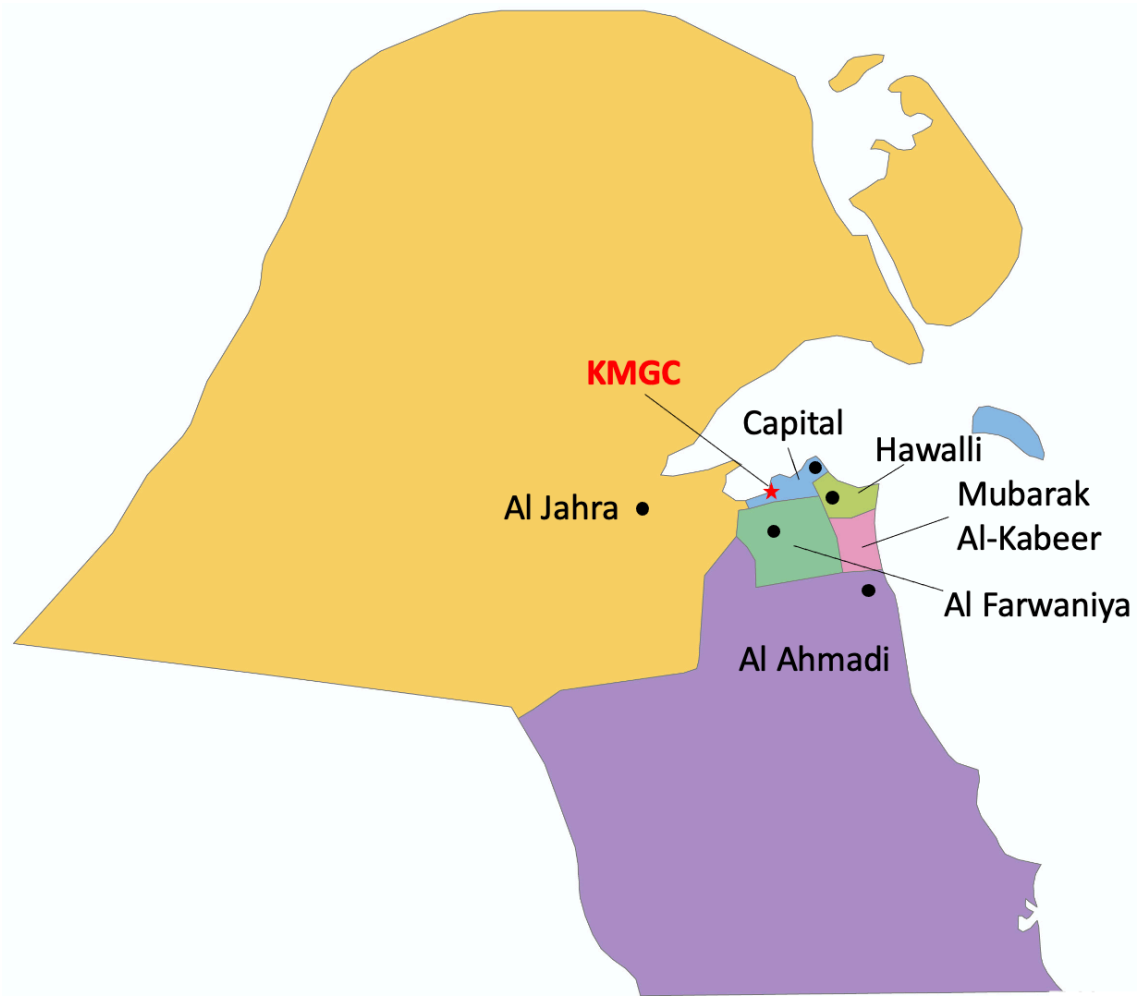

Figure 3.1 Map of Kuwait Governorates and locations of main hospitals that refer cases to KMGC in the Al-Sabah Health Region

A map of Kuwait with its 6 governorates labelled and shaded in different colours. Circles are locations of the main public hospitals that refer cases to KMGC. The red star is the location of KMGC within the Al-Sabah Health Region where patients are referred to. (Adapted from Vemaps.com (Vemaps, 2019))

3.3.1 Selection of patients suspected of mitochondrial disease in Kuwait for study cohort

The recruitment scheme used for recruitment of patients in Kuwait is outlined in **Figure 3.2** with the number of cases. This section describes the review steps in detail.

3.3.1.1 Paediatric metabolic specialist review

Paediatric cases in Kuwait suspected of mitochondrial disease were reviewed by Dr Buthaina Albash a paediatric metabolic specialist based at KMGC. Out of a total of 250 cases reviewed and investigated 136 were excluded from recruitment by the metabolic specialist based on clinical expertise due to poor clinical details, missing investigational results, or suspicion of alternative disorders other than mitochondrial disease. The remaining 114 cases were recruited for this study and consents were obtained from participating patient families. Of the recruited cases, 21 cases were previously investigated by WES. The majority of reviewed families were related either as first cousins, second cousins, or distant cousins due to high rate of consanguinity within the population of Kuwait which results from societal practices.

3.3.1.2 Mitochondrial Disease Criteria Scoring

The remaining 93 cases were scored using Mitochondrial Disease Criteria (MDC) based on the Morava criteria that is aimed at assessing paediatric cases suspected of mitochondrial disease involvement (**Figure 3.3**) (Morava *et al.*, 2006). Modifications to the published criteria include the renaming of the morphology column to “tissue findings” after the addition of respiratory chain enzyme activities to morphological tissue findings. Furthermore, an additional row separating “Highly Suggestive Findings” was added to “Suggestive Findings”. Patients were scored based on findings identified from personal history, family history, and clinical examination.

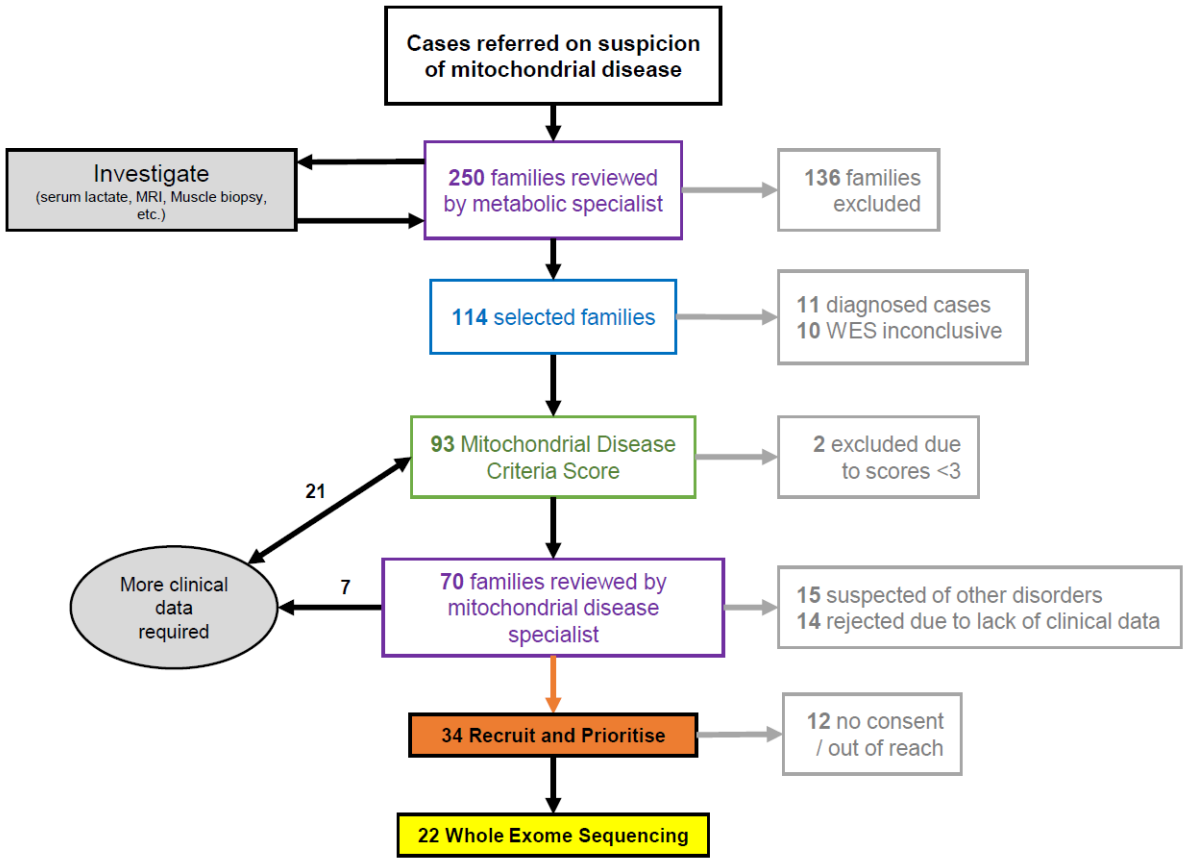

Figure 3.2 Flowchart outlining filtration and selection scheme of patients suspected of mitochondrial disease in Kuwait for the study cohort

The flowchart outlines how candidate cases from Kuwait are reviewed, investigated and excluded at different stages of the recruitment process. Cases referred to the Kuwait Medical Genetics Centre are reviewed and investigated by a metabolic specialist and cases were excluded based on clinical opinion. Selected families were then excluded based on genetic analysis status and the remaining were reviewed and scored with the MDC. Cases not pending investigation results, nor excluded based on score, were reviewed by a mitochondrial disease specialist. Cases were either excluded, investigated, or approved for the study based on clinical expertise in the field. Approved cases were prioritised and recruited, but some cases were not reachable or consent for research was not obtained resulting in a reduction in number of cases recruited.

Categories	Muscular	CNS	Multisystem	Metabolic / Imaging	Tissue Findings
Highly Suggestive Findings (2 points each)	Ophthalmoplegia Facies myopathica	Developmental regression Ataxia		MRI suggestive Elevated CSF lactate **Elevated serum lactate**	RCC enzyme deficiency* Reduced COX staining** Ragged red fibres** Abnormal mitochondria/ EM
Suggestive Findings (1 point each)	Hypotonia Muscle Weakness Exercise intolerance Rhabdomyolysis Abnormal EMG	Epilepsy Pyramidal Signs Extrapyramidal Signs Brainstem involvement Abnormal EEG	Haematology GI Tract (dysmotility) Heart (abnormal ECHO or arrythmia) Kidney (Fanconi's syndrome) Liver Vision (retinitis pigmentosa or optic neuropathy) Hearing (SNHL) Neuropathy (axonal) Failure to thrive Family history	Elevated pyruvate Elevated L/P ratio Elevated alanine Abnormal urine organic acids MRI symmetric lesions MRI cerebral atrophy MRS elevated lactate	Reduced SDH staining
Max Limit	**2**	**2**	**3**	**4**	**4**

Figure 3.3 Mitochondrial disease criteria used to score presentations and investigation results of patients referred to the study.

CSF; cerebrospinal fluid; CNS: central nervous system; COX: Cytochrome *c* oxidase; EEG: electroencephalogram; EM: electron microscopy; EMG: electromyogram; GI tract: gastrointestinal tract; ECHO: echocardiogram; RCC: respiratory chain complex; SNHL: sensorineural hearing loss. Scores 2-4: possible mitochondrial disease; Scores 5-7: probable mitochondrial disease; Scores ≥8: definite mitochondrial disease. * 2 points for isolated complex deficiency, 4 points for multiple complex deficiency. ** 4 points each

Scoring using these criteria emphasised highly suggestive findings paving the way to compile and score cases to recruit for the study. Based on the Morava *et al.* (2006) criteria, maximum limits are placed for all categories. This resulted in the sacrifice of criteria sensitivity to mitochondrial disease in order to maintain high specificity towards mitochondrial disease characterisation. The maximum limits were not changed for any of the categories.

3.3.1.2.1 Neuromuscular / CNS

The first category scores Neuromuscular presentations and highlights ophthalmoplegia and facies myopathica as presentations highly associated with mitochondrial disease. The second category scored central nervous system (CNS) presentations and investigational findings were developmental regression and ataxia in patients were emphasised as highly suspected of mitochondrial disease involvement. The first two categories each had a maximum of 2 points each to avoid inflation of scores in these categories where multiple presentations and findings are not necessarily suggestive of mitochondrial disease only but other disorders as well.

3.3.1.2.2 Multiple system involvement

The third category scored the involvement of multiple systems in patient presentations. Organs included high energy dependent organs such as the heart, GI tract, kidneys, and liver. Affected functions commonly associated with mitochondrial disease such as vision and hearing were also included along with neuropathy, failure to thrive and a family history of mitochondrial disease. This category's maximum limit is set to 3 to account for multisystem involvement in scored patients without inflating the score. That is to say, once multisystem involvement is established there is no additional diagnostic benefit from simply scoring more organ involvement

3.3.1.2.3 Metabolic and Imaging

The fourth category scores "Metabolic and Imaging" findings after investigations. This includes blood, cerebrospinal fluid (CSF) and urine investigations along with MRI neuroradiological scans. Elevated lactate in blood and CSF were highlighted as findings highly associated with mitochondrial disease. MRI findings suggestive of mitochondrial disease involvement such as Leigh syndrome and basal ganglia disease were also highly associated with mitochondrial disease (Lake *et al.*, 2016). The maximum limit for this category was set to 4 to account for investigative results.

3.3.1.2.4 Tissue findings

The fifth and final category was modified compared to the Morava criteria that focused solely on cell morphology in tissue samples. The category scores "Tissue findings" and includes respiratory chain enzyme activities in tissue, which deficiencies are likely indicators of mitochondrial disease in patients in addition to reduced staining of complex IV, ragged red fibres, and electron microscope findings showing abnormal mitochondrial structures. The maximum limit for this category was also set to 4.

3.3.1.2.5 Scoring patients

Highly suggestive findings score 2 points each, while suggestive findings score 1 point each. Morphological findings of reduced complex IV activity and ragged red fibres score 4 points each as they are clear indicators of mitochondrial disease (Zafeiriou *et al.*, 1995). As suggested by the Morava criteria, the scores were grouped into 3 categories. Scores between 2 and 4 points suggest a possible mitochondrial disease involvement, a score between 5 and 7 points suggest probable mitochondrial disease involvement, and a score of 8 and greater suggest definite mitochondrial disease involvement.

Mitochondrial disorders fall under the umbrella of inborn errors of metabolism (IEM) disorders often with overlapping clinical features such as axial hypotonia, developmental delay and failure to thrive. Consequently, patients were thoroughly investigated at KMGC to exclude any other IEM disorders prior to consideration for the study.

Most mitochondrial diagnostic criteria heavily relied on functional and biochemical findings from patient biopsy samples, which were not always available for this patient cohort. As biopsy investigations are not routinely performed in Kuwait, we were concerned that his would influence the scoring system, depleting patient scores and suggestive of no mitochondrial disease involvement. To compensate for this in the recruitment process, more emphasis was placed on the availability of radiological MRI findings and corresponding clinical presentations suggestive of mitochondrial disease such as bilateral symmetric involvement of the basal ganglia, brainstem, corpus callosum, and the cerebellum (Lake *et al.*, 2016). The availability of laboratory and test results supported candidacy of patients for recruitment. Consequently, the adapted version of the Morava criteria relied more on the first four categories that can be reported, investigated and scored in most patients. Only a few referred cases had muscle biopsies collected and

analysed which heavily increased their chances of recruitment based on the biopsy findings.

3.3.1.2.6 Paediatric neurologist review

The highest scoring patients were further reviewed by a paediatric neurologist and one of my Ph.D. supervisors, Prof Robert McFarland, a specialist in mitochondrial disease based at the Wellcome Centre for Mitochondrial Research Newcastle University. This allows the input of longstanding clinical expertise to select those patients most likely to have a mitochondrial disease and where possible, classify them further on clinical grounds e.g., Leigh Syndrome, Congenital Progressive External Ophthalmoplegia (CPEO), mtDNA depletion syndrome (MDDS) as well as confirming selected patients or excluding cases that were suggestive of disorders other than mitochondrial disease. Many patients were excluded from the study due to the lack of clinical data, laboratory findings or radiological imaging.

On a number of occasions, the metabolic specialist at KMGC shortlisted several mitochondrial disease patients and invited Prof McFarland to Kuwait to view the cases in clinic. This resulted in the recruitment of a further seven families to our study. The cases were scored, and consent was obtained for recruitment. DNA from probands and their family members was extracted from peripheral blood and sent to the Wellcome Centre from Mitochondrial Research (WCMR) in Newcastle. Proband DNA samples were submitted to unbiased WES.

3.4 Results

3.4.1 Clinical reports of recruited patients

This section describes the clinical phenotypes and finding of patients recruited in our cohort.

3.4.1.1 Family 1

Patient 1-I (MDC score: 7) was a Kuwaiti Arab Bedouin female patient born to consanguineous first cousin parents. She was born by normal delivery at 37 gestation weeks with birth weight of 2.9 kg. She presented from birth with hypertrophic cardiomyopathy with echocardiography showing ventricular hypertrophy and small arterial septal defect (ASD). At the age of 4 months, she was considered to be developmentally delayed and was noted to have generalised hypotonia, abnormal hearing, nystagmus, and was found to have a pericardial effusion. Brain MRI scan showed a thin corpus callosum. She passed away at the age of 1 year and 2 months and the cause of death was not reported. She had 2 affected older brothers who also passed away early in life. No mtDNA mutations were reported for Patient 1-I.

The older (affected) brother of I-1 (Patient 1-II; MDC score: 11) was born at full term after an uneventful pregnancy with birth weight of 2.9 kg. He was developmentally delayed from early life only being able to hold his head and show a social smile at 6 months. After his immunisation at 6 months, he became febrile and floppy. His development progressed slowly achieving the ability to roll at the age of 1 year and later developed hearing problems and nystagmus. Severe hypotonia was later noted with normal reflexes and he was fitted with hearing aids and started wearing glasses. Blood investigations showed a slight increase in lactate, thyroid stimulating hormone (TSH) and uric acid levels and mildly elevated aspartate aminotransferase (AST) level. A muscle biopsy was obtained from the patient and respiratory chain enzyme activity analysis showed reduced overall activities in complexes I to IV. There are conflicting reports on whether he developed hypertrophic cardiomyopathy. He passed away around the age of 2 years and 9 months and the cause of death was not reported.

The younger (affected) brother of I-1 (Patient 1-III; MDC score: 5) was born at 36 weeks gestation with birth weight of 2.7 kg. His mother had gestational diabetes. He presented with concentric cardiomyopathy from birth, showed developmental delay, and became

hypotonic with episodes of lactic acidosis with elevated pyruvate and increased lactate to pyruvate ratio. In addition, blood investigations revealed elevated Creatine Kinase (MM and MB), ALT, and 3-β-hydroxybutyrate levels increased as well. He passed away around the age of 1 year and 3 months and the cause of death was not reported.

Upon comparison of presentations and progress of disease in the affected siblings of this family, the proband and her younger brother presented more similarly than their older affected brother.

3.4.1.2 Family 2

Patient 2 (MDC score: 10) is a 5 year-old Jordanian Arab female patient living in Kuwait born to consanguineous paternal first cousin parents. She was born at full term with birth weight 3.0 kg. Family history revealed multiple neonatal deaths. The patient was exclusively breast fed. Around the age of 1 month, the patient developed excessive crying with abnormal movements for 3 days before becoming lethargic and admitted to the hospital. She developed 2 episodes of general tonic-clonic seizures during her admission and were controlled by IV phenobarbitone. CSF lactate (3.83 mmol/l), blood lactate (7.33 mmol/l) and blood pyruvate (111 μmol/l) were all elevated with a significantly high lactate/pyruvate ratio (66) reported. CT head scan at 1 month showed areas of hypodensity in the central brain stem and thalami suggestive of a metabolic disorder. The EEG rhythms in the awake state were slow but there was no evidence of epileptiform discharges. This finding supported the suggestion of metabolic disease involvement.

MRI brain scan at 1 month showed bilateral symmetric high T2 signals in the lentiform nuclei (sparing the caudate), pons and medulla oblongata suggestive of mitochondrial disease involvement (**Figure 3.4**). The patient was started on L-carnitine, coenzyme Q, Thiamine and a ketogenic diet. Blood lactate levels normalised during the following month. Sequencing of mtDNA in Patient 2 did not identify any pathogenic variants.

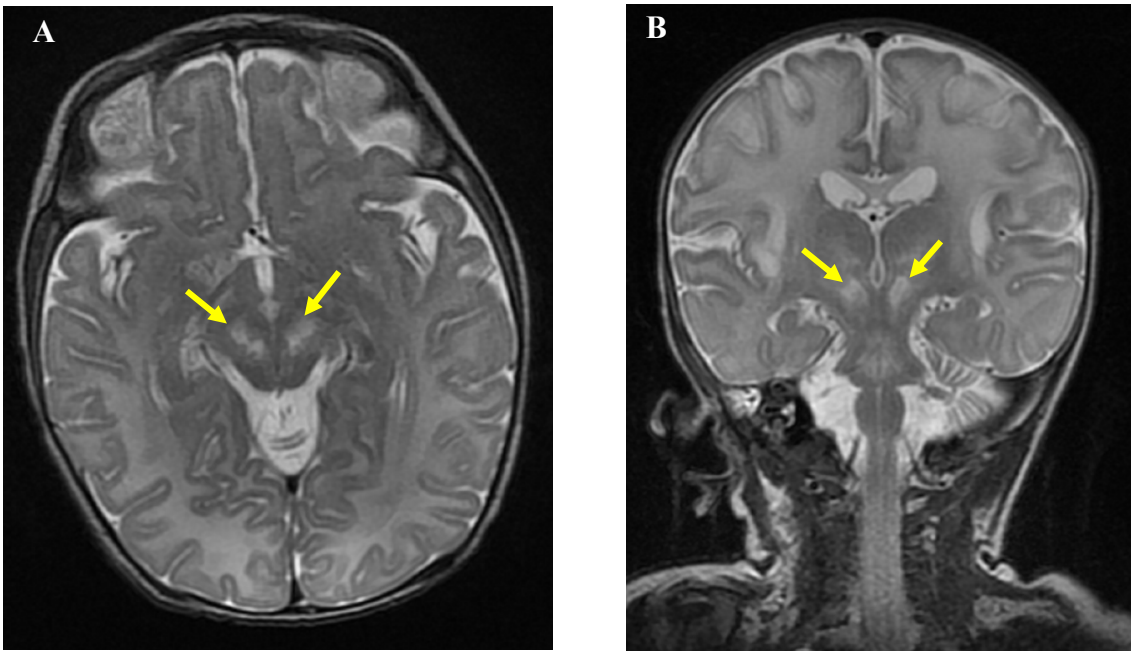

Figure 3.4 Brain MRI neuroradiological images for Patient 2

Axial (**A**) and coronal (**B**) MRI brain scan images for Patient 2 at 1 month showing bilateral symmetric T2 signals in the thalami (yellow arrows)

3.4.1.3 Family 3

Patient 3 (MDC score: 7) is a 10 year-old Syrian Arab male patient living in Kuwait born to consanguineous first cousin parents. He was born at full term by normal delivery with birth weight 3.2 kg and Apgar scores of 9 and 10 at 1 minute and 5 minutes respectively. He presented from birth with seizures and tachypnoea accompanied by elevated CK and alanine levels in blood, elevated lactate in both CSF and blood (>13 mmol/L) and elevated blood pyruvate levels resulting in a high lactate/pyruvate ratio. Developmental delay was noted from the second month of life and hypotonic limbs with persistent lactic acidosis were later observed at the age of 5 months. He had a generalised tonic-clonic seizure at the age of 5 years.

Brain MRI scan at 5 years revealed T1, T2 and FLAIR signals in the upper pons and midbrain of the left side and bilateral signals in globus pallidus with involvement of internal capsule. Restricted diffusion also reported bilaterally in globi pallidi. Thinning of the posterior part of the corpus callosum was also reported along with mild dilatation of lateral and third ventricles. The EEG report noted abnormal background activity and focal epileptic form abnormalities. He experienced episodes of recurrent lactic acidosis

that were controlled using sodium bicarbonate. No mtDNA mutations were reported for Patient 3. Family history revealed Patient 3 has an older affected brother who presented with a similar phenotype.

3.4.1.4 Family 4

Patient 4-I (MDC score: 8) was the first-born Syrian Arab female child to consanguineous first cousin parents who live in Kuwait. She was born at full term by normal delivery after an uneventful pregnancy with birth weight of 3.6 kg. She was investigated in Syria for hypertrichosis at the age of 2 years and was diagnosed with congenital adrenal hyperplasia prompting treatment with oral hydrocortisone; this clinical diagnosis was later revoked when serum cortisol, 17 hydroxyprogesterone, androstenedione and testosterone levels were normal before and after adrenocorticotropic hormone (ACTH) stimulation test. At 2 years and 8 months, she was noted to have developmental delay with body measurements below the 5th centile (weight: 9.5 kg, height: 83 cm; head circumference: 46 cm. She was slightly hypotonic with reduced DTRs; besides synophrys and hirsutism no dysmorphic features were noted. Measured serum lactate was slightly elevated (2.8 mmol/l). An MRI brain scan at 2 years 9 months showed bilateral high T2 signals involving the caudate nuclei, cerebral peduncles, dorsal midbrain, colliculi and distal medulla. Furthermore, high T2 signals in the cerebellar white matter just below the level of middle cerebellar peduncles at the region of dentate nuclei were also reported. At 3 years and 5 months, she was noted to exhibit a long philtrum, hypertelorism, brachycephaly, mild clinodactyly, generalised hypertrichosis and normal female genitalia. At 4 years and 6 months, she developed a severe pneumonia requiring intubation and assisted ventilation, but unfortunately, she passed away.

Her first younger brother, Patient 4-II (MDC score: 9), was born at full term after an uneventful pregnancy with birth weight of 3.5 kg. He was healthy until the age of 2 months when he became floppy and started to lose weight. At 12 months, he was noted to have delayed development, hypotonia with hyporeflexia, generalised muscle weakness, muscle wasting and failure to thrive. His body measurements were all below the 5th centile. Serum lactate was elevated on several occasions (over 3.0 mmol/l). An MRI brain scan at 15 months showed diffuse cerebral atrophy and high signal intensity lesions involving the cerebral peduncles, periaqueductal grey and the cerebral white matter. His development started to regress and became bed bound. His vision and feeding were deteriorating, and he developed ophthalmoplegia, ptosis, bulbar weakness, and wasting

and weakness of all muscles. He was socially interactive but had a clear intellectual disability. A follow-up MRI brain scan at 20 months revealed changes in deep white matter of frontal, parietal, temporal and occipital lobes as well as increased signal intensity in cerebral peduncles, dorsal brain stem, cerebellar white matter and dentate nuclei. He was admitted in an unconscious state shortly after this MRI scan but recovered after 3 days of assisted ventilation on the paediatric intensive care unit. He later developed hypoventilation associated with bradycardia. His respiration deteriorated until he passed away at the age of 21 months.

Their younger affected brother, patient 4-III (MDC score: 7), was born at 37 gestation weeks by emergency caesarean section due to oligohydramnios complication during pregnancy. His birth weight was 3.0 kg with Apgar scores of 8 and 9 at 1 minute and 5 minutes respectively He was doing well until the age of 14 months when his development started to regress, and he became spastic. Serum lactate levels were elevated (4.2 mmol/l) and an MRI brain scan at 18 months showed bilateral symmetrical high T2 and T2-FLAIR signal areas in deep cerebellar white matter, deep pyramidal tract of lower pons, medulla and in midbrain (**Figure 3.5**). At 19 months, he presented with ptosis, hypertonia in both upper and lower limbs with hypotonic neck and axial muscles and was microcephalic (head circumference below 3rd centile). Investigations confirmed elevated lactate levels (3.75 mmol/l) and uncovered elevated levels of pyruvate (173 μmol/l), creatine kinase (540 U/L), and creatinine (84 μmol/l). He arrested suddenly and passed away at home.

No mtDNA mutations were reported for any of the patients from family 4.

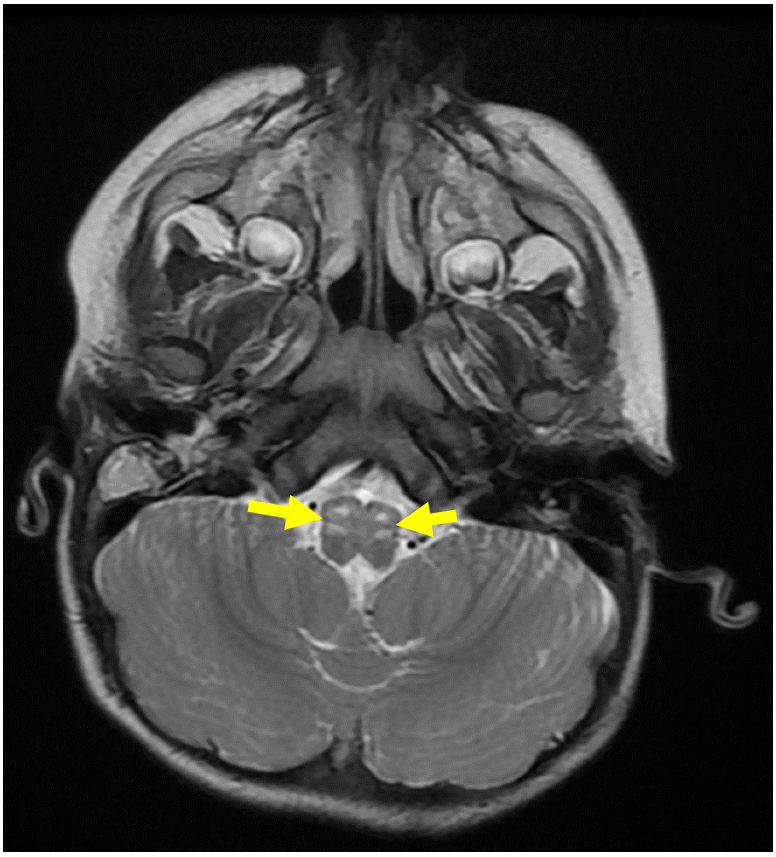

Figure 3.5 Brain MRI neuroradiological image for Patient 4-III.

Axial MRI image of Patient 4-III at 18 months showing bilateral symmetric high T2-FLAIR signals in the medulla oblongata (yellow arrows).

3.4.1.5 Family 5

Patient 5-I (MDC score: 8) is a 13 year-old Arab Bedouin male patient born at full term to consanguineous first cousin parents who live in Kuwait. His delivery was by caesarean section due to pre-eclampsia with birth weight 3.2 kg followed by an uneventful postnatal period. He was repeatedly admitted with a wheezy chest and gastro-oesophageal reflux disease (GORD). At 3 months, he was admitted due to recurrent seizures presenting as cyanosis and apnoea and was diagnosed with epilepsy. He was started on Phenobarbitone to control his seizures and domperidone and cimetidine to treat his GORD. He stopped his medication at the age of 2 with no reports of seizures or GORD thereafter. At 6 months, he was presented with lactic acidosis and was started on Thiamine and sodium bicarbonate. At 15 months, he was reported to have global developmental delay and only started walking at the age of 2 years; he did not form sentences until the age of 9 years.

At 4 years, his weight was at the 50th centile and his head circumference was <5th centile. Routine blood investigations were normal except for elevated lactate (4.5 mmol/l). At 13 years, he was noted to have a short stature, thin body habitus, mild brachycephaly and mild dysmorphic features with no facial weakness. No mtDNA mutations were reported for Patient 5-I.

The younger brother, Patient 5-II (MDC score: 9), is a 9 year-old male patient born full term by caesarean section due to breech presentation with birth weight 3.520 kg. He was admitted to NICU for 12 days due to transient tachypnoea of the newborn and lactic acidosis. His serum lactate and ammonia levels were elevated (9.2 mmol/l and 124.9 μmol/l respectively). His ammonia levels normalised but his serum lactate remained slightly elevated at 3.15 mmol/l. At 1 month, he was diagnosed with GORD and was started on domperidone and ranitidine. For his lactic acidosis, he was also started on sodium carbonate and commenced a ketogenic diet. At 13 months he was noted to be hypotonic, had global developmental delay (delayed gross motor skills and speech), and had mild dysmorphic features. He started walking at 22 months but by 30 months he was frequently falling especially while running. At 9 years, he was noted to have a short stature, thin body habitus and mild brachycephaly.

Their younger sister, patient 5-III (MDC score: 5), is a 2 year-old female patient that was admitted to the NICU due to respiratory distress, cyanosis and reluctance to feed; she was diagnosed with GORD. By the age of 7 months, she had repeat attacks of lactic acidosis. She was started on Thiamine and sodium bicarbonate in an attempt to treat the lactic acidosis and is now on a ketogenic diet managed by a dietician.

3.4.1.6 Family 6

Patient 6 (MDC score: 6) was an Egyptian Arab male patient born to consanguineous first cousin parents who live in Kuwait. His mother had pregnancy induced hypertension but gave birth to him at full term with a birth weight of 2.7 kg with no neonatal issues reported. At 4 months of age, he presented with nystagmus, myopia and hypotonia. At 18 months he experienced a seizure attack. At 20 months he was diagnosed with bilateral sensorineural hearing loss and was fitted with hearing aids 2 months later. By the age of 2 years, the patient was noted for midfacial hypoplasia and was developmentally delayed (delayed speech, only sounds). At 3 years, he was admitted due to hypoglycaemia and had metabolic acidosis. Laboratory tests revealed low blood glucose level (2.0 mmol/L,

normal range 3.9 - 7.1 mmol/L), elevated serum lactic acid (10 mmol/L) which normalised after the hypoglycaemic attack, elevated liver function enzymes ALT 187 IU/L and AST 225 IU/L (normal range < 40 IU/L for both), and urine organic acid showed significantly elevated adipic acid. An ECHO at 3 years revealed mild left ventricular hypertrophy, pericardial effusion, and minimal mid cavity obstruction. He later developed cataracts and subsequently developed vision loss. A brain MRI scan at 3 years showed mild reduction in brain volume. The patient developed another seizure attack at the age of 8 years and passed away shortly after; no report on the cause of death was available. No mtDNA mutations were reported for Patient 6.

3.4.1.7 Family 7

Patient 7-I (MDC score: 8) was a Syrian Arab female born to consanguineous second cousin parents. She was born at full term by caesarean section delivery due to breech position with a birth weight of 2.7 kg and Apgar scores of 2 at 1 minute, 7 at 5 minutes, and 9 at 10 minutes. She was admitted to the NICU for 7 days due to mild respiratory distress, subgaleal haematoma and jaundice. At 2 years, her development was delayed but no regression was noted. She continued to gain skills (walking, speech, vision and hearing) until the age of 4 years when she suddenly lost her ability to speak. She gradually lost her motor skills, developed progressive hypertonia, became ataxic then wheelchair-bound, and lastly developed dysphagia. According to her family, she still maintains her cognitive skills. Brain MRI scan at 7 years revealed bilateral symmetric high T2 signals and low T2 signals in the caudate and putamen (**Figure 3.6**). At 11 years, she was cachectic with dystonia and areflexia. She passed away soon after at the age of 11 years and 6 months. No mtDNA mutations were reported for Patient 7-I.

Her younger brother, patient 7-II (MDC score: 5), is a 10 year-old male who had normal development until the age of 9 years when he changed his preferred writing hand from the right to the left hand and then developed problems moving his right arm. He later developed slurred speech and ataxia. MRI brain scan at 9 years revealed bilateral symmetric high T2 signals in the lentiform nuclei, signals in the right caudate head, and signals in the left medulla oblongata all with corresponding high FLAIR signals and low T1 signals. At 10 years, he developed dystonia with increased tone, decreased power in shoulders and hips, and had generally slow movement and bradycardia.

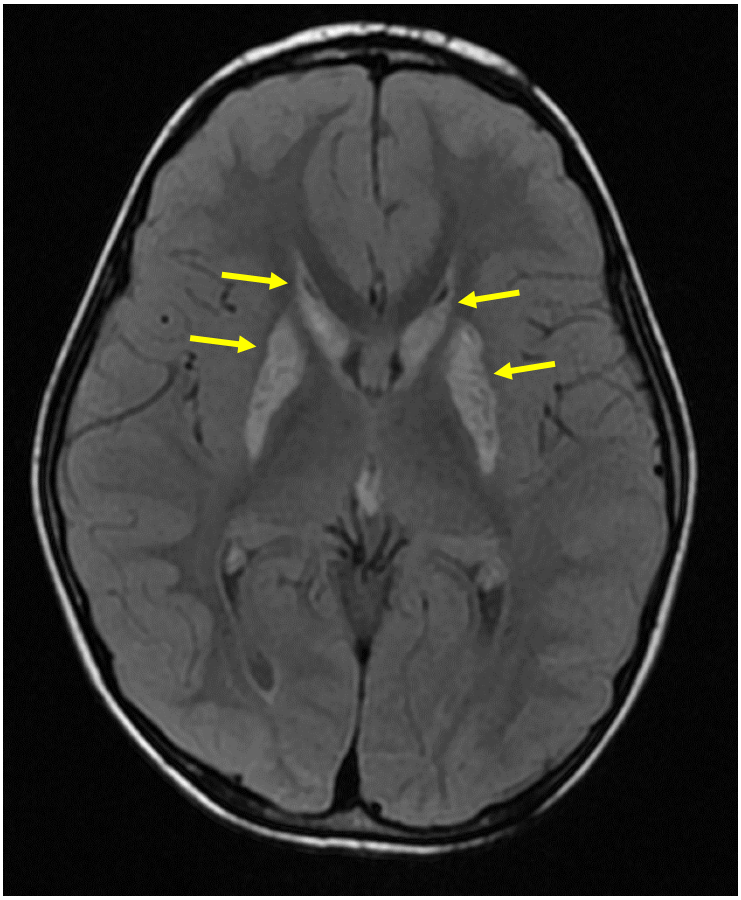

Figure 3.6 Brain MRI neuroradiological image for patient 7-I

Axial MRI image of Patient 7-I at 7 years showing bilateral symmetric high T2-FLAIR signals in the caudate and putamen (yellow arrows).

3.4.1.8 Family 8

Patient 8 (MDC score: 7) is a 2 year-old Kuwaiti Arab Bedouin female who is a product of an IVF pregnancy to consanguineous distant cousin parents. Her maternal cousin is reported to be blind. She presented with nystagmus at 4 months and a brain MRI scan result suggested possible optic neuritis. She improved after she was started on prednisolone. She had motor developmental delay and her CSF lactate was slightly elevated when measured (2.8 mmol/l). She was noted to be ataxic at 6 months with a follow-up MRI brain scan at 10 months revealed new bilateral bright T2-FLAIR signals in the subthalamic regions (**Figure 3.7**). At 2 years, she was noted to have a convergent strabismus and had hypotonic arms and legs. No mtDNA mutations were reported for Patient 8

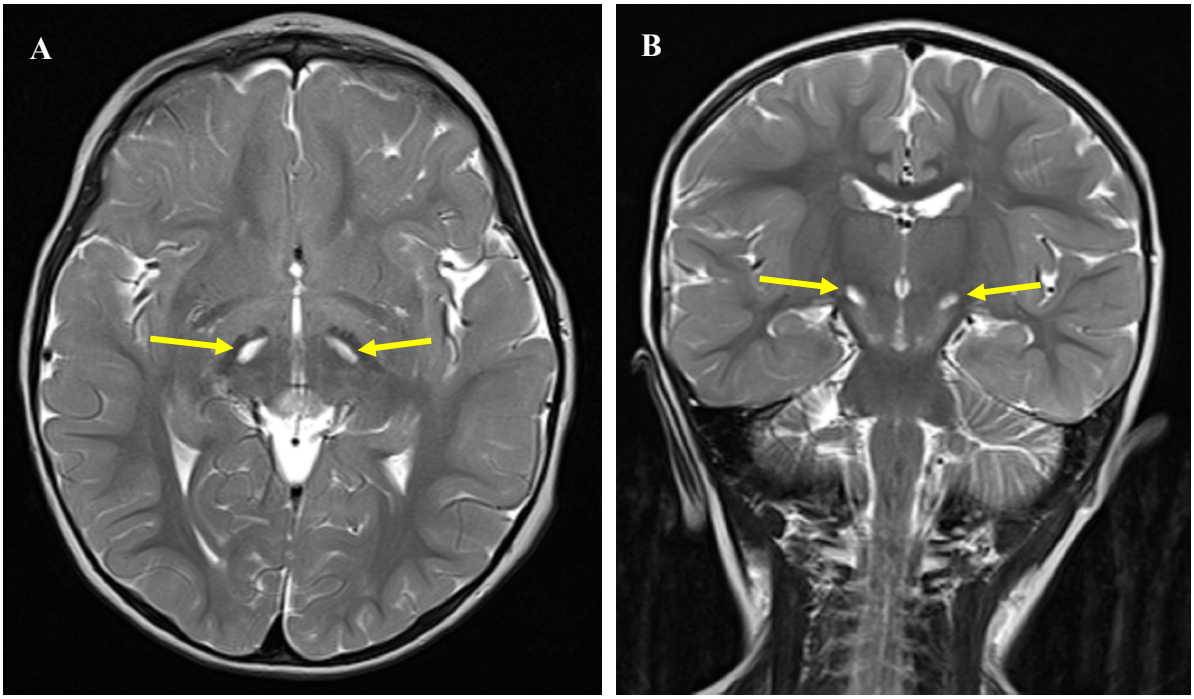

Figure 3.7 Brain MRI radiological images of Patient 8

Axial (**A**) and coronal (**B**) MRI images of Patient 8 at the age of 10 months showing bilateral symmetric high T2 signal in the sub thalamic region (yellow arrows).

3.4.1.9 Family 9

Patient 9 (MDC score: 9) is a 5 year-old Syrian Arab male patient born to consanguineous first cousin parents. He was born full term and was diagnosed antenatally to have intrauterine growth retardation (IUGR). At 5 months, his mother noticed his failure to thrive, and by 8 months he developed nystagmus and strabismus. MRI brain scan at 18 months revealed abnormal areas of white matter signal intensity in periventricular white matter as well as cerebellar white matter (**Figure 3.8**). At 2 years, he had developmental delay, failure to thrive and walked at 27 months. He was only saying 2 words at that time and later was diagnosed with have moderate to severe hearing loss. His lactate levels increased to 9.7 mmol/l after a period of fasting in preparation for an audiometry test; this was normalised using sodium bicarbonate and he was started on thiamine, L-carnitine and coenzyme Q supplements. At 5 years, he was noted for having a thin build, short stature, wearing glasses to correct hypermetropia, had alternating strabismus, nystagmus, blue sclerae, was hypotonic with muscle weakness affecting his shoulder and hip girdles, experiences fatigue during the day, and has a broad-based gait. No mtDNA mutations were reported for Patient 9.

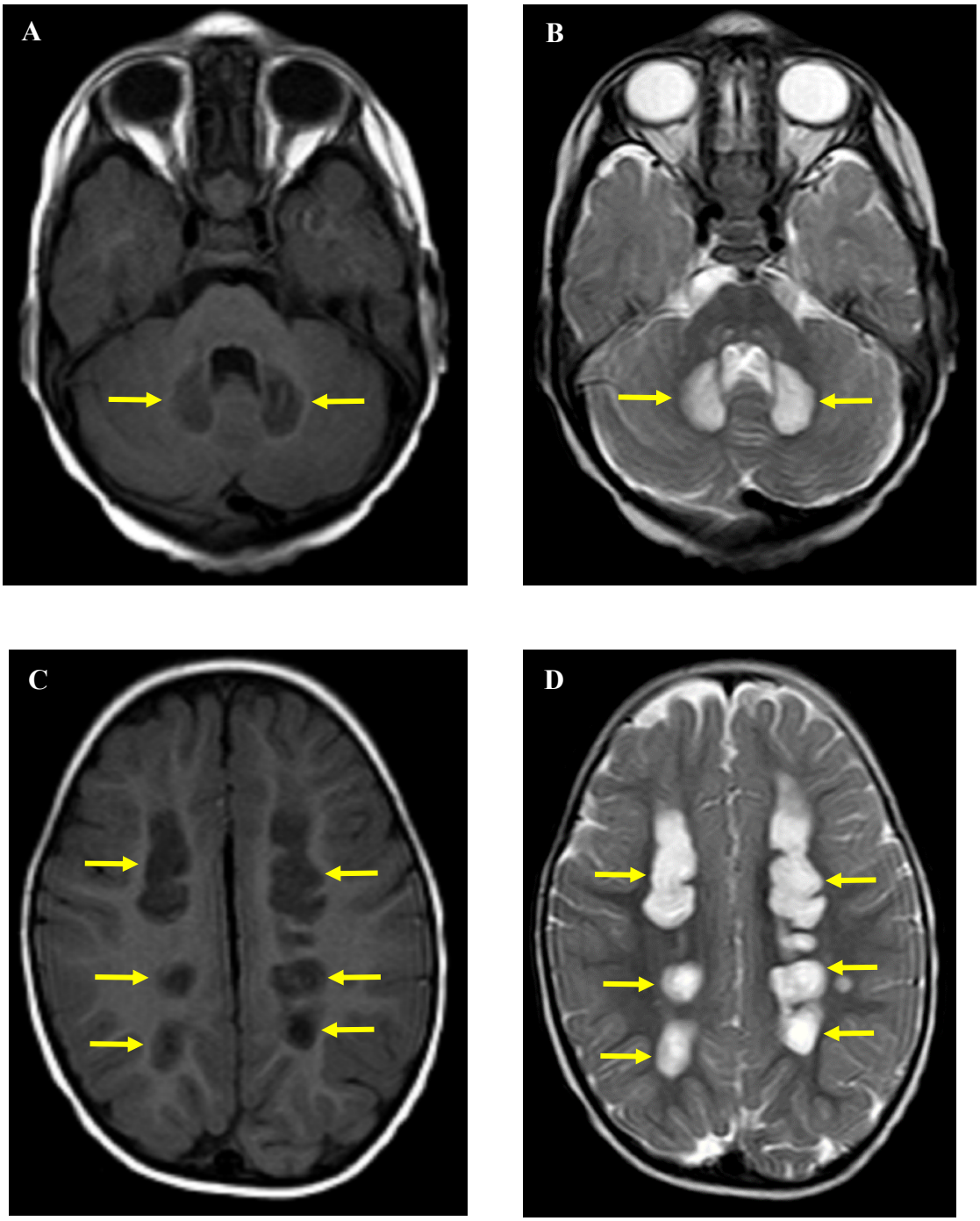

Figure 3.8 Brain MRI radiological findings in Patient 9

Axial MRI images of Patient 9 at 18 months showing bilateral symmetric low T1 signals (yellow arrows; **A** and **C**) and high T2 signals (yellow arrows; **B** and **D**) in the cerebellum (yellow arrows; **A** and **B**) and periventricular regions (yellow arrows; **C** and **D**).

3.4.1.10 *Family 10*

Patient 10 (MDC score: 5) is a 60 year-old Kuwaiti female with non-consanguineous parents. She presented at 34 years with bilateral ptosis and progressive external ophthalmoplegia; a surgery to correct her ptosis was done at the age of 40 years. She experienced post-operative pain in the left side of her face; thereafter, she reported impaired sensation in the same area. She reported difficulty chewing and choking at times which required her to adjust her diet. She had mildly spasticity in her lower limbs with a stiff (not ataxic) gait, experienced exercise intolerance and fatigue, had weak proximal muscles, and experienced constipation for which she took laxatives.

3.4.1.11 Family 11

Patient 11-I (MDC score: 8) is a 6 year-old Kuwaiti Arab Bedouin female born to consanguineous first cousin parents. Delivery was by caesarean section followed by an uneventful neonatal period with birth weight of 3.0 kg. She had an epileptic episode at age of 4 months and later presented with global developmental delay, hypotonia, epilepsy, and lactic acidosis. She is microcephalic and has micrognathia. She also has bilateral hearing loss; mild hearing loss in the right ear and moderate hearing loss in the left ear. MRI brain scan at 4 months reported severe cortical atrophy, hypomyelination of frontal, occipital and temporal lobes with calcification of basal ganglia. CT head scan 4 months reports multiple bilateral symmetrical foci of calcification in both basal ganglia and thalami and bilateral periventricular regions and left cerebellum suggestive of a metabolic disorder. No mtDNA mutations were reported for Patient 11-I

The medical report of the Patient 11-I's older sister, Patient 11-II (MDC score: 4), reported she was born after an uneventful pregnancy with birth weight 3.0 kg and was kept in the incubator for 1 day. At 5 months of age, she presented with microcephaly, dysmorphic features, developmental delay and hepatitis. She also presented with spasticity and brisk DTRs with clonus and had large ears. Patient 11-II passed away and the age and cause of death were not available.

Patient 11-I has an affected 5 year-old female double first cousin, Patient 11-III (MDC score: 6), whose parents are also consanguineous first cousins; Patient 11-III's mother is the full-sister of Patient 11-I's mother and the cousin's father is the first cousin of both the Patient 11-I's mother and father. Patient 11-III was born at full term by caesarean section with no perinatal issues and birth weight of 3.0 kg. At the age of 2 years and 2 months,

for a period of 2-3 weeks, she presented with sudden jerky movements during her sleep which lasted 2-3 minutes and occurred 2-3 times a day. Frequency increased to 10 times a day accompanied by nystagmus both vertical and horizontal. Poor feeding and reduced activity reported by parents along with increased irritability. No fever, diarrhoea, vomiting, head trauma, cyanosis, or intake of medication reported. Blood test revealed mild increase in lactate (2.78 mmol/l) and CBC test showed lymphocytic leucocytosis. CT head scan reported prominent sulci and ventricular cyst and an MRI brain scan reported brain atrophy.

3.4.1.12 Family 12:

Patient 12 (MDC score: 7) is a 6 year-old Kuwaiti Arab male born to non-consanguineous parents. Delivery was at full term by caesarean section following an uneventful pregnancy with birth weight 3.71 kg and no neonatal issued reported. He developed progressive stiffness in his limbs, trunk and head from the age of 1 month. By 3 months, he had difficulties starting a feed, had poor social interaction as he did not make eye contact or smile to his mother or caretakers, and was crying excessively but without any reported seizures. He had generalised hypertonia and hyperreflexia and serum and CSF lactate levels were slightly elevated (3.1 mmol/l and 3.0 mmol/l respectively). MRI brain scan at 3 months showed abnormal diffuse white matter signal. At 5 months, he was noted to start following with his eyes and smile, but he also became dystonic when irritable or crying. He was treated with Clonazepam and later commenced Baclofen; the dosage was gradually increased as he got older. At 11 months he started recognising and interacting with his parents and had stranger anxiety. Follow-up MRI brain scan at 3 years revealed diffuse high T2-FLAIR signal in the white matter and noted a thin corpus callosum (**Figure 3.9**). A muscle biopsy was taken at 19 months and showed mild histochemical changes not suggestive of mitochondrial disorder. Nonetheless, he was started on a mitochondrial cocktail including L-carnitine (300 mg, twice a day), coenzyme Q (5 mg twice a day), and vitamin C (100 mg twice a day). mtDNA analysis on DNA extracted from peripheral blood and muscle did not identify the m.3243A>G or m.8344A>G variants. At 3 years 5 months, the patient had a febrile seizure due to a respiratory infection and was started on Phenobarbitone. He had recurring generalised tonic-clonic seizures 6 months later prompting the increase in Phenobarbitone, yet he continued to have seizures at a rate of about once a month.

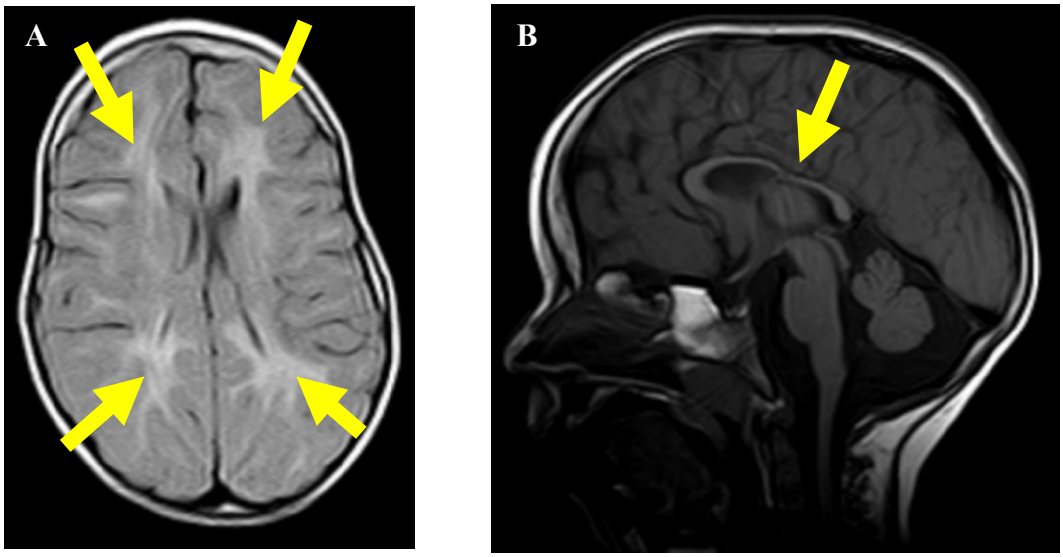

Figure 3.9 Brain MRI neuroradiological images for Patient 12

MRI brain scan for Patient 12 at 3 years
A Axial T2-FLAIR image showing high signal in the white matter near the ventricle horns (yellow arrows)
B Sagittal T1 image highlights thinning of the corpus callosum (yellow arrow)

3.4.1.13 *Family 13*

Patient 13 (MDC score: 9) is a 15 year-old Kuwaiti Persian male born to consanguineous first cousin parents. He was born full term by caesarean section with birth weight 3.5 kg. Apgar scores were 2 at 1 minute and 5 at 5 minutes and he was ventilated for 9 hours after birth. He was found to have bilateral hydronephrosis and was diagnosed to have posterior urethral valve and was operated on when he was 2 weeks old. He had developmental delay since early infancy; he sat at the age of 1 year, walked at 6 years, exhibited delayed speech and a low IQ. He developed unilateral ptosis that was corrected at 6 years. At 15 years, he was noted to have a short stature, synophrys, mild turricephaly, had bilateral cataracts which were removed, was generally weak and had an abnormal EMG disclosing non-irritative myopathy in his weak and wasted shoulder and hip girdle muscles. He also had secondary sexual characteristics such as facial and axillary hair and gynaecomastia. Family history revealed the patient has a similarly affected paternal aunt.

3.4.1.14 Family 14

Patient 14-I (MDC: 8) is a 21 year-old Kuwaiti Arab Bedouin female patient and firstborn to consanguineous parents from the same tribe. Following a normal pregnancy, she was born at full term after a long labour and required resuscitation, but persistent ventilation was not required; her birth weight was 2.8 kg. At the age of 1 month, her parents became concerned reporting minimal movement of her limbs, but she was aware of her surroundings. At 5 months, she presented with global developmental delay, generalised hypotonia, and muscle wasting. An MRI at the age of 20 months revealed cerebral atrophy and an EEG at the age of 3 years showed abnormal background activity that was slow for her age. Auditory test results were unremarkable, and EMG and nerve conduction studies were unremarkable too. ECG and ECHO results were also unremarkable.

The patient had slow development and by the age of 8 years she presented with microcephaly (<3rd centile), failure to thrive (weight <3rd centile), bilateral ptosis and ophthalmoplegia, myopathic face, generalised muscle wasting, diminished DTRs, and most notably developed choreoathetotic movements. Haematological and biochemical profiles including lactate, ammonia, and creatine kinase levels were within normal range. Furthermore, peroxisomal, lysosomal, blood and urine amino acids, and urine organic acid studies were all unremarkable.

By the age of 13 years, choreoathetoid movements in her arms, hands, and fingers were clearly noted in addition to contractures in both her knees. Both horizontal and vertical gaze palsy were noted, and subsequent ophthalmological tests revealed bilateral tigroid fundi with a small halo to each disc, high myopia (>-20.00), and VEP results revealed macular pathway dysfunction suggesting the patient had moderate to poor levels of vision. Brain MRI at 13 years confirmed generalised reduction of cerebral white matter bulk and EEG showed a slow rhythm. Spinal curvature emerged over several years; likely a consequence of truncal hypotonia, continued growth and weakness to the extent that she was unable to support herself when sitting. She underwent surgery in the UK to correct the scoliosis with spinal rods. The patient lost her motor skills after the spinal surgery.

Upon suspicion of underlying genetic disease by specialists in the UK, various genetic tests were performed including chromosomal karyotyping and targeted gene sequencing of *POLG* (on suspicion of Alpers-Huttenlocher syndrome) but all results were normal. A

muscle biopsy was obtained for analysis, and results showed myopathy with a mild generalised increase of lipids in muscle fibres while respiratory chain enzyme activities were normal. By the age of 19 years, the patient had developed epilepsy that was controlled by sodium valproate.

The patient has 4 healthy siblings and one affected brother (Patient 14-II; MDC score: 5) who is 9 years old and was born at 36 weeks after an uncomplicated pregnancy with a birth weight of 2.3 kg. The mother noticed he was hypotonic with head lag and constipation from the first month of life. At the age of 13 months, he was noted to be developmentally delayed with microcephaly (2^{nd} centile) and he presented with choreiform flicking movements which his mother noticed were increasing in frequency and severity. Hypotonia was noted in the neck, shoulders and trunk in addition to muscle weakness in the upper limbs. The patient had problems with all automatic reactions. EMG and nerve conduction studies were unremarkable. Blood sugar and lactate levels were within normal range. Brain MRI scans at 6 months and 14 months both revealed mild generalised reduction of white matter.

A number of genetic tests were requested to rule out suspected genetic disorders. Patient results for karyotyping, Prader-Willi and Angelman syndrome methylation, Fragile X testing, *SMN1* exons 7 and 8 deletions, and array-CGH were all normal. A muscle biopsy was obtained from the patient and respiratory chain enzyme test revealed a marginal loss of complex IV activity. Histological tests showed non-specific mild myopathic features with slow hypotrophy and increased fibre size variation. No evidence of structural congenital myopathy was identified. Upon suspicion of mitochondrial disease involvement, mtDNA analysis was undertaken for mutations associated with neuropathy, ataxia and retinitis pigmentosa/ maternally inherited Leigh Syndrome (NARP/MILS), MELAS and MERRF and results were unremarkable.

Patient 14-II's carnitine profile and very long chain fatty acid levels in blood were normal. Blood sugar and lactate levels were normal, and CSF protein, sugar, and lactate levels were also normal. Other CSF tests assessed amino acid, monoamine metabolites, dihydrobiopterin, and 5-methlytetrahydrofolate on suspicion of which were all normal. Urinary glycosaminoglycan and reducing substance tests were normal, urine amino acid test showed an increase in taurine levels, and urine purine screen showed no sulphocysteine. Urine organic acids revealed ketosis with dicarboxylic aciduria, elevated

levels of homovanillic and vanillomandelic acids, with generalised tricarboxylic acid cycle stress.

3.4.1.15 Family 15

Patient 15 (MDC score: 8) was a Kuwaiti Arab Bedouin female born to consanguineous paternal first cousin parents, born at term following a normal pregnancy and birth weight 3.2 kg. She was the third of six siblings. Her growth and development progressed normally, but at the age of 6 years and 6 months, she developed a febrile illness and was diagnosed with influenza H1N1 infection. She was treated with Tamiflu and improved, however shortly after she became lethargic and sleepy staying in bed most of the day for days at a time. 3 months later, while visiting Thailand for medical investigations, she developed seizures. EEG records and brain MRI scans were both unremarkable. She returned to Kuwait and her lethargy became exaggerated and she would sleep for 10 days and then function normally for a couple of days after which she would sleep for another group of days. At the age of 7 years, she collapsed while playing on a trampoline and was having trouble breathing and likely suffered a cardiac arrest. She was taken to the nearest hospital within approximately 25 minutes and was revived but later suffered four more episodes of cardiac arrest. A brain MRI scan showed evidence of hypoxic ischaemic damage with global cerebral and deep grey matter involvement with preserved brainstem and cerebellar function. She was boarded to Great Ormond Street Hospital (GOSH) in London, UK, for further management. Investigations identified she had cardiomyopathy and was suggested to have an underlying metabolic disorder. Neurological assessment confirmed she sustained severe hypoxic ischaemic brain damage and had severe visual impairment, but her hearing seemed intact. She developed dystonia, was fitted with a PEG due to her feeding problems and was noted have labile blood pressure. On examination, she had contractures affecting her arms (flexed at the elbows and wrists), her legs were extended, and she had scoliosis. Further assessment revealed she had significant GORD. A muscle biopsy was taken, and respiratory chain enzyme activity assay revealed low complex IV activity.

3.4.1.16 Family 16

Patient 16 (MDC score: 10) is a 10 year-old Kuwaiti female patient born to consanguineous first cousin Kuwaiti parents. She was born at 29 gestation weeks as one of triplet IVF pregnancy with a birth weight 1.340 kg and Apgar scores 9 at 1 minute and

10 at 5 minutes. She developed respiratory distress and was monitored in the NICU for 3 days and treated with surfactants I and V. Her motor and cognitive skills development were delayed and a brain MRI scan at 9 months showed delayed myelination and prominent CSF spaces. She developed strabismus at the age of 1 year which was operated on and corrected. She did not achieve independent walking until the age of 3 years, a skill which she subsequently lost at the age of 5 years. In addition, she developed ptosis, dysphagia, and spastic diplegia. Blood lactate was repeatedly elevated (6-10 mM) and so were potassium levels. ECHO at 6 years was unremarkable, her dysphagia subsided, and her cognitive skills remain mildly delayed, but she has a very good memory. By the age of 10 years, she had developed bilateral ophthalmoplegia with minimal movement in any direction with no facial weakness, had truncal muscle weakness leading to her inability to rise from lying down to sitting without support and had increased tone in both legs with brisk DTRs in both lower limbs. No mtDNA mutations were reported for Patient 16.

3.4.1.17 Family 17

Patient 17 (MDC score: 4) is a 7 month-old Egyptian male, fourth of four children born to non-consanguineous parents. He was born by elective caesarean section due to maternal hypertension during pregnancy and his birth weight was 2.7 kg. At the age of 2 months, he developed afebrile seizures in the form of generalised spasms, head nod, and flexion of trunk and hips which occurred in clusters 6 - 7 times per day; he was well in between episodes. Seizures were controlled by Levetiracetam and adrenocorticotropic hormone treatments for 20 days that was later switched to Vigabatrin for 20 days and then switched to Topiramate. His seizures continued into the age of 4 months reducing to 4 - 5 clusters per day. A brain MRI scan was unremarkable, but EEG records showed multifocal epilepsy. Investigations revealed persistent elevated serum lactate (3.4 - 7.1 mM), elevated pyruvate (255.1 μM), and lactic aciduria. Liver function and serum glucose levels were unremarkable. On examination at 7 months of age, he was noted to be well nourished with no dysmorphic facial features, but he had gross motor developmental delay and an exaggerated head lag.

3.4.1.18 Family 18

Patient 18-I (MDC score: 12) was a male patient born to consanguineous (distant relatives) Kuwaiti parents. No problems were reported during the pregnancy and he was born at full term with a birth weight of 3.75 kg. He was floppy and slow to respond at

birth and was later noted to be developmentally delayed as he did not fixate, nor follow and did not acquire a social smile. At 3 months of age, he had recurrent seizures in the form of up-rolling eyes and tonic-clonic movements of the upper limbs and was admitted to the hospital due to chest infections and seizures. Neurological findings showed he had spastic paraplegia with increased deep tendon reflexes (DTRs), and he was not following or responding to external stimuli. Laboratory test showed elevated CSF lactate (5.1 mmol/L, normal range 0.6 - 2.2 mmol/L), persistent elevated serum lactate (4.0 - 15.0 mmol/L, normal range 0.5 - 2.2 mmol/L), and elevated pyruvate (144 μmol/L, normal range 41 - 67 μmol/L). A brain MRI scan showed basal ganglia involvement and biochemical analysis of respiratory chain enzyme activity in a muscle biopsy showed complex I and IV activities were deficient. Patient 18-I passed away around the age of 1 year with cause of death report available.

Family history revealed Patient had 2 older brothers who presented with a similar phenotype (suggestive of Leigh syndrome) and passed away. One of the decease brothers was boarded to the UK where they investigated respiratory chain enzyme activity in a muscle biopsy and identified complex I and IV deficiency. They have 3 living sisters who developed similar symptoms having developmental delay, epilepsy, microcephaly and clasp knife rigidity. Brain MRI scan of one of the affected sisters revealed bilateral symmetric abnormal signals in the lateral aspect of the putamen. The affected siblings have 2 healthy sisters.

Patient 18-II (MDC score: 7) was a male patient and the double first cousin of Patient 18-I (their mothers are sisters, and their fathers are brothers). He was born at full term by normal delivery with a birth weight of 3.25 kg and he presented with mild jaundice but no other neonatal issues. He had a seizure at the age of 8 months and was noted to be developmentally delayed on examination. He was not following, presented with a head lag, mild hypertonia in the upper limbs with generalised hyperreflexia. A brain CT scan showed hypoattenuation involving the head of the caudate and anterior aspect of the putamen along with mild cerebral atrophy. He was prescribed phenobarbitone to control his seizures but sadly passed away around the age of 1 year with no record of cause of death available. Patient 18-II had an affected brother who presented with a febrile illness early in life and passed away around the age of 1 year. Brain MRI scan suggested post-encephalitis brain atrophy and respiratory chain enzyme activity in a muscle biopsy showed complex IV deficiency. The deceased siblings have an older, affected sister (28

years old) who has had seizures since the age of 4 years, is developmentally delayed, had an ataxic gait, and developed kyphoscoliosis at the age of 10 years. Brain MRI scan showed she had diffuse minimal cerebral atrophy, and respiratory chain enzyme activity in muscle tissue showed no deficiency. The affected siblings have 3 healthy younger brothers.

3.4.1.19 Family 19

Patient 19 (MDC score: 5) is a 7 year-old Kuwaiti male born to non-consanguineous parents at full term by normal delivery after an uneventful pregnancy with birth weight 3.0 kg. At 5 months, he had a 'staring look' when awakening and developed recurrent myoclonic jerks in his left leg. He was started on Phenobarbitone to treat the abnormal movements he developed. EEG records were abnormal, but a brain MRI scan was unremarkable. Auditory assessment reported bilateral impaired hearing for which he was fitted with hearing aids, and an ophthalmology assessment due to poor eye contact identified hypermetropia and he was prescribed glasses. At 16 months, his Phenobarbitone was halted and replaced by Sodium Valproate and had was noted to be global developmental delay. He developed intractable seizures at the age of 5 and a half years and his Sodium Valproate dose was increased. On examination, he was reported to be microcephalic, had a stereotypic movement of the head, had a spastic gait, and had increased tone in legs with brisk DTRs. Investigations into serum lactate, ammonia, electrolytes, thyroid function, and complete blood count revealed unremarkable results.

He gradually developed autistic behaviours including self-mutilation (hand biting) and was prescribed Risperidone. At the age of 7 years, he was examined and was reported to be irritable, bilateral toe walking gait with support, and had left convergent strabismus. No mtDNA mutations were reported for Patient 19.

3.4.1.20 Family 20

Patient 20 (MDC score: 6) is an 8 year-old Omani male born to consanguineous parents (first cousins once removed). He was born with a low birth weight indicating intrauterine growth restriction. He has global developmental delay, failure to thrive, congenital cataracts, generalised hypotonia, and a brain MRI scan at 2 years revealed mild cerebral atrophy. Serum lactate (1.8 mM) and CK levels (82 mM) were within normal range. Family history revealed similarly affected relatives including a younger sibling presenting

with primary microcephaly, generalised hypotonia, congenital cataracts, and developmental delay with difficulty in learning.

3.4.1.21 Family 21

Patient 21-I (MDC score: 6) was a Yemeni female, second born to consanguineous first cousin parents, born at full term by caesarean section. Her birth weight was 4.0 kg and she had no reported neonatal issues. At the age of 21 months, she developed recurrent fever attacks associated with intractable seizures that later became afebrile seizures leading to status epilepticus. She was developmentally delayed, had general hypotonia, and investigations revealed elevated liver enzymes in the blood (AST and GGT). EEG results showed an abnormal record and a brain MRI scan revealed encephalitis suggestive of viral aetiology. The patient passed away at the age of 26 months with no known cause reported.

Her younger sister, Patient 21-II (MDC score: 6) is 1 year-old and was born by normal delivery. At 6 months of age, she developed infantile spasms and a brain MRI scan was unremarkable. The patient's spasms were controlled until the age of 1 year when she developed an episode of severe infection and septic shock after which she developed uncontrollable epilepsy in the form of generalised tonic-clonic seizures and abnormal eye movements. She suffered from convulsive and non-convulsive status epilepticus. Brain MRI scan at 1 year revealed global cerebral atrophy and bilateral signal changes involving the thalami, caudate nuclei, globus pallidi, post-parietal cortical and subcortical regions, midbrain, pons, and cerebellum. Radiological findings were suggestive of a mitochondrial disease involvement. Investigations revealed normal findings for serum amino acid and acylcarnitine profiles, urine organic acids, and CSF lactate, protein and glucose. EEG results showed severely abnormal records.

3.4.1.22 Family 22

Patient 22-I (MDC score: 6) is a 17 year-old Kuwaiti female born to consanguineous maternal first cousin parents. She was born at full term by normal delivery with no pregnancy or neonatal issues reported and her birth weight was 2.5 kg. At the age of 9 years, she developed an unsteady gait, tremor, and impaired communication skills. She developed scoliosis and myopia for which she was prescribed glasses. She was fitted with a brace for her scoliosis in the USA. EMG results were suggestive of an axonal/demyelinating neuropathy. Genetic analysis using microarray-CGH revealed

multiple duplication regions in chromosome Xq28 (75kb and 88kb) not previously reported in association with disease. Family history revealed multiple relatives with short stature.

Her younger sister, Patient 22-II (MDC score: 4), is a 13 year-old female born at full term with a history of oligohydramnios near the end of pregnancy, and her birth weight was 3.1 kg. At the age of 10 years, she became easily fatigued and on examination was noted to have a thin build with failure to thrive, but psychomotor development was normal for her age. ECHO revealed mild to moderate concentric left ventricular hypertrophy.

3.5 Summary of recruited families and cases

The presentations and findings of all the patients were tabulated to help review and compare the available information amongst the selected and recruited patients. Clinical presentations of the patients are tabulated in **Table 3.1**, available investigation results are tabulated in **Table 3.2**, and available neuroradiological findings are tabulated in **Table 3.3**.

Table 3.1 Table of clinical presentations in patients recruited for the study

(continued on next page).

						Muscle										CNS			Pyramidal		Extra Pyramidal		Brain Stem			Cerebellum	Audi -tory	
Patient	MDC	Sex	Family History	Age at onset (months)	Consanguinity	Hypotonia	Spasticity	Ptosis	Ophthalmoplegi	Dysmorphic	Muscle wasting	Muscle Weakness	Muscle fatigue	Failure to thrive	Brachycephaly	Microcephaly	Dev delay	Dev regress	Epilepsy	Hypertonia	DTR	Dystonia	Athetosis/ Chorcoathetosis	Nystagmus	Dysphagia	Strabismus	Ataxia	Bilateral Hearing Loss	Notes
1-I	5	F	+	Birth	+	+	-	-	-	-	-	-	-	-	-	-	+	-	-	-	-	-	-	+	-	-	-	+	
1-II	11	M	+	7	+	+	-	-	-	+	+	-	-	+	-	-	+	-	-	-	-	-	-	+	-	-	-	+	Constipation
1-III	7	M	+	4	+	+	-	-	-	-	-	-	-	-	-	-	-	-	-	-	-	-	-	-	-	-	-	-	
2	10	F	+	1	+	+	-	-	-	-	-	-	-	-	-	-		-	+	-	-	-	-	-	-	-	-	-	
3	7	M	-	Birth	+	+	-	-		-	-	-	-	-	-	-	+		+	-	-	-	-	-	-	-	-	-	
4-I	8	F	+	24	+	-	-	-	-	+	-	-	-	+	-	-	+	-	-	-	D	-	-	-	-	-	-	-	
4-II	9	M	+	2	+	+	-	+	+	-	+	+	-	+	-	-	-	+	-	-	-	-	-	-	-	-	-	-	
4-III	7	M	+	14	+	+	+	+	+	-	-	-	-	+	-	-	-	+	-	-	-	-	-	-	-	-	-	+	-	
5-I	8	M	+	Birth	+	+	-	-	-	+	-	-	-	-	+	-	+	-	-	-	-	-	-	-	-	-	-	-	Short stature, GORD
5-II	9	M	+	3	+	+	-	-	-	+	-	-	-	-	+	-	+	-	+	-	-	-	-	-	-	-	-	-	Short stature, GORD
5-III	5	F	+	N/A	+	-	-	-	-	-	-	-	-	-	+	-	+	-	-	-	-	-	-	-	-	-	-	-	
6	6	M	+	4	+	+	-	-	-	+	-	-	-	-	-	-	+	-	+	-	-	-	-	+	-	-	-	-	Myopia,
7-I	8	F	+	54	+	-	+	-	-	-	+	-	-	+	-	-	-	+	-	-	-	+	-	-	+	-	+	-	
7-II	5	M	+	108	+	-	-	-	-	-	-	-	-	-	-	-	-	+	-	-	-	-	-	-	-	-	+	-	Dysarthria
8	7	F	-	4 months	+	+	-	-	-	-	-	-	-	-	-	-	+	-	-	-	-	-	-	+	-	+	+	-	
9	9	M	-	N/A	-	+	-	-	-	-	-	-	-	+	-	-	+	-	-	-	-	-	-	+	-	-	-	-	IUGR
10	5	F	-	34 years	-	-	-	+	+	-	-	+	+	-	-	-	-	-	-	-	-	-	-	-	-	-	-	-	
11-I	8	F	+	4	+	+	-	-	-	-	-	-	-	-	-	+	+	-	+	-	-	-	-	-	-	-	-	+-	Micrognathia
11-II	4	F	+	5	+	-	+	-	-	+	-	-	-	-	-	+	+	-	-	-	B	-	-	-	-	-	-	-	Hepatitis
11-III	6	F	+	26	+	-	-	-	-	-	-	-	-	-	-	-	-	-	-	-	B	-	-	+	-	-	-	-	Jerky during sleep

Patient	MDC	Sex	Family History	Age at onset (months)	Consanguinity	Hypotonia	Spasticity	Ptosis	Ophthalmoplegia	Dysmorphic features	Muscle wasting	Muscle weakness	Muscle fatigue	Failure to thrive	Brachycephaly	Microcephaly	Dev delay	Dev regress	Epilepsy	Hypertonia	DTR	Dystonia	Athetosis/ Choreoathetosis	Nystagmus	Dysphagia	Strabismus	Ataxia	Bilateral Hearing Loss	Notes
12	7	M	-	1	+	+	-	-	-	-	-	-	-	-	-	-	+	-	+	-	-	-	-	-	+	+	-	-	
13	9	M	+	Birth	+	+	-	+	-	+	+	-	-	-	+	-	+	-	-	-	-	-	-	-	-	-	-	-	Hydroureteronephrosis
14-I	8	F	+	1	+	+	-	+	+	+	+	-	-	+	-	+	+	+	+	-	D	-	+	-	-	-	-	-	Scoliosis, myopia, pale optic discs, peripheral neuropathy
14-II	5	M	+	5	+	+	-	-	-	-	-	-	-	+	-	+	+	-	-	+	-	+	-	-	-	-	-	-	
15	8	F	-	N/A	+	-	-	-	-	-	-	-	-	-	-	-	-	-	-	-	-	-	-	-	-	-	-	-	
16	19	F	+	N/A	+	-	+	+	+	-	-	-	-	-	-	-	+	-	-	-	D	-	-	-	+	-	-	-	Cerebral palsy
17	4			3	-	-	-	-	-	-	-	-	-	-	-	-	-	-	-	-	-	-	-	-	-	-	-	-	
18-I	12	M	+	3	+	-	+	-	-	-	-	-	-	-	-	+	+	-	+	-	Ex	-	-	-	-	+	-	-	
18-II	7	M	+	8	+	-	-	-	-	-	-	-	-	-	-	-	+	-	+	+	-	-	-	-	-	-	-	-	
19	5	M	-	1	-	-	+	-	-	-	-	-	-	-	-	-	+	-	+	-	B	-	-	-	-	-	-	-	
20	6	M	+	N/A	+	+	-	-	-	-	-	-	-	+	-	+	+	-	-	-	-	-	-	-	-	-	-	-	Cataracts
21-I	6	F	+	21	+	+	-	-	-	-	-	-	-	-	-	-	+	-	+	-	-	-	-	-	-	-	-	-	
21-II	6	F	+	6	+	-	-	-	-	-	-	-	-	-	-	-	-	-	+	-	-	-	-	+	-	-	-	-	
22-I	6	F	+	108	+	-	-	-	-	-	-	-	-	-	-	-	+	-	-	-	-	-	-	-	-	+	-	-	Tremor, scoliosis, myopia, F/H short stature
22-II	4	F	+	120	+	-	-	-	-	-	-	-	+	+	-	-	-	-	-	-	-	-	-	-	-	-	-	-	

B: brisk ; CNS: central nervous system; D: diminished; DTR: deep tendon reflexes; Ex: exaggerated; MDC: Mitochondrial Disease Criteria; N/A: not available

Table 3.2 Table of investigation results of patients recruited for the study

(continued on next page).

						Auditory		Vision	Heart	Metabolic					CNS	PNS	Muscle Biopsy	
Patient	MDC	Sex	Family History	Age at onset (months)	Consanguinity	SNHL	Conductive hearing loss	Visual Acuity	Cardiomyopathy	Elevated serum lactate	Elevate serum pyruvate	Elevated Alanine	Elevated CSF lactate	Abnormal urine organic acids	Abnormal EEG	Abnormal EMG	Reduced OXPHOS activity	Notes
1-I	5	F	+	Birth	+	-	-	-	+	-	-	-	-	-	-	-	-	
1-II	11	M	+	7	+	-	-	+	-	+	-	-	-	+	-	-	CI, CII, CIII, CIV	
1-III	7	M	+	4	+	-	-	-	+	+	-	-	-	-	-	-	-	
2	10	F	+	1	+	-	-	-	-	+	+	-	+	-	+	-	-	
3	7	M	-	Birth	+	-	-	-	-	+	+	-	+	-	+	-	-	
4-I	8	F	+	24	+	-	-	-	-	+	-	-	-	-	-	-	-	
4-II	9	M	+	2	+	-	-	-	-	+	-	+	-	-	-	-	-	
4-III	7	M	+	14	+	-	-	-	-	+	+	-	-	-	-	-	-	Elevated CK, creatinine
5-I	8	M	+	Birth	+	-	+	-	-	+	-	-	-	-	-	-	-	
5-II	9	M	+	3	+	-	+	-	-	+	-	-	-	-	+	-	-	
5-III	5	F	+	N/A	+	-	-	-	-	+	-	-	-	-	-	-	-	
6	6	M	+	4	+	+	-	+	+	+	-	-	-	-	-	-	-	hypoglycaemia, metabolic acidosis
7-I	8	F	+	54	+	-	-	-	-	-	-	-	-	-	-	-	-	
7-II	5	M	+	108	+	-	-	-	-	-	-	-	-	-	-	-	-	
8	7	F	-	4	+	-	-	-	-	-	-	-	+	-	-	-	-	
9	9	M	-	N/A	-	+	-	-	-	+	-	-	-	-	-	-	-	
10	5	F	-	34 years	-	-	-	-	-	-	-	-	-	-	-	-	-	
11-I	8	F	+	4	+	-	-	-	-	-	-	-	-	-	-	-	-	
11-II	4	F	+	5	+	-	-	-	-	-	-	-	-	-	-	-	-	
11-III	6	F	+	26	+	-	-	-	-	+	-	-	-	-	-	-	-	

						Auditory		Vision	Heart	Metabolic					CNS	PNS	Muscle Biopsy	
Patient	MDC	Sex	Family History	Age at onset (months)	Consanguinity	SNHL	Conductive hearing loss	Visual Acuity	Cardiomyopathy	Elevated serum lactate	Elevate serum pyruvate	Elevated Alanine	Elevated CSF lactate	Abnormal urine organic acids	Abnormal EEG	Abnormal EMG	Reduced OXPHOS activity	Notes
12	7	M	-	1	-	-	-	-	-	+	-	-	+	-	-	+	-	
13	11	M	+	Birth	+	-	-	+	-	-	-	-	-	-	-	+	-	Hydroureteronephrosis
14-I	8	F	+	1	+	-	-	+	-	-	-	-	-	-	+	-	CIV	lactic aciduria
14-II	5	M	+	5	+	-	-	-	-	-	-	-	-	+	-	-	-	
15	8	F	-	N/A	+	-	-	-	+	-	-	-	-	-	-	-	CIV	
16	19	F	+	N/A	+	-	-	-	-	+	+	-	-	-	-	-	-	elevated anion gap
17	4			3	-	-	-	-	-	+	+	-	-	-	-	-	-	
18-I	12	M	+	3	+	-	-	+	-	+	+	+	-	-	-	-	CI, CIV	
18-II	7	M	+	8	+	-	-	+	-	+	-	+	-	-	-	-	CI, CIV	
19	5	M	-	1	-	+	-	-	-	-	-	-	-	-	-	-	-	
20	6	M	+	N/A	+	-	-	-	-	-	-	-	-	-	-	-	-	
21-I	6	F	+	21	+	-	-	-	-	-	-	-	-	-	+	-	-	Elevated AST/GGT
21-II	6	F	+	6	+	-	-	-	-	-	-	-	-	-	+	-	-	
22-I	6	F	+	108	+	-	-	-	+	-	-	-	-	-	-	+	-	
22-II	4	F	+	120	+	-	-	-	+	-	-	-	-	-	-	-	-	

CI: complex I; CIV: complex IV; CNS: Central Nervous System; CSF: cerebrospinal fluid; MDC: Mitochondrial Disease Criteria; N/A: not available; PNS: Peripheral Nervous System; SNHL: sensorineural hearing loss;

Table 3.3 Table of neuroradiological findings in patients recruited for the study

(continued on next page).

Patient	Sex	Scan type	Leukodystrophy	Cerebral atrophy	Corpus callosum	Ventricles/ periventricular	Semiovale	Basal ganglia	Globus pallidus	Internal capsule	External capsule	Thalamus	Substanita nigra	Midbrain	Pons	Cerebral peduncles	Medulla	Brainstem	Dentate nuclei	Cerebellum	MRS lactate peak	Notes
1-I	F	MRI	-	-	+	+	-	-	-	-	-	-	-	-	-	-	-	-	-	-	+	
1-II	M	MRI	-	-	-	+	+	-	-	-	-	-	-	-	-	-	-	-	-	-	-	
1-III	M	N/A																				
2	F	MRI	-	-	-	-	-	+	-	-	+	+	-	-	-	-	-	-	-	-	-	
3	M	MRI	-	-	+	-	-	-	+	+	-	-	-	+	+	-	-	-	-	-	+	Involving left hemisphere
4-I	M	MRI	+	-	-	-	-	-	-	-	-	-	-	-	-	-	-	-	-	-	-	
4-II	F	MRI	-	-	-	-	-	+	-	-	-	-	-	+	-	+	+	-	+	+	-	
4-III	M	MRI	-	+	-	+	-	-	-	-	-	-	-	-	-	+	-	+	+	-	-	
5-I	M	N/A																				
5-II	M	N/A																				
5-III	F	N/A																				
6	M	MRI	-	+	-	-	-	-	-	-	-	-	-	-	-	-	-	-		-	-	
7-I	F	MRI	-	-	-	-	-	+	-	-	-	-	-	-	-	-	-	-	-	-	+	
7-II	M	MRI	-	-	-	-	-	+	-	-	-	-	-	-	-	-	-	-	-	-	-	
8	F	MRI	-	-	-	-	-	-	-	-	-	+	+	-	-	-	-	+	-	-	-	
9	M	MRI	-	-	-	+	-	-	-	-	-	-		-	-	+	-	+	-	+	-	
10																						
11-I	F	CT/MRI	-	+	-	+	-	+	-	-	-	+	-	-	-	-	-	-	-	+	-	Calcification, Hypomyelination frontal, occipital, temporal lobes
11-II	F	N/A																				
11-III	F	MRI	-	+	-	-	-	-	-	-	-	-	-	-	-	-	-	-	-	-	-	

Patient	Sex	Scan Type	Leukodystrophy	Cerebral atrophy	Corpus callosum	Ventricles/ periventricular	Semiovale	Basal ganglia	Globus pallidus	Internal capsule	External capsule	Thalamus	Substantia nigra	Midbrain	Pons	Cerebral peduncles	Medulla	Brainstem/	Dentate nuclei	Cerebellum	MRS lactate peak	Notes
12	M	MRI	+	-	+	-	-	-	-	+	-	-	-	-	-	-	-	+	-	-	-	
13	M	MRI	-	-	-	-	-	-	-	-	-	-	-	-	-	-	-	-	-	+	-	Left side
14-I	F	MRI	-	+	-	-	-	-	-	-	-	-	-	-	-	-	-	-	-	-	-	
14-II	M	MRI	-	+	-	-	-	-	-	-	-	-	-	-	-	-	-	-	-	-	-	
15	F	MRI	-	-	-	-	-	-	-	-	-	-	-	-	-	-	-	-	-	-	-	Hypoxic ischaemic damage to cerebral and grey matter
16	F	MRI	-	-	-	+	-	-	-	-	-	-	-	-	-	-	-	-	-	-	-	delayed myelination, prominent CSF spaces
18-I	M	MRI	-	-	-	-	-	+	-	-	-	-	-	-	-	-	-	-	-	-	-	
18-II	M	MRI	-	+	-	-	-	+	-	-	-	-	-	-	-	-	-	-	-	-	-	
20	M	MRI	-	+	-	-	-	-	-	-	-	-	-	-	-	-	-	-	-	-	-	
21-I	F	MRI	-	-	-	-	-	-	-	-	-	-	-	-	-	-	-	-	-	-	-	encephalitis suggestive of viral infection
21-II	F	N/A																				
22-I	F	N/A																				
22-II	F	N/A																				

3.6 Discussion

Mitochondrial disease cases have been poorly diagnosed in Kuwait in the past 10 years. The tool of choice to genetically analyse and diagnose cases suspected of mitochondrial disease is Sanger sequencing of patient DNA that was extracted from peripheral blood. In a highly consanguineous population such as in Kuwait autosomal recessive diseases are likely more prevalent (Skladal *et al.*, 2003; Shawky *et al.*, 2013). A new approach was required to improve the diagnosis rates of mitochondrial disease cases in Kuwait. This initiated a collaboration with the Wellcome Centre for Mitochondrial Research, based at Newcastle University, where clinical and research staff have a wealth of knowledge and expertise in this specialised field.

For my PhD project, cases suspected of mitochondrial disease in Kuwait were recruited, reviewed and scored. The recruitment process required the review of many suspected cases, but many were excluded due to the lack of clinical history, lack of clinical follow-up, or lack of investigation results. Clinical history and progress of disease in patients was important during the recruitment process but some medical reports only contained a summary of presentations and investigation results from a single patient visit with no clinical history or follow-up afterwards. In addition, investigations such as blood investigations and neuroradiological imaging that could reveal highly suggestive findings that would increase the likelihood of recruitment were not requested. Another issue that was faced was families of patients suspected of mitochondrial disease involvement were either unreachable for a follow-up appointment to request investigations or they declined to attend a follow-up appointment at KMGC.

Cases from most recruited families had neuroradiological MRI findings that were either suggestive of mitochondrial disease involvement or showed cerebral atrophy or leukodystrophy. These findings played a major role in their recruitment since subjects who did not have neuroradiological findings were not prioritised and thus not recruited to the study. Blood and urine investigations also played a very important role in the recruitment process as their outcomes could be highly suggestive findings such as elevated blood lactate or elevated tricarboxylic acid cycle intermediates in urine. Results of CSF investigations are challenging to obtain, but elevated lactate in CSF is one of the key findings associated with mitochondrial disease. Only seven patients had a lumbar puncture performed and obtains results of CSF analyses including lactate levels. Even though muscle biopsies are a last resort to confirm mitochondrial disease involvement in

patients, muscle biopsies are not routinely obtained and analysed for mitochondrial disease in Kuwait which renders the fifth category of the utilised MDC of no use for almost all cases. Only a few cases had a muscle biopsy taken and analysed in the UK and findings supported their recruitment to the study.

The scoring of patient presentations and investigation results using the MDC scale helped identify missing clinical details that can be requested to support the suspicion of mitochondrial disease involvement. Family history of disease also influenced the recruitment of families with a few consanguineous families having multiple affected siblings raising their chances of recruitment.

The utilised MDC was developed using previously published criteria, but no extensive evaluation or validation of the MDC has been carried out. The utilised MDC could have been used to score published cases (be it of mitochondrial disease patients or known non-mitochondrial disease patients) to evaluate how accurately it can predict the suspicion of mitochondrial disease. Given the criteria categories used in the MDC, it is likely that patient scores might be skewed to increasing the suspicion of mitochondrial disease involvement. These steps could be carried out to help improve the utilised MDC, however the involvement of expert clinicians in the selection process helped overcome such an effect by using the MDC and genuinely select cases that are suspected of mitochondrial disease.

Diagnosing mitochondrial disease patient is a difficult task. Numerous studies attempted to utilise criteria in diagnosed mitochondrial disease cases to assess how successful they are in predicting diagnosis and assessed specificity and sensitivity of the criteria (Diogo *et al.*, 2009; Puusepp *et al.*, 2018; Witters *et al.*, 2018). No specific mitochondrial disease criteria are defined as the universal standard thus far. Predicting mitochondrial disease in patients is challenging and requires tools and expertise to assess and evaluate available clinical data and investigation results. The review of high MDC scoring cases by a mitochondrial specialist (Prof Robert McFarland) assisted in excluding cases and prioritising patients for WES analysis. It is important to point out that the chronological order of cases investigated was dependant on the time of review and recruitment from KMGC. Prioritisation based on high scoring cases occurred when there were a number of cases awaiting analysis; the highest scoring cases were prioritised for WES analysis. The method of WES investigations and the results of variant filtration are outlined and

presented in the next chapter (**Chapter 4**); segregation studies were also carried out when possible.

Chapter 4. Whole exome sequencing of paediatric patients from Kuwait suspected of mitochondrial disease

4.1 Introduction

Consanguineous marriages are common practice in many parts of the world with this preference estimated in at least 20% of the global population and more than 8.5% of children worldwide born to consanguineous parents (Modell and Darr, 2002). Consanguinity rates reaching and exceeding 50% have been reported in many Arab countries with rates of first cousin marriages exceeding 20% (Tadmouri *et al.*, 2009). Prevalence of inherited disorders among consanguineous populations is often higher than in non-consanguineous populations (Skladal *et al.*, 2003; Shawky *et al.*, 2013).. This has been observed in Kuwait where levels of consanguinity exceeding 50% have been reported (Al-Awadi *et al.*, 1985; Radovanovic *et al.*, 1999; Tadmouri *et al.*, 2009; Al-Kandari and Crews, 2011).

Genetic investigations into causative mutations in genetic disorders can be performed using a number of tools depending on available findings and history of disease in the family. Genetic analysis methods include the following: targeted gene sequencing of suspected genes; linkage analysis studies based on inheritance within a family; and homozygosity/autozygosity mapping within families of known consanguinity (Alkuraya, 2010; Ott *et al.*, 2015; Frazier *et al.*, 2019). High-throughput NGS is a set of powerful tools that have been a driving factor in diagnosing genetic diseases (Shendure and Ji, 2008). In human genetics, different NGS approaches that can be used to sequence specifically targeted genes (targeted gene panels), sequence the protein coding regions of the genome (WES and clinical exome sequencing), or sequence the full human genome (WGS) (**Figure 4.1**). NGS technology can sequence the 16.6 kb mitochondrial genome to identify mutations and targeted assessment of mtDNA heteroplasmy levels can also be determined using pyrosequencing. NGS technology amplifies the target DNA of choice (target gene panels, clinical exome sequencing, WES and WGS) and reads the sequenced in stretches of DNA 100-200 bp in length (Buermans and den Dunnen, 2014). These sequences are aligned to a reference human genome sequence, annotated with genetic information such as the location of the sequence within the genome, the location of a variant within a gene, and then analysed for *in silico* prediction of pathogenicity and

frequency of the variant within control databased such as gnomAD (Wadapurkar and Vyas, 2018). The NGS approach amplifies and sequences targeted regions of the genome multiple times (named read "depth") to determine its zygosity and the quality of the variant call by reading the variant multiple times and sometimes exceeding 100x reads. The technology also attempts to read all the targeted regions of the genome (named read "coverage") and advances in the technology have increased the percent coverage of WES from 80% to 95% (Lelieveld *et al.*, 2015). The cost of gene sequencing has dropped in the past two decades due to the introduction of NGS technologies and thus have become a first-tier approach to diagnosing patients suspected of genetic disorders (Wadapurkar and Vyas, 2018). However, NGS has limitations within these parameters as variants might be located outside the covered regions or the depth and quality of the read may be rendered as poor, and thus not called.

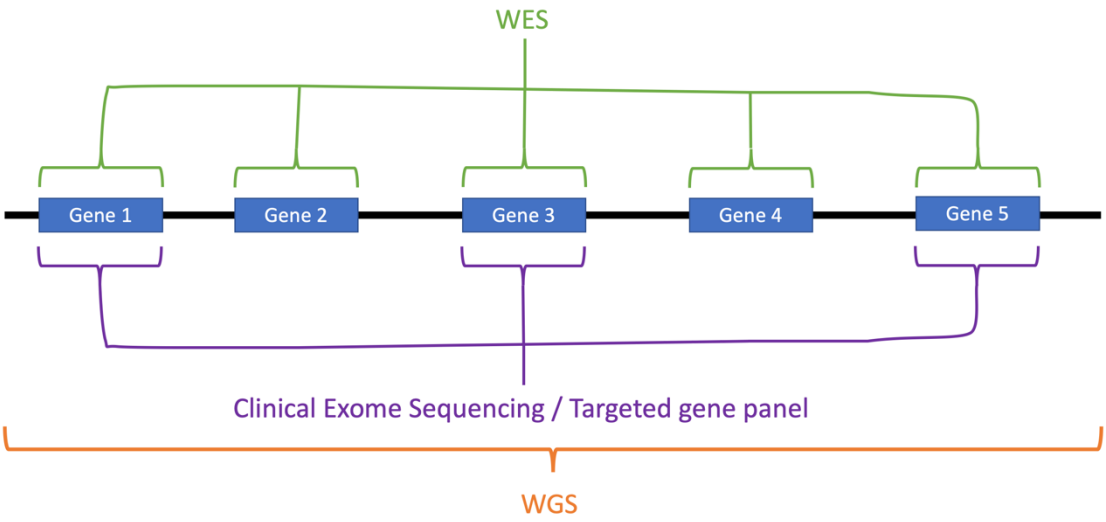

Figure 4.1 Genome regions targeted by different NGS techniques

All protein coding regions of the human genome are targeted and sequenced by the WES approach (green). Specific genes of interest are targeted and sequenced when using the clinical exome sequencing and targeted gene panel approaches (purple). The whole human genome is sequenced when the WGS approach is used (orange).

NGS tools have been utilised in diagnosing cases suspected of genetic disorders using targeted gene panel sequencing (Morgan *et al.*, 2010), WES (Choi *et al.*, 2009; Bolze *et al.*, 2010; Ng *et al.*, 2010), and WGS (Lupski *et al.*, 2010). Later studies employed NGS on patient cohorts with various clinical presentations and resulted in varying successful diagnosis rates within each study (Saunders *et al.*, 2012; Yang *et al.*, 2013; Gilissen *et al.*, 2014; Soden *et al.*, 2014).

Mitochondrial disease patients have been initially associated with mutations in mtDNA mutations, rearrangements and deletions in DNA from muscle and blood samples (Holt *et al.*, 1988; Wallace *et al.*, 1988; Goto *et al.*, 1990; Shoffner *et al.*, 1990). However, mtDNA mutations are not the sole source of pathogenicity in mitochondrial disease patients since mutations in nuclear encoded genes were also associated with mitochondrial disease (Endo *et al.*, 1989; Liu *et al.*, 1993; Bourgeron *et al.*, 1995). With 1,158 proteins associated with mitochondrial function, mutations in over 300 nuclear genes have been associated with disease so far (Stenton and Prokisch, 2020; Thompson *et al.*, 2020a). NGS methods, including WES and targeted gene panels, have been successful in identifying nDNA mutations in genes associated with mitochondrial function (Haack *et al.*, 2010; Gotz *et al.*, 2011; Calvo *et al.*, 2012). Studies that used WES on patient cohorts suspected of mitochondrial disease yielded diagnosis rates higher than 60% (Haack *et al.*, 2012; Lieber *et al.*, 2013; Taylor *et al.*, 2014; Wortmann *et al.*, 2015). NGS methods have a shorter turnover time for results compared to earlier approaches such as targeted gene sequencing, linkage analysis and homozygosity mapping since NGS methods identify the suspected mutations in each patient or family.

There have been numerous studies based in countries neighbouring Kuwait that utilised NGS technology to diagnose patient cohorts suspected of genetic disorders (Dixon-Salazar *et al.*, 2012; Alazami *et al.*, 2015; Yavarna *et al.*, 2015; Alfares *et al.*, 2017; Anazi *et al.*, 2017; Monies *et al.*, 2017). The cohorts of these studies were mostly from consanguineous families and the overall rate of diagnosis was 45% (Alahmad *et al.*, 2019). These cohort studies identified 178 novel candidate genes associated with disease including 14 gene associated with mitochondrial function most of which were identified in consanguineous families in the cohort. In addition, founder mutations in at least 10 genes associated with mitochondrial disease were identified in unrelated families.

4.2 Aims

The aim of this chapter is to describe the genetic analysis approach and outline the filtration of called variants in the recruited patients from 22 families. In cases with variants in previously reported genes, phenotype comparisons are performed to expand clinical spectrums of associated disease. Addressing aetiology of disease is also performed to elucidate pathogenicity in novel candidate genes as well and pathogenicity of novel variants identified.

4.3 Methods

4.3.1 Whole exome sequencing

Whole exome sequencing was performed as outlines in ***Section 2.2.5***.

4.3.2 In silico analysis of candidate gene variants

In silico analysis of the effect of detected variants were performed as outlines in ***Section 2.2.6***.

4.3.3 Sanger Sequencing

DNA for Sanger sequencing was extracted from peripheral blood of patients and their family members as described in ***Section 2.2.3***.

Sanger sequencing of the identified variants was performed as follows outlined in ***Sections 2.2.7***, ***2.2.8***, ***2.2.9***, ***2.2.10, 2.2.11***, ***2.2.12***, ***2.2.13*** and ***2.2.14***

4.3.4 Filtration of variants called in WES

A flowchart of the following description of the filtration process is outlined in **Figure 4.2**.

4.3.4.1 Rare or novel homozygous variants

Variants called in WES were filtered to identify protein coding variants that were novel or rare; rare variants have a minor allele frequency of less than 1% in the gnomAD and ESP6500 databases (Lek et al., 2016). Since the majority of families were consanguineous, variants were filtered for homozygous variants since autosomal recessive inheritance of variants was likely. Depending on the availability of an in-house exome variant database (consisting of results from 384 previous WES analysis results from a cohort of mitochondrial and neurological disease patients and controls that were analysed at Newcastle University), the results were filtered for variants that were not previously homozygous in the in-house exome database. This step helps narrow down the search for pathogenic variants in my cohort but can be omitted or modified to include variants with less than 4 reported homozygotes in the database due to presence of patients within the in-house exome database. The individuals in the in-house exome database are recruited in Newcastle and therefore will be of different ethnicity (likely European) compared to families in my recruited cohort. Due to high rates of consanguinity within the families, there might be polymorphic variants that have not been reported previously.

4.3.4.2 Mitochondrial proteins

The list of identified genes was filtered for proteins localising to the mitochondria and is listed in the MitoCarta2.0 database of mitochondrial proteins (Calvo et al., 2015). The panel of WES results were then filtered to eliminate homozygous variants identified in other patients in the panel (excluding relatives of the patient).

4.3.4.3 'In silico' predictions of pathogenicity

The resulting variants were prioritised based on genes previously associated with disease, previously reported pathogenic variants, loss-of-function variants (frameshift deletions or insertions or nonsense variants), *in silico* predictions of pathogenicity of missense variants, absence of homozygotes in gnomAD or ESP6500 databases, protein function and location of affected protein residue within the protein sequence. These filtrations steps help narrow down the scope of search for candidate variants and genes.

4.3.4.4 Modifications to the prioritisation scheme

Should the prior steps not suggest a clear variant to investigate, a few modifications to the filtration process can be done to include more variants and genes. The first suggested modification (**Figure 4.2, A**) is to omit the filtration of proteins localising to the mitochondria and look for variants in all genes. This might yield a candidate variant to investigate that so far has not been associated with mitochondrial function. The second modification (**Figure 4.2, B**) is to include heterozygous variants and continue the search for candidate bi-allelic (compound heterozygous) variants that might explain disease in the patient. The last suggested modification (**Figure 4.2, C**) would be to include splice-site variants as they might be the causative variants in some cases and need to be investigated. A combination of the previous suggested modifications might lead to the identification of candidate variants in the patients.

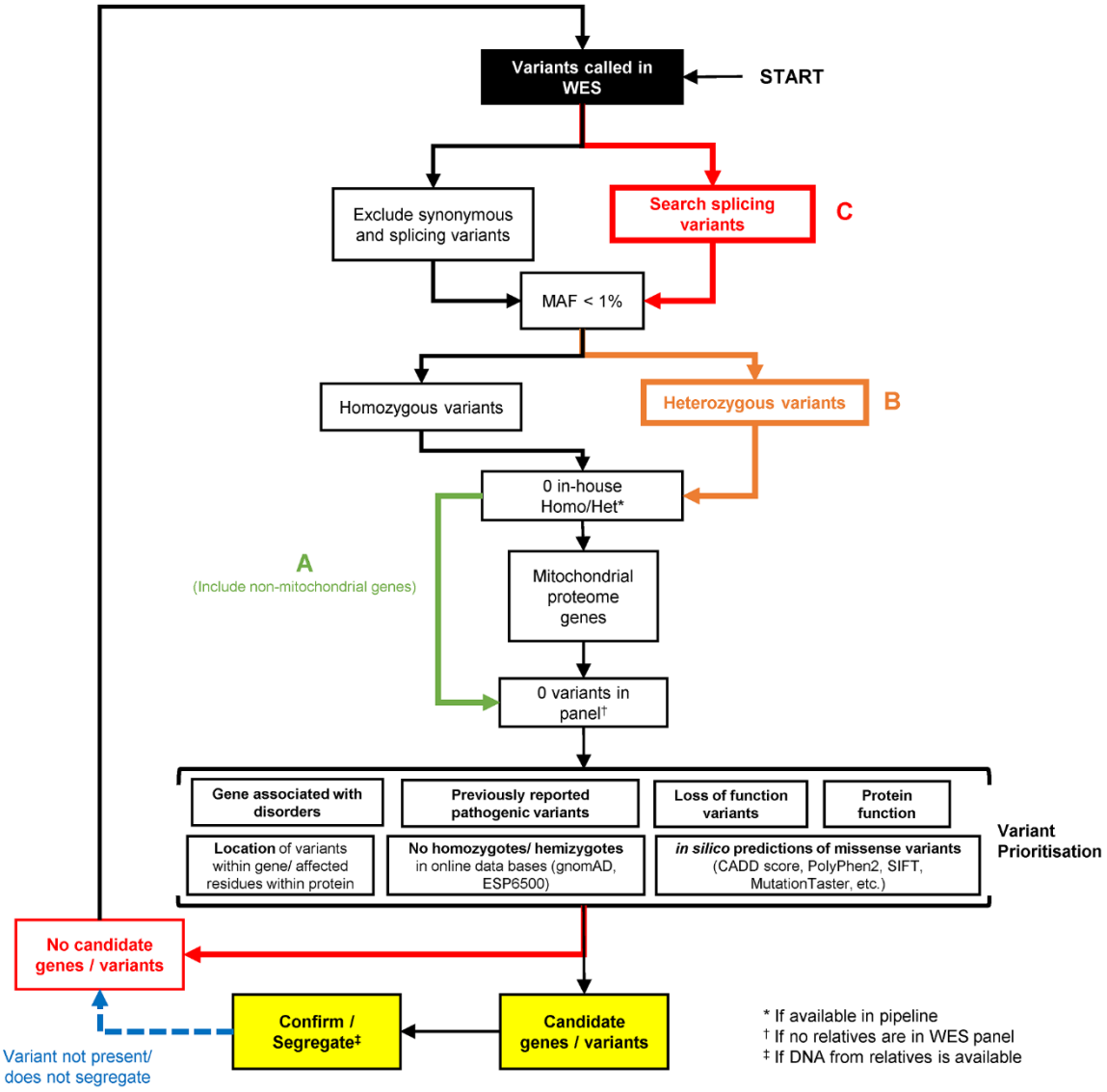

Figure 4.2 Whole exome sequencing variant filtration flowchart

Whole exome sequencing filtration pipeline utilised to search for variants in candidate disease causing genes in patients suspected of mitochondrial disease. Steps **A**, **B**, and **C** are different filtration steps that were used to identify candidate gene in non-mitochondrial disease patients (e.g. steps **A** and **B** were used to filter for compound heterozygous variants regardless of mitochondrial localisation or function).

4.4 Results

4.4.1 Average coverage and depth of utilised WES kits and platforms

For patients from families 1-13 and families 15-17, the Nextera Rapid Exome Capture kits used on an Illumina NextSeq500 platform reported an average coverage at 50-80% of bases at 30x depth.

For patients from family 14 and families 18-22, the Twist capture kit used on the Illumina NovaSeq 6000 platform reported an average coverage exceeding 95% of bases at 30x depth of more.

4.4.2 LETM1

4.4.2.1 Family 1

Patient 1-I was a female patient born to consanguineous Kuwaiti Bedouin parents. She presented with hypertrophic cardiomyopathy, developmental delay, hypotonia, hearing impairment, and nystagmus (**Table** 4.1). A brain MRI showed a thin corpus callosum. She had a family history of 2 brothers who passed away early in life. She passed away at the age of 1 year and 2 months.

WES was carried out on DNA from Patient 1-I and results suggested she was homozygous for a novel codon deletion in exon 5 of the *LETM1* (leucine zipper-EF-hand containing transmembrane protein 1) gene resulting in the deletion of the lysine residue at position 252 of the protein (NM_012318.2; c.754_756delAAG; p.Lys252del). LETM1 is an IMM transmembrane protein that plays a crucial role in calcium homeostasis by acting as a Ca^{2+}/H^{+} antiporter and plays an important role in maintaining mitochondrial morphology (Shao et al., 2016; Piao et al., 2009). *In silico* analysis of the effect of the codon deletion using the protein prediction tool PROVEAN suggested that the amino acid deletion was deleterious (Choi et al., 2012; Choi and Chan, 2015). A single individual, who was heterozygous for a missense mutation at the location of the deleted residue, was reported in the gnomAD database - the missense mutation had a minor allele frequency of 4.6×10^{-6} - and *in silico* missense prediction tools Polyphen-2 and SIFT both predicted that the missense mutation was likely deleterious (Lek et al., 2016; Adzhubei et al., 2010; Ng and Henikoff, 2001; Kumar et al., 2009). However, a database dedicated to the reporting and analysis of background de novo mutations in humans analysed the missense mutation through 14 *in silico* protein damage predicting tools and concluded that the

variant was not damaging since not enough prediction tools reported the mutation as such (Jiang et al., 2017).

Sanger sequencing confirmed that Patient 1-I was homozygous for the codon deletion. A segregation study confirmed both parents were heterozygous carriers of the codon deletion, all healthy brothers were wild-type, and all healthy sisters were heterozygous carriers (**Figure 4.3**). DNA extracted from a homogenised muscle sample from her older affected brother, Patient 1-II (muscle sample was taken during his visit to Great Ormond Street Hospital in London in 2007) confirmed that he was also homozygous for the codon deletion in *LETM1* (**Figure 4.3**). No DNA was available for the younger affected brother who passed away. Since all affected siblings and the patient passed away, no muscle or skin biopsy could be obtained for further biochemical, histochemical or immunofluorescent analysis.

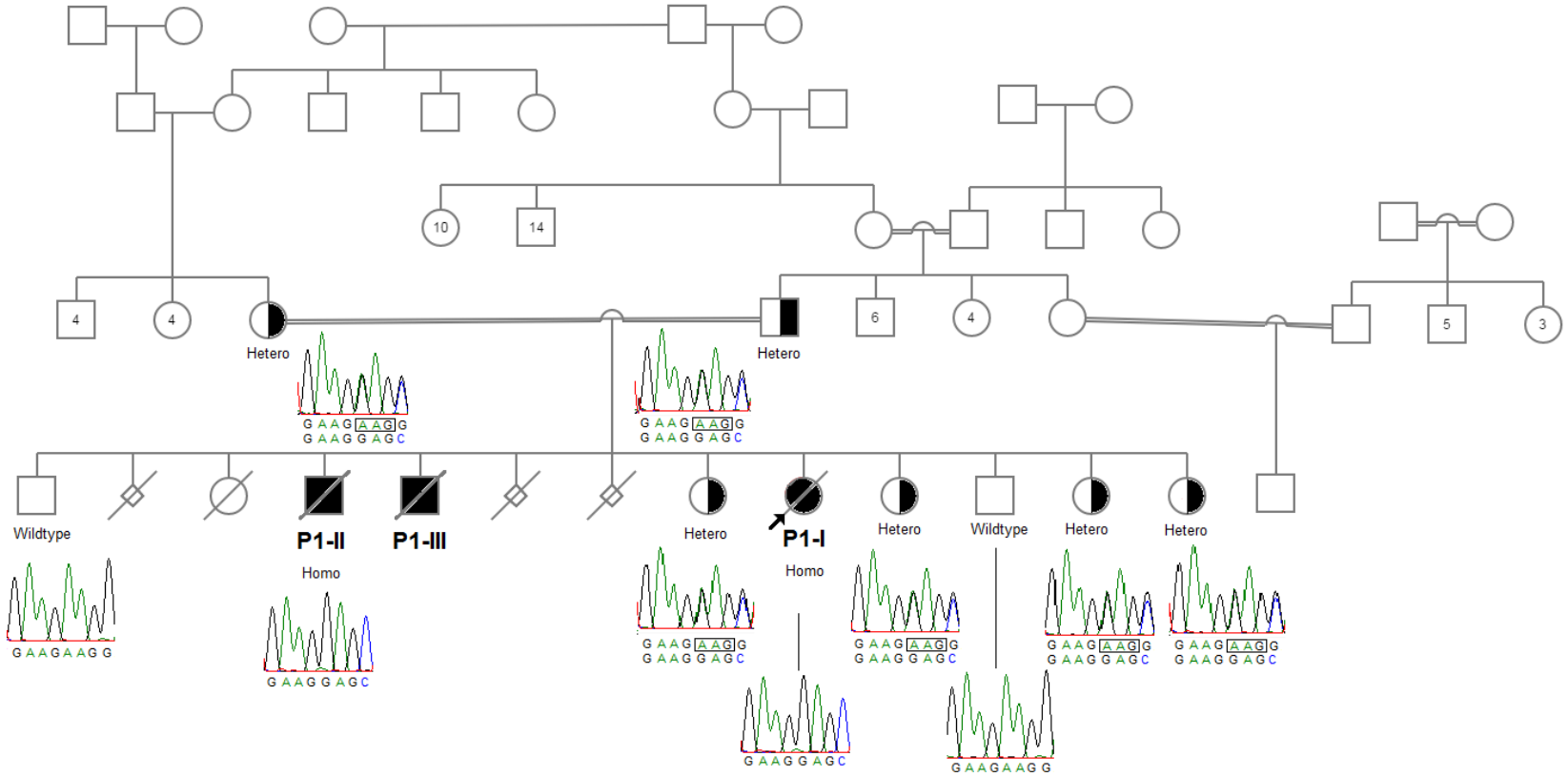

Figure 4.3 Segregation of *LETM1* deletion in Family 1.

Pedigree showing the segregation of the *LETM1* codon deletion (c.754_756delAAG; p.Lys252del) in Family 1 members. Genotyping of Patients P1-I and P1-II (P1-I and P1-II respectively), which are 2 of the 3 affected siblings that passed away, found them to be homozygous for the codon deletion. Sequencing chromatograms highlight the deleted nucleotides in the heterozygous individuals (black box).

4.4.2.2 Family 6

Patient 6 was a male born to consanguineous Egyptian parents. He presented with nystagmus, myopia, hypotonia, sensorineural hearing loss, cataracts, and hypertrophic cardiomyopathy (**Table** 4.1). He experienced 2 separate seizure attacks and a brain MRI showed mild reduction in brain volume.

WES analysis identified a rare homozygous *LETM1* missense mutation in Patient 6 (c.881G>A; p.Arg294Gln). The variant results in a non-synonymous change of a highly conserved residue and the database dedicated to *in silico* analysis of background *de novo* mutations in humans (mirDNMR) reported the variant as damaging in 10 various *in silico* protein damage predicting tools including PolyPhen-2, PROVEAN, CADD and MutationTaster (Kumar et al., 2009; Adzhubei et al., 2010; Choi et al., 2012; Schwarz 2014; Choi and Chan, 2015; Jiang et al., 2017). The identified variant was reported in 4 heterozygous controls of European ancestry by gnomAD database with a MAF of 1.6×10^{-5} (Lek et al., 2016). Two other controls of European descent were heterozygous for another variant that affects the same residue (c.880C>T; p.Arg294Trp) and a European control was heterozygous for a frameshift deletion (c.880delC; p.Arg294Glyfs). The total MAF for all heterozygous variants reported is 2.8×10^{-5}. This variant segregated in the family as Patient 6 was homozygous while parents and healthy siblings were heterozygous (**Figure 4.4**). This affected residue is located in a highly conserved region of the protein and homozygotes have not been previously reported making is an ideal candidate gene to investigate.

A

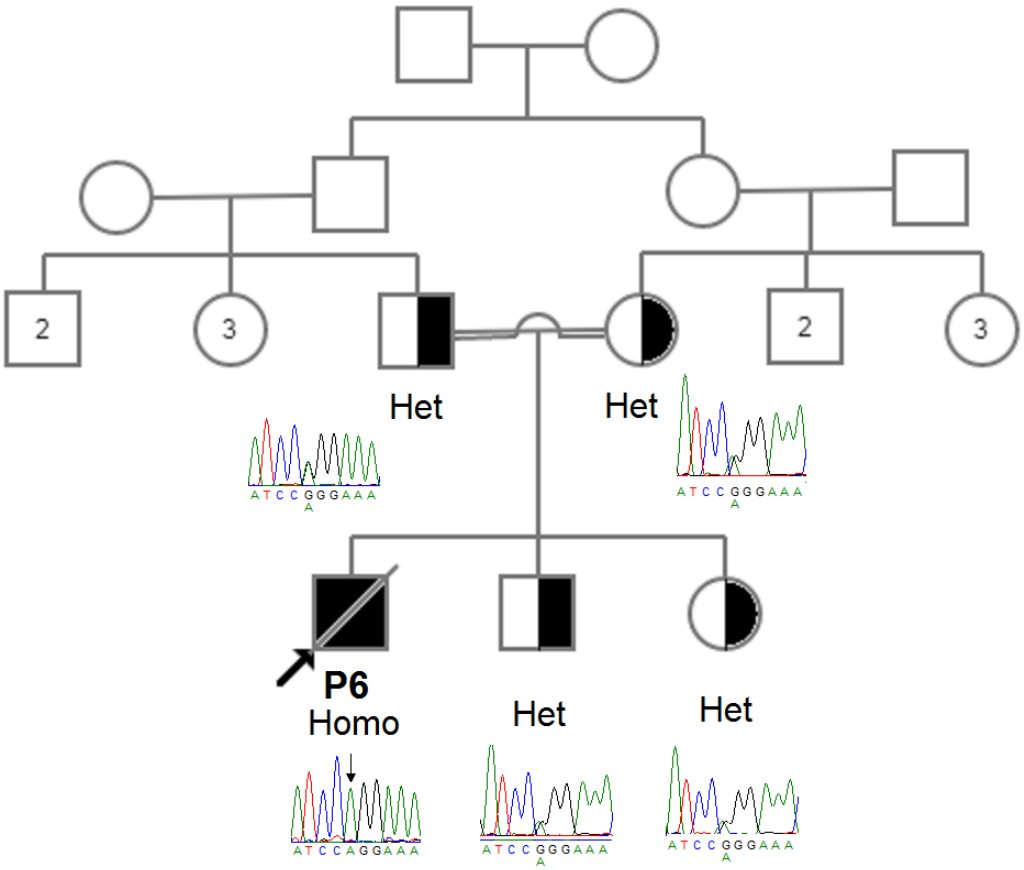

B

```
                                        *
Patient                 AKGSATKDFSVFFQKIQETGE----RPSNEEI
Homo sapiens            AKGSATKDFSVFFQKIRETGE----RPSNEEI
Mus musculus            AKGNATKDFSAFFQKIRETGE----RPSNEEI
Rattus norvegicus       AKGNATKDFSAFFQKIRETGE----RPSNEEI
Danio rerio             SKGNVTEEFSTFFQKIRDSGE----IPSNEQI
Drosophila melanogaster HSSEEAKQFEAFFTKIRNPTE----PVSNDEI
Saccharomyces cerevisiae ENAEKKQKFLNFFRKLYSAKEGKIMTFQHDEI
                          ...  :.*  ** *: .  *      .:::*
```

Figure 4.4 Segregation of *LETM1* variant in Family 6.

A Pedigree showing the segregation of the rare missense *LETM1* variant (c.881G>A; p.Arg294Gln) in Family 6 members. Patient 6 (P6) was homozygous for the missense mutation. Sequencing chromatograms of identified missense variant in Patient 6 highlighting the nucleotide change (red arrow).
B Clustal Omega alignment of LETM1 protein residues in model organisms showing high conservation of the substituted Arginine 294 residue (highlighted).
.

Table 4.1 Phenotypes of *LETM1* patients

Patient	1-I	P1-II	1-III	6
Mutation	c.754_756delAAG; p.Lys252del	c.754_756delAAG; p.Lys252del	c.754_756delAAG; p.Lys252del	c.881G>A; p.Arg294Gln
Age of onset	Birth	6 months	Birth	30 months
Age of death	14 months	26 months	15 months	N/A
Phenotype	Hypotonia Developmental delay Nystagmus SNHL Cardiomyopathy	Hypotonia Dysmorphic features Muscle wasting Failure to thrive Developmental delay Nystagmus SNHL Visual acuity Elevated lactate Abnormal urine organic acids Constipation	Hypotonia Cardiomyopathy Elevated lactate	Hypotonia Dysmorphic features Developmental delay Epilepsy Nystagmus Visual acuity Cardiomyopathy Elevated lactate Myopia Hypoglycaemia Cataracts

N/A: not available; SNHL: Sensorineural hearing loss

4.4.3 Family 8

Patient 8 is a 2 year-old female born to consanguineous Kuwaiti Arab Bedouin parents following IVF. She presented with nystagmus, developmental delay, ataxia, hypotonia and convergent strabismus. Her CSF lactate levels were elevated, and a brain MRI revealed bilateral symmetric signals in the subthalamic regions. Family history revealed her maternal cousin was blind.

WES was carried out on DNA from Patient 8 and results suggested she was homozygous for a novel truncating variant in exon 1 of the *NDUFA13* (complex I structural subunit FA13, *GRIM19*) gene resulting in the premature truncation at position 8 of the protein (NM_015965; c.22C>T; p.Gln8*). Sanger sequencing confirmed that the proband was homozygous for the truncating variant and a segregation study identified both parents as unaffected heterozygous carriers (**Figure 4.5**). A younger brother was born after the segregation and was reported to be a heterozygous carrier by colleagues at KMGC.

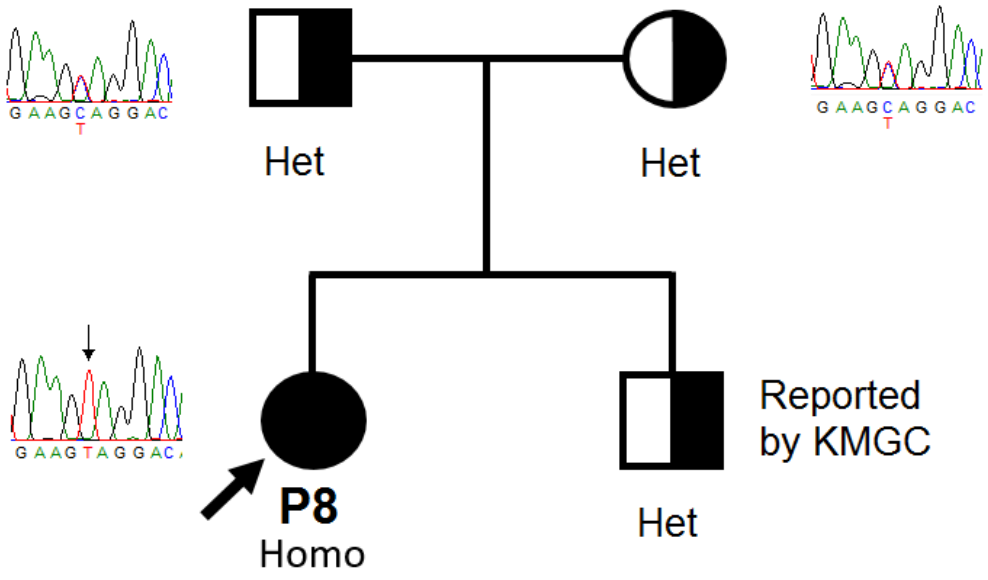

Figure 4.5 Segregation of *NDUFA13* variant in Family 8

Pedigree of Family 3 showing the segregation of the identified truncating *NDUFA13* mutation (c.22C>T; p.Gln8*). Sequencing chromatograms of identified homozygous missense variant in Patient 8 (P8) highlighting the nucleotide change (black arrow).

4.4.4 Family 5

Patient 5-II is a 9 year-old male born to consanguineous Arab Bedouin parents. He presented with developmental delay, hypotonia, short stature, mild dysmorphic features, GORD, and persistently elevated serum lactic acid. DNA from Patient 5-II from family 5 was selected for WES.

WES analysis identified a novel homozygous *MPC1* missense mutation in Patient 5-II (c.109C>T; p.Pro37Ser). *MPC1* encodes the IMM protein Mitochondrial Pyruvate Carrier 1 that forms a heterodimer complex with its paralog Mitochondrial Pyruvate Carrier 2 (*MPC2*) to facilitate the uptake of pyruvate by mitochondria (Bricker et al., 2012). The variant results in a non-synonymous change of a highly conserved residue located in a transmembrane domain of the protein and is the residue that follows the first residue of exon 6 (McCommis and Finck, 2015). *In silico* tools including PolyPhen-2, PROVEAN, CADD and MutationTaster predicted the change to be deleterious (Kumar et al., 2009; Adzhubei et al., 2010; Choi et al., 2012; Schwarz 2014; Choi and Chan, 2015). The variant segregated in the family where the proband and his affected siblings were homozygous, parents were heterozygous and unaffected siblings were wild-type (**Figure 4.6**).

A

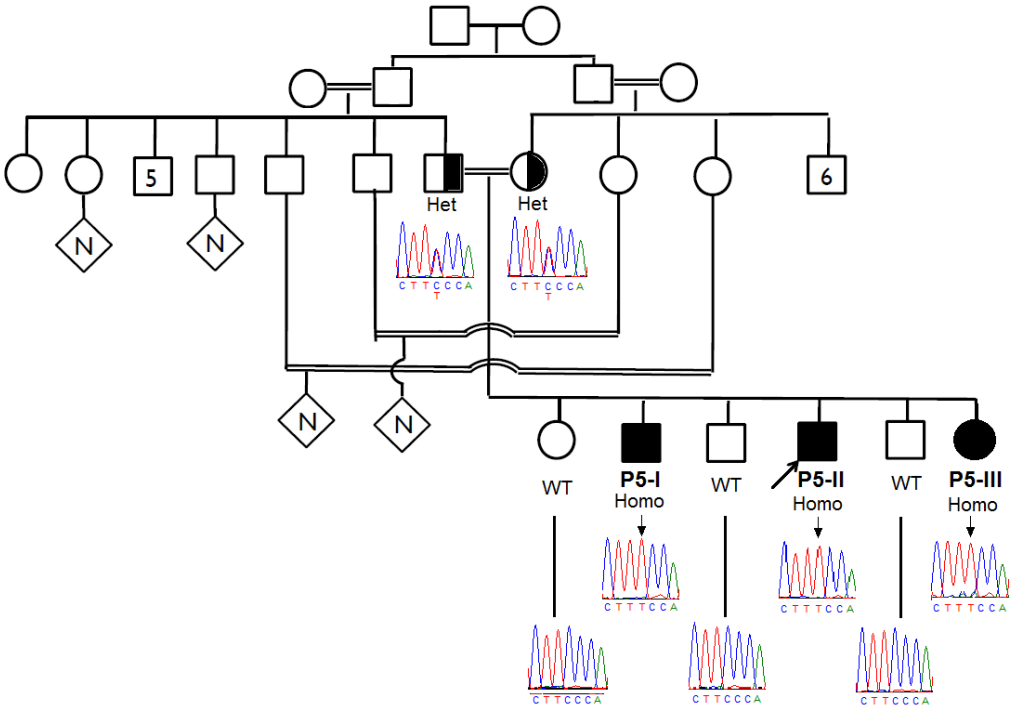

B

```
                                        *
Patient                 DYLMSTHFWGPVANWGLSIAAINDMKKSPEIISGRMT
Homo sapiens            DYLMSTHFWGPVANWGLPIAAINDMKKSPEIISGRMT
Mus musculus            DYLMSTHFWGPVANWGLPIAAINDMKKSPEIISGRMT
Rattus norvegicus       DYLMSTHFWGPVANWGLPIAAINDMKKSPEIISGRMT
Danio rerio             DYLMSTHFWGPVANWGLPIAAISDMKKSPEIISGRMT
Drosophila melanogaster DYFMSTHFWGPVANWGIPVAALADTQKSPKFISGKMT
Saccharomyces cerevisiae KYIFTTHFWGPVSNFGIPIAAIYDLKKDPTLISGPMT
                        .*:::*******:*:*:*:**: * :*.* :*** **
```

Figure 4.6 Segregation of *MPC1* variant in Family 5

A Pedigree of family 7 showing the segregation of the identified *MPC1* missense mutation (c.109C>T; p.Pro37Ser). Sequencing chromatograms highlight the identified missense variant in Patients 5-1, 5-II and 5-III (P5-I, P5-II and P5-III respectively) highlighting the nucleotide change (black arrows).
B Clustal Omega alignment of MPC1 protein residues in vertebrates showing high conservation of the substituted Proline 37 residue (highlighted).

4.4.5 Family 7

Patient 7-I was a female Syrian Arab patient born to consanguineous parents. She presented with developmental delay then lost her motor skills, developed progressive hypertonia, became ataxic, then wheelchair-bound and lastly developed dysphagia. A brain MRI scan revealed bilateral symmetric signals in the caudate and putamen. She passed away at the age of 11 years and 6 months.

Patient 7-I has a younger brother (Patient 7-II) who developed slurred speech, ataxia dystonia, decreased muscle power in in shoulders and hips, and bradycardia at the age of 10 years. A brain MRI scan revealed bilateral symmetric signals affecting the basal ganglia and brainstem. DNA from both Patient 7-I and Patient 7-II were selected for WES as a sibling duo.

WES identified a truncating *TTC19* frameshift deletion in both affected siblings, patients 7-I and 7-II (c.779_780delAT; p.Tyr260*). TTC19 is a complex III assembly factor that colocalises with the respiratory chain protein in the IMM (Ghezzi et al., 2011). The deletion was segregated in the family where both patients were homozygous, parents and an unaffected sibling were heterozygous, and 3 unaffected siblings were wild-type (**Figure 4.7**).

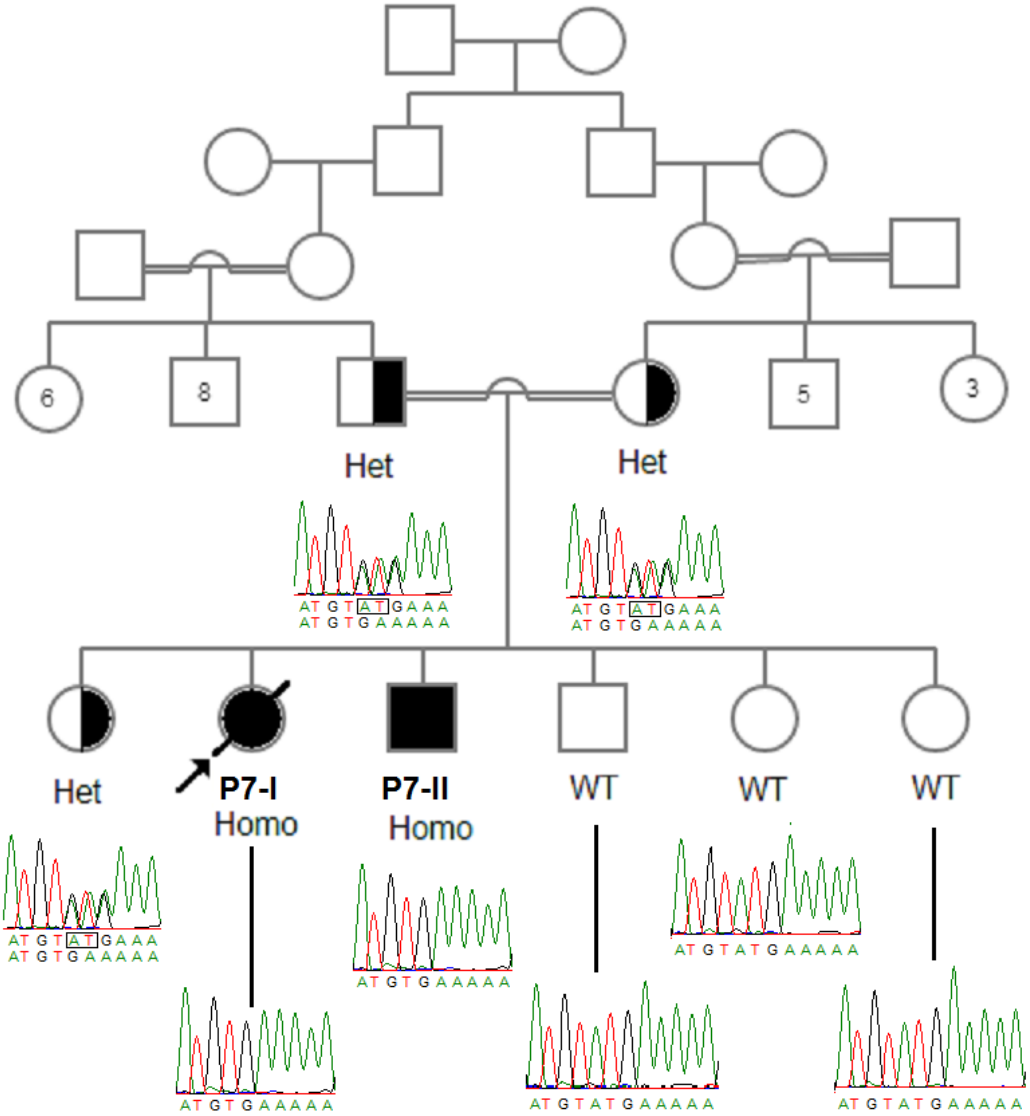

Figure 4.7 Segregation of *TTC19* deletion in Family 7

This pedigree shows the segregation of the truncating *TTC19* frameshift deletion (c.779_780delAT; p.Tyr260*) within Family 7. Sequencing chromatograms of the genotyped family members highlight the deleted nucleotides in heterozygous individuals such as the parents (black box). Patients 7-I and 7-II are labelled P7-I and P7-II respectively.

4.4.6 Family 2

Patient 2 is a 5 year-old female born to consanguineous Jordanian Arab parents. She presented with seizures early in life and elevated lactate levels in CSF and serum with a high serum pyruvate and lactate/pyruvate ratio also reported. A head CT scan at 1 month showed a hypodensity in the central brainstem and thalami.

WES was carried out on the DNA from Patient 2 and results suggested she was homozygous for a novel missense mutation in exon 3 of the transmembrane protein encoding gene *SLC19A3* (solute carrier family 19 member 3) resulting in the substitution of the tryptophan residue at position 59 with an arginine residue (NM_025243; c.175T>C; p.Trp59Arg). The mutation was predicted to be damaging by almost all *in silico* prediction tool including Polyphen-2, SIFT and PROVEAN (Adzhubei et al., 2010; Ng and Henikoff, 2001; Kumar et al., 2009; Choi et al., 2012; Choi and Chan, 2015).

Sanger sequencing confirmed that Patient 2 was homozygous for the suggested missense mutation and a segregation study showed both parents and her 2 siblings were all heterozygous carriers of the variant (**Figure 4.8**).

A

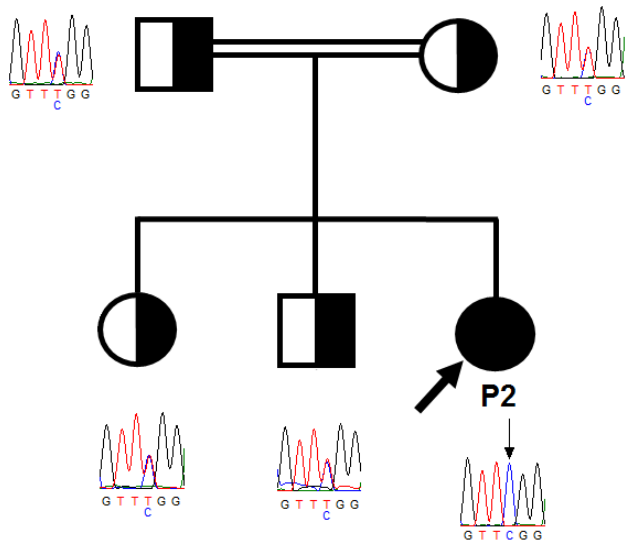

B

```
                                        *
Patient                                 ITNEIFPVRTY-SYLVLLLPVFVLTDYVR
Homo sapiens                            ITNEIFPVWTY-SYLVLLLPVFVLTDYVR
Mus musculus                            MTNEILPVWTY-SYLATLPPVFVLTDYLR
Rattus norvegicus                       MTNEILPVWTY-SYLAMLPPVFVLTDYLR
Danio rerio                             LNNQIFPVWTY-SYLAVLVPVFLLTDWLR
Drosophila melanogaster                 IYQDVYPFGTY-SVLAQLVIVFLITDLVR
Saccharomyces cerevisiae                SANQTWGFWSNFAYWG--VMSFSVGTWMS
                                          ::    . :  :         * :   :
```

Figure 4.8 Segregation of novel missense *SLC19A3* variant in Family 2.

A Family 2 pedigree showing the segregation of the novel *SLC19A3* missense mutation (c.175T>C, p.Trp59Arg) with the remaining unknown genotype of the patient's sister. Sequencing chromatograms of identified missense variant in genotyped family members and highlighting the nucleotide change in Patient 2 (P2) (black arrow).
B Clustal Omega alignment of SLC19A3 protein residues in model organisms showing high conservation of the substituted Tryptophan 59 residue except in *Drosophila melanogaster* (highlighted).

4.4.7 Family 4

Patient 4-III was the youngest of the 3 affected siblings in Family 4. He was born to consanguineous first cousin Syrian parents. At the age of 14 months, he began to lose his acquired milestones, became spastic and had elevated serum lactate levels. A brain MRI scan showed bilateral symmetric signals in the cerebellum, and the brainstem. At 19 months, he presented with ptosis, hypertonia in his limbs, and hypotonia in his axial muscles and microcephaly was noted . DNA from Patient 4-III was selected for WES.

WES was carried out on the DNA from Patient 4-III and results suggested she was homozygous for a novel frameshift deletion in exon 5 of the transmembrane protein encoding gene *SURF1* (surfeit-1) resulting in the premature truncation after 4 residues (NM_003172; c.367_368delAG; p.Arg123Glyfs*4). Sanger sequencing confirmed that Patient 4-III was homozygous for the novel frameshift mutation and a segregation study showed all affected siblings (Patients 4-I and 4-II) were homozygous while parents and unaffected siblings were heterozygous carriers of the variant (**Figure 4.9**).

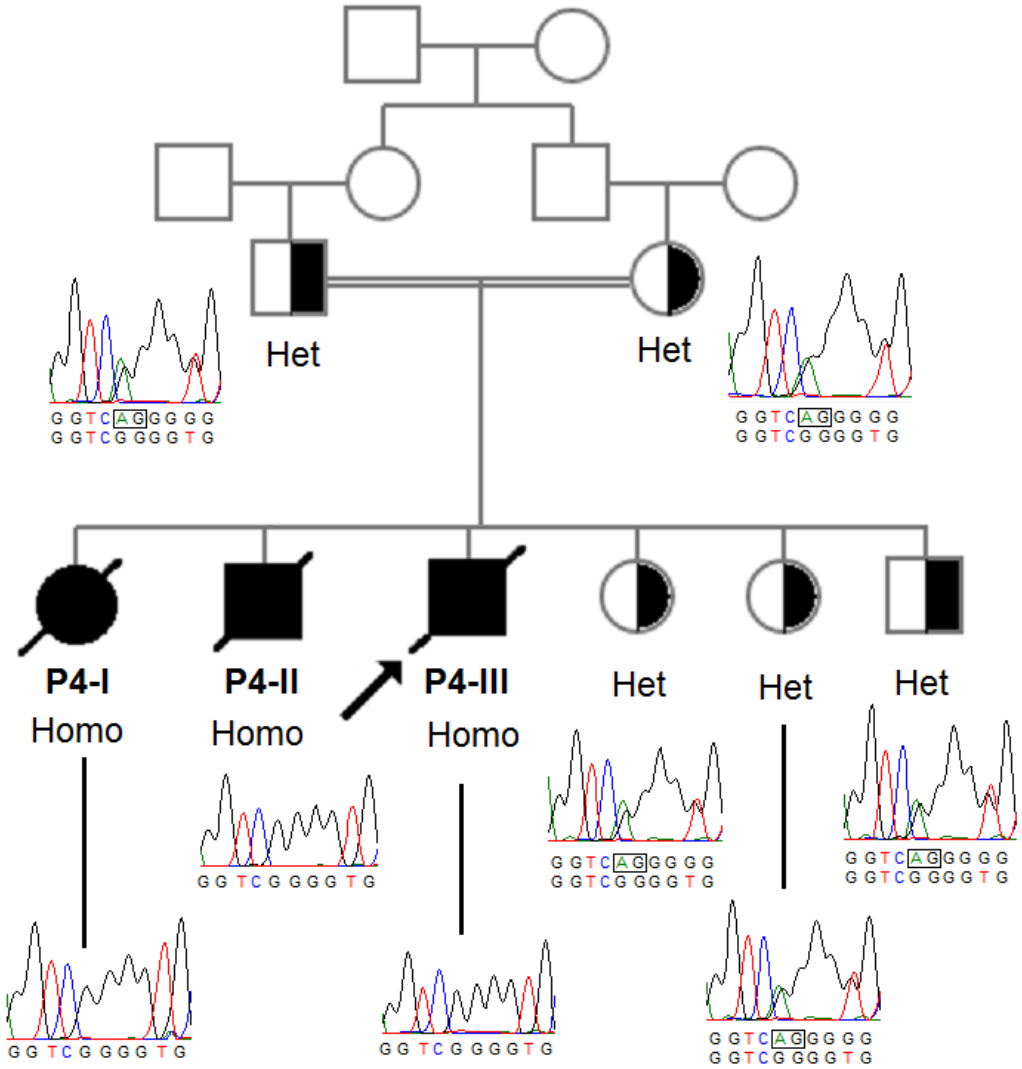

Figure 4.9 Segregation of *SURF1* deletion in Family 4.

Pedigree of family 4 showing the segregation of the identified truncating *SURF1* deletion (c.367_368delAG). Sequencing chromatograms highlight the deleted nucleotides in heterozygous individuals (black box). Patients 4-I, 4-II and 4-III (P4-I, P4-II and P4-III respectively) were homozygous for the deletion.

4.4.8 Family 10

Patient 10 is a 60 year-old adult female patient born to non-consanguineous Kuwaiti parents. She developed ptosis and progressive external ophthalmoplegia at the age of 34 years. She developed difficulty chewing and choking when eating, experienced exercise-intolerance, had weak proximal muscles and spastic lower limbs with a stiff gait, and experienced constipation.

WES was carried out on DNA from Patient 10 and results suggested she was homozygous for a rare missense variant in exon 6 of the *RRM2B* (Ribonucleotide Reductase subunit M2B) gene resulting in the substitution of the leucine residue at position 64 of the protein with a proline (NM_015713; c.574G>A; p.Ala192Thr). Sanger sequencing confirmed that the proband was homozygous for the rare missense variant and a segregation study could not be carried out due to absence of parental DNA (**Figure 4.10**). Carrier status of her children was not performed either.

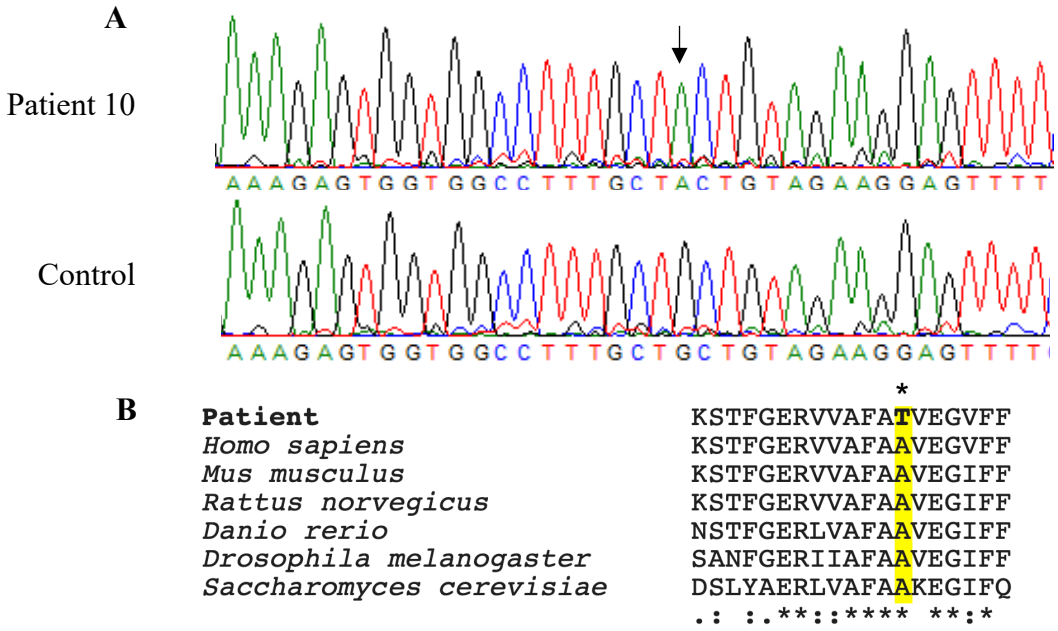

Figure 4.10 Confirmation of missense *RRM2B* mutation in Patient 10.

A Sequencing chromatogram highlighting the confirmed missense *RRM2B* variant (c.574G>A; p.Ala192Thr) in Patient 10 (black arrow).
B Clustal Omega alignment of RRM2B protein residues in model organisms showing high conservation of the substituted Alanine 192 residue (highlighted).

4.4.9 Family 9

Patient 9 is a 5 year-old male patient born to consanguineous Syrian Arab parents. He presented at birth with IUGR and later presented with developmental delay, failure to thrive, short stature, hypermetropia, nystagmus, blue sclerae, strabismus, moderate hearing loss, fatigue, hypotonia, muscle weakness affecting shoulders and hip girdles, and a broad-based gait. A brain MRI scan revealed abnormal areas in the periventricular white matter and cerebellum. Serum lactate levels elevated following a period of fasting prior to an audiometry test.

WES was carried out on DNA from Patient 9 and results suggested he was homozygous for a previously reported missense variant in exon 2 of the *NDUFB9* (complex I structural subunit FB9) gene resulting in the substitution of the leucine residue at position 64 of the protein with a proline (NM_005005; c.191T>C; p.Leu64Pro). Sanger sequencing confirmed that the proband was homozygous for the missense *NDUFB9* variant and a segregation study of identified parents and siblings as unaffected heterozygous carriers (**Figure 4.11**).

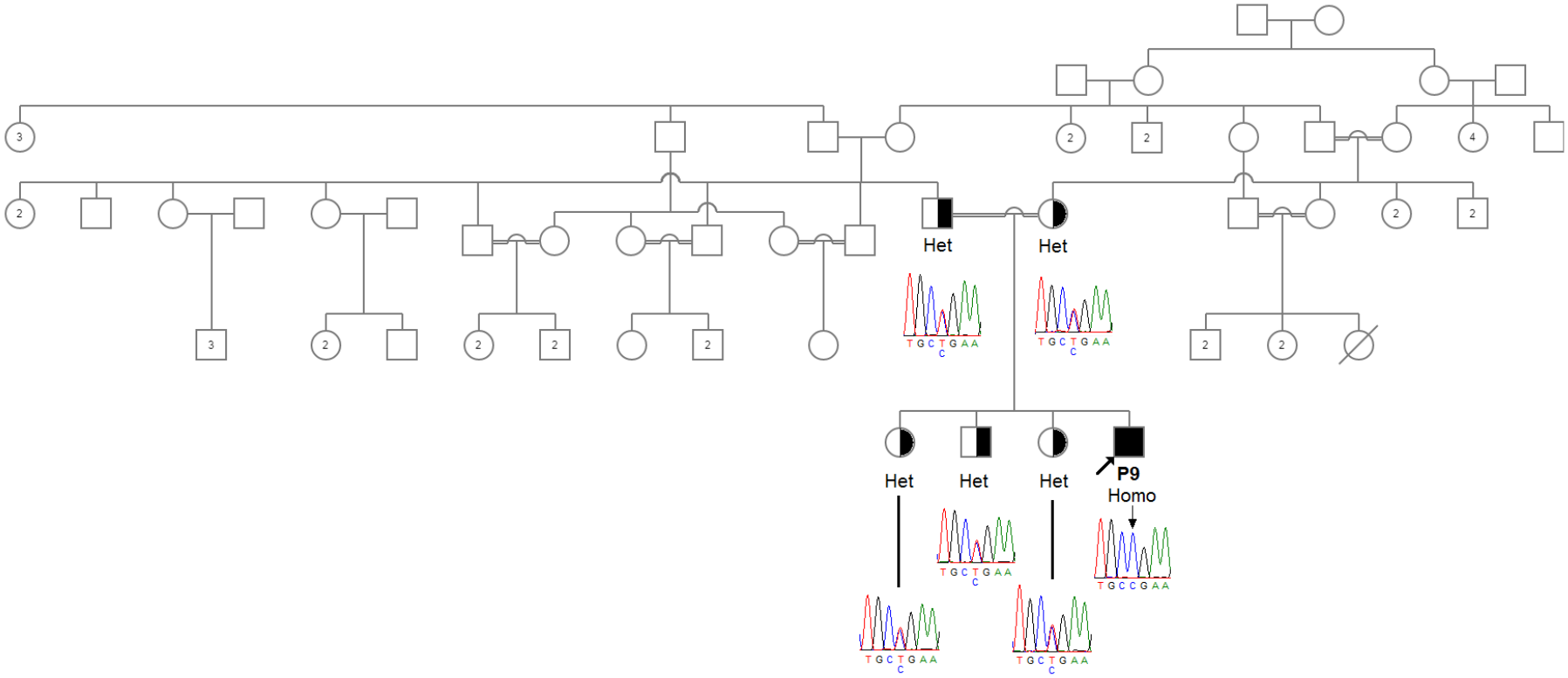

Figure 4.11 Segregation of *NDUFB9* variant in Family 9

Pedigree of family 9 showing the segregation of the identified *NDUFB9* mutation in family members. Sequencing chromatograms show the heterozygous state of carriers and highlights the nucleotide change in Patient 9 (P9) (black arrow).

4.4.10 Family 3

Patient 3 is a 10 year-old male patient born to consanguineous Syrian Arab parents. He presented with seizures and tachypnoea from birth accompanies by elevated lactate in serum and CSF and elevated pyruvate, alanine and creatine kinase in blood. He became hypotonic with persistent elevated serum lactate. He developed another seizure at the age of 5 years and a brain MRI revealed abnormal signals in the basal ganglia and brainstem along with a thin corpus callosum and dilatation of lateral and third ventricles.

WES was performed on DNA from Patient 3 and this indicated he was homozygous for a previously reported nonsense mutation that terminated protein translation of the *PDHX* gene (Pyruvate Dehydrogenase Complex component X) in the middle of exon 6 resulting in protein truncation (NM_003477; c.742C>T; p.Gln248*). The reported MAF of this mutation in the gnomAD database is 1.22×10^{-5} with 3 heterozygous individuals reported, one African and two European controls (Lek et al., 2016). Sanger sequencing confirmed Patient 3 was homozygous for the nonsense mutation. A segregation study revealed both parents, 1 brother, and 2 healthy sisters were heterozygous carriers of the variant, a healthy brother and a healthy sister were wild-type, and an affected brother was found to be homozygous for nonsense variant (**Figure 4.12**).

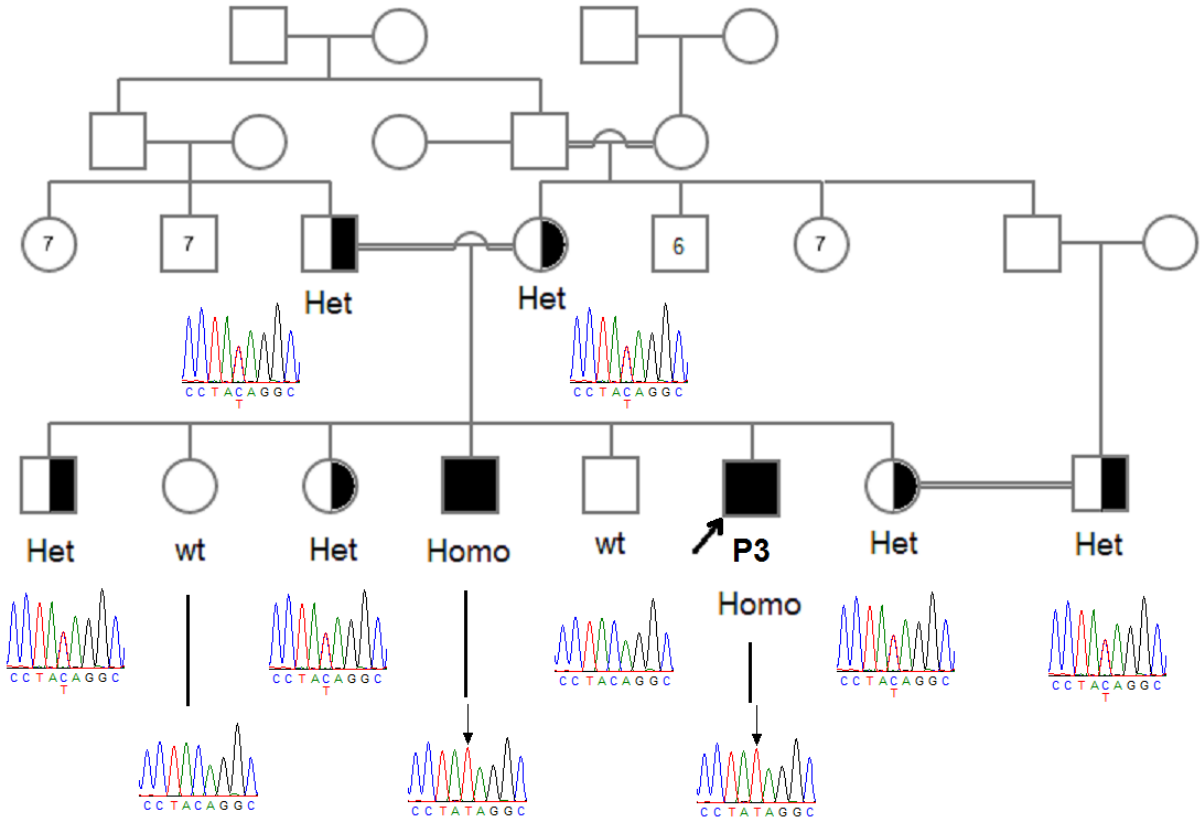

Figure 4.12 Segregation of *PDHX* truncating variant in Family 3.

Pedigree showing the segregation of the truncating *PDHX* variant among family1. Patient 3 (P3) and an affected older brother were both homozygous for the nonsense mutation. Sequencing chromatograms highlight the identified homozygous *PDHX* truncating variant in Patient 3 and his affected sibling (black arrow).

4.4.11 Family 11

Patient 11-I is a 6 year-old female patient born to consanguineous Kuwaiti Arab parents. She presented with global developmental delay, hypotonia, epilepsy, microcephaly, micrognathia, bilateral hearing loss and lactic acidosis. A brain MRI revealed severe cortical atrophy, hypomyelination of the frontal, occipital and temporal lobes, and calcification of the basal ganglia. A head CT scan revealed multiple bilateral symmetric foci of calcification in the basal ganglia, thalami, periventricular regions and left cerebellum.

Patient 11-III is the double first cousin of Patient 11-I. Patient 11-III is a 5 year-old female who presented with jerky movements during her sleep, nystagmus, poor feeding, reduced activity, irritability, and a mild increase in serum lactate. A brain MRI scan revealed brain atrophy. DNA from Patient 11-I and Patient 11-III were selected for WES analysis as first cousin duo.

WES was carried out on the DNA from Patient 11-I and her affected double first cousin Patient 11-III with results suggesting that they were both homozygous for a novel missense variant in exon 2 of the *RNASEH2C* (Ribonuclease H2 subunit C) gene, resulting in the substitution of a leucine residue at position 68 with a valine residue (NM_032193; c.202C>G; p.Leu68Val). RNASEH2C is one of three subunits that comprise the endonuclease RNase H2 complex that is responsible for cleaving ribonucleotides from RNA:DNA and DNA:DNA duplexes (Crow et al., 2006). The mutation was predicted to be damaging by the *in silico* prediction tools Polyphen-2 and PROVEAN (Adzhubei et al., 2010; Kumar et al., 2009; Choi et al., 2012; Choi and Chan, 2015). Sanger sequencing confirmed that Patients 11-I and 11-III were both homozygous for the suggested missense mutation and a segregation study showed parents of both patients were heterozygous carriers of the variant (**Figure 4.13**). Healthy siblings of both affected patients are yet to be genotyped to complete the segregation study and ensure full segregation.

A

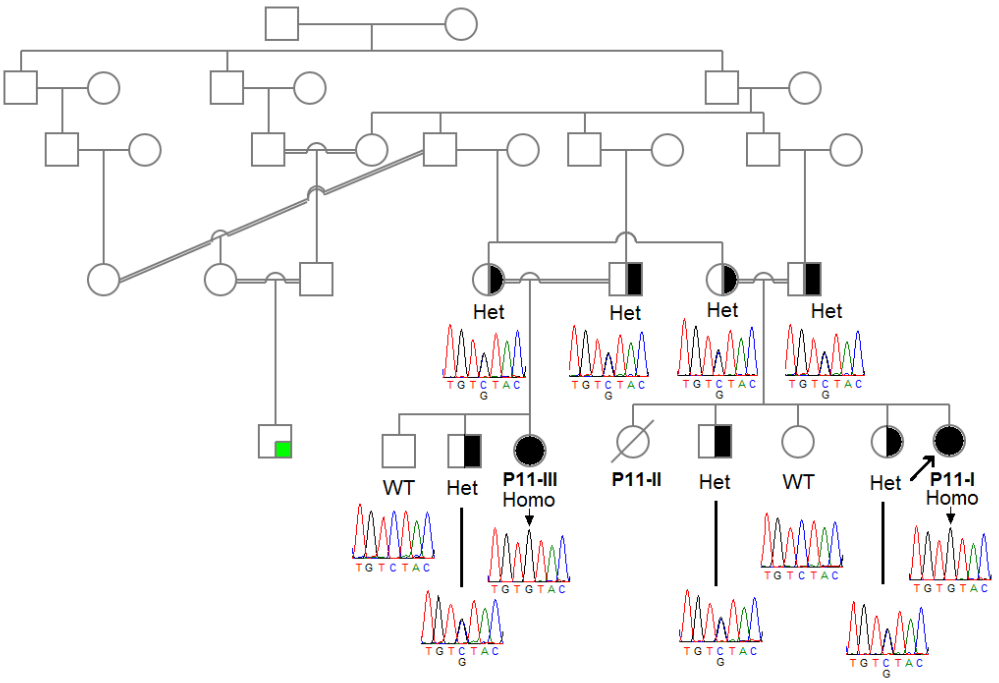

B

```
                                  *
Patient                           VSFRGRCVRGEEVAVPPGLVGYVM
Homo sapiens                      VSFRGRCLRGEEVAVPPGLVGYVM
Mus musculus                      ASFRGRGLRGEEVAVPPGFAGFVM
Rattus norvegicus                 VSFRGRGLRGEDVAVPPGFAGFVM
Danio rerio                       VSFRGRGLKGQELQCPQGYTGVVL
                                  .***** *:*:::  * * .* *:
```

Figure 4.13 Segregation of *RNASEH2C* variant in Family 11.

A Pedigree of family 11 showing the segregation of the identified *RNASEH2C* missense mutation (c.202C>G, p.Leu68Val). Sequencing chromatograms highlight the homozygous missense variant in Patients 11-I and 11-III (P11-I and P11-III respectively) (black arrow).
B Clustal Omega alignment of RNASEH2C protein residues in model organisms showing high conservation of the substituted Leucine 68 residue (highlighted).
.

4.4.12 Family 12

Patient 12 is a 6 year-old male patient born to non-consanguineous Kuwaiti Arab parents. He presented with generalised hypertonia and hyperreflexia, mildly elevated serum and CSF lactate levels, became dystonic, irritable, and developed epilepsy. A brain MRI scan revealed diffuse signal in the white matter and a thin corpus callosum.

WES was carried out on DNA from Patient 12 and results identified 2 variants in exon 2 *TREX1* (Three Prime Repair Exonuclease 1). One variant was a novel frameshift duplication (NM_033629; c.50dupT; p.Asp18Argfs) and the other heterozygous variant was a previously reported missense variant (NM_033629; c.341G>A; p.Arg114His) (Crow et al., 2006). Sanger sequencing confirmed that Patient 12 was compound heterozygous for the 2 identified variants and segregation study revealed that his father was heterozygous for the nucleotide duplication allele while his mother was heterozygous for the previously reported missense variant

Figure 4.14).

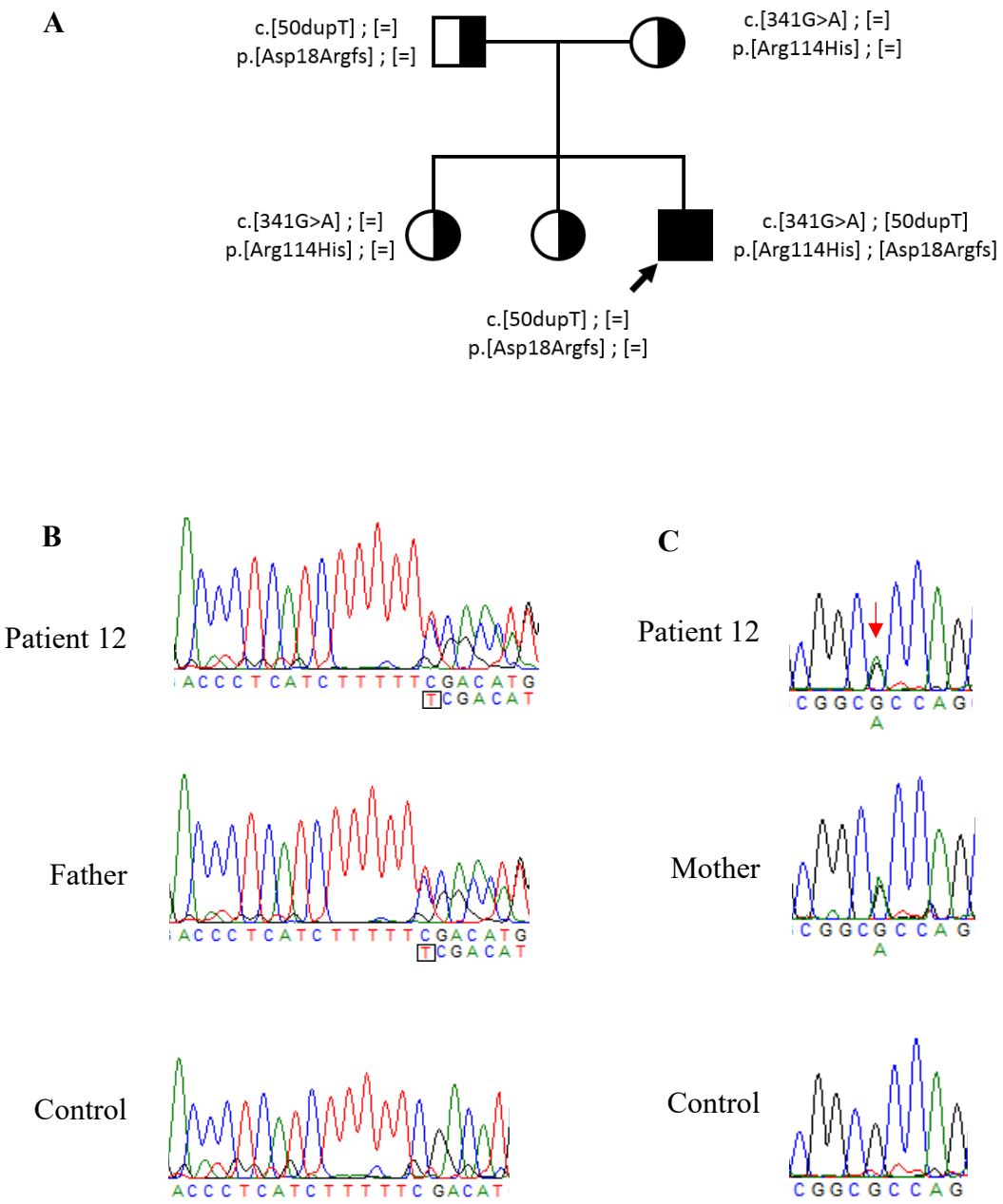

Figure 4.14 Segregation of *TREX1* variant in Family 12

A Pedigree of family 12 showing the segregation of the identified *TREX1* variant.
B. Sequencing chromatograms of identified *TREX1* frameshift duplication (c.50dupT) in Patient 12 highlighting the nucleotide insertion (black box).
C. Sequencing chromatograms of identified *TREX1* missense variant (c.341A>G) in Patient 12 highlighting the nucleotide change (red arrow).

4.4.13 Family 13

Patient 13 is a 15 year-old male patient born to consanguineous Kuwaiti Persian parents. He presented with developmental delay, unilateral ptosis, short stature, synophrys, mild turricephaly, bilateral cataracts, general weakness, and EMG disclosing non-irritative myopathy wasted shoulder and hip girdle muscles.

WES was carried out on DNA from Patient 13 and results suggested he was homozygous for a novel frameshift deletion in exon 11 of the *VPS13B* (*COH1*, Vacuolar Protein Sorting 13 homolog B) gene resulting in the substitution of the leucine residue at position 64 of the protein with a proline (NM_152564.4; c.1512delA; p.Glu505Lysfs). VPS13B is a plasma membrane protein associated with vesicle-mediated transport and intracellular protein sorting (Kolehmainen et al., 2003). Sanger sequencing confirmed that the proband was homozygous for the frameshift deletion, but a segregation study was not performed due the absence of DNA from the family (

Figure 4.15).

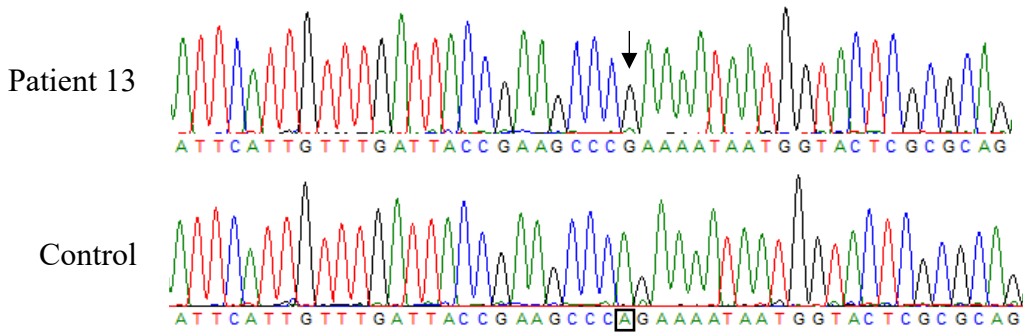

Figure 4.15 Confirming identified VPS13B frameshift deletion in Patient 13

Sequencing chromatograms of identified *VPS13B* frameshift deletion (c.1512delA) in Patient 13 highlighting the nucleotide deletion (black arrow and black box).

4.4.14 Family 14

Patient 14-I is a 21 year-old female patient born to consanguineous Kuwaiti Arab Bedouin parents from the same tribe. She presented with global developmental delay, failure to thrive, microcephaly, gaze palsy, myopia, bilateral ptosis and ophthalmoplegia, myopathic face, generalised hypotonia, generalised muscle wasting, scoliosis, and developed choreoathetotic movements. A brain MRI scan revealed cerebral atrophy and an EEG showed slow abnormal background activity.

Patient 14-II is Patient 14-I's 9 year-old brother. He presented with developmental delay, microcephaly, hypotonia, muscle weakness, constipation, and developed choreiform flicking movements. A brain MRI scan revealed mild generalised reduction of white matter. DNA from both Patient 14-I and 14-II were selected for WES.

WES analysis was performed on DNA from both Patients 14-I and 14-II and filtering for protein coding homozygous and heterozygous variants in genes coding for mitochondrial and non-mitochondrial proteins suggested no variants. However, including splice-site variants in the filtration steps suggested both patients were homozygous for a novel splice-site altering variant in *ATP8A2* (NM_016529; c.321+1G>T; p.?). The variant is predicted to result in the retention of intron 3. Sanger sequencing confirmed both sibling patients were homozygous for the splice-site variant, and a segregation study showed both parents were heterozygous carriers (**Figure 4.16**). DNA from the 4 healthy siblings were not available to complete the segregation due to the family not consenting to genotyping of healthy siblings.

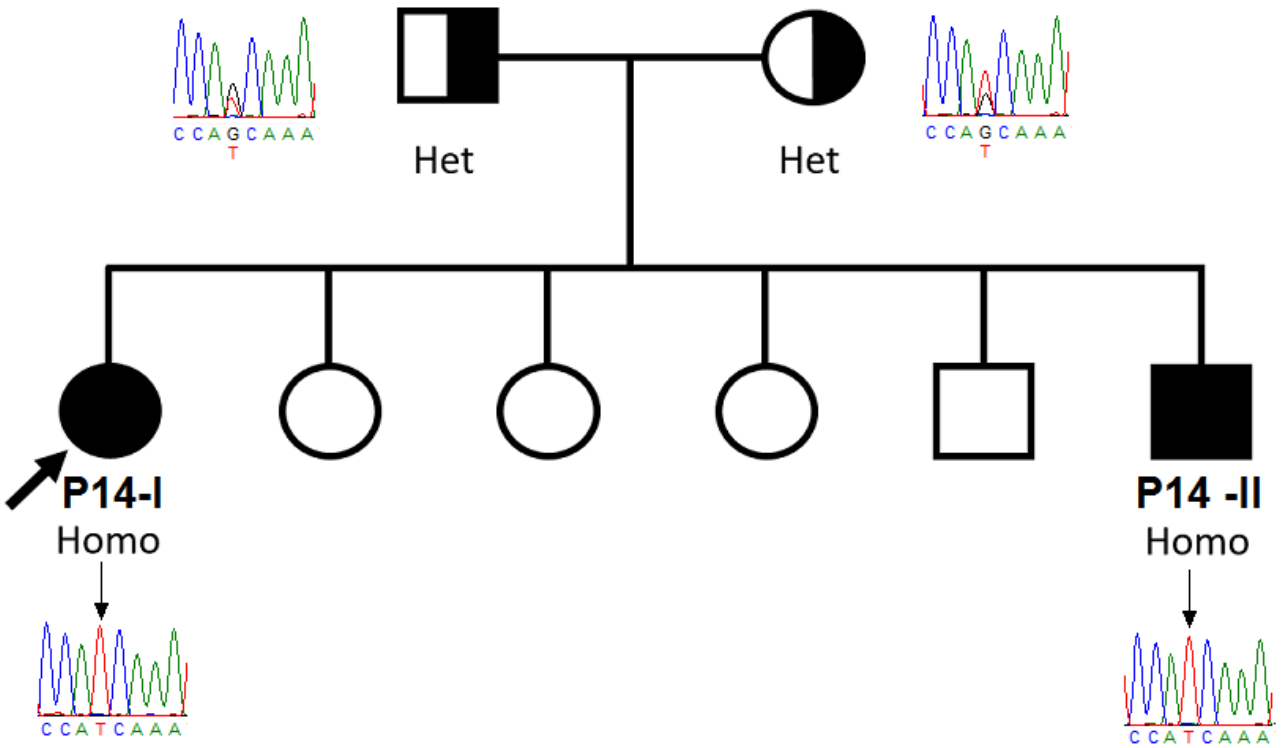

Figure 4.16 Segregation of *ATP8A2* variant in Family 14

Pedigree of family 14 showing the segregation of the identified *ATP8A2* variant (c.321+1G>T). Sequencing chromatograms of identified homozygous splice-site variant in Patient 14-I highlighting the nucleotide change (black arrow).

4.4.15 Undiagnosed cases

No candidate variants were identified in 8 of the 22 recruited families. The various filtration modifications were applied as described in ***Section 4.3.4,*** but no candidate variants were confirmed in these families.

4.4.15.1 Family 16

WES analysis revealed Patient 16 was heterozygous for a previously reported truncating *MGME1* variant (c.456G>A; p.Trp152*) (Kornblum et al., 2013). MGME1 is a mitochondrial nuclease that plays a role in DNA maintenance during mtDNA replication. Sanger sequencing of the truncating variant confirmed the patient was homozygous while sequencing of an exon with low read depth coverage identified no variants within it. Reanalysis of WES variants did not identify any other candidate variants.

4.5 Summary of findings

4.5.1 Variants in patients from consanguineous unions

Since the majority of recruited patients were born in consanguineous families, homozygous variants were the main focus of the WES variants filtration process. Of the 14 diagnosed families, 12 patients had consanguineous and 2 had non-consanguineous parents. All diagnosed patients from consanguineous families harboured homozygous genetic mutations, while one of the non-consanguineous families harboured a homozygous mutation and the other harboured compound heterozygous mutations (**Table 4.2**).

4.5.2 Rate of candidate variants identified

Of the 22 recruited families, 14 genetic diagnoses have been reached (63.6%). This is an expected yield as this was a similar diagnosis rate in previous research involving WES of patients suspected of mitochondrial disease (Taylor et al., 2014; Wortmann et al., 2015; Pronicka et al., 2016). Of the 14 diagnosed families, 10 families (71%) were diagnosed with or suspected of mitochondrial disease involvement, and 4 families (29%) were diagnosed with phenocopies of mitochondrial disease such as AGS and Cohen syndrome.

A total of 15 variants were identified in 13 genes. Of the 15 variants, 10 were novel variants (*LETM1*, *SLC19A3*, *SURF1*, *MPC1*, *NDUFA13*, *TTC19*, *RNASEH2C*, *VPS13B*, *TREX1*, *ATP8A2*), 2 were rare variants previously reported in a heterozygous state in

controls (*RRM2B*, *LETM1*), 3 were previously reported in patients (*PDHX*, *NDUFB9*, *TREX1*). Categories of the mutations are as follows: 7 missense mutations (*SLC19A3*, *MPC1*, *NDUFB9*, *LETM1*, *RRM2B*, *RNASEH2C*, *TREX1*), 2 truncating mutations (*PDHX*, *NDUFA13*), 3 frameshift deletions (*SURF1*, *TTC19*, *VPS13B*), 1 non-frameshift deletion (*LETM1*), 1 duplication (*TREX1*), 1 splice-site variant (*ATP8A2*). Of the 13 identified genes, 12 were previously reported as associated with disease in patients, and only *LETM1* was a novel candidate gene with mitochondrial localisation and function.

Table 4.2 Summary of variants identified using WES in recruited patients showing in silico predictions of pathogenicity in missense mutations

(continued on next page).

Family	Gene	RefSeq	Exon/ Intron	mRNA transcript	Protein substitution	Variant	MAF	PPh2	SIFT	Mutationtaster	CADD
1	*LETM1*	NM_12318.2	Exon 5	c.754_756del	p.Lys252del	Novel candidate gene	-	-	-	-	-
2	*SLC19A3*	NM_025243	Exon 3	c.175T>C	p.Trp59Arg	Novel variant	-	0.998	0.15	0.99999	24.5
3	*PDHX*	NM_003477	Exon 6	c.742C>T	p.Gln248*	Reported pathogenic variant	1.22×10^{-5}	NA	0.81	-	35
4	*SURF1*	NM_003172	Exon 5	c.367_368del	p.Arg123Glyfs*4	Novel frameshift deletion	-	-	-	-	-
5	*MPC1*	NM_016098	Exon 3	c.109C>T	p.Pro37Ser	Novel variant	-	0.991	0.27	0.9999	27
6	*LETM1*	NM_12318	Exon 6	c.881G>A	p.Arg294Gln	Novel candidate gene; rare variant	-				
7	*TTC19*	NM_017775	Exon 8	c.779_780del	p.Tyr260*	Novel frameshift deletion	-	-	-	-	-
8	*NDUFA13*	NM_015965	Exon 1	c.22C>T	p.Gln8*	Novel truncating variant	-	-	-	-	38
9	*NDUFB9*	NM_005005	Exon 2	c.191T>C	p.Leu64Pro	Reported pathogenic variant	1.6×10^{-5}	0.999	0.02	0.99999	26.3
10	*RRM2B*	NM_015713	Exon 6	c.574G>A	p.Ala192Thr	Rare missense variant	4.0×10^{-6}				31

Family	Gene	RefSeq	Exon/ Intron	mRNA transcript	Protein substitution	Variant	MAF	PPh2	SIFT	Mutationtaster	CADD
11	*RNASEH2C*	NM_032193	Exon 2	c.202C>G	p.Leu68Val	Novel variant	-	-	-	-	25
12	*TREX1*	NM_033629	Exon 2	c.50dupT c.341G>A	p.Asp18Argfs p.Arg114His	Novel duplication Reported pathogenic variant	- 2.0×10^{-4}	- 1.00	- 0.00	- 0.986	- 28.1
13	*VPS13B*	NM_015243	Exon 11	c.1512del	p.Glu505Lysfs	Novel frameshift deletion	-	-	-	-	-
14	*ATP8A2*	NM_016529	Intron 3	c.321+1G>T	p.? retaining intron 3?	Novel splicing variant	-	-	-	-	-

CADD: Combined Annotation Dependent Depletion; MAF: gnomAD minor allele frequency; PPh2: PolyPhen2; RefSeq: Reference Sequence; SIFT: Sorting Intolerant from Tolerant algorithm.

4.6 Discussion

4.6.1 Mitochondrial disease diagnoses

4.6.1.1 LETM1

LETM1 is a hexameric transmembrane protein, embedded in the mitochondrial inner membrane that plays a crucial role in calcium homeostasis by acting as a Ca^{2+}/H^{+} antiporter (Shao *et al.*, 2016). The protein also helps maintain mitochondrial morphology since overexpression of the protein leads to the fragmenting of mitochondria and knockdown results in the swelling of mitochondrial cristae and necrotic cell death (Nowikovsky *et al.*, 2004; Tamai *et al.*, 2008; Piao *et al.*, 2009). The protein was determined to have one transmembrane domain with the C-terminus located in the matrix (Shao *et al.*, 2016), but a more recent study identified another transmembrane domain of the protein with both the N and C-termini locating to the matrix (Lee *et al.*, 2017).

The *LETM1* gene was first reported as a deleted gene in Wolf-Hirschhorn Syndrome (WHS) patients (Endele *et al.*, 1999). It is one of several genes in the WHS critical region, located on the p arm of chromosome 4, that is hemizygously deleted in WHS patients. Symptoms of WHS include a characteristic facial dysmorphology, microcephaly, developmental delay, cardiac defects, epilepsy and hypotonia (Hirschhorn *et al.*, 1965; Wolf *et al.*, 1965; Hart *et al.*, 2014). Many of these phenotypes are present in patients with mitochondrial disease as well as other neurological disorders.

Patient 1-I and both her affected brothers (Patients 1-II and 1-III) presented with developmental delay and hypotonia, but cardiomyopathy was only observed in the patient and her younger brother while its presence was speculated in her older brother as it was not investigated or reported; all these clinical features fall under WHS and mitochondrial disorder symptoms. However, Patient 1-I and her older, affected brother presented with ophthalmological and auditory issues, both her brothers had elevated serum lactate levels and a muscle biopsy from her older brother showed reduced overall respiratory chain defect in all OXPHOS complexes. Observation of these accompanying clinical symptoms strongly supports a diagnosis of mitochondrial disorder in this family rather than WHS. This is further supported by the absence of the facial dysmorphic features of WHS and the absence of seizures in any of the siblings. Since WHS is associated with the hemizygous deletion in chromosome 4, the finding of a homozygous deletion in 2 of the

3 affected siblings with unaffected heterozygous parents is the final indicator that haploinsufficiency does not result in clinical presentation in this family (Hart et al., 2014).

The LETM1 amino acid residues affected in the 2 families are located in the C-terminal domain (CTD) that protrudes from the IMM into the matrix with the LETM1 protein having a single transmembrane domain (Shao *et al.*, 2016). Residues 252 and 294 are predicted to be part of a coiled-coil domain but the UniProt knowledge base reports the residue 252 to be the first residue in the ribosome binding domain (Endele *et al.*, 1999; Prasad *et al.*, 2009; The UniProt Consortium, 2017). Using this determined model, the mitoribosomal protein L36 (MRPL36) binds to LETM1 and localises to the IMM (Piao et al., 2009). MRPL36 plays a key role in binding the large ribosomal subunit to the small ribosomal subunit (Prestele *et al.*, 2009). The deletion of the *MRPL36* gene results in an overall respiratory chain complex defect since it contributes to the insertion of OXPHOS complex subunits by anchoring the mitoribosome close to the IMM where the expressed proteins are inserted by the IMM transmembrane protein OXA1 (Prestele *et al.*, 2009; Bauerschmitt *et al.*, 2010). It is likely that the deletion of the residue disrupted the binding of MRPL36 to LETM1 resulting in OXPHOS complex defects like those observed as a result of the C-terminal extension (CE) domain of the MRPL36 protein (Prestele *et al.*, 2009). This defect was reported in the OXPHOS complex activity carried out on the muscle biopsy from the Patient 1-I's older brother further supporting this hypothesis. The Ca^{2+} binding domain of the LETM1 polypeptide is located near the C-terminal of the LETM1 protein leading to the dismissal of the effect of the homozygous on the protein's calcium antiporter activity.

The conflicting model presented by Lee *et al.* (2017) places the residues in the IMS with a proposed coiled-coil region for binding ribosomal proteins. This might suggest that a reaction might be taking place in the IMS that could explain the observed swelling of the mitochondria in knockdown cell lines. It is unfortunate that no biopsy may be obtained to further research the effect of this variant on mitochondrial function and how it may have contributed to their clinical symptoms.

A submission of the identified *LETM1* variants in GeneMatcher (Sobreira *et al.*, 2015) matched us with a cohort of patients with variants in the same gene that are being compiled into a collaborative study that can highlight tissue result from surviving patients. A total of 7 families so far, including the 2 families from this study, have been assessed. One of the patients harboured the same rare homozygous mutation identified in

Patient 6 (c.881G>A; p.Arg294Gln) in a 34 year-old female patient born to consanguineous Italian parents. The patient presented with developmental delay, myopathy, hypotonia, ataxia, nystagmus, divergent strabismus, ptosis, bilateral cataracts, and lactic acidosis. A brain MRI scan at the age of 8 years revealed cerebral atrophy and cerebellar hypoplasia. Histochemical analysis of muscle biopsy revealed ragged red fibres and COX-deficient fibres, and respiratory chain enzyme activity assessment revealed combined OXPHOS deficiency of complexes I, III and IV. The patient's presentations match those identified in Patient 1-II with both presenting with hypotonia, myopathy, nystagmus, lactic acidosis, and combined OXPHOS enzymes deficiency in muscle.

Another family with two sibling patients who have compound heterozygous *LETM1* variants with one variant affecting a residue neighbouring the mutation identified in Patient 6 [c.878T>A; p.Ile293Asn] while the other was a frameshift deletion [c.2094del; p.Asp699Metfs]. Both affected siblings presented with developmental delay, diabetes, epilepsy, deafness, and facial dysmorphism. Other varying presentations were spasticity and clonus in one sibling while the other had neuropathy and MRI brain revealed hypoplasia in the pons and cerebellum. Interestingly, no elevated lactate was reported in either siblings.

The collaborative work on *LETM1* patients will provide a clinical spectrum of presentations that helps diagnose similar patients, while available tissue samples will help shed light on the aetiology of disease in the patients. It is surprising that 2 unrelated patients in this cohort who were from different ethnicities harboured mutations in a single novel candidate gene (*LETM1*). This was a promising finding; however, all the patients were deceased, and no tissue samples were available to pursue functional studies; only genotyping and segregation studies were possible.

4.6.1.2 NDUFA13

The identified *NDUFA13* nonsense mutation is located very early on in the translated polypeptide and the synthesised protein is likely degraded due to non-sense mediated decay. *NDUFA13* encodes a supernumerary complex I subunit located on the membrane arm of the inner mitochondrial membrane protein complex (Zhu *et al.*, 2016; Guo *et al.*, 2017). The protein was previously identified as *GRIM19* due to its function in inducing cell death by interferon-β and all-trans-retinoic acid (Angell *et al.*, 2000). Mutations in *NDUFA13* were first identified in thyroid Hurthle cell carcinomas and in other organ

cancers suggesting its function as a tumour (Máximo *et al.*, 2005; Pinto and Màximo, 2018). Knocking out *NDUFA13* expression in HEK293T cells, using TALENs tools, results in the disruption of complex I assembly (Stroud *et al.*, 2016).

The first identified inherited pathological mutation in *NDUFA13* was reported in patient siblings suspected of mitochondrial disease where both presented with developmental delay, hypotonia, lower limb spasticity, lactic acidosis, optic atrophy, abnormal eye movements, and complex I deficiency in muscle (Angebault *et al.*, 2015). Additionally, one of the siblings presented with epilepsy, choreoathetotic movements, auditory neuropathy, and global akinesia; the other presented with truncal ataxia, distal dyskinesia, and bradykinesia. Radiological MRI findings in both affected siblings revealed high signal in the dentate nucleus in addition to an elevated lactate peak in the basal ganglia on MRS. Functional analysis of skin fibroblasts from both patients revealed decreased levels of CI subunit proteins including NDUFA13, NDUFA9 and NDUFB8, decreased levels of assembled CI and OXPHOS supercomplexes, and lower oxygen consumption rates compared to controls.

Bi-allelic compound heterozygous *NDUFA13* variants were reported in another patient who presented with early-onset Leigh syndrome (Gonzalez-Quintana *et al.*, 2020). This patient presented before the age of 2 years with nystagmus, hypotonia, lactic acidosis, moderate neurological symptoms and bilateral lesions in the basal ganglia. By the age of 16 years, he had developed spastic tetraparesis, difficulty swallowing, low weight and mild hypertrophic cardiomyopathy. Biochemical OXPHOS enzyme analysis in patient biopsy revealed isolated CI activity. In addition, functional analysis of patient skin fibroblasts showed decreased levels of NDUFA13 and NDUFA9 proteins, decreased levels of assembled respirasomes, a slower growth rate, and lower oxygen consumption rates compared to controls.

The identified homozygous *NDUFA13* mutation in this study is the third identified family thus far. Progression of Patient 8's clinical presentations is similar that of the *NDUFA13* affected siblings reported by Angebault *et al.* (2015). Radiological MRI findings are consistent with a mitochondrial disease diagnosis and also overlap with regards to the involvement of the optic nerve (**Figure 3.7**). The early presentation of the *NDUFA13* patient reported by Gonzalez-Quintana *et al.* (2020) is similar to Patient 8 regarding developmental delay, nystagmus, hypotonia and lactic acidosis. The variation in clinical

presentations and findings show clinical heterogeneity with regards to mutations identified within a single gene associated with mitochondrial function.

The identified *NDUFA13* variant results in an early termination of protein translation likely meaning there is no protein expression. A skin biopsy from Patient 8 was requested to run functional studies to confirm variant pathogenicity and support the genetic diagnosis that this patient is complex I deficient.

4.6.1.3 MPC1

MPC1 encodes the IMM protein Mitochondrial Pyruvate Carrier 1 that forms a heterodimer complex with its paralog Mitochondrial Pyruvate Carrier 2 (*MPC2*) to facilitate the uptake of pyruvate by mitochondria (Bricker *et al.*, 2012; Vanderperre *et al.*, 2015). Both paralogs are required to form the complex and facilitate pyruvate transportation into the matrix.

Patients from three families suspected of mitochondrial disease were genetically investigated and 2 missense mutations in *MPC1* were identified (Brivet *et al.*, 2003; Bricker *et al.*, 2012). The patients presented with developmental delay, lactic acidosis, microcephaly, facial dysmorphism, hypotonia, nystagmus, hepatomegaly, and hypoglycaemia. Investigations revealed elevated plasma pyruvate and lactate, and Kreb's cycle intermediates in urine. Radiological brain MRI revealed cerebral atrophy, slight ventricular dilatation, and periventricular leukomalacia and calcification in addition to high lactate peak in caudate ganglia on MRS. Oxygen consumption in pyruvate driven respiration conditions was decreased in patient fibroblasts compared to control fibroblasts indicating the cells' dependence on anaerobic glycolysis to generate energy. Transfection of the patient fibroblasts with a vector carrying a wild-type human *MPC1* gene rescued the oxygen consumption supporting the genetic diagnosis of both *MPC1* mutations.

Patients 5-I and 5-II presented with clinical phenotypes similar to those reported in the *MPC1* patients. Some of the similar phenotypes are developmental delay, lactic acidosis, microcephaly/brachycephaly, and facial dysmorphism. Their younger sister (Patient 5-III) also presented with these features with the exception of the facial dysmorphism.

The novel *MPC1* missense mutation these patients harbour is the third reported mutation in *MPC1*. Skin biopsies from Patients 5-I and 5-II have been requested to functionally investigate the effect of the novel variant on MPC1 activity and expression in fibroblasts.

4.6.1.4 TTC19

TTC19 is a complex III assembly factor that colocalises with the respiratory chain protein in the IMM (Ghezzi *et al.*, 2011). Bi-allelic mutations in *TTC19* are associated with a group of heterogeneous phenotypes in both paediatric and adult patients; presentations include progressive neurodegenerative disease, psychosis, ataxia, and occasionally elevated lactate reported in patients (Ghezzi *et al.*, 2011; Nogueira *et al.*, 2013; Atwal, 2014; Melchionda *et al.*, 2014; Morino *et al.*, 2014; Ardissone *et al.*, 2015; Koch *et al.*, 2015; Kunii *et al.*, 2015; Mordaunt *et al.*, 2015). Radiological findings in patients commonly show involvement of the basal ganglia and the cerebellum. Most identified mutations are truncating, or frameshift indels that result in the loss of TTC19 protein expression in patient muscle and fibroblasts. Complex III enzyme activity is reduced in patient muscle and in fibroblasts grown in galactose, however immunoblotting and blue native gel electrophoresis (BNGE) do not show any reduction in the expression of complex III subunits and protein complex intermediates.

Recent research revealed that TTC19 is responsible for cleaving the N-terminal chain of the ubiquinol:cytochrome *c* reductase, Rieske iron-sulphur polypeptide (UQCRFS1) in the fully assembled protein complex (Bottani *et al.*, 2017). The accumulation of these N-terminus chains results in an inactive fully assembled complex III protein. The clinical progression of symptoms in Patient 7-I and her brother along with the lack of reported plasma lactate elevation and radiological findings involving the caudate and putamen (**Figure 3.6**) reflect a similar phenotype to that reported by Mordaunt *et al.* (2015) in an Iraqi patient. Skin biopsies from both affected siblings has been requested to functionally investigate the expression of TTC19 protein in fibroblast cell lines using immunoblotting, BN-PAGE and possibly respiratory chain enzyme activity. Findings will support the diagnosis of complex III deficiency and reinforce the phenotype-genotype relationship between *TTC19* mutations and clinical and functional finding in previously reported patients.

4.6.1.5 SLC19A3

SLC19A3 encodes a thiamine/H+ antiporter that is a member of the SLC19 folate/thiamine transporter family found in the plasma membrane that takes up thiamine while simultaneously expelling protons (Rajgopal *et al.*, 2001; Ganapathy *et al.*, 2004). Bi-allelic mutations in its gene are associated with biotin-thiamine responsive basal

ganglia disease (BTRBGD) (Ferreira *et al.*, 2017). BTRBGD is an autosomal recessive disorder that presents initially as encephalopathy with seizures and is accompanied by development delay or regression often leading to hypotonia and muscle fatigue (Aljabri *et al.*, 2016; Algahtani *et al.*, 2017). Lactic acidosis was also reported in some cases and was treated with thiamine and biotin (Pérez-Dueñas et al., 2013). However, treatment at late stages of BTRBGD does not reverse the effects leading to long-term symptoms that eventually lead to death (Algahtani *et al.*, 2017).

The clinical presentations of Patient 2 sit well with the BTRBGD diagnosis and she has been treated with thiamine and other supplements but there is no report of any biotin being administered. The homozygous mutation in exon 3 of the *SLC19A3* gene results in the non-synonymous substitution of a non-polar tryptophan residue at position 59 with a basic arginine residue in a transmembrane domain of the SLC19A3 protein (Prasad *et al.*, 2009; The UniProt Consortium, 2017). This substitution likely disrupts the secondary folding of the transmembrane protein leading to a reduction in thiamine/H+ antiporter activity resulting in the development of BTRBGD. Thiamine (also known as vitamin B1) has an active phosphorylated form thiamine pyrophosphate (TPP) which is an important cofactor in cellular metabolism including pyruvate dehydrogenase (PDH) activity (Depeint *et al.*, 2006).

Alaskan Husky Encephalopathy (AHE) is an animal disorder that presents with brain lesions similar to Leigh syndrome (Vernau *et al.*, 2013) AHE is caused by the truncation of the SLC19A3.1 paralog of the SLC19A3 protein due to compound heterozygous variants involving a 4bp insertion and a single nucleotide polymorphism in the gene (c.624insTTGC, c.625C>A) (Vernau *et al.*, 2015). The SLC19A3.1 paralog is expressed in the brain and spinal cord of Alaskan Huskies. Functional analysis of brain tissue from affected Huskies showed thiamine deficiency, reduction in OXPHOS activity and an increase in oxidative stress. These results do not reflect what happens in humans since *SLC19A3* gene is expressed ubiquitously in humans (Vernau *et al.*, 2013).

No functional study has been reported in the literature to investigate the effects of *SLC19A3* mutations on mitochondrial function in patients. Obtaining a biopsy sample and performing protein and mitochondrial functional analyses would expand our knowledge on the aetiology of this disease.

4.6.1.6 SURF1

SURF1 encodes a complex IV assembly factor that is embedded in the inner mitochondrial membrane (Zhu *et al.*, 1998). In addition to its role in assembly, SURF1 is also suggested to play an important role in the incorporation of heme a as part of the complex IV biogenesis pathway (Hannappel *et al.*, 2012). Bi-allelic *SURF1* mutations were first identified in Leigh syndrome patients with associated complex IV deficiency in 1998 (Tiranti *et al.*, 1998; Zhu *et al.*, 1998; Wedatilake *et al.*, 2013).

Leigh syndrome was reported by Denis Leigh in 1951 and is now considered the most common diagnosis in paediatric mitochondrial disease patients (Leigh, 1951; Lake *et al.*, 2015). Radiological MRI findings of symmetrical lesions involving the basal ganglia and brainstem are the most consistent features in Leigh syndrome. Genetic mutations associated with Leigh syndrome were first reported in 1991; since then, mutations in more than 75 genes (mitochondrial and nuclear) have been associated with Leigh syndrome (Hammans *et al.*, 1991; Lake *et al.*, 2016). *SURF1* is one of these genes and is commonly linked with complex IV deficiency associated with Leigh syndrome; cases with other *SURF1* mutations are associated with leukodystrophy (Rahman *et al.*, 2001; Wedatilake *et al.*, 2013).

Patients 4-I, 4-II and 4-III all presented with clinical phenotypes suggestive of mitochondrial disorder. Radiological brain MRI findings in all 3 patients were supportive of the diagnosis. For example, brain MRI findings for patient 4-III showed lesions involving the brainstem consistent with the radiological findings of Leigh syndrome patients (**Figure 3.5**). Patient 4-I also presented with hypertrichosis which is frequently reported in patients with *SURF1* mutations (Kleist-Retzow *et al.*, 2001; Østergaard *et al.*, 2005; Yüksel *et al.*, 2006; Baertling *et al.*, 2013).

No functional studies to support the *SURF1* mutation can be carried out due to the lack of skin and muscle biopsies or a cell line for any of the patients. Nonetheless, clinical and radiological findings support the genetic diagnosis of the three siblings having a pathogenic frameshift *SURF1* deletion.

4.6.1.7 RRM2B

RRM2B encodes the cytosolic protein Ribonucleotide Reductase regulatory TP53 inducible subunit M2B, which is a part of the ribonucleotide reductase complex responsible for the reduction of ribonucleoside diphosphates to deoxyribonucleoside

diphosphates (Bourdon *et al.*, 2007). which is a crucial step in replenishing cellular deoxyribonucleoside triphosphate levels for DNA synthesis, most importantly mtDNA synthesis. *RRM2B* mutations have been associated with mtDNA depletion and multiple mtDNA deletions in patients (Pitceathly *et al.*, 2012; Keshavan *et al.*, 2020). Patients with *RRM2B* mutations either present early in life or in adulthood with the most commonly reported phenotypes in adults being ptosis and progressive external ophthalmoplegia (PEO).

Patient 10's presentation and age at onset fit well with the genetic diagnosis of bi-allelic *RRM2B* mutations. Even though her MDC score was only suggestive of probable mitochondrial disease involvement, as the only adult in the cohort, her presentations of ptosis, PEO, and exercise intolerance and fatigue were highly suggestive of mitochondrial disease. The MDC used in the study was specified for use with paediatric cases rendering it unreliable in this case. Furthermore, the lack of medical reports and investigation results likely depleted the MDC score. The decision to recruit was based on Prof McFarland's expertise and assessment of her clinical presentation during his visit to Kuwait. As the only adult patient, her parents were deceased, and no segregation study was possible.

4.6.1.8 NDUFB9

The identified variant is the only *NDUFB9* reported in patients who were homozygous and their fibroblasts revealed a defect in complex I activity that was rescued when wild-type *NDUFB9* cDNA was expressed (Haack *et al.*, 2012). *NDUFB9* encodes a supernumerary complex I subunit located within the membrane arm of the protein embedded in the inner mitochondrial membrane (Zhu *et al.*, 2016; Guo *et al.*, 2017). NDUFB9 plays a role in the interaction between complexes I and III when forming supercomplexes (Wu *et al.*, 2016a). Knocking out *NDUFB9* expression in HEK293T cells, using TALENs and CRISPR/Cas9 methods, results in the disruption of complex I assembly (Stroud *et al.*, 2016). The first reported pathogenic mutation in *NDUFB9* was associated with reduced expression of NDUFB9 and other complex I subunits in fibroblasts in addition to reduced complex I activity (Haack *et al.*, 2012). One of the affected siblings presented before the age of 6 months with progressive hypotonia and lactic acidosis.

Patient 9 is homozygous for the same mutation reported and his symptoms occurred before the age of 6 months. His elevated lactate and hypotonia are also consistent yet the

ophthalmologic and auditory presentations are additional clinical presentations not reported before. Since no up-to-date clinical data is available for the reported patient's symptoms, the additional symptoms could be considered as clinical variations in patients with *NDUFB9* mutations.

4.6.1.9 PDHX

Pyruvate dehydrogenase complex (PDHc) is a protein that localises in the mitochondrial matrix and catalyses the final step of glycolysis by converting pyruvate to acetyl-CoA (Brown *et al.*, 2006). The *PDHX* gene codes for the E3 binding protein (E3BP), also known as PDHc component X, which binds to the protein's catalytic subunit E2 to the E3 subunit of the PDHc. Mutations in the *PDHX* gene are predominantly associated with patients exhibiting lactic acidosis, due to pyruvate dehydrogenase deficiency, mostly accompanied by symptoms of developmental delay, encephalopathy, and occasionally reported seizures, or hypotonia (Barnerias *et al.*, 2010; Tajir *et al.*, 2012; Ivanov *et al.*, 2014). Patient 3's presentation with episodic lactic acidosis, developmental delay, hypotonia, epilepsy and encephalopathy are clearly associated with PDHc deficiency.

In Kuwait, two previously reported patients that were homozygous for protein truncating mutations in *PDHX* presented with similar symptoms including the reported thinning of the corpus callosum (Ramadan *et al.*, 2004). One of them was homozygous for a mutation that led to the termination of translation in exon 6 at residue position 248 (c.742C>T, p.Gln248*) and the other was a nonsense mutation that terminated translation in exon 1 at the 5th residue position (c.14A>G, p.Typ5*). Pyruvate dehydrogenase activity was reduced in both patient and histochemical analysis showed both patients were deficient for E3BP. Truncating mutations were reported elsewhere in the literature with similar reported symptoms and deficiencies as previously described (Brown *et al.*, 2006; Tajir *et al.*, 2012).

More importantly, the genotyped homozygous mutation in Patient 3 was reported in a case that was compound heterozygous for the truncating variant plus the insertion of a long-interspersed element-1 that resulted in the deletion of exons 3 to 9 of the *PDHX* gene (Miné *et al.*, 2007). Reported clinical symptoms overlapped with Patient 3 pyruvate dehydrogenase activity was reduced and the E3BP deficiency was reported.

Even though the truncating mutation was previously reported in the literature, this is the first time it is present in a homozygous state. Repeating biochemical and histochemical

and confirming the effects of the mutation on pyruvate dehydrogenase activity and E3BP expression will provide further support to the effects of truncating mutations in the *PDHX* gene.

4.6.2 Non-mitochondrial diagnoses

4.6.2.1 RNASEH2C

Cleavage of ribonucleotides from RNA:DNA and DNA:DNA duplexes is performed by the endonuclease RNase H2 (Crow *et al.*, 2006b). Three subunits (RNASEH2A, RNASEH2B and RNASEH2C) comprise the fully functioning enzyme. Mutations in genes coding for these subunits are associated with Aicardi-Goutières syndrome (AGS) an autosomal recessive disorder that usually presents in childhood with microcephaly and an encephalitic-like syndrome that leads to psychomotor delay, irritability, hypotonia, abnormal movements and many develop epilepsy (Rice *et al.*, 2007b; Crow *et al.*, 2015). Calcification of the basal ganglia and white matter abnormalities in MRI brain scans are also characteristic of AGS.

In the *RNASEH2C* gene, a homozygous missense mutation (c.205C>T; p.Arg69Trp) directly neighbouring the genotyped variant found in Patient 11-I and her cousin Patient 11-III (c.202C>G; p.Leu68Val) was reported in at least 24 families with AGS (Crow *et al.*, 2015). The presentation of developmental delay, hypotonia, microcephaly, epilepsy and MRI scans showing calcification of the basal ganglia in Patient 11-I points towards a diagnosis of AGS. The reported symptoms of Patient 11-II in addition to Patient 11-III's presentation with jerky movements, irritability and reported encephalopathy further support the AGS diagnosis. However, elevated lactate reported in both affected cousins, hearing loss in Patient 12-I and nystagmus in Patient 11-III suggest the possible involvement of mitochondrial dysfunction. Analysis of biopsy samples from both affected cousins could uncover any mitochondrial involvement in this AGS suggested diagnosis.

4.6.2.2 TREX1

TREX1 was the first gene associated with AGS and is also associated with adult-onset autosomal dominant retinal vasculopathy with cerebral leukodystrophy (RVCL) (Richards *et al.*, 2007; DiFrancesco *et al.*, 2015). *TREX1* encodes a 3'-5' DNA exonuclease that degrades single stranded DNA during DNA damage repair and in a cellular apoptosis pathway (Höss *et al.*, 1999; Lee-Kirsch *et al.*, 2007). AGS patients with

TREX1 mutations were the most severely affected compared to patients with variants in other associated genes (*ADAR, IFIH1, RNASEH2B,* and *SAMHD1*) (Adang *et al.*, 2020). RVCL patients with heterozygous mutations in the C-terminal of *TREX1*

Patient 12 presented with leukodystrophy, epilepsy, spasticity, developmental delay, and elevated serum and CSF lactate; no interferon alpha levels were measured in the patient's serum or CSF. The patient's phenotype, notably the elevated serum and CSF lactate, was highly suggestive of mitochondrial disease or other neurological disorders, but AGS was not suspected. The lack of thorough clinical investigations such as cranial CT scan and assessment of serum α-interferon levels in the *TREX1* patient resulted in the misinterpretation of the phenotype. The elevated lactate levels reported might be a result of distress at the time of sample collection. Leukodystrophy is another finding that has been reported in mitochondrial disease patients adding to the suggestiveness of the phenotype. Although not yet measured, the patient's serum interferon alpha levels might have been suggestive of AGS; this should be followed-up and confirmed in the patient.

4.6.2.3 VPS13B

VPS13B encodes vacuolar protein sorting 13 homolog B, a transmembrane protein of the plasma membrane associated with vesicle-mediated transport and intracellular protein sorting (Kolehmainen *et al.*, 2003). The *VPS13B* gene spans 864 kb with 4 protein coding transcripts identified the largest containing 62 exons. The VPS13B protein localises to the Golgi apparatus and siRNA knockdown of *VPS13B* resulted in Golgi fragmentation, defects in endosome and lysosome formation, and defects in Golgi glycosylation indicating VPS13B is required to maintain Golgi morphology and glycosylation and plays a role in the endosomal - lysosomal pathway (Seifert *et al.*, 2011; Duplomb *et al.*, 2014). Furthermore, siRNA knockdown of the rat homolog *Coh1* in rat hippocampal neurons reduced the length of neurites formed compared to siRNA scramble knockdown suggesting the protein in involved in neuritogenesis (Seifert *et al.*, 2015).

Mutations in *VPS13B* are associated with Cohen syndrome, an autosomal recessive disorder with variable clinical presentations patients (Kolehmainen *et al.*, 2003). More than 200 patients diagnosed with Cohen syndrome from different parts of the world including Finland, Italy, Greece, Iran, Pakistan, India, Japan, and China (Bugiani *et al.*, 2008; Seifert *et al.*, 2009; Douzgou and Petersen, 2011; Rafiq *et al.*, 2015; Zhao *et al.*, 2019; Alipour *et al.*, 2020; Kaushik *et al.*, 2020). Most reported mutations result in loss

of protein function (i.e., frameshift deletions and truncating mutations). Patients typically present with microcephaly, infantile hypotonia, non-progressive developmental delay, typical craniofacial features (in the form of short philtrum, high arched or wave shaped eyelids, thick hair, and low hairline), hyperextensibility of the joints, slender extremities, motor incoordination, intermittent neutropenia, and a cheerful disposition (Kivitie-Kallio and Norio, 2001; El Chehadeh-Djebbar *et al.*, 2013). Variable reported presentations include abnormal truncal fat distribution (observed in mid-childhood), typical facial characteristics, retinitis pigmentosa, myopia, cataract, and chorioretinal dystrophy (Douzgou and Petersen, 2011; Douzgou *et al.*, 2011).

Patient 13's clinical presentations fit well with this genetic diagnosis as he presented with developmental delay, facial dysmorphic features, mild turricephaly, bilateral cataract (which was treated), generalised muscle weakness, wasted shoulder and hip muscles supported by an abnormal EMG indicating myopathy and a brain MRI revealing mild cerebellar atrophy. The MRI findings were previously highlighted as a key finding in some patients with bilateral cerebellar hypoplasia, but Patient 13 only had unilateral (left) hypoplasia (Waite *et al.*, 2010). No blood investigation results were available to report on lactate levels and neutrophil levels which would further support a clinical Cohen syndrome. Patient 13 had a high MDC score of 9 meaning he was a good candidate for the study as a suspected mitochondrial disease patient born to first cousin parents with family history of an affected paternal aunt. The lack of clinical history regarding disease progression did not prompt the exclusion of the patient from recruitment highlighting a limitation of the recruitment process. The patient's family did not provide DNA samples to perform a segregation study therefore we could not confirm segregation of the identified deletion and genotype the affected aunt.

4.6.2.4 ATP8A2

ATP8A2 encodes a P4-type ATPase, a plasma membrane protein that translocates the aminophospholipid phosphatidylserine across the membrane's lipid bilayer from the exocytoplasmic to the cytoplasmic leaflet; *ATP8A2* is expressed in the retina, testes and brain where it is mostly expressed in the cerebellum (Coleman *et al.*, 2009; Cacciagli *et al.*, 2010). The translocation of aminophospholipids maintains lipid bilayer asymmetry which is crucial for maintaining the curvature of cellular membranes and is associated with numerous cellular functions including cell division, vesicle formation, membrane permeability, and apoptosis.

A number of patients with *ATP8A2* mutations have been reported and presented with cerebellar ataxia, mental retardation and dysequilibrium syndrome 4 (CAMRQ4) and manifested severe neuromuscular phenotypes (Cacciagli *et al.*, 2010; Onat *et al.*, 2013). The first reported case presented with severe mental retardation and hypotonia and had a balanced chromosomal translocation between chromosomes 10 and 13 resulting in the splitting of the *ATP8A2* gene. The second family were primarily diagnosed with Unertan syndrome, a syndrome characterised by mental retardation, primitive language and quadrupedal gait. Patients from the second family presented with mental retardation, truncal ataxia, mild atrophy of cerebral cortex, cerebellum and corpus callosum, and most had quadrupedal gait. A missense *ATP8A2* mutation involving a highly conserved residue (Ile376Met) was identified and segregated in the affected individuals.

Patients 14-I and 14-II presented with similar phenotypes to those reported in the Unertan family, but no quadrupedal gait was noted. The presence of ptosis and ophthalmoplegia along with lactic aciduria in Patient 14-I raises the question of whether metabolic or mitochondrial function is involved in the disease aetiology. This is supported by the presence of metabolic findings in Patient 14-II. Unfortunately, no patient cell line was available to run cDNA analysis to assess the effect of the splice-site variant on mRNA splicing.

4.7 Summary

The aim of my study was to recruit paediatric patients residing in Kuwait who are highly suspected of mitochondrial disease involvement. With this in mind, my selected cohort was from a highly consanguineous population with a focus on diagnosing mitochondrial disease resulted in a rate of diagnosis that reflects the high proficiency of the implemented recruitment scheme and adapted MDC scoring criteria. The clinical phenotypes of patients were not suggestive of any specific genes to be targeted initially since the majority of patients did not have biochemical or histological results from muscle biopsies. Utilisation of WES resulted in the diagnosis of 14 out of 22 families without the need for linkage analysis or homozygosity mapping. The rate of diagnosis (63.6%) was similar to diagnosis rate reported in cohorts of suspected mitochondrial disease patients investigated using WES (Haack *et al.*, 2012; Taylor *et al.*, 2014; Wortmann *et al.*, 2015; Pronicka *et al.*, 2016).

4.8 Conclusion

The use of agnostic WES had an advantage over targeted gene sequencing of genes associated with mitochondrial function since WES allowed for the diagnosis of 4 families with disorders that were phenocopies of mitochondrial disease (Lieber *et al.*, 2013). Nonetheless, there were limitations to the WES method since coverage and depth of variant calls varied between patients (see ***Section 4.4.1***) which could have resulted in reduced capture of some genes associated with mitochondrial function (Sims *et al.*, 2014). Moreover, WES is not reliable in identifying translocations and inversions in chromosomes, identifying copy number variants (CNVs), sequencing repeat regions and GC-rich regions, identifying methylation patterns due to epigenetics or unipaternal disomy, or identify deep intronic variants that could result in cryptic splicing or affect microRNA function (Seaby *et al.*, 2015; Sheppard *et al.*, 2018). These limitations are expected when using WES as a first-tier diagnostic tool to diagnose patients suspected of a genetic disorder, but the resulting diagnostic rates keep it as a promising diagnostic tool.

Another limitation was the databases of control genotypes used in determining variant frequencies in the world population (such as gnomAD); these databases do not include Arabs as an exclusive subgroup. There are no databases with Arab population genotypes available publicly, however a number of databases are being developed in Saudi Arabia and Qatar (Team, 2015; Zayed, 2016). The disadvantage of using gnomAD as a reference database for controls is that some common variants in the Arab population might be under-reported in the database and thus could lead to a false-positive classification of a variant that has a higher frequency in the population than reported. Nonetheless, the availability of variants from over 60,000 sequenced individuals is a great starting point and a resource to rule out variants that are already identified.

The input from clinical experts in Kuwait and Newcastle along with the use of the developed MDC played a major role in increasing the rate of mitochondrial disease diagnoses within my study cohort. Such input and analysis of patients could help diagnose patients without the need for invasive muscle biopsies to confirm mitochondrial disease. Although the MDC has limited sensitivity in its analysis, its high specificity enables patients with mitochondrial disease to be recruited for WES analysis. However, the utilised MDC was not thoroughly evaluated and validated using known mitochondrial and non-mitochondrial disease cases. The result of these scores was the identification of variants associated with non-mitochondrial diseases in 4 families. This finding suggests

a limitation of the MDC that can suggest a case to be suspected of mitochondrial disease due its scoring methods. The utilisation of the MDC scoring system helped establish a comparison between the recruited cases, but its specificity needs to be re-evaluation to help identify patients suspected mitochondrial disorders more accurately.

It was surprising to see patients from 2 unrelated families with mutations affecting the same gene (*LETM1*), a novel candidate gene associated with mitochondrial function. Studies involving understudied populations such as the Middle East can help identify novel candidate genes due to the high consanguinity rate within the population leading to high rates of recessive genetic disorders. It was unfortunate that patients from both families were not available

The remaining 8 undiagnosed cases were investigated for variants that might explain their phenotypes using WES, but no clear candidates were identified; these included mtDNA variant that were sequenced in the process. Due to the presence of consanguinity within the population and the lack of a clear phenotype associated with mtDNA mutations, no mtDNA variants were identified in these patients. Further investigations are required to help identify the cause of disease in the patients but the lack of access to skin biopsies and functional analysis hinders the progress of diagnosis in these patients.

For interesting cases in my cohort with novel variants identified, we were able to obtain skin biopsies to establish fibroblast cell lines and functionally investigate the steady-state levels of protein subunits and OXPHOS complex assemblies which are highlighted and discussed in the following chapter (**Chapter 5**).

Chapter 5. The functional validation of genetic variants identified by whole exome sequencing

5.1 Introduction

Traditional mitochondrial disease investigations have depended on functional findings in patient biopsies suggestive of impaired mitochondrial function prior to initiating, and guiding, diagnostic genetic analyses (Wortmann *et al.*, 2017). This has routinely involved the acquisition of a muscle biopsy from the patient and analysing OXPHOS complex enzyme activities histochemically and biochemically. With the introduction of NGS methods in the forms of WES/WGS and/or large gene panels, improved diagnostic rates have prompted a shift in the approach to diagnosis to a "genetics-first" approach. Genetic diagnoses in mitochondrial disease patients using NGS technologies may result in a number of scenarios that might prompt further investigations to validate the identified variants as causative. A range of functional analysis methods are utilised for this purpose and multiple factors influence the selected methods of validation. A flowchart outlining the process of functional investigations has recently been proposed by our group and is found in **Figure 5.1** (Thompson *et al.*, 2020a).

If the identified variants are known, validated pathogenic variants in a gene previously associated with mitochondrial disease and the clinical phenotype correlates with previously reported patients with the same genotype, no investigation beyond the segregation study within the patients' families is warranted. If the identified variant is a novel variant in a known mitochondrial disease gene, investigating steady-state protein levels of the protein and related proteins (e.g. OXPHOS subunits) in patient tissue (e.g. muscle biopsy) or fibroblast cell lines using SDS-PAGE and immunoblotting will highlight the effect of the variant on the expression of the protein of interest and related proteins (Schägger, 2006), while investigating the assembly of OXPHOS complexes using BN-PAGE will assess the effect of the variant on complex assembly (Wittig *et al.*, 2006). In addition, assessment of gene transcription via qPCR of cDNA generated from patient mRNA can highlight the effect of the identified variant on gene expression (Wong and Medrano, 2005). Furthermore, splice-site variants can be investigated by sequencing cDNA to conclude how the variant affects splicing and if it results in intron retention or exon skipping (Anna and Monika, 2018).

If the variant is identified in a novel candidate gene of known mitochondrial function, SDS-PAGE and BN-PAGE phenotypes were assessed in patient tissue and/or cell lines to evaluate the effect of the variant on protein levels and, when necessary, OXPHOS complex assembly and protein levels. Assessment of respiratory chain complex enzyme activities can support SDS-PAGE and BN-PAGE findings (Schägger, 2006; Wittig *et al.*, 2006; Frazier *et al.*, 2020). If the novel candidate gene plays a role in mtDNA expression, analysis of the incorporation of [^{35}S] labelled methionine and cysteine can assess the synthesis rates of newly transcribed mtDNA encoded proteins in patient cell lines compared to control cell lines (Richter *et al.*, 2013). Furthermore, a rescue experiment expressing a wild-type copy of the protein in the patient cell lines and assessing the effect on previously established phenotype helps validate that the identified variant is pathogenic (Murphy *et al.*, 2016). GeneMatcher (https://genematcher.org/) is a platform that matches researchers that have identified variants in the same novel candidate genes fostering collaboration to build larger patient cohorts, something that is a constant challenge in the study of rare disease (Sobreira *et al.*, 2015). This can lead to parallel functional studies on multiple variants and provide functional evidence validating the pathogenicity of the variants in novel candidate genes and establishing an association with mitochondrial disorders and/or other genetic disorders.

The previously mentioned functional methods depend on the availability of cell lines, typically skin fibroblasts, from patients. In circumstances where patient tissues and cell lines are not available (e.g., the affected individual may be deceased or parental consent has not allowed the collection of tissues or cells for functional testing), other tissue culture models and animal models may be studied. Cellular phenotypes can be assessed in human cell lines using a number of methods: knocking down gene expression using RNA interference methods (Han, 2018); knocking out gene expression using gene editing methods such as TALENs and Crispr-Cas9 (Stroud *et al.*, 2016); knocking in mutations in homologs of the gene in other organisms such as yeast (Bricker *et al.*, 2012); or using mouse knock-in or knock-out models (Agostino *et al.*, 2003; Yatsuga and Suomalainen, 2012; Li *et al.*, 2014). An example of this is the generation of knock-out *Slc19a3* mice which showed decreased uptake of thiamine compared to wild-type mice (Reidling *et al.*, 2010). This is an excellent model with regards to *SLC19A3* mutations in LS patients that revealed the consequence of the mutations on protein function. However, the outcomes of model experiments are not always representative of human knock-out experiments or

present with phenotypes similar to human phenotypes. For example, mutations in *SURF1* are associated with LS due to complex IV deficiency, but *Surf1* knock-out mice presented with a mild decrease in complex IV activity upon tissue analysis, absence of neurodegeneration, and increased lifespans compared to controls (Dell'Agnello *et al.*, 2007). The phenotype observed in this mouse model is not representative of the phenotypes observed in *SURF1* LS patients. Therefore, caution needs to be observed when generating and investigating these models.

At KMGC, the only functional analysis tool available is a tandem mass spectrometer used as part of Kuwait's national new-born screening programme. It assesses acylcarnitine and amino acid levels in dried blood spots optimally acquired on day 3 of life. These screening results can identify neonates with treatable metabolic disorders including disorders related to the fatty acid oxidation and amino acid metabolism pathways. However, as a screening step, follow-up validation of possible metabolic disease is carried out on peripheral blood at a specialised biochemistry lab and genetic investigation is not necessarily performed to elucidate the cause of the disease phenotype. However, in cases that do have follow-up genetic analyses (e.g., very-long-chain acyl-CoA dehydrogenase deficiency, phenylketonuria and biotinidase deficiency), Sanger sequencing is performed on *ACADVL*, *PAH* and *BTD* genes, respectively, in search of known founder mutations in the populations or novel variants in these genes due to the high phenotype-genotype correlations. This approach has been utilised for the past 5 years and has identified a large number of patients with these disorders and genotyped and segregated variants in families. Genetic counselling services are provided to families with such results (highly likely with consanguineous parents). This process utilises a "function first" approach to diagnosing neonates and is an optimal follow-up for the new-born screening programme results.

In patients with suspected genetic disease, genetic results may be carried out at a commercial facility that carries out NGS analyses most commonly WES. Segregation studies are carried out at KMGC using Sanger sequencing, but novel variants or variants of unknown significance (VUS) are not followed up with functional analyses when required for validation and are assumed to be causative. This lack of functional investigations is concerning and establishing a functional lab that utilises methods to validate pathogenicity of genetic variants is critical in Kuwait and KMGC requires such facilities to expand its service and provide support for its genetic findings.

5.2 Aims

The Aim of this chapter is to validate the genetic findings in patients from 4 families recruited from Kuwait using functional analysis techniques available. This chapter includes patients from 3 additional families that were referred from the King Saud University, Riyadh, Kingdom of Saudi Arabia, and the NHS Highly Specialised Service for Rare Mitochondrial Disorders in Newcastle upon Tyne, UK. These additional cases harboured novel variants in known mitochondrial disease genes that required validation. Evidence of pathogenicity in these cases with novel or rare variants allows for a definitive diagnosis to be made and feedback to the treating clinicians can provide support to patient families through genetic counselling. Functional findings can also inform about new mitochondrial biology and help to characterise novel mitochondrial disease genes (see **Chapter 6**).

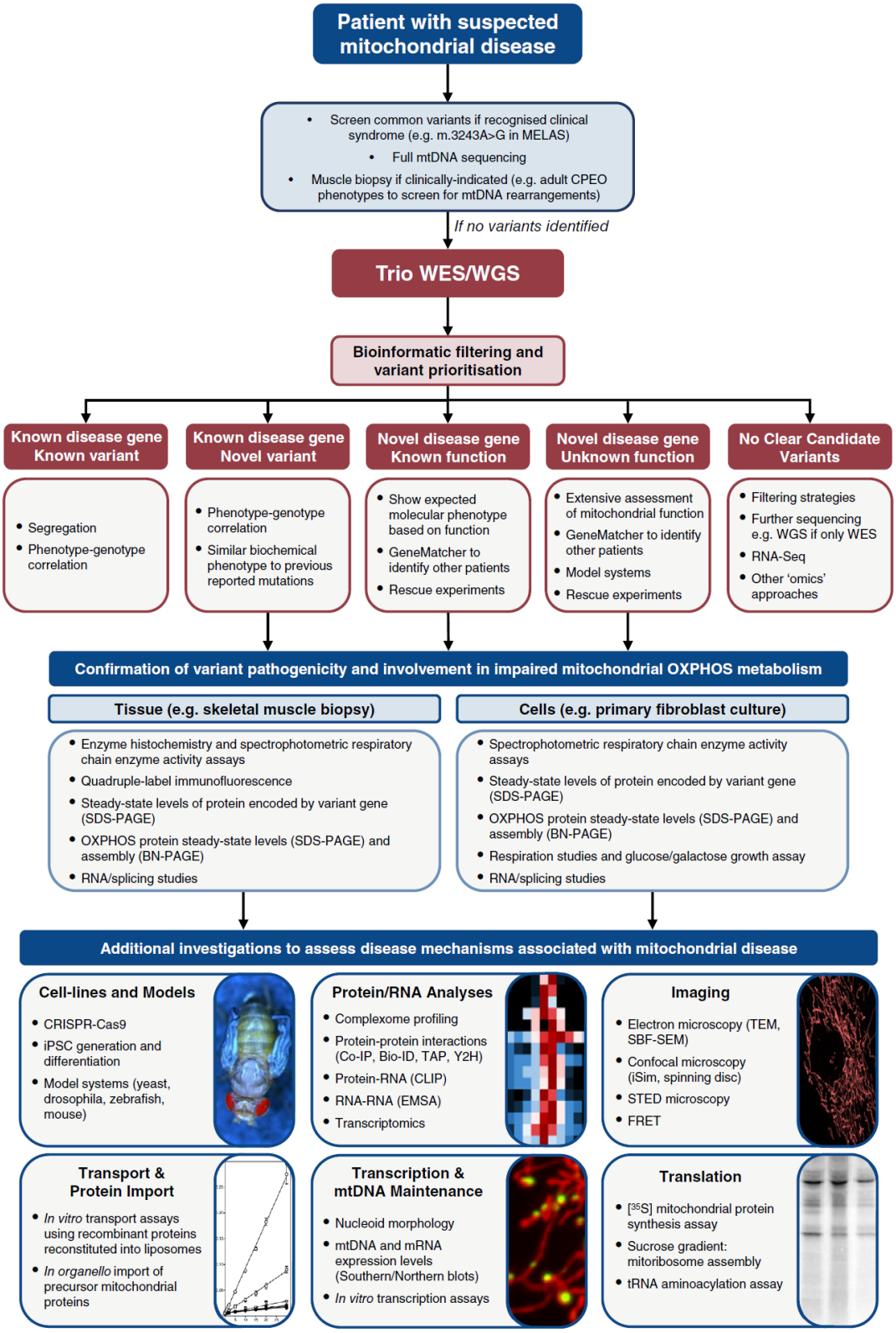

Figure 5.1 An overview of workflow utilised in identifying variants and validating their pathogenicity in association with mitochondrial disease.

(Legend on next page)

Figure 5.1 An overview of workflow utilised in identifying variants and validating their pathogenicity in association with mitochondrial disease.

Genetic investigations are initiated upon suspicion of mitochondrial disease. Methods include preliminary sequencing of mtDNA in search of possible mutations. Upon identification, follow-up functional techniques can be used to validate pathogenicity of the variant and elucidate aetiology of disease.
The following are examples of additional investigations used to validate and assess the consequence of identified variants:
Cell-lines and Models: a yeast model was used to validate the pathogenicity of *MPC1* mutations identified by expressing the mutant *MPC1* genes in *mpc1*-knockout yeast which did not restore yeast growth rates and did not restore rates of oxygen consumption to control levels (Bricker *et al.*, 2012).
Protein/RNA Analyses: complexome profiling of OXPHOS complex assembly was assessed in patients with *NDUFA6* mutations and highlighted stalled complex I assembly and the absence of complex I's N-module (Alston *et al.*, 2018).
Imaging: Transmission electron microscopy (TEM) of fibroblasts from a Leigh syndrome patient homozygous for *SLC25A46* mutations revealed reduced numbers and lengths of cristae in mitochondria suggesting SLC25A46 plays a role in mitochondrial dynamics (Janer *et al.*, 2016).
Transport and Protein Import: Inhibition of complex I resulted in impaired protein import into the mitochondrial which was assessed by expressing a gene tagged with a mitochondrial target sequence and assessing protein localisation and mitochondrial import (Franco-Iborra *et al.*, 2018).
Transcription and mtDNA Maintenance: A northern blot assessing the expression of *MT-ATP6* in fibroblasts of a patient with a dinucleotide deletion revealed a reduction in the mRNA expression of *MT-ATP6* (JeŠIna *et al.*, 2004).
Translation: Following on from the aforementioned reduction in mRNA expression of *MT-ATP6*, JeŠIna *et al.* (2004) performed a [^{35}S] methionine mitochondrial protein synthesis which confirmed the reduction in ATP6 protein synthesis in the mitochondria (Thompson *et al.*, 2020a).

5.3 Methods

5.3.1 Recruitment of Patients

Patients were recruited via my research cohort from the Kuwait Medical Genetics Centre as outlined in ***Section 3.3.1***. Additional patients were referred from the King Saud University, Riyadh, Kingdom of Saudi Arabia, and from the NHS Highly Specialised Service for Rare Mitochondrial Disorders in Newcastle upon Tyne, UK. Clinical summaries and growing fibroblast cell lines were provided by the respective centres.

5.3.2 Acquiring patient fibroblast cell lines from skin biopsies

Surviving patients living in Kuwait with novel variants of interest had a skin biopsy obtained by Ahmad Alaqeel, a clinical colleague at the KMGC. An outline of how samples were acquired is provided in ***Section 2.2.15***. The biopsy samples were sent to the NHS Highly Specialised Service for Rare Mitochondrial Disorders in Newcastle upon Tyne, UK.

5.3.3 Establishing primary cell lines from skin biopsies

Gavin Falkous established the primary fibroblast cell line from the obtained patient skin biopsies by explanting the samples in T25 flasks. They were treated as outlined in ***Section 2.2.16***. The established fibroblast cell lines were split once they reached 80% confluency.

5.3.4 Cell culture

Cultured fibroblast cell lines of patients were performed as outlined in ***Sections 2.2.17***, ***2.2.18***, ***2.2.19*** and ***2.2.20***.

Cells were expanded once they reached 60-80% confluency. Larger flasks were used when necessary to obtain larger numbers of cells for analysis.

5.3.5 Cell lysing in preparation for protein steady-state analysis using western blotting

Fibroblasts from control were harvested and lysed as outlined in ***Section 2.2.21.1*** and the protein concentrations were determined as described in ***Section 2.2.21.2***.

5.3.6 Assessment of protein steady-state levels using western blotting

An outline of the Western blotting method is provided in ***Section 2.2.21.3*** and a description of the immunoblotting technique is outlined in ***Section 2.2.23***.

5.3.7 Enrichment of mitochondria

Mitochondrial enrichment was performed on harvested patient fibroblasts to provide a higher quantity and concentration of mitochondrial proteins for analysis of OXPHOS complex assembly. An outline of the mitochondrial enrichment method is provided in ***Section 2.2.22.1***.

5.3.8 Solubilisation of enriched mitochondria

Enriched mitochondria were solubilised using 1% DDM as outlined in ***Section 2.2.22.2***.

5.3.9 Assessment of OXPHOS complex assembly using BN-PAGE

An outline of the BN-PAGE method is provided in ***Section 2.2.22.4*** and a description of the immunoblotting technique is outlined in ***Section 2.2.23***.

5.3.10 Analysis of respiratory chain complex activity

These studies were performed by Langping He at the NHS Highly Specialised Service for Rare Mitochondrial Disorders in Newcastle upon Tyne, UK. A description of the methods is outlined in ***Section 2.2.24***.

5.4 Results

5.4.1 Clinical summaries of investigated patients

The following are clinical and genetic summaries of patients investigated and diagnosed at indicated centres or at the NHS Highly Specialised Service for Rare Mitochondrial Disorders in Newcastle upon Tyne, UK.

5.4.1.1 Patient 23

Patient 23 was investigated and diagnosed by the NHS Highly Specialised Service for Rare Mitochondrial Disorders in Newcastle upon Tyne, UK.

Patient 23 was born in 1991 and presented with seizures and myoclonus with brain MRI reporting basal ganglia calcification. mtDNA and *POLG* mutations were investigated and excluded. WES identified a rare homozygous *COX15* variant: NM_078470; c.1019T>C; p.Leu340Pro. *In silico* predictions tools including PolyPhen2, PROVEAN, CADD and Mutationtaster predict the mutation to be deleterious (Kumar *et al.*, 2009; Adzhubei *et al.*, 2010; Choi *et al.*, 2012; Schwarz *et al.*, 2014; Choi and Chan, 2015). The variant was reported in a single control from South Asia in the gnomAD database with MAF of 4.0×10^{-6} (Lek *et al.*, 2016). The variant affects a residue that is embedded in a transmembrane domain of COX15 and could possibly disrupt the structure of the protein (**Figure 5.2**).

COX15 codes for Heme A Synthase, a protein that catalyses the conversion of Heme O to Heme A. Heme A is an important Complex IV cofactor that is incorporated into COX1 by SURF1. It has been shown that COX15 plays an important role in Complex IV assembly and binds COX1 (Bareth *et al.*, 2013). A small number of patients with clinical presentations consistent with mitochondrial disease and skeletal muscle biopsy results indicating complex IV deficiency were subsequently found to harbour *COX15* mutations (Antonicka *et al.*, 2003; Oquendo *et al.*, 2004; Bugiani *et al.*, 2005; Alfadhel *et al.*, 2011; Miryounesi *et al.*, 2016).

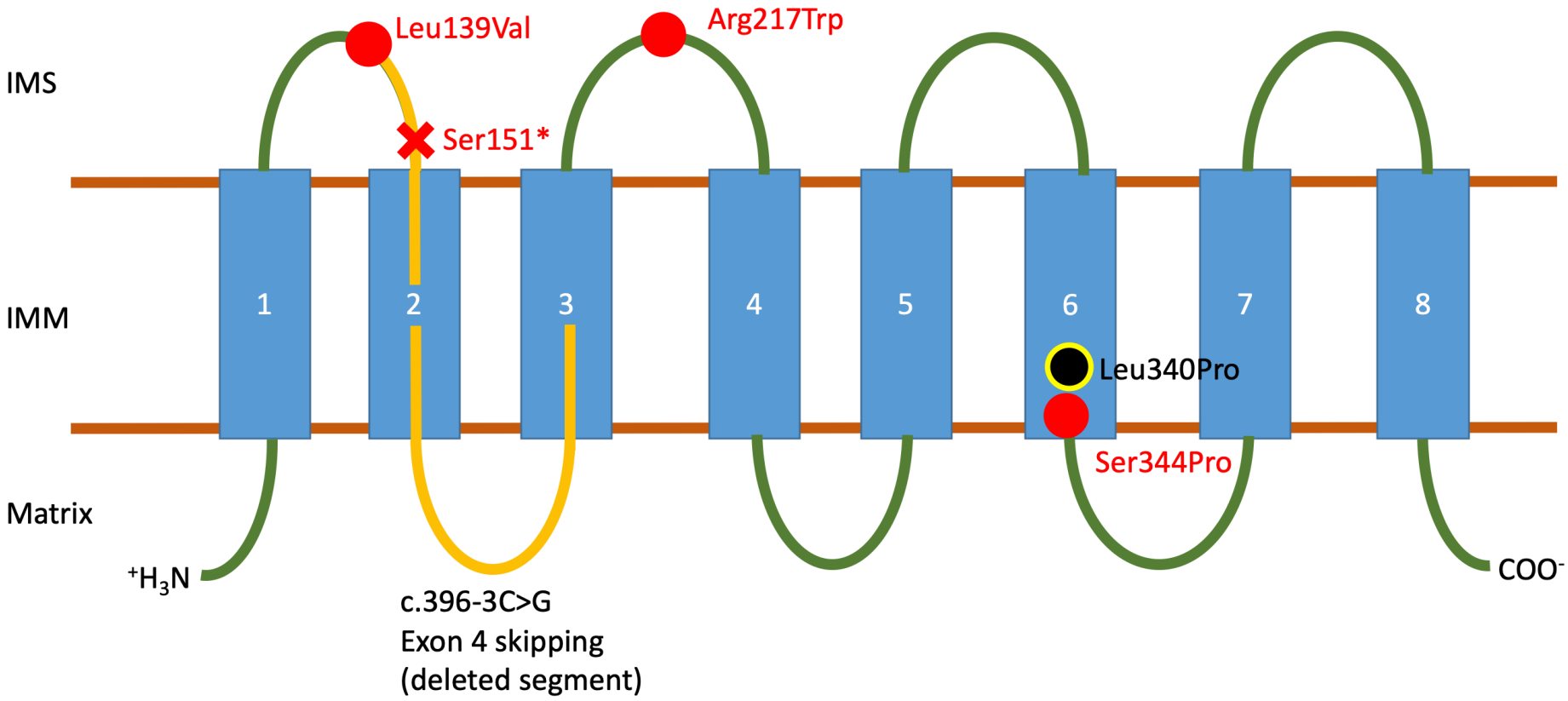

Figure 5.2 Locations and consequences of identified and previously reported COX15 variants.

Structural scheme of transmembrane COX15 protein highlighting the locations of previously reported mutations: missense mutations (red circles); truncating variant: red cross; splicing variant predicted to result in exon skipping (yellow segment), and missense variant reported in this project (black and yellow circle).
IMS: Mitochondrial intermembrane space; IMM: inner mitochondrial membrane.

5.4.1.2 Patients 24-I and 24-II

Patients 24-I and 24-II were referred by Malak Alghamdi, a Saudi Arabian paediatrician at King Saud University, Riyadh, Kingdom of Saudi Arabia.

Patient 24-I is a 16 year-old female born to consanguineous Saudi Arabian parents. She was the third pregnancy and born at full term after an uneventful pregnancy. She presented with language delay and said her first word at the age of 3 years with a mild learning disability resulting in a limited vocabulary. She developed a progressive ataxic gait since the age of 12 years, experienced recurrent falls and was noted to have gaze evoked nystagmus. A brain MRI scan revealed bilateral symmetrical hyperintense signals in the brainstem, hypothalamic structures and deep grey matter with moderate diffuse cerebellar and vermin atrophy. She was suspected of having Wernicke's encephalopathy and was started on Vitamin B1 therapy. After 2 years, brain MRI scans showed resolution of medial thalami, mammillary bodies, periaqueductal grey matter in midbrain, head of caudate and right globus pallidus, plus moderate cerebellar atrophy (**Figure 5.4**). MRS in the basal ganglia showed lactate peaks, and decreased NAA and creatine peaks, which suggested underlying mitochondrial disease. At the age of 16 years, she cannot walk, is wheelchair bound, mute, and completely dependent on her mother. Plasma amino acid analysis showed elevated alanine/lysine ratio, and urine sample analysis revealed lactic aciduria.

Patient 24-I's younger brother (Patient 23-II) is a 7 year-old male patient born at full term after an uneventful pregnancy. At the age of 6 years, he developed ataxia associated with recurrent falls. His serum lactate levels were elevated (3.1 mmol/L) and plasma amino acid analysis showed elevated alanine/lysine ratio, suggestive of mitochondrial dysfunction.

Commercial NGS services provided by CentoGene (Germany) were used to perform WES analysis on DNA from Patients 24-I and 24-II. WES analysis identified the following non-frameshift *TTC19* deletion in both patients that resulted in the deletion of 10 protein residues: NM_017775; c.680_709del; p.Glu227_Leu236del. Sanger sequencing of the variant in the family identified both parents and 3 unaffected siblings to be heterozygous and confirmed both Patients 24-I and 24-II were homozygous for the identified variant (**Figure 5.3**). The function of TTC19 has been previously described in ***Section 4.6.1.4***.

Fibroblast cell lines were obtained from both patients and sent for functional investigation to the NHS Highly Specialised Service for Rare Mitochondrial Disorders in Newcastle upon Tyne, UK.

These patients were investigated with Patient 7-II (a *TTC19* patient from my cohort) to functionally assess the expression of TTC19 and its effect on OXPHOS complex subunit expression, assembly and activity. Clinical and genetic findings for Patient 7-II are described in ***Sections 3.4.1.7*** and ***4.4.6*** respectively.

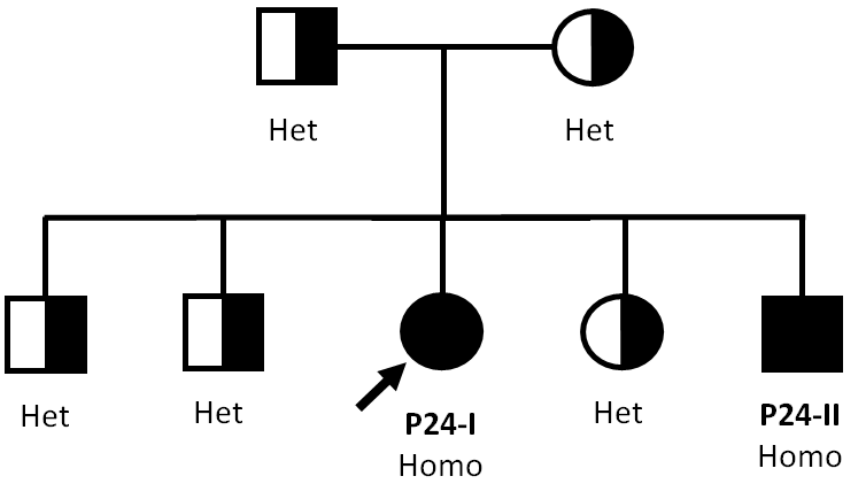

Figure 5.3 Family pedigree of Patients 24-I and 24-II

A family pedigree of Patients 24-I and 24-II (labelled P24-I and P24-II respectively) showing the segregation of the identified TTC19 non-frameshift deletion (c.680_709del; p.Glu227_Leu236del) in the family.

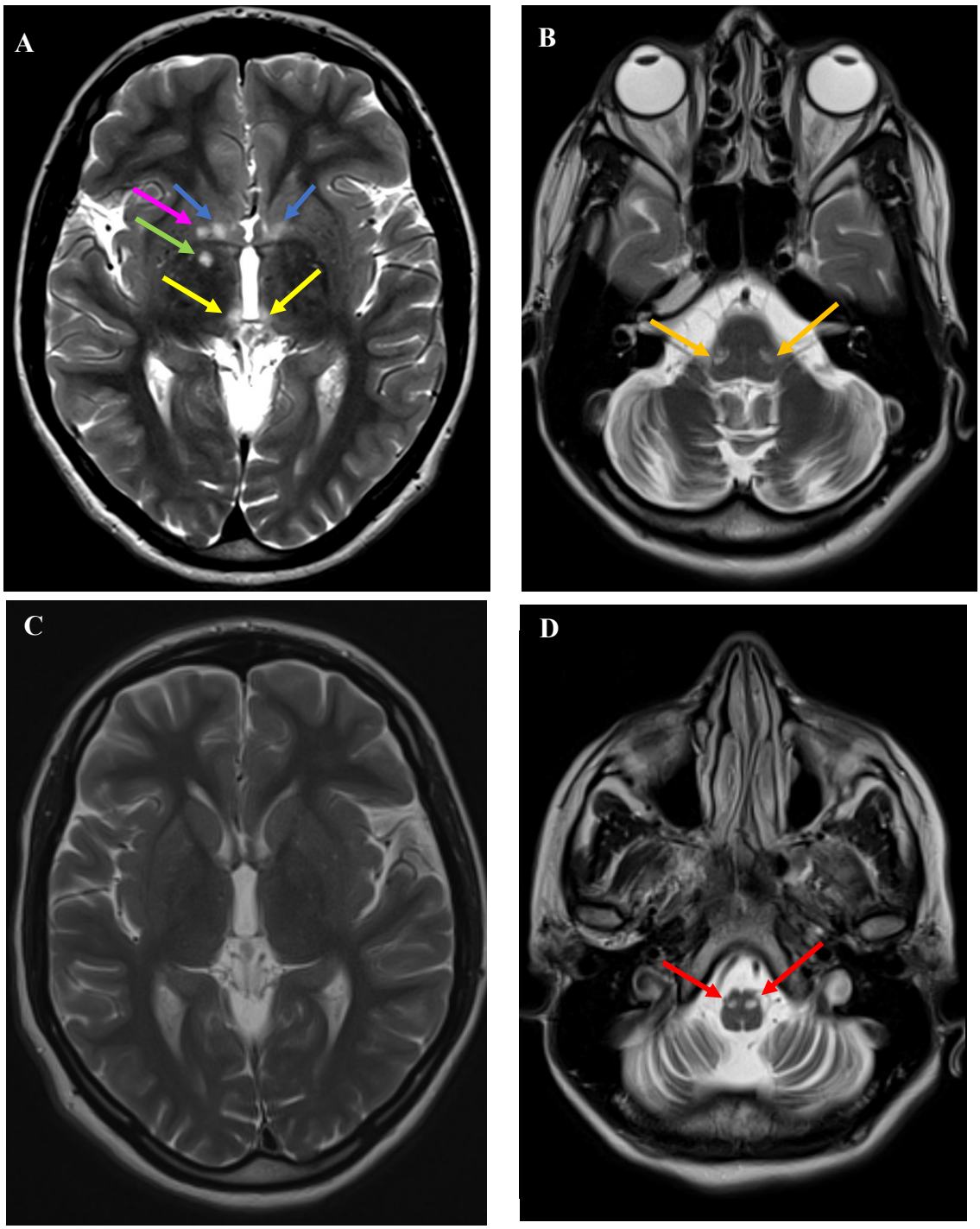

Figure 5.4 Brain MRI Neuroradiological Images of Patient 24-I

T2 weighted brain MRI scans of Patient 24-I showing:
A At age of 12 years, bilateral symmetric lesions in the medial thalami (yellow arrows), caudate head (blue arrows), right putamen (pink arrow) and right globus pallidus.
At 14 years after 2 years of vitamin B1 therapy:
B Bilateral symmetric lesions in pontomedullary junction (orange arrows)
C Resolution of basal ganglia and medial thalami lesions seen in panel **A**.
D Bilateral symmetric lesions in inferior olivary nucleus.

5.4.1.3 Patient 25

Patient 25 was investigated and diagnosed by the NHS Highly Specialised Service for Rare Mitochondrial Disorders in Newcastle upon Tyne, UK.

Patient 25 was born to consanguineous parents and presented with tachypnoea and metabolic acidosis. The patient's blood lactate levels were highly elevated (8.0 mmol/L). WES analysis identified a rare homozygous *NDUFAF3* variant: NM_199069.2; c.335T>G; p.Ile112Arg. *In silico* predictions tools including PolyPhen2, PROVEAN, CADD and Mutationtaster predict the mutation to be deleterious (Kumar *et al.*, 2009; Adzhubei *et al.*, 2010; Choi *et al.*, 2012; Schwarz *et al.*, 2014; Choi and Chan, 2015). Furthermore, the variant resides near a splice-site and could possibly affect the splicing of the transcribed gene. The variant was reported in a single control from Africa in the gnomAD database with MAF of 4.0×10^{-6} (Lek *et al.*, 2016).

NDUFAF3 is a complex I assembly factor that is plays a role in the assembly of complex I's Q module alongside the complex I assembly factor NDUFAF4 (Guerrero-Castillo *et al.*, 2017). A number of patients presenting with Leigh syndrome and complex I deficiency have previously been reported with bi-allelic *NDUFAF3* mutations (Saada *et al.*, 2009; Baertling *et al.*, 2017b; Ishiyama *et al.*, 2018).

5.4.2 Functional analysis results

The following are functional analysis results of investigated patient cell lines from the recruited patients.

5.4.2.1 NDUFA13

Clinical and genetic findings for Patient 8 are described in ***Sections 3.4.1.8*** and ***4.4.4*** respectively. Patient 8 was homozygous for a novel truncating *NDUFA13* variant (NM_015965; c.22C>T; p.Gln8*). Immunoblotting of the NDUFA13 protein in the Patient 8 showed a clear defect in protein expression (**Figure 5.5A**). Immunoblotting of OXPHOS subunits showed a defect of NDUFB8 related to the NDUFA13 defect. Immunoblotting of BN-PAGE showed a clear complex I defect in the patient (**Figure 5.5B**).

5.4.2.2 COX15

Patient 23 was homozygous for a rare missense *COX15* variant (NM_078470; c.1019T>C; p.Leu340Pro; MAF = 4.0×10^{-6}). Immunoblotting of OXPHOS protein subunits in the Patient 23 showed a clear defect in protein expression of complex IV subunits COX1 and COX2 (**Figure 5.6A**). Immunoblotting of the COX15 protein was attempted using a number of antibodies but results were inconclusive due to no bands showing or an array of unspecific bands appeared. Immunoblotting of BN-PAGE showed a clear complex IV defect in the patient (**Figure 5.6B**).

A

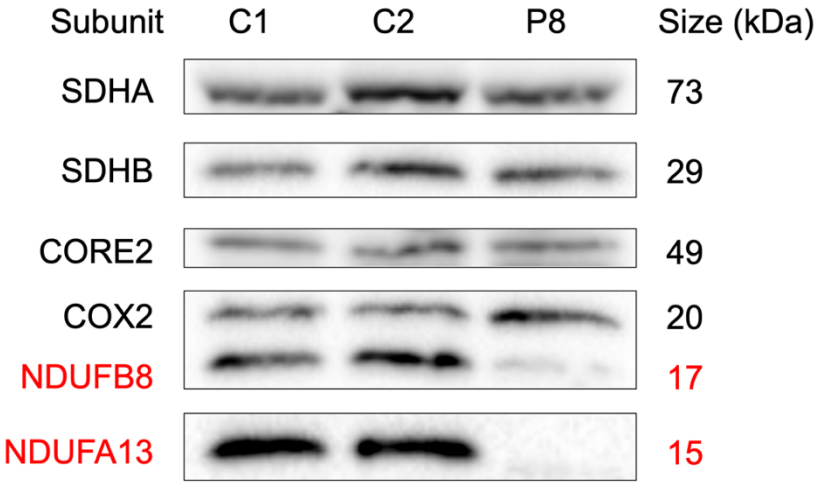

B

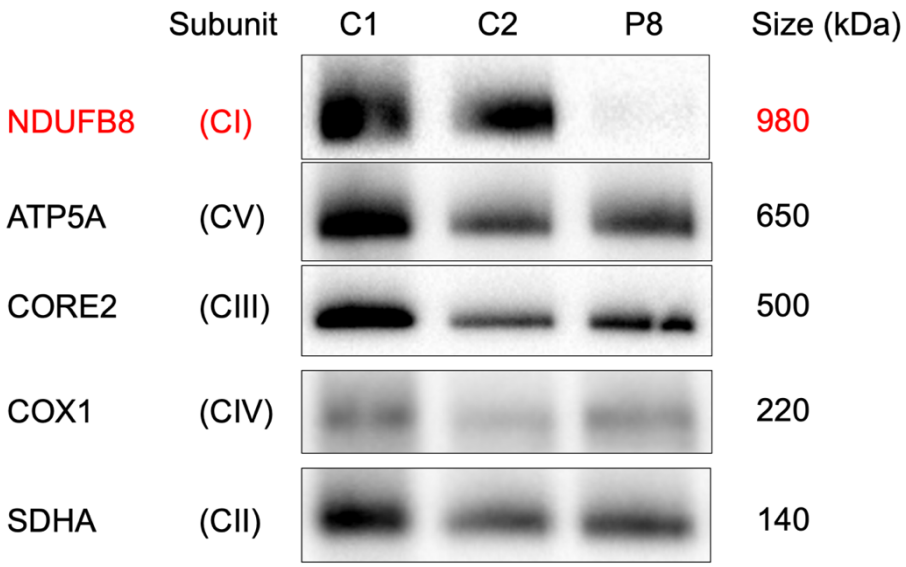

Figure 5.5 Investigating NDUFA13 expression and Complex I assembly in Patient 8 fibroblasts

A Immunoblotting of OXPHOS subunits in NDUFA13 patient (P8) and age-matched control fibroblasts (C1 and C2) showing a defect in the 2 complex I subunits NDUFA13 and NDUFB8 in the patient (red). These results represent finding of 3 biological repeats.
B Immunoblotting OXPHOS complexes in NDUFA13 patient (P8) and age-matched control fibroblasts (C1 and C2) showing a complex I defect in the patient. This was the result of the only biological experiment performed.

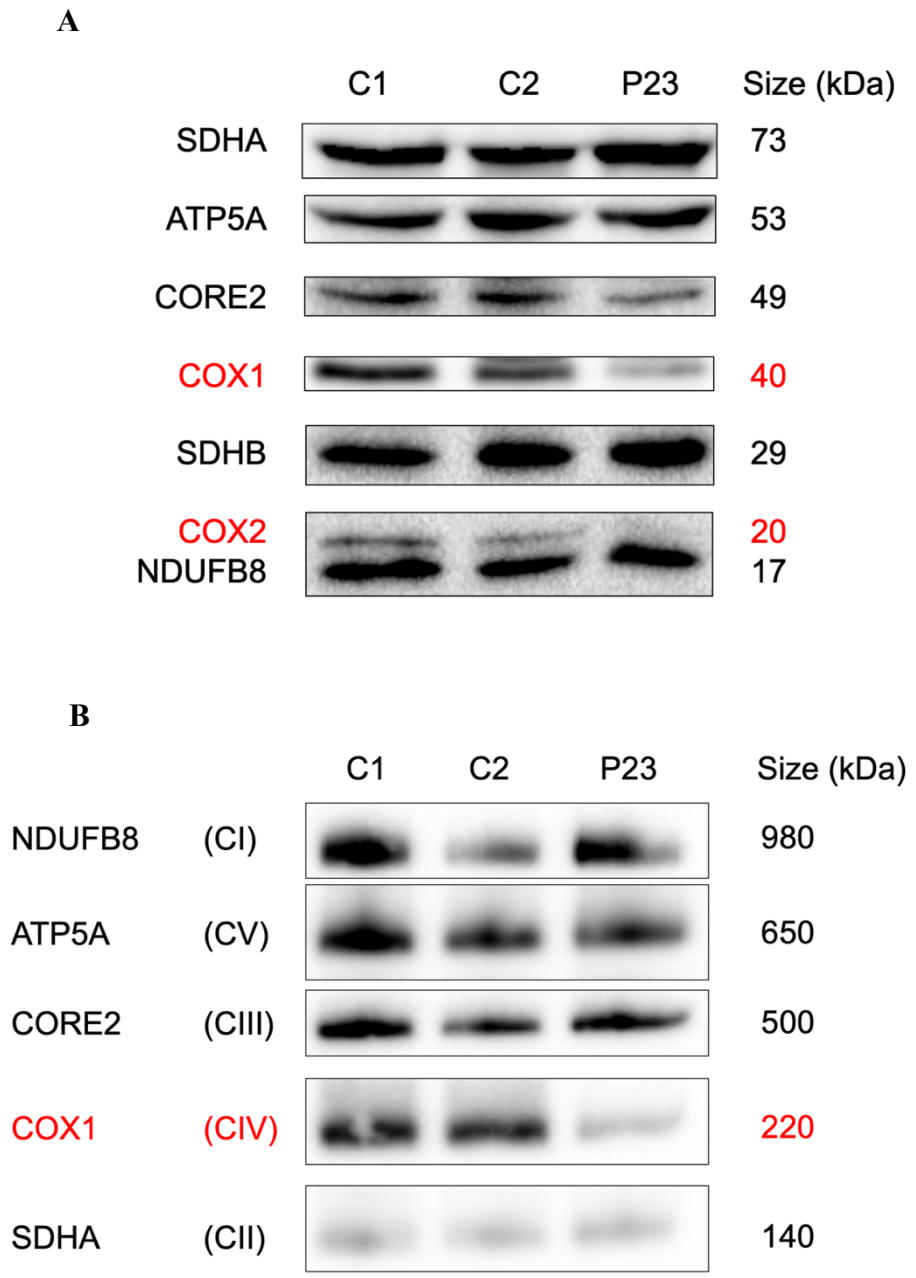

Figure 5.6 Steady-state analysis of OXPHOS subunits and complex assembly analysis of OXPHOS complexes in Patient 23.

A Steady-state analysis of OXPHOS subunits in Patient 23 (P23) using Western blotting shows a deficiency in COX I and COX II protein expression compared to age-matched control fibroblasts. These results represent findings of 4 biological repeats.
B BN-PAGE analysis of OXPHOS complex assembly shows a defect in fully assembled complex IV in Patient 23 (P23) compared to age-matched control fibroblasts. These results represent findings of 2 biological repeats.

5.4.2.3 NDUFAF3

Patient 25 was homozygous for a rare *NDUFAF3* variant (NM_199069.2; c.335T>G; p.Ile112Arg; MAF = 4.0 $\times 10^{-6}$). Immunoblotting of the NDUFAF3 protein in the Patient 25 showed a clear defect in protein expression (**Figure 5.7**). Immunoblotting of OXPHOS subunits showed a defect in the expression of complex I subunits NDUFA9, NDUFB8 and NDUFC2 compared to controls.

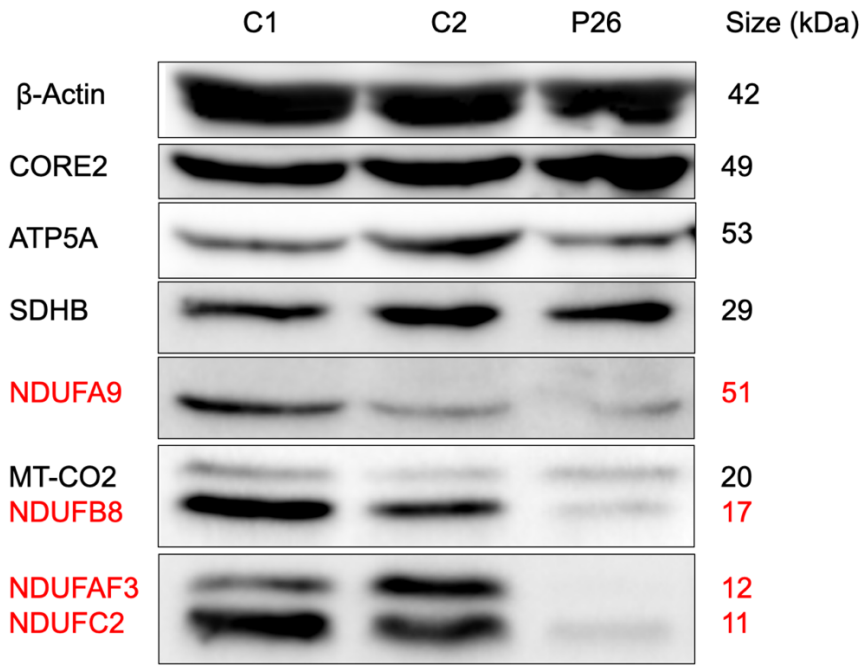

Figure 5.7 Investigating protein steady-state in Patient 25

Immunoblotting of OXPHOS subunits Patient 25 (P25) and age-matched control fibroblasts showing a defect in expression of the complex I assembly factor NDUFAF3 and complex I subunits (red). These results represent findings of 3 biological repeats.

5.4.2.4 TTC19

Two recruited families harboured novel homozygous *TTC19* deletions. Patients 7-I and 7-II harboured a truncating deletion (NM_017775; c.779_780del; p.Tyr260*) and Patients 24-I and 24-II harboured a non-frameshift deletion that resulted in the deletion of 10 protein residues (c.680_709del; p.Glu227_Leu236del).Fibroblasts were obtained for Patients 7-II, 24-I and 24-II, however Patient 24-II fibroblast cell line could not be expanded and therefore was not assessed. Immunoblotting of the TTC19 protein in Patient 7-II from Kuwait (P7-II) and Saudi Arabia (Patient 24-I) showed no clear defect in protein expression nor a defect in complex III subunits CORE2 and UQCRFS1 (**Figure 5.8A**). Immunoblotting of BN-PAGE showed no OXPHOS defect in Patient 7-II (**Figure 5.8B**); the fibroblasts cell line from Patient 24-I did not expand to the amount required for complex assembly analysis and therefore OXPHOS assembly could not be assessed using BN-PAGE. Residual OXPHOS enzyme activity did not show any defect in complex III enzyme activity in either cell lines which supports the immunoblotting results presented (data not shown).

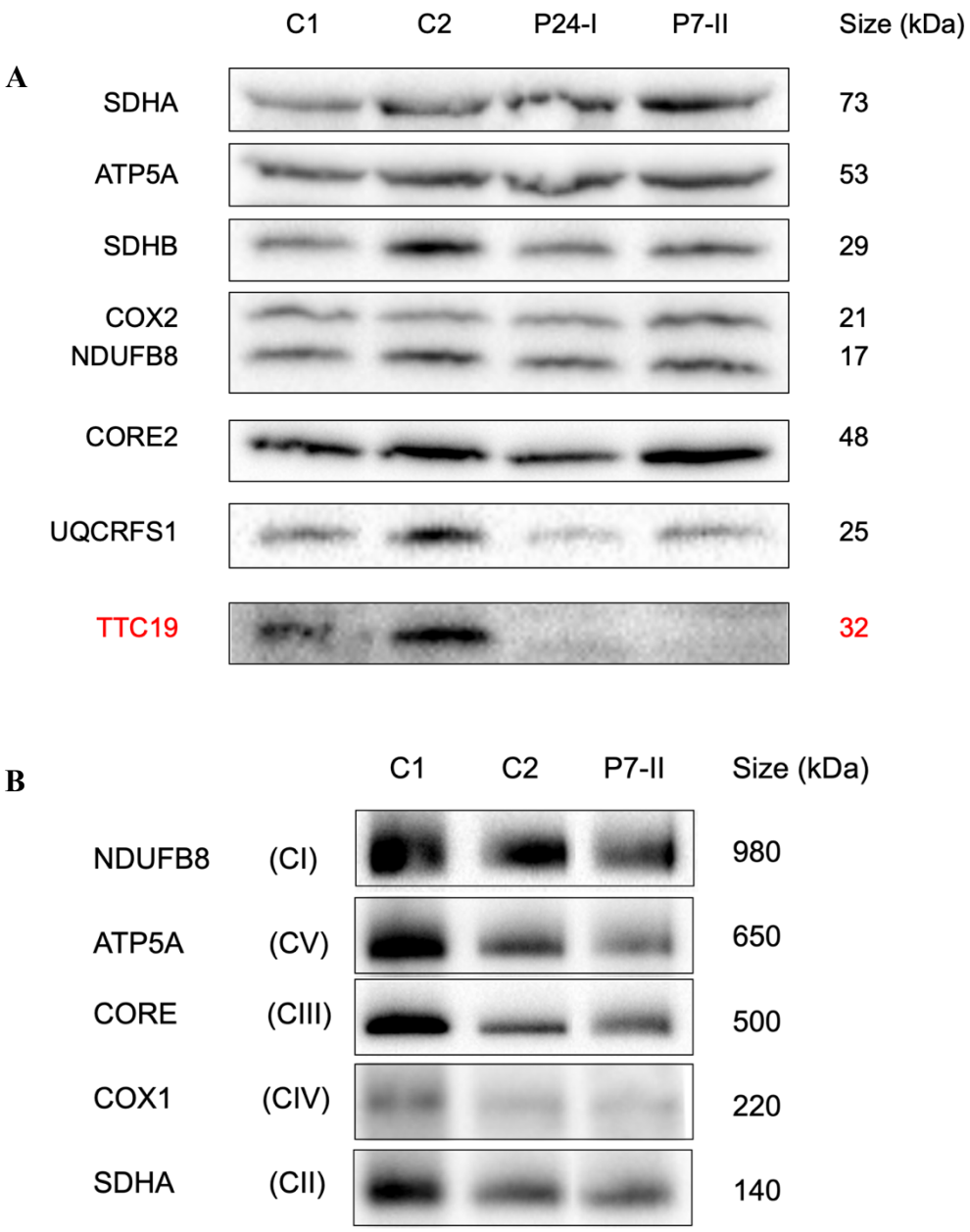

Figure 5.8 Investigating TTC19 expression and Complex III assembly in fibroblasts of TTC19 patients

A Immunoblotting of OXPHOS subunits and TTC19 in Patients 7-II and 24-I (P7-II and P24-I respectively) and age-matched control fibroblasts showing TTC19 defect in patients (red) but no complex III defect (CORE2 and UQCRFS1). These results represent findings of 3 biological repeats for both patients.
B. Immunoblotting of OXPHOS complexes in *TTC19* patient 7-II (P7-II) and control fibroblasts showing no complex III (CORE2) defect in patient. These results represent findings of 2 biological repeats for Patient 7-II

5.4.2.5 MPC1

Clinical and genetic findings for Patients 5-I and 5-II are described in ***Sections 3.4.1.5*** and ***4.4.5*** respectively. Patients 5-I and 5-II harboured a novel *MPC1* missense variant (NM_016098; c.109C>T; p.Pro37Ser). Immunoblotting of the MPC1 protein in the diagnosed siblings (patients 5-I and 5-II) showed a clear defect in protein expression (**Figure 5.9**). Immunoblotting of OXPHOS subunits does not show any effect on protein expression due to MPC1 defect.

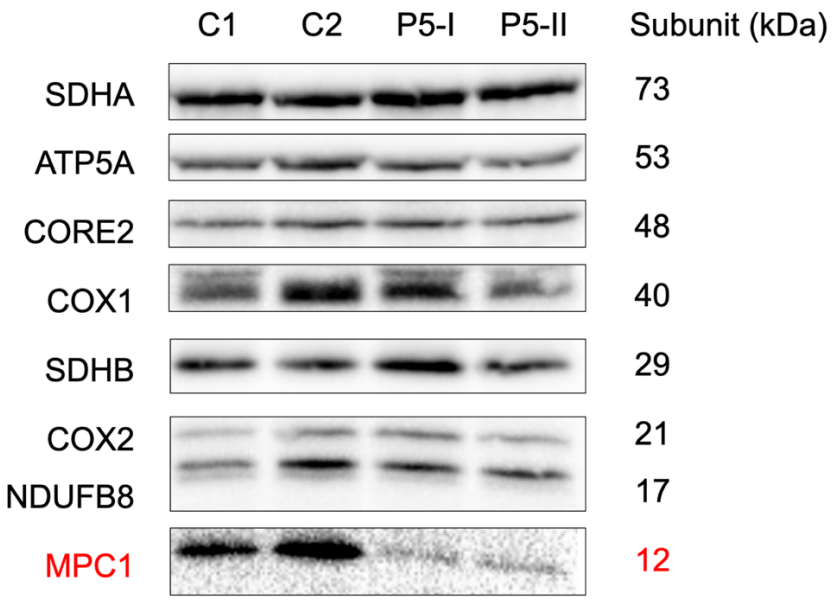

Figure 5.9 Investigating protein steady-state in Family 5

Immunoblotting of OXPHOS subunits and MPC1 in *MPC1* patients (5-I and 5-II) and age-matched control fibroblasts showing an MPC1 defect in patients (red). These results represent finding of 2 biological repeats for both patients.

5.4.2.6 TREX1

Clinical and genetic findings for Patient 12 are described in ***Sections 3.4.1.12*** and ***4.4.13*** respectively. Patient 12 harboured compound heterozygous *TREX1* mutations. One mutation is a pathogenic missense variant that was previously reported in Aicardi-Goutières syndrome patient (NM_033629; c.341G>A; p.Arg114His) while the other is a novel frameshift duplication (c.50dupT; p.Asp18Argfs). Immunoblotting of the TREX1 protein in Patient 12 showed a clear defect in protein expression (**Figure 5.10**). Immunoblotting of OXPHOS subunits does not show any functional defects.

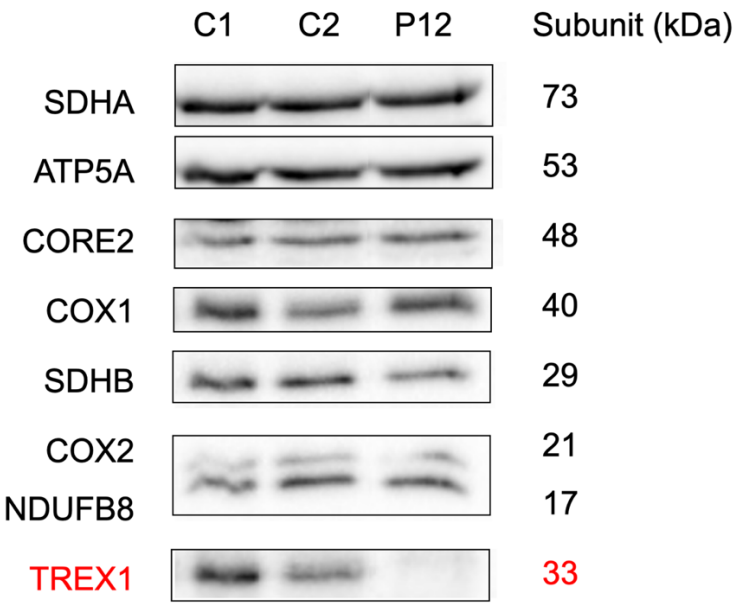

Figure 5.10 Investigating protein steady-state in Patient 12

Immunoblotting of OXPHOS subunits and TREX1 in Patient 12 (P12) and age-matched control fibroblasts showing a TREX1 defect in patient (red). These results represent findings of 2 biological repeats.

5.5 Discussion

Discovering genetic variants associated with disease is the first step to establishing a cause for suspected genetic disease in patients. If the identified variant has been previously associated with disease, and a clear phenotype-genotype correlation is established and observed, then no validation is required. However, if a novel variant has been identified in a gene that is already associated with disease, pathogenicity of the variant requires functional validation. To pursue this, patient tissue and cell lines are required to assess the functional consequences of the putative pathogenic variant. In cases genotyped with possible mitochondrial disease, steady-state protein levels of the affected protein and related proteins provide insight into the effect of the identified variant on cellular biology and assessment of OXPHOS complex assembly and activity further support these findings.

Clinical and functional phenotypes of patients can be compared to previously reported patients and help expand clinical and functional phenotype in the scope of the effected gene and protein. Furthermore, functional findings help researchers understand mitochondrial biology by providing evidence of mitochondrial dysfunction related to the mutated protein.

5.5.1 NDUFA13

The identified *NDUFA13* variant (NM_015965; c.22C>T; p.Gln8*) in Patient 8 is a novel truncating mutation that is associated with a defect in complex I assembly in Patient 8. The functional analysis results support a diagnosis of complex I deficiency and assessing respiratory chain enzyme activity is not necessary to confirm the findings. A single family with and identified *NDUFA13* mutation were previously reported where functional analysis results revealed decreased expression of NDUFA13 and other complex I subunits in addition to showing a defect in complex I assembly in the investigated patients (Angebault *et al.*, 2015). The study silenced the *NDUFA13* gene expression using siRNA in control fibroblasts and functional analysis results showed a similar phenotype to that observed in patient fibroblasts. Another study knocked out *NDUFA13* expression using the TALENs technique in HEK293T cells and analysis of complex I assembly revealed a clear absence of assembled complex I (Stroud *et al.*, 2016). These findings support the pathogenicity of the truncating *NDUFA13* in patient 8.

5.5.2 COX15

The identified *COX15* mutation in Patient 23 (NM_078470; c.1019T>C; p.Leu340Pro; MAF = 4.0×10^{-6}) is a rare mutation that has not been previously reported in a homozygous state in controls. As a complex IV assembly factor, functional analysis on fibroblast cells and muscle biopsies from patients previously reported with bi-allelic *COX15* mutations showed a deficiency in complex IV activity in addition to decreased complex IV assembly (Antonicka *et al.*, 2003; Oquendo *et al.*, 2004; Bugiani *et al.*, 2005; Alfadhel *et al.*, 2011). Clinical findings in these studies reported heterogeneous clinical presentations and findings that are suggestive of mitochondrial disease involvement including developmental delay, failure to thrive, nystagmus, tremor, hypotonia, muscle wasting, elevated CSF and serum levels, and lesions in the basal ganglia and cerebral white matter. The reported presentation and clinical findings in patient 23 fit with those of mitochondrial disease including the presence of seizures, myoclonus, and basal ganglia calcification. However, this is an expansion of the spectrum of presentations associated with *COX15* mutations in mitochondrial disease patients.

Assessment of steady-state levels of COX15 in some of these patients revealed varying effects on protein expression but unfortunately no COX15 antibody presented reliable results to assess the levels of COX15 in patient 23 (Swenson *et al.*, 2016). The introduction of a proline in a transmembrane domain helix introduces a “kink” into the structure which will likely affect the final structure of the inner membrane bound COX15 protein (Law *et al.*, 2016). This is a possible explanation for the reduced complex IV subunits and a reduced complex IV assembly observed in Patient 23 fibroblasts and supports a diagnosis of complex IV deficiency.

5.5.3 NDUFAF3

The identified *NDUFAF3* mutation in Patient 25 (NM_199069.2; c.335T>G; p.Ile112Arg; MAF = 4.0×10^{-6}) is a rare mutation that has not been previously reported in a homozygous state in controls. As a complex I assembly factor, functional analysis on fibroblast cells and muscle biopsies from patients previously reported with bi-allelic *NDUFAF3* mutations showed a deficiency in complex I activity in addition to decreased complex I assembly and decreased expression of complex I subunits (Saada *et al.*, 2009; Baertling *et al.*, 2017b; Ishiyama *et al.*, 2018). Further investigations included the silencing of *NDUFAF3* in HeLa cells using small interfering RNA (siRNA) which

resulted in a functional phenotype similar to that observed in NDUFAF3 patient cell lines (Saada *et al.*, 2009), and complementation experiment using lentiviral transduction of *NDUFAF3* patient cell lines which rescued the observed phenotype in the patient cell lines (Baertling *et al.*, 2017b). None of the previously mentioned studies assessed the steady-state protein levels of NDUFAF3 in their patients. Patient 25 had a defect in steady-state levels of NDUFAF3 and other complex I subunits which support the diagnosis of complex I deficiency.

5.5.4 TTC19

The *TTC19* deletions identified in Family 7 (NM_017775; c.779_780del; p.Tyr260*) and Patients 24-I and 24-II (c.680_709del; p.Glu227_Leu236del) are novel and have not been previously reported. A total of 19 patients harbouring *TTC19* mutations have been reported previously (Ghezzi *et al.*, 2011; Nogueira *et al.*, 2013; Melchionda *et al.*, 2014; Morino *et al.*, 2014; Ardissone *et al.*, 2015; Koch *et al.*, 2015; Kunii *et al.*, 2015; Mordaunt *et al.*, 2015; Conboy *et al.*, 2018; Habibzadeh *et al.*, 2019). As a complex III assembly factor, functional analyses were performed on some *TTC19* patients which revealed varying deficiencies in complex III activity in patients' muscles (Ardissone *et al.*, 2015) and no defect in steady-state levels of complex III subunits in patient fibroblasts or muscle samples (Ghezzi *et al.*, 2011; Nogueira *et al.*, 2013; Koch *et al.*, 2015). The role of TTC19 is to cleave the N-terminus of UQCRFS1 after the assembly of complex III homodimer (Bottani *et al.*, 2017). The defect in TTC19 expression does not necessarily result in a defect in complex III assembly (Nogueira *et al.*, 2013; Melchionda *et al.*, 2014; Koch *et al.*, 2015). The functional findings in Patient 7-II and Patient 24-I show a defect the steady-state of TTC19, while complex III assembly in not affected in Patient 7-II. This is similar to functional findings observed in cell lines of previously reported *TTC19* patients. The unaffected complex III activity in fibroblasts of Patients 7-II and 24-I might be due to the fact that the defect in complex III assembly was observed in patient muscle samples. The functional analyses provide evidence that support a diagnosis of mitochondrial disease due to complex III deficiency.

5.5.5 MPC1

The identified *MPC1* variant in Family 5 (NM_016098; c.109C>T; p.Pro37Ser) is novel and has not been previously reported. Patients with *MPC1* mutations have been reported and their mutations were investigated using a yeast model to assess the effect of the

mutations on protein expression (Bricker *et al.*, 2012). Further investigations into the expression of MPC1 steady-state levels showed a decrease in MPC1 expression in addition to a decrease in MPC2 (Oonthonpan *et al.*, 2019). Patient phenotypes of reported *MPC1* patients included facial dysmorphism, developmental delay, hypotonia and lactic acidosis all of which were observed in patients from Family 5. The defect in steady-state MPC1 levels in Patients 5-I and 5-II in addition to their observed clinical phenotypes fit with a diagnosis of MPC1 deficiency as reported previously in patients.

5.5.6 TREX1

One of the *TREX1* variants identified in Patient 12 was previously reported in patients with AGS (NM_033629; c.341G>A; p.Arg114His) (Crow *et al.*, 2006a), while the other variant was a novel frameshift duplication (c.50dupT; p.Asp18Argfs). Patient 12 presented at the age of 1 month with progressive stiffness of neck, limb and trunk muscles and by 3 months he was noted to be irritable with excessive crying. By the age of 5 months 4 limb dystonia was evident. CSF and serum lactate levels were elevated. Similar clinical presentations were observed in a cohort of genetically diagnosed AGS patients including patients with *TREX1* mutations (Rice *et al.*, 2007a; Crow *et al.*, 2015; Livingston and Crow, 2016). Brain MRI scans of patient 12 at 3 years of age revealed high intensity T2 signals in white matter regions near the ventricle horns and a thin corpus callosum which also fits with the spectrum radiological findings in AGS patients. Furthermore, patient 12 had a febrile seizure at the age of 3 years and 5 months due to a respiratory infection and 6 months later he had recurring general tonic-clonic seizures which is also reported in AGS patients. The elevated CSF and serum lactate levels in addition to other observed clinical presentations in patient 12 greatly overlap with presentations of mitochondrial disease patients which led to an MDC score of 7 suggesting mitochondrial disease involvement.

Crow *et al.* (2006a) functionally investigated the effect of the identified *TREX1* variant (p.Arg114His) in a number of AGS patients by assessing the activity of the 3'-5' endonuclease which *TREX1* encodes

Rice *et al.* (2007a) suggest that the identified variant (p.Arg114His) is an ancient founder mutation and have investigated the variant functionally by assessing the activity of the 3'-5' endonuclease which *TREX1* encodes and by assessing the expression of interferon genes due to the reported elevation of interferon alpha levels in AGS patients (Crow *et*

al., 2006a; Rice *et al.*, 2007a; Silva *et al.*, 2007; Ellyard *et al.*, 2014). Steady-state levels were never assessed or reported in these patients. The steady-state level of TREX1 protein in Patient 12 was severely decreased. Since this diagnosis was not of a mitochondrial disorder, the finding of TREX1 deficiency in Patient 12's fibroblast cell line due a known reported *TREX1* variant and a loss-of-function frameshift duplication variant, it is indicative of an Aicardi-Goutières syndrome diagnosis which is a phenocopy disorder of mitochondrial disease.

5.6 Summary

A summary of the functional findings described in the aforementioned Results section is tabulated in **Table 5.1**.

Table 5.1 Summary of functional results in patient fibroblasts

Patient	Source	Gene	GenBank Ref	Genotype	Residue	Variant trait	WB	BN-PAGE	OXPHOS enzyme activity
5-I and 5-II	Kuwait	*MPC1*	NM_016098	c.109C>T	p.Pro37Ser	Novel variant	MPC1 deficiency	N/A	N/A
7-II	Kuwait	*TTC19*	NM_017775	c.779_780del	p.Tyr260*	Novel frameshift deletion	TTC19 deficiency	Normal	Normal
8	Kuwait	*NDUFA13*	NM_015965	c.22C>T	p.Gln8*	Novel truncating variant	NDUFA13 and complex I subunit deficiency	Complex I deficiency	N/A
12	Kuwait	*TREX1*	NM_033629	c.50dupT c.341G>A	p.Asp18Argfs p.Arg114His	Novel duplication Reported pathogenic variant	TREX1 deficiency	N/A	N/A
23	Newcastle	*COX15*	NM_078470	c.1019T>C	p.Leu340Pro	Rare missense variant	COX-1 and COX-2 deficiency	Complex IV deficiency	N/A
24-I	Saudi Arabia	*TTC19*	NM_017775	c.680_709del	p.Glu227_Leu236del	Novel non-frameshift deletion	TTC19 deficiency	N/A	Normal
25	Newcastle	*NDUFAF3*	NM_199069	c.335T>G	p.Ile112Arg	Rare missense variant	NDUFAF3 and complex I deficiency	N/A	N/A

BN-PAGE: Blue native polyacrylamide gel electrophoresis; N/A: Not available; OXPHOS; oxidative phosphorylation; WB: Western blot.

5.7 Final discussion

My research cohort is comprised of 22 patients living in Kuwait who were recruited based upon clinical suspicion of a diagnosis of mitochondrial disease. Of the 22 recruited patients, 10 harboured bi-homozygous variants in genes associated with mitochondrial disease or function, and 4 harboured bi-allelic variants in genes associated with diseases that are phenocopies of mitochondrial disease. Skin biopsies were acquired from patients from 4 of the Kuwait cohort families with segregated novel variants, 3 were associated with mitochondrial disease and 1 was associated with a phenocopy of mitochondrial disease. The acquisition of skin biopsies depended on a number of factors including the exclusion of patients with previously reported variants (*PDHX* and *NDUFB9* variants in families 3 and 9 respectively), the lack of samples from patients who were deceased (such as patients from families 1, 4, 6 and 7), and the absence of consent from patients or their guardians (families 2 and 10). In cases where variants segregated in the families, phenotype-genotype correlations in patients between mutations in the affected gene and previously reported cases supported the genetic diagnoses reached. This includes cases with phenocopies of mitochondrial disease that were diagnosed using WES (families 11, 12, 13 and 14). In addition to the Kuwait cohort, patients from 3 families who harboured homozygous novel variants in mitochondrial disease genes were referred to our research project for functional validation of pathogenicity from King Saud University, Riyadh, Kingdom of Saudi Arabia, and the NHS Highly Specialised Service for Rare Mitochondrial Disorders in Newcastle upon Tyne, UK.

As demonstrated in the study's cohort, many patients in Kuwait harbour novel variants or variants in novel candidate genes with associated cellular functions. Reporting of these variants as possibly pathogenic, or variants of unknown significance, is practiced at KMGC without functional evidence supporting variant pathogenicity which should be accessible within the centre. Expanding the laboratories at KMGC would provide functional support of genetic diagnoses and this requires setting up a functional laboratory that follows up patients with identified novel mitochondrial disease variants and novel candidate genes associated with mitochondrial function. This would require an independent tissue culture laboratory and a functional laboratory to perform functional studies including western blotting and BN-PAGE. Where consent is available, skin biopsies would be obtained to establish and expand fibroblast cell lines from patients. These fibroblasts would be primarily analysed using western blotting and BN-PAGE to

investigate steady-state protein levels and OXPHOS complex assembly where required to provide functional evidence for the effects of the identified variants affecting mitochondrial function and other cellular functions. Furthermore, fibroblasts can be used to assess gene expression by measuring mRNA transcript levels using quantitative PCR techniques, while mRNA analysis can also identify alternative splicing transcripts due to splice-site variants using PCR amplification, agarose gel electrophoresis and Sanger sequencing. To further validate pathogenicity of the identified variants, the availability of fibroblast cell lines would also provide material for biochemical assessment of OXPHOS complex activities in patients. These would be the first steps towards functionally validating novel mitochondrial disease variants and novel candidate gene variants at associated with mitochondrial function at KMGC. These functional analyses can be expanded to include the validation of many other genetic disorders when functional validation of variants is required.

Functional investigations provide support for pathogenicity of a certain variant. But the effect of the variant is only limitedly assessing to the expression of the effected protein and any associated proteins such as the OXPHOS subunits. The tissue source (skin or muscle) can also affect the observed phenotype since some proteins are expressed at varying levels depending on the tissue. For example, the *MPC1* variant identified in family 5 is associated a reduction in MPC1 expression, but no other functional or biochemical assessments of pyruvate import were performed that might have provided further support to pathogenicity. Another example is the extremely modifying *TTC19* variants identified in a family from Kuwait and a family from Saudi Arabia. Since the function of the complex III assembly factor is the cleaving of UQCRFS1 at the end of complex assembly, no clear changes were observed in the levels of assembled complex III or complex III subunits. The availability of muscle biopsies might've provided more accurate evidence of pathogenicity since muscle is more energy dependant than skin and could show deficiencies in the biochemical enzyme activity of complex III and provide better evidence of functional pathogenicity. Although clear deficiencies are observed using the available tools, further assessment of pathogenicity is sometimes required to solidify findings. Due to the heterogeneity of clinical phenotypes in mitochondrial disease patients, causative association of variants, functional findings, and observed phenotypes are important to establish and are strongly supported with a larger number of cases reported.

Limitations to this study include the difficulty in accessing patient tissue samples (skin biopsies) until late in the study. This limited the time available to establish the fibroblast cell line and later functionally analyse the cell lines using the available functional analysis methods. Other analysis methods such as oxygen consumption rate and cell growth rate could have been performed to further support pathogenicity of the identified variants, but time was limited and thus these analyses were not carried out. Furthermore, maintaining cell line growth was a challenge that limited the ability to run OXPHOS complex assembly analysis using BN-PAGE on cell lines from the NDUFAF3 patient (Patient 25) and one of the TTC19 patients (Patient 24-I). Nonetheless, western blotting and BN-PAGE results provided evidence supporting the pathogenicity of the identified variants. In light of these challenges, a "genetics-first" approach has resulted in rapid identification of novel candidate variants that were validated using functional analysis methods. **Chapter 6** outlines a thorough investigation of a novel mitochondrial disease in patients from 2 unrelated families and how patient cell lines were assessed and investigated to determine aetiology of disease and to expand our understanding of mitochondrial biology.

Chapter 6. *NDUFC2* mutations are a novel cause of Complex I deficiency in Leigh syndrome patients.

6.1 Introduction

Leigh syndrome is the most common neurodegenerative disorder reported in paediatric mitochondrial disease patients (Rahman *et al.*, 2017). Mutations in more than 90 genes including examples from both the nuclear and mitochondrial genomes have been associated with Leigh syndrome so far (Lake *et al.*, 2019). Clinical heterogeneity in Leigh syndrome patients is observed with commonly reported presentations including developmental delay, loss of acquired skills, hypotonia, elevated CSF lactate levels, and multisystem involvement. Typical radiological findings in patients reveal bilateral and symmetric involvement of the basal ganglia and/or brainstem (Rahman *et al.*, 1996).

Complex I deficiency is a common biochemical phenotype affecting paediatric mitochondrial disease patients; more than a third of reported Leigh syndrome patients have complex I deficiency (Lake *et al.*, 2016; Lake *et al.*, 2017; Rahman *et al.*, 2017). Complex I is the largest of the mitochondrial respiratory chain enzymes, is comprised of 44 different subunits and requires at least 14 assembly factors for its biosynthesis (Stroud *et al.*, 2016; Zhu *et al.*, 2016; Guerrero-Castillo *et al.*, 2017; Formosa *et al.*, 2020). Knocking out complex I subunits resulted in defective or stalled complex I assembly and supported the modular assembly of complex I previously established (Stroud *et al.*, 2016).

Complexome profiling is a method that helps elucidate the pattern of assembly in protein complexes by combining BN-PAGE and mass spectrometry to analyse proteins present in intermediate subassemblies of complex assembly. This method has been used in cell lines from several mitochondrial disease patients with pathogenic variants in complex I subunits and has furthered our understanding of the assembly and stability of complex I (Alston *et al.*, 2016a; Alston *et al.*, 2018; Alston *et al.*, 2020).

There have so far been 42 different genes encoding either subunits or assembly factors of complex I associated with mitochondrial disorders; 29 of these genes are associated with Leigh syndrome patients (**Figure 6.1**) (Rahman *et al.*, 2017; Rouzier *et al.*, 2019; Alston *et al.*, 2020; Thompson *et al.*, 2020a). Genetic diagnoses of mitochondrial disease are challenging due to the genetic heterogeneity, with more than 330 genes already associated

with disease, including those associated with Leigh syndrome (Lake *et al.*, 2019; Stenton and Prokisch, 2020; Thompson *et al.*, 2020a). NGS in the form of targeted gene panels (Legati *et al.*, 2016; Plutino *et al.*, 2018) and unbiased WES (Taylor *et al.*, 2014; Wortmann *et al.*, 2015; Pronicka *et al.*, 2016; Theunissen *et al.*, 2018) has resulted in diagnostic rates of cohorts mitochondrial disease patients exceeding 60% (notably when using WES) and identified novel candidate genes associated with mitochondrial disease in patients.

6.2 Aims

The aim of this chapter is to describe the clinical, biochemical and molecular findings of patients from two unrelated consanguineous families who presented with Leigh syndrome due to variants in *NDUFC2,* which encodes a complex I structural subunit. These unrelated patients were identified independently in Saudi Arabia and Italy and were referred as part of a collaboration. I will discuss investigations carried out to assess the effect of the *NDUFC2* variants on gene expression, protein expression, complex I assembly and respiratory enzyme activity. Furthermore, complexome profiling was utilised to characterise the effect of the variants on complex I assembly and variant pathogenicity was validated further by expressing wild-type *NDUFC2* in patient cell lines and assessing the rescue effect on protein expression and complex I assembly.

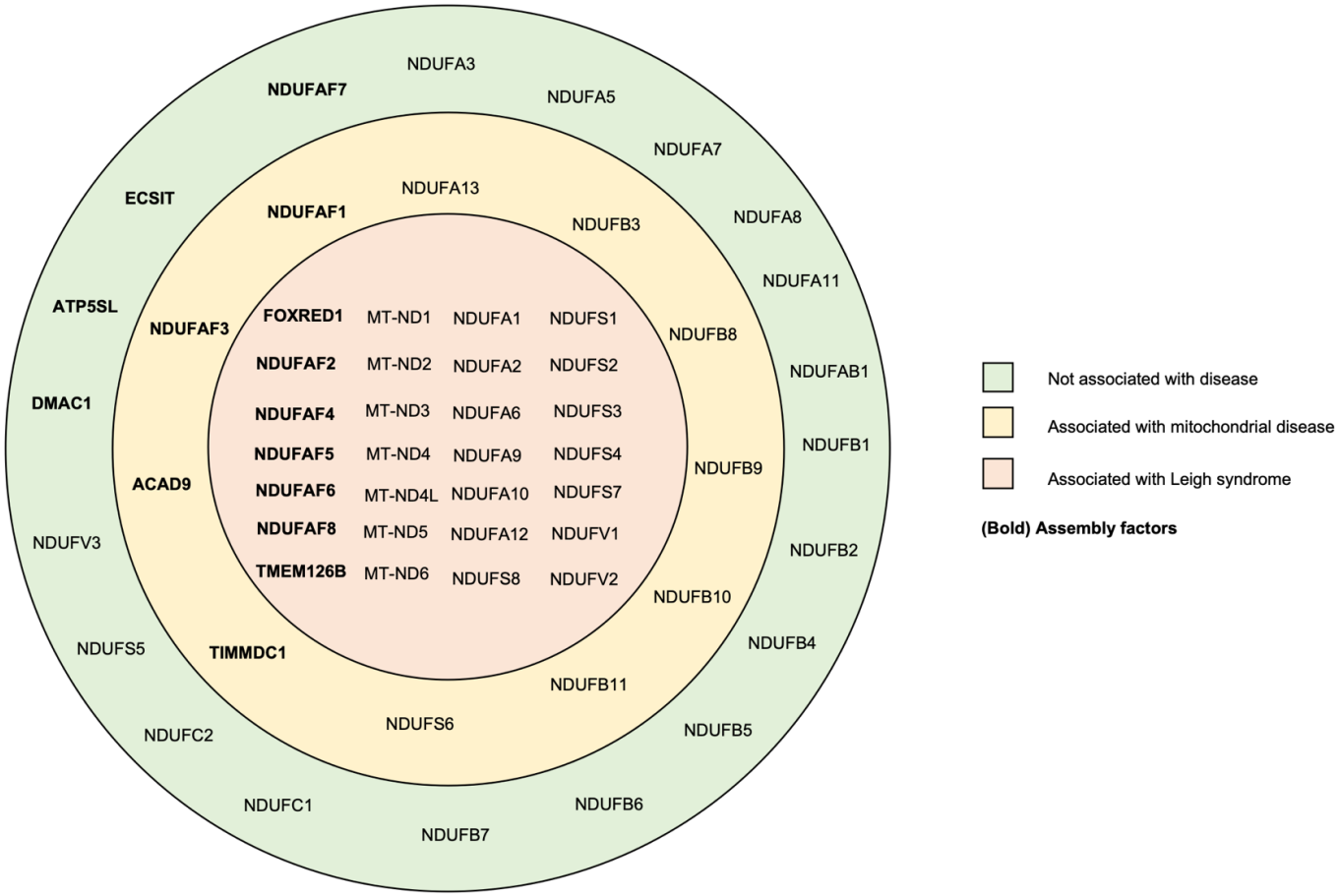

Figure 6.1 Complex I subunits and factors categorised based on association with disease.

Venn diagram of all currently known complex I subunits and assembly factors grouped into 3 categories: green: not currently associated with disease; yellow: associated with mitochondrial disease; orange: associated with Leigh syndrome. Proteins in bold are assembly factors.

6.3 Methods

6.3.1 Patient consent

Informed consent for diagnostic and research studies was obtained for all subjects in accordance with the Declaration of Helsinki protocols and approved by local institutional review boards at King Saud bin Abdulaziz University for Health Sciences in Jeddah, Kingdom of Saudi Arabia, and at the Fondazione IRCCS Istituto Neurologico Carlo Besta Milan, Italy.

6.3.2 Next-generation sequencing

6.3.2.1 Patient A-1

Commercial NGS services provided by CentoGene (Germany) were used to perform WES analysis on DNA from Patient A-1.

6.3.2.2 Patient B

Genetic studies were performed on Patient B using a custom 300 gene targeted gene-panel of nuclear genes previously associated with mitochondrial disease, candidate genes that take part in the same molecular pathway, and included all genes encoding complex I subunits. Library capture and enrichment were performed using a custom panel (SureSelectXT Custom library, Agilent, US) and sequencing was performed on an Illumina MiSeq platform according to the manufacturer's protocol. Bioinformatic analysis was performed as previously described (Legati *et al.*, 2016).

6.3.3 Sanger Sequencing

DNA for Sanger sequencing was extracted from peripheral blood of patients and their family members. The used primers targeting the identified *NDUFC2* (NM_004549.6) deletion in Patient A-1 were as follows:

Forward: 5'-ACATGAACATTCAGACCACAGC-3'

Reverse: 5'-CAAGGTGTCAACATACAGATTAGCA-3'

Sanger sequencing of the identified variants was performed on Family A as follows:

A 25µl PCR reaction mixture consisted of 13.3µl nuclease free water, 5.0µl GoTaq X5 reaction buffer (Promega), 2.5µl 2mM dNTPs (Promega), 3.0µl 10µM mixture of forward

and reverse primers (IDT), 0.2µl GoTaq polymerase (Promega) and 1.0 µl of the patient's DNA.

The PCR reaction heating steps were as follows: an initiation step at 94°C for 4 minutes, then 30 cycles of denaturation step at 94°C for 45 seconds, and annealing step at 62°C for 45 seconds and an extension step at 72°C for 45 seconds, and a final extension step at 72°C for 5 minutes concluding with a hold step at 4°C.

Sanger sequencing of Family B was performed by collaborators at the Fondazione IRCCS Istituto Neurologico Carlo Besta in Milan, Italy.

6.3.4 RNA transcript levels

This method was performed by collaborators at the Fondazione IRCCS Istituto Neurologico Carlo Besta in Milan, Italy.

RNA purification and cDNA retrotranscription were performed using RNeasy mini kit (QIAGEN) and GoTaq 2-Step RT-qPCR System (Promega), respectively, according to the manufacturers' protocols. RNA was extracted from skin fibroblasts, and 1 µg was used as template for RT-PCR, with the following oligonucleotides sequences: q-NDUFC2-F 232_251 and q-NDUFC2-R 358_377 for *NDUFC2* (NM_004549.6); q-ACTB-F 425_442 and q-ACTB-R 502_521 for *ACTB* (NM_001101.5), used for normalisation.

6.3.5 Cell culture

Fibroblast cell lines of patients were cultured as outlined in ***Sections 2.2.17***, ***2.2.18***, ***2.2.19*** and ***2.2.20***. During the lentiviral rescue experiment, HEK293T cells and skin fibroblasts were initially cultured in Growth Media substituting FBS with dialysed FBS (Gibco, 26400044) for 3 to 4 weeks.

6.3.6 Oxygen consumption

This method was performed by collaborators at the Fondazione IRCCS Istituto Neurologico Carlo Besta in Milan, Italy. Alessia Nasca, Andrea Legati, Eleonora Lamantea, Menuela Spagnolo, Danielle Ghezzi).

Mitochondrial respiration of intact cells was measured using high-resolution respirometry (Oxygraph-2k, Oroboros Instruments, Innsbruck, Austria) with DatLab software 7.1.0.21 (Oroboros Instruments, Innsbruck, Austria) (Pesta and Gnaiger, 2011). Measurements

were performed at 37°C in Growth Media (***Section 2.1.4.3***). Basal respiration was measured for 20 minutes followed by titration of Oligomycin (2.5 µM final concentration; f.c.) to measure oligomycin-inhibited LEAK respiration. Subsequently, the respiratory uncoupler carbonyl cyanide-4-phenylhydrazone (FCCP) (Sigma Aldrich, Munich, Germany) was titrated stepwise until maximal uncoupled respiration (ETS) was reached. Residual oxygen consumption (ROX) was determined after sequential inhibition of complex I with Rotenone and complex III with Antimycin A. Absolute respiration rates were corrected for ROX and normalised for cell number.

6.3.7 Respiratory chain enzyme activities

These studies were performed by Langping He at the NHS Highly Specialised Service for Rare Mitochondrial Disorders in Newcastle upon Tyne, UK. A description of the methods is outlined in ***Section 2.2.24***.

6.3.8 Blue native PAGE and in gel activity stains

These experiments were performed by collaborators at Goethe-Universität in Frankfurt, Germany (Juliana Heidler, Jana Meisterknecht and Ilka Wittig).

Sample preparation and BN-PAGE of cultured cell pellets were essentially performed as previously described (Wittig *et al.*, 2006). Equal protein amounts of samples were loaded on top of a 3 to 18% acrylamide gradient gel (dimension 14x14 cm). After native electrophoresis in a cold chamber, blue-native gels were fixed in 50% (v/v) methanol, 10% (v/v) acetic acid, 10 mM ammonium acetate for 30 min and stained with Coomassie (0.025% Serva Blue G, 10% (v/v) acetic acid). In gel activity stains were performed as described in (Wittig et al. 2007).

6.3.9 Western blotting & blue native-PAGE

An outline of the western blotting method is provided in ***Section 2.2.21*** and an outline of the BN-PAGE method is provided in ***Section 2.2.22***. A description of the immunoblotting technique is outlined in ***Section 2.2.23***.

6.3.10 Complexome profiling

These analyses were undertaken by collaborators at Goethe-Universität in Frankfurt, Germany.

Complexome profiling was performed on fibroblasts from Patient A-1 and Patient B and an age-matched control cell line as previously described (Heide *et al.*, 2012; Fuhrmann *et al.*, 2018).Sample preparation, mass spectrometry, data processing and raw data have been deposited to the ProteomeXchange Consortium (http://proteomecentral.proteomexchange.org) via the PRIDE partner repository (https://www.ebi.ac.uk/pride/archive/) (Vizcaíno *et al.*, 2013) with the dataset identifier <PXD014936>." Complexome data were further analysed using NOVA (Giese *et al.*, 2015). Complex I and identified assembly intermediates were visualised using the Cryo-EM structure of murine complex I (PDB: 6g2j) (Agip et al., 2018) and PyMOL (The PyMOL Molecular Graphics System, Version 2.3.3. Schrödinger, LLC.).

6.3.11 Lentiviral rescue

Wild-type *NDUFC2* was expressed in patient fibroblasts using the Lenti-X TetOne Inducible Expression System with the pLVX-TetOne-Puro vector. Wild-type *NDUFC2* insert was generated by PCR using cDNA from control fibroblasts and the following primers containing EcoRI and BamHI restriction sites respectively (underlined sections are part of the pLVX-TetOne-Puro vector, bold nucleotides are restriction enzyme sites followed by nucleotides from the wild-type *NDUFC2*):

Forward: pLVX-TetOne-Puro-2537_2522-NDUFC2-1_21:

5'-CCCTCGTAAA**GAATTC**ATGATCGCACGGCGGAACCCA-3'

Reverse: pLVX-TetOne-Puro-2486_2501-NDUFC2-360_327:

5'-GAGGTGGTCT**GGATCC**TCAACGTATTGGATGGAATTTTTCAAAAATTTCA-3'

The insert was cloned into the linearised pLVX-TetOne-Puro plasmid vector (Takara Bio / Clonetech) using the In-Fusion HD Cloning Kit (Takara Bio / Clonetech). The *NDUFC2* containing vector was packaged into infectious lentiviral particles using Lenti-X Packaging Single Shots (Takara Bio / Clonetech) to transfect HEK293T cultured in Growth Media containing dialysed FBS according to manufacturer's guidelines. The presence of doxycycline/tetracycline in FBS could induce gene expression of the doxycycline induced vector, therefore Growth Media containing dialysed FBS (dialysed Growth Media) was used according to manufacturer's guidelines. Dialysed Growth Media containing infectious lentivirus was harvested after 48 hours, centrifuged at 500 *g* for 10 minutes to remove cellular debris and the supernatant was retained. This virus

containing supernatant was used to transduce patient fibroblast cell lines at a ratio of 1:2 with fresh dialysed Growth Media and 4 μg/ml polybrene overnight. The dialysed Growth Media was replaced and puromycin (2 μg/ml) added to select for successfully transduced cells. Transduced cells were cultured in puromycin for at least 7 days by which time all patient fibroblasts used as non-transduced controls had died. Expression of wild-type *NDUFC2* was induced by adding doxycycline (Takara Bio / Clonetech; 100 - 200 μg/ml) to the media and incubating for 48 - 96 hours. The cultured cells were then harvested and analysed using the SDS-PAGE and western blotting (***Section 2.2.21***) or subjected to mitochondrial enrichment and subsequent BN-PAGE analysis (***Section 2.2.22***). Fibroblast cell lines were later maintained in regular Growth Media after comparing the effect of Growth Media and dialysed Growth Media on protein expression.

6.4 Results

6.4.1 Clinical presentations of patients

6.4.1.1 Family A

Patient A-1, a female infant, is the second child born to healthy consanguineous first cousin Saudi parents (Family 1). She was born by normal vaginal delivery at 37 weeks gestation (birth weight 2.0 kg, 2nd – 9th centile) with no antenatal issues. Developmental delay was noted at 2 years when she was unable to walk. At 6 years, her height and weight remained below the 5th centile and clinical examination revealed facial dysmorphic features, spasticity and brisk deep tendon reflexes. She was unable to stand without support and unable to speak. A hearing assessment was unremarkable, but an ophthalmological examination revealed bilateral optic disc pallor. She did not develop seizures and had no cardiac, renal, or hepatic abnormalities. Serum lactate ranged from 3.6 to 7.6 mmol/L (normal range 0.7–2.2 mmol/L), while ammonia, blood glucose and thyroid function were unremarkable. Plasma amino acid analysis detected elevated alanine (724 μmol/L, normal range 143–439 μmol/L) and elevated proline (366 μmol/L, normal range 52–298 μmol/L). Urine organic acid analysis showed increased fumaric acid excretion (151 mM/M creatinine, normal range < 20 mM/M). Leukocyte enzyme assay for arylsulfatase A, arylsulfatase B and galactocerebrosidase was unremarkable, as was abdominal ultrasound and array comparative genomic hybridisation (aCGH) testing. Brain MRI at 21 months showed bilateral areas of abnormal high signal intensity at the corticospinal tract level of the corona radiata with loss of white matter volume at these areas. This was associated with irregularity in the outline of the lateral ventricles suggestive of periventricular leukomalacia. Bilateral symmetrical abnormal T2 high signals of the medial aspect of the thalami, substantia nigra and posterior tract of the medulla oblongata were also identified (**Figure 6.2**).

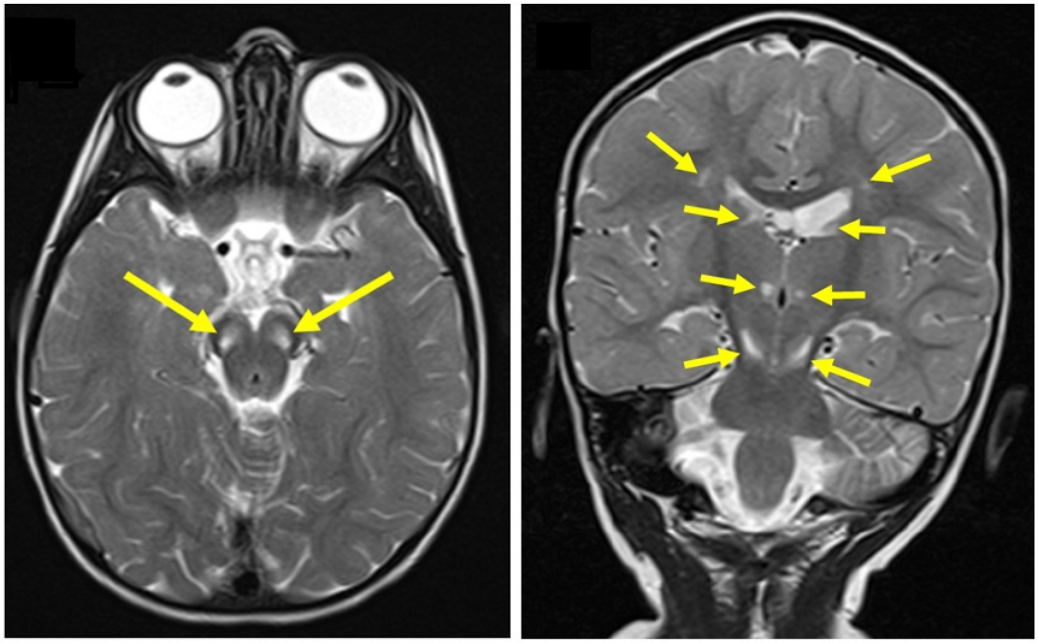

Figure 6.2 Neuroimaging of Patient A-1

(Left) Axial T2-weighted imaging of Patient A-1 at 21 months showed bilateral hyperintense signals in the pons (arrows).
(Right) Coronal T2-weighted imaging of Patient A-1 at 21 months showed bilateral hyperintense signals in the periventricular regions, caudate, thalami and substantia nigra (arrows).

Patient A-2 was the younger brother of Patient A-1; foetal echocardiogram showed mild cardiomegaly, dilated superior vena cava and a small ventricular septal defect (VSD). Antenatal ultrasound showed dilated cisterna magna and ventriculomegaly. He was born by normal vaginal delivery at 36 weeks gestation (birth weight 2.020 kg, 2nd centile). Postnatal echocardiography revealed a perimembranous VSD with left pulmonary artery stenosis. Following birth, he was noted to have persistently elevated serum lactate (4.0–10.0 mmol/L; normal range 0.7–2.2 mmol/L). He exhibited global developmental delay and poor growth with his weight and length remaining below the 3rd centile. Brain MRI at the age of 10 days demonstrated bilateral abnormal high T2 signal intensity of the frontal periventricular area within the regions of caudo-thalamic grooves and associated irregularity of the outline of the lateral ventricles. Also noted were the foci of abnormal T2 signal in the lentiform nuclei with paucity of periventricular white matter and oedema. The MRI also revealed a Dandy-Walker malformation with partial agenesis of the corpus callosum (**Figure 6.3**). At 5 months of age, there was a rapid increase in head size. Brain

CT scan detected acute hydrocephalus with significant dilatation of the third and lateral ventricles. He underwent urgent ventriculoperitoneal shunt insertion. At the age of 19 months, he developed a severe respiratory infection requiring paediatric intensive care unit support and lactate levels were elevated in excess of 20.0 mmol/L (normal range 0.7–2.2 mmol/L). With this intercurrent illness, he developed seizures, regressed and lost all of his previously acquired developmental skills. Recurrent chest infections and pulmonary aspirations suggested an unsafe swallow and he was placed on nasogastric tube feeding. His clinical course was dominated by progressive spasticity, muscle atrophy development of a left hydronephrosis and a persistent lactic acidosis. Serum ammonia, creatine kinase, liver function, thyroid function, plasma amino acids, urinary organic acids, and newborn screening results were all unremarkable. He passed away at the age of 3 years as a consequence of pneumonia with associated severe metabolic acidosis.

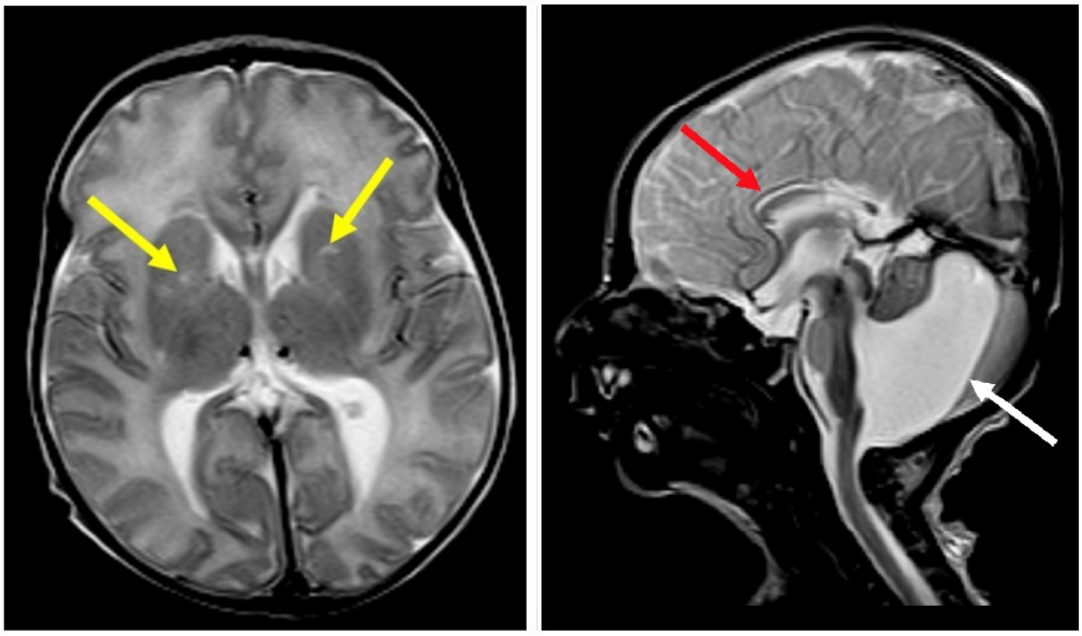

Figure 6.3 Neuroimaging of Patient A-2

(Left) Axial T2-weighted imaging of Patient A-2 at 10 days of age showed bilateral hyperintense signals in the basal ganglia (yellow arrows).
(Right) Sagittal T2 imaging of Patient A-2 at 10 days of age showed Dandy-Walker malformation (white arrow) and thinning of the corpus callosum (red arrow).

6.4.1.2 Family B

Patient B, a male infant, was the third child from healthy consanguineous (first cousin) parents of Moroccan origin with an unremarkable family history. He was born at term after an uneventful pregnancy. Vomiting, failure to thrive, psychomotor delay and poor eye contact were reported from the first months of life. Clinical evaluation performed at 5 months showed impaired growth (weight and length < 3rd centile), microcephaly (< 3rd centile), poor eye contact, non-paralytic strabismus, truncal hypotonia with limb hypertonia, paucity of spontaneous movements and lack of postural control. Brain MRI revealed bilateral abnormal high T2 signal intensity within the thalami (**Figure 6.4**), the basal ganglia and brainstem, though spinal cord MRI was normal. EEG and peripheral nerve conduction studies were unremarkable, but brainstem auditory and visual evoked potentials showed severe central conduction abnormalities. Epilepsy was not reported, however when under anaesthesia to perform MRI, he developed intermittent clonic seizures of both upper limbs which were successfully treated with midazolam. Routine blood investigations including plasma amino acid levels were reported normal, but serum lactate and pyruvate levels were elevated (3.2 mmol/L, normal range 0.8–2.1 mmol/L, and 194 µmol/L, normal range 55–145 µmol/L, respectively). Following severe respiratory deterioration, the patient died at 8 months of age.

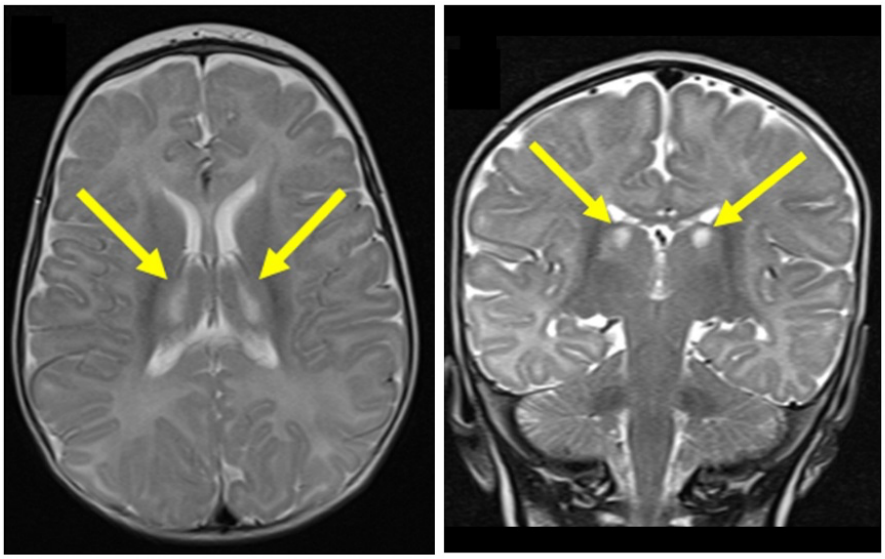

Figure 6.4 Neuroimaging of Patient B

Axial (left) and coronal (right) T2-weighted imaging of Patient B at 5 months of age showed bilateral hyperintense signals in the thalami (arrows).

6.4.2 Genetic investigations

6.4.2.1 Family A

Patient A-1 was initially investigated using commercially available WES that prioritised identification of variants in known disease genes in their analysis. No candidate variants were identified using this NGS method. Subsequent unbiased WGS identified a homozygous 22-nucleotide deletion within the last exon of *NDUFC2* predicting a stop loss mutation in the NDUFC2 protein (GenBank: NM_004549.6; c.346_*7del; p.His116_Arg119delins21). Segregation analysis using Sanger sequencing found both parents and a healthy brother were heterozygous for the c.346_*7del variant; DNA was not available from Patient A-2 (affected sibling) to confirm his genotype (**Figure 6.5**). The identified c.346_*7del variant is absent in variant databases and no healthy controls were homozygous for any loss-of-function *NDUFC2* variants within the gnomAD database (Lek et al., 2016)

6.4.2.2 Family B

Biochemical investigation in Patient B's muscle biopsy revealed an isolated complex I deficiency. This prompted genetic studies in the form of targeted gene-panel analysis which targeted 299 genes associated with mitochondrial function and disease including 54 genes related to complex I assembly and previously associated with complex I deficiency (**Appendix C**). which identified a homozygous c.173A>T p.(His58Leu) *NDUFC2* variant affecting a highly conserved histidine residue (**Figure 6.6A**). Three healthy controls in gnomAD were heterozygous for a rare variant affecting the same residue (c.172C>T, p.(His58Tyr), MAF = 1.21×10^{-5}) (Lek *et al.*, 2016). The residue change was assessed using numerous *in silico* prediction tools and all tools predict it to be pathogenic (PolyPhen2: 1.000 [probably damaging]; SIFT: 0.000 [deleterious]; PROVEAN: -6.733 [deleterious]; raw CADD: 3.99; scaled CADD: 27.9) (Ng and Henikoff, 2001; Kumar *et al.*, 2009; Adzhubei *et al.*, 2010; Choi *et al.*, 2012; Choi and Chan, 2015; Rentzsch *et al.*, 2018). Sanger sequencing confirmed that both parents were heterozygous carriers for the c.173A>T variant; the healthy siblings of Patient B were not tested (**Figure 6.6B and C**).

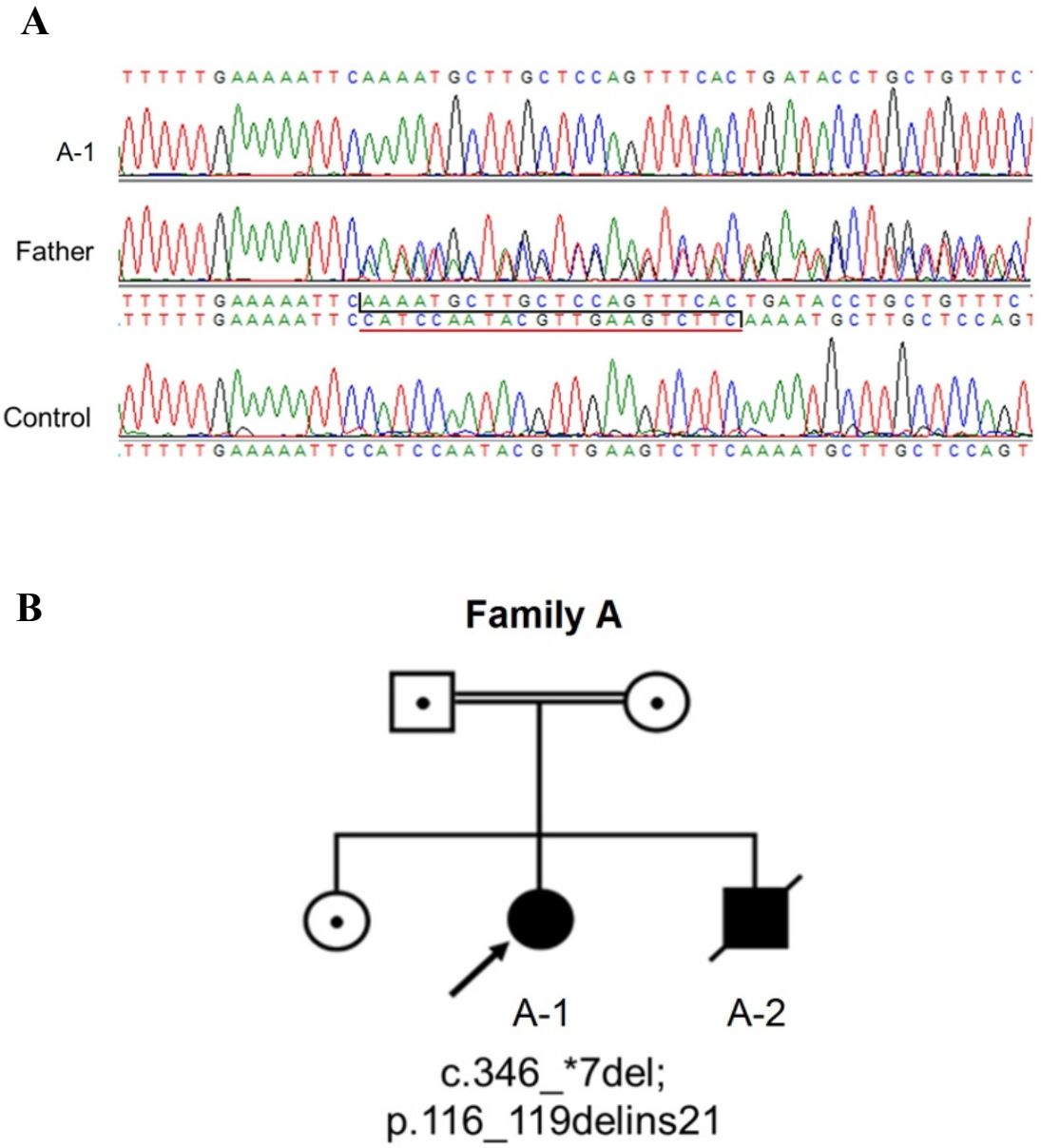

Figure 6.5 Identification and segregation of *NDUFC2* deletion in Family A

A Sequencing chromatograms depicting the identified 22 nucleotide deletion (c.346_*7del) identified in Patient A-1 (A-1), the heterozygous state of the deletion in the father, and the wild-type *NDUFC2* sequence in Control DNA.
B Pedigree showing segregation of variant in Family A. Patient A-2 was not genotyped due to unavailability of DNA

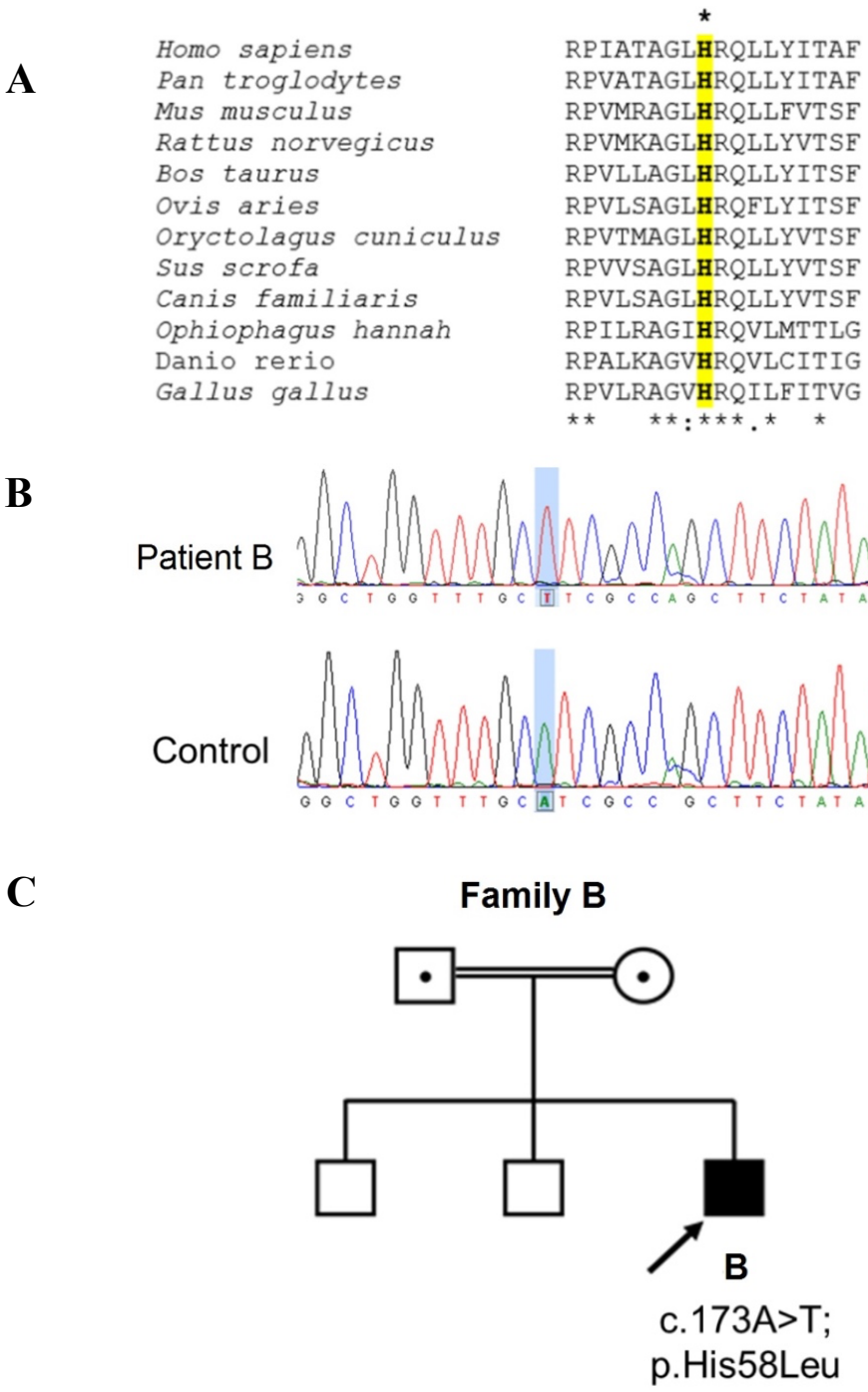

Figure 6.6 Identification and segregation of *NDUFC2* missense variant in Family B

A Clustal Omega sequence alignment shows evolutionary conservation of the p.His58 residue (highlighted) along with its neighbouring residues (human NDUFC2: NP_004540.1).
B Sequencing chromatograms depicting the identified missense variant (c.173A>T; p.(His58Leu)) in Patient B and the wild-type *NDUFC2* sequence in Control DNA.
C Pedigree of Family confirming carrier status of both parent for the identified missense variant (c.173A>T; p.(His58Leu)).

6.4.3 Assessment of NDUFC2 mRNA gene expression in patients' fibroblasts

Quantitative real-time PCR (qRT-PCR) analysis of mRNA transcript levels derived from patient fibroblasts revealed a decrease in *NDUFC2* mRNA expression in Patient A-1 fibroblasts (43% of controls), while mRNA levels in Patient B were similar to controls (**Figure 6.7**).

6.4.4 Assessment of respiratory chain enzyme activity in patients' tissue and cell lines

Mitochondrial respiratory chain enzyme analysis revealed isolated complex I deficiency in Patient A-1's fibroblasts (16% residual activity compared to controls) and Patient B's fibroblasts and muscle (19% and 48% residual activity compared to controls, respectively) (Error! Reference source not found.**A and B**). High-resolution respirometry a nalysis on both patients' fibroblast cell lines revealed a severe decrease in oxygen consumption rates (Error! Reference source not found.**C**).

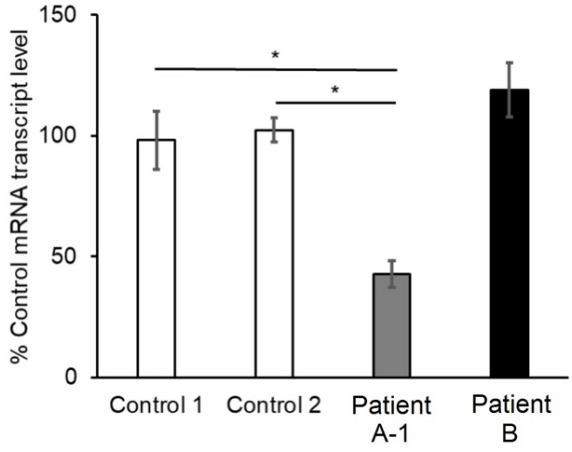

Figure 6.7 NDUFC2 mRNA transcript levels in *NDUFC2* patients' fibroblasts

NDUFC2 mRNA transcript levels in fibroblast cell lines of controls (white), Patient A-1 (grey) and Patient B (black). Quantification of *NDUFC2* mRNA transcript levels (normalised to *ACTB*) showed diminished transcript levels in Patient A-1 while transcript levels were unaffected in Patient B. Bars correspond to standard deviations of two independent experiments, performed in duplicate; *$p<0.05$.

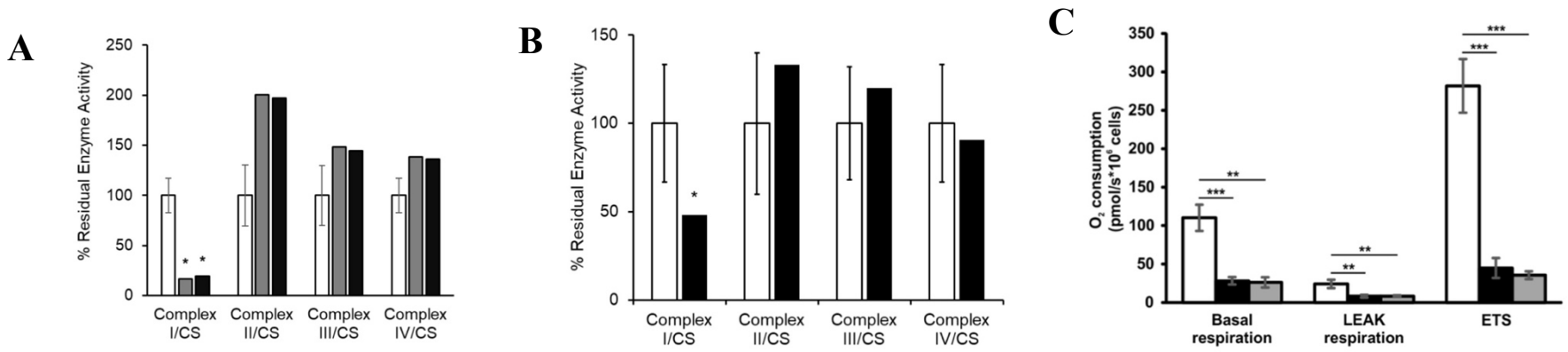

Figure 6.8 Analysis of respiratory chain complex activities in NDUFC2 patients' fibroblasts

A Assessment of respiratory chain enzyme activities, normalised to citrate synthase (CS), in fibroblast cell lines from controls (white), Patient A-1 (grey) and Patient B (black). Mean residual enzyme activities of control fibroblasts (n = 8) are set at 100% and error bars represent 1 standard deviation of control activities. Asterisks (*) denote enzyme activity below control range.
B Assessment of respiratory chain enzyme activities, normalised to citrate synthase (CS), in skeletal muscle from controls (white) and Patient B (black). Mean residual enzyme activities of control skeletal muscle (n>100 samples) are set at 100% and bars are 1 standard deviation of control activities. Asterisks (*) denote enzyme activity below control range.
C Respiration of Patient B and Patient A-1 derived fibroblasts (black and grey, respectively) compared to control fibroblasts (white) using high-resolution respirometry. ROX-corrected analysis of basal respiration, Oligomycin inhibited LEAK respiration and maximum uncoupled respiration (ETS). Both patient fibroblasts exhibited a severe mitochondrial respiration defect as measured by oxygen consumption. Data are mean ± SD from at least 3 experiments. **p<0.01, ***p<0.001.

6.4.5 Steady-state protein levels of complex I subunits in patient cell lines

SDS-PAGE was utilised to assess steady-state protein levels of complex I subunits in fibroblast lysates from patients and controls. Immunoblotting using antibodies against various complex I structural subunits (NDUFC2, NDUFB8, NDUFA9) revealed an overall decrease in steady-state levels of complex I subunits in both patients compared to controls (Error! Reference source not found.)

6.4.6 Complex I assembly in patient cell lines

BN-PAGE was utilised to assess the assembly of respiratory chain complexes in enriched mitochondria from patient and control fibroblast cell lines that were solubilised using DDM. Immunoblotting using antibodies against a subunit from each of the five respiratory chain enzymes (Complex I: NDUFB8; Complex II: SDHA; Complex III: UQCRC2; Complex IV: MT-CO1; Complex V: ATP5A) showed an absence of fully assembled complex I in Patient A-1 and a severe decrease in assembled complex I in Patient B compared to controls (**Figure 6.10**). Assessment of supercomplex formation in enriched mitochondria from patient and control fibroblast cell lines that were solubilised using digitonin showed a severe decrease in complex I-containing supercomplexes (**Figure 6.11**).

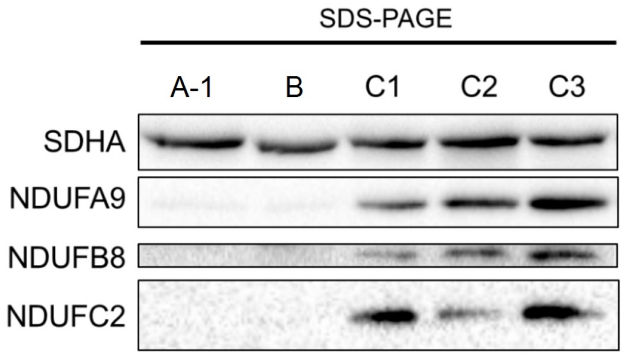

Figure 6.9 Western blot analysis of complex I subunits in *NDUFC2* patient fibroblasts.

Western blot analysis of various structural subunits of complex I in fibroblasts from Patient A-1 and Patient B (A-1 and B respectively) with three age-matched controls (C1, C2, and C3) (results are representative of 3 biological repeats; n=3).

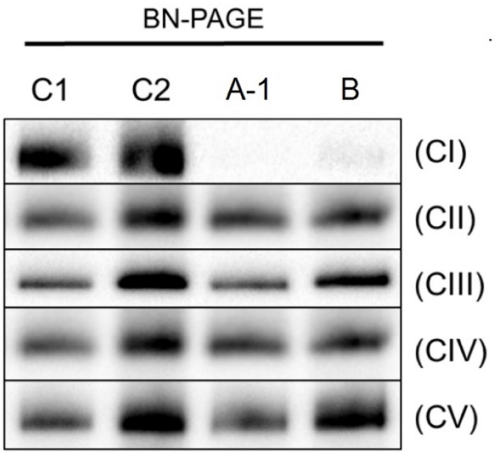

Figure 6.10 Assessment of OXPHOS complex assembly in *NDUFC2* patients' fibroblasts using BN-PAGE.

BN-PAGE analysis of OXPHOS complex assembly in enriched mitochondria from patients and control fibroblasts solubilised using DDM. Immunoblotting was performed using antibodies to structural subunits from each OXPHOS complex (CI [NDUFB8], CII [SDHA], CIII [UQCRC2], CIV [MT-CO1], and CV [ATP5A]) (results are representative of 3 biological repeats; n=3).

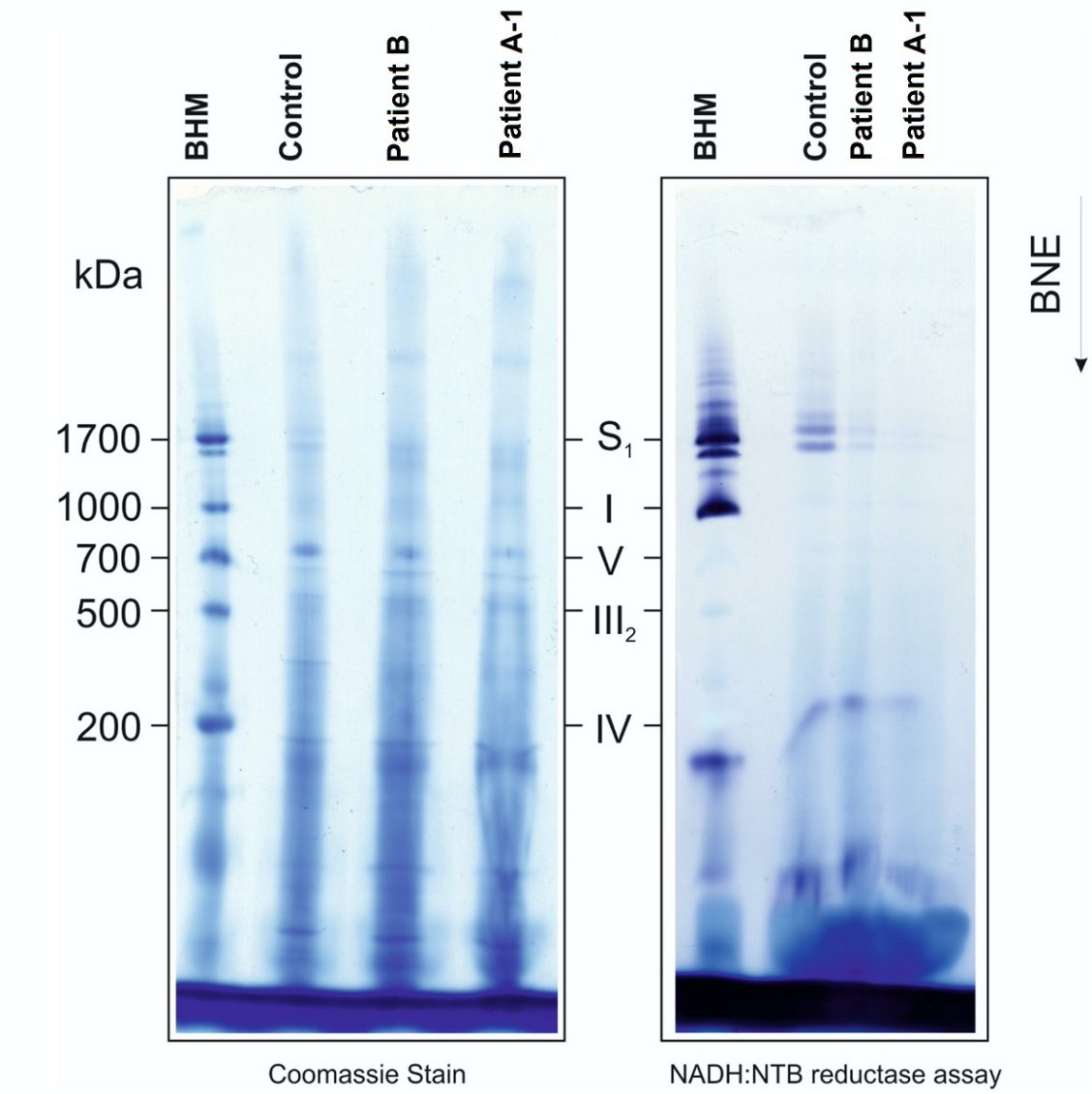

Figure 6.11 Assessment of assembly of complex I containing supercomplexes in Patient B

Coomassie stain (left panel) and an in-gel complex I assay (right panel) in BN-PAGE showed decreased complex I-containing supercomplexes in subject mitochondria. Analysis of complex assembly and stability detected a drastic deficiency of complex I-containing supercomplexes.
S_1, supercomplex containing complex I, dimer of complex III and 1 copy of complex IV; V, ATP synthase; I-III-IV, complexes I-III-IV. BHM, Bovine heart mitochondria solubilised with digitonin as native mass ladder.

6.4.7 Doxycycline inducible lentiviral rescue experiment

To support the pathogenicity of the identified variants and assess the effect of expressing wild-type *NDUFC2* in the patients' fibroblast cell lines, a lentiviral rescue experiment was carried out. This involved lentiviral transduction of each patient fibroblast cell line with a doxycycline-inducible pLVX-TetOne-Puro vector containing wild-type *NDUFC2*.

6.4.7.1 Optimisation of doxycycline dosage by assessing steady-state protein levels of NDUFC2 and other complex I subunits in transduced patient cell lines

To optimise doxycycline induction, various doxycycline concentrations and periods of incubation were used to determine the optimal conditions for the rescue experiment by assessing the effect of induction on the steady-state levels of NDUFC2 and other complex I subunits. Initially, incubation of transduced patient cell lines in a gradient of doxycycline concentrations (25, 50, 100 and 200 ng/ml) for 96 hours showed increased steady-state protein levels of NDUFC2 and other complex I subunits (NDUFB8 and NDUFA9) with 200 ng/ml having the highest levels as expected (**Figure 6.12A**). NDUFC2 protein levels in the induced Patient A-1 cell line showed a gradual increase in expression but did not reach levels comparable to controls; in contrast, the induced Patient B cell line did reach NDUFC2 levels comparable to controls but there was not an obvious difference in steady-state protein levels between the doses of doxycycline tested (25-200 ng/ml) (**Figure 6.12A**). NDUFB8 protein levels in the induced Patient A-1 cell line also did not show a gradual increase in protein levels corresponding to the doxycycline concentration. Subsequently, induction of transduced patient fibroblast cell lines with doxycycline concentrations of 100 ng/ml for 48 hours was compared to those induced with 200 ng/ml for 96 hours and showed an increase in complex I subunit expression in both conditions (**Figure 6.12B**). There was only a slight increase in NDUFC2 and NDUFB8 levels between the samples induced with 200 ng/ml doxycycline for 96 hours compared to 100 ng/ml doxycycline for 48 hours demonstrating that 48 hours is sufficient to allow for NDUFC2 expression and subsequent complex I assembly. Again, steady state levels of complex I subunits including NDUFC2 were not comparable to controls in Patient A-1, but they were comparable to controls in Patient B (**Figure 6.12B**).

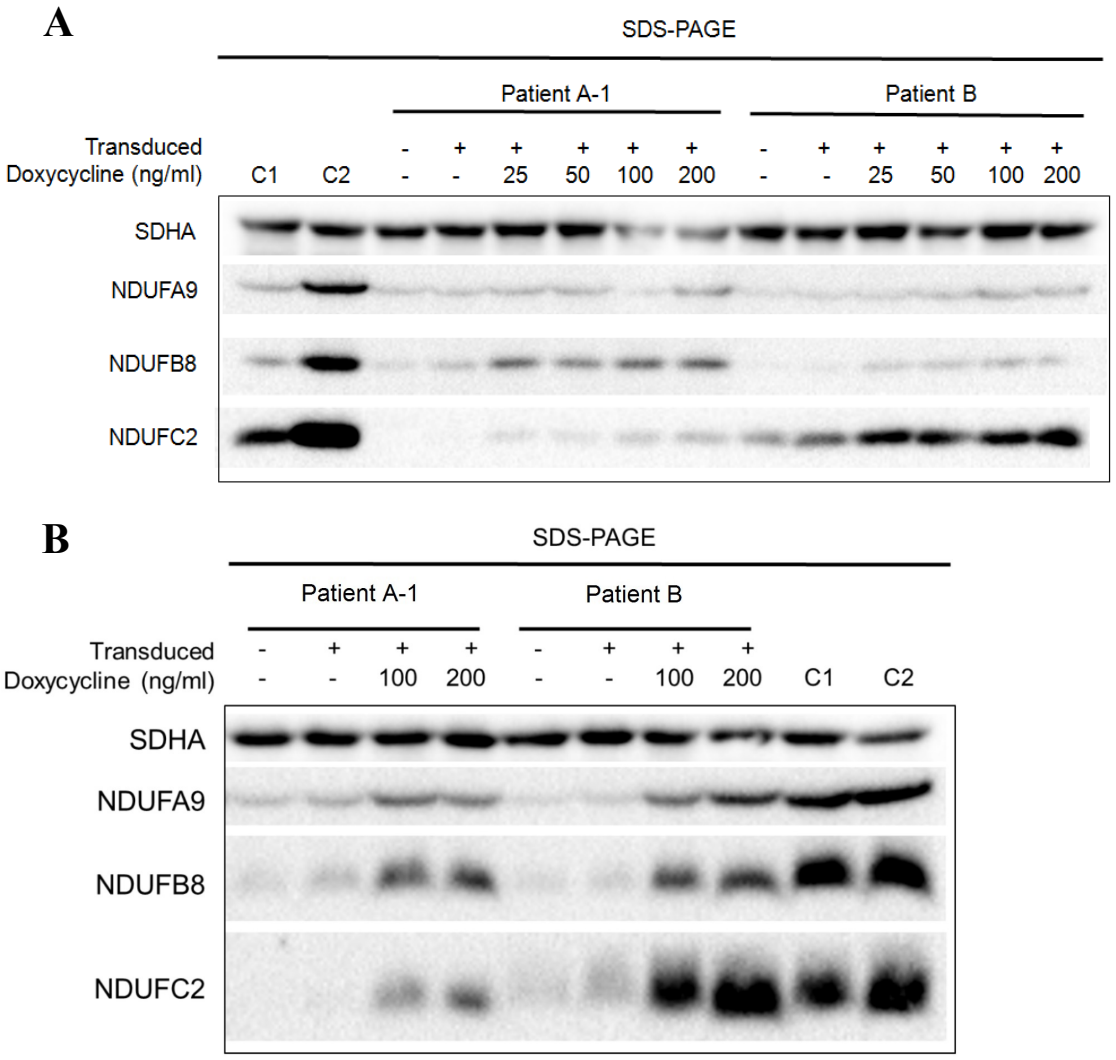

Figure 6.12 Assessing the effect of lentiviral transduction of wild-type NDUFC2 cDNA on steady-state complex I subunit levels in patient cell lines.

A Western blot analysis of whole cell lysates from controls (C1 and C2) and patient cell lines (Patient A-1 and B) that were either untransduced (-) or transduced with the lentiviral vector (pLVX) containing wild-type *NDUFC2* (+). Transduced cell lines were either uninduced or induced using a sequence of doxycycline concentrations of 25, 50, 100 or 200 ng/ml for 96 hours where indicated (results are representative of 1 experiment; n=1).
B Western blot analysis of whole cell lysates from controls (C1 and C2) and patient cell lines (Patient A-1 and B) that were either untransduced (-) or transduced with the lentiviral vector (pLVX) containing wild-type *NDUFC2* (+). Transduced cell lines were either uninduced or induced with 100 ng/ml doxycycline for 48 hours or 200 ng/ml doxycycline for 96 hours where indicated (results are representative of 2 biological repeats; n=2).

6.4.7.2 Assessment of Complex I assembly in induced patient cell lines

The optimisation of doxycycline induction conditions described above showed that induction using 100 ng/ml doxycycline for at least 48 hours (**Figure 6.12**) was sufficient to increase steady-state protein levels of NDUFC2 and other complex I subunits in both transduced patients' fibroblast cell lines to close to maximal levels within this system, though using 200 ng/ml did increase the expression slightly. Thus, due to the minimum requirement of 72 hours for fibroblasts to reach optimal confluency for harvesting for mitochondrial enrichment and subsequent BN-PAGE analysis, the induction was performed using 200 ng/ml doxycycline for 72 hours. Enriched mitochondria from induced patient cell lines were assessed using BN-PAGE and revealed an increase in complex I assembly compared to controls and their respective uninduced and untransduced cell lines (**Figure 6.13**). These results mirror the SDS-PAGE results with levels of fully assembled complex I in induced Patient B cell lines increased more than that observed in Patient A-1 cell lines but complex I levels in neither induced patient cell line reached levels similar to controls.

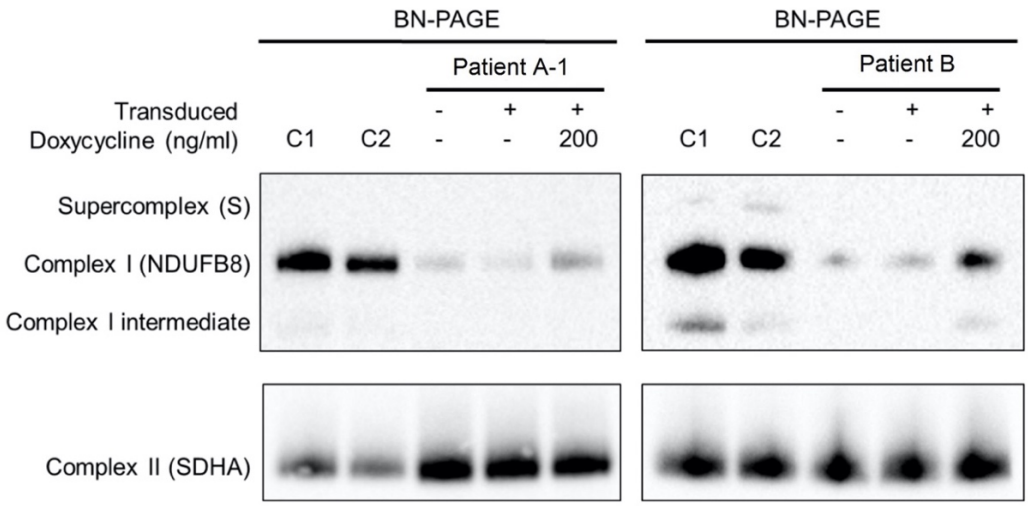

Figure 6.13 Assessing the effect of lentiviral transduction of wild-type NDUFC2 cDNA on complex I assembly in patient cell lines

BN-PAGE analysis of OXPHOS complex assembly in enriched mitochondria isolated from controls (C1 and C2) and patient cell lines that were either untransduced (-) or transduced with the lentiviral vector (pLVX) containing wild-type *NDUFC2* (+). Transduced cell lines were either uninduced or induced with 200 ng/ml doxycycline for 72 hours (results are representative of 2 biological repeats; n=2).

6.4.8 Complexome profiling of patient fibroblast cell lines

Complexome profiling was performed on fibroblast cell lines of both patients and an age matched control to investigate the role of NDUFC2 in complex I assembly and stability. In support of previous functional findings, there was a severe decrease in complex I-containing supercomplexes (S) (

Figure 6.14 **and Figure 6.15A-C**). In addition, no NDUFC2 was detected in patient A-1 and only a small amount was detected in Patient B (

Figure 6.14, grey horizontal line). Complex III and IV levels were unaffected compared to the control, however they formed smaller supercomplexes lacking complex I and remained as individual complexes (**Figure 6.15B-C,** black arrows). Close analysis of complex I assembly intermediates in the patients reveal the important role of NDUFC2 in complex I biosynthesis. Assembly of the Q module appears unaffected by the variants identified in both patients. The Q module subunits (NDUFA5, NDUFS2, NDUFS3, NDUFS7 and NDUFS8) were detected with its assembly factors (NDUFAF3 and NDUFAF4) bound to it (**Figure 6.16A-B**). In contrast to the control profile, Q-module is shown to form an intermediate binding with the NDUFA13 subunit and the assembly factor TIMMDC1 (Q*~300 kDa,

Figure 6.14**,** orange dashed boxes; **Figure 6.16A**) in both patients indicating that the identified intermediate is bound to the membrane. A larger Q intermediate with the NDUFA13 and TIMMDC1 is formed with components of the mitochondrial complex I assembly complex (MCIA) ACAD9, ECSIT, NDUFAF1 and the transmembrane protein TMEM126B resulting in a 715-800 kDA complex I intermediate (**Figure 6.16A**). In addition, a preassembled intermediate comprised of the ND4 module and the assembly factors TMEM70 and FOXRED1 was detected in both patients (**Figure 6.16B**). No intermediates of the N, ND2 and ND5 modules were detected in either patients. The complexome profiling findings suggest that in the absence of the NDUFC2 subunit complex I assembly is stalled at the Q module intermediate stage.

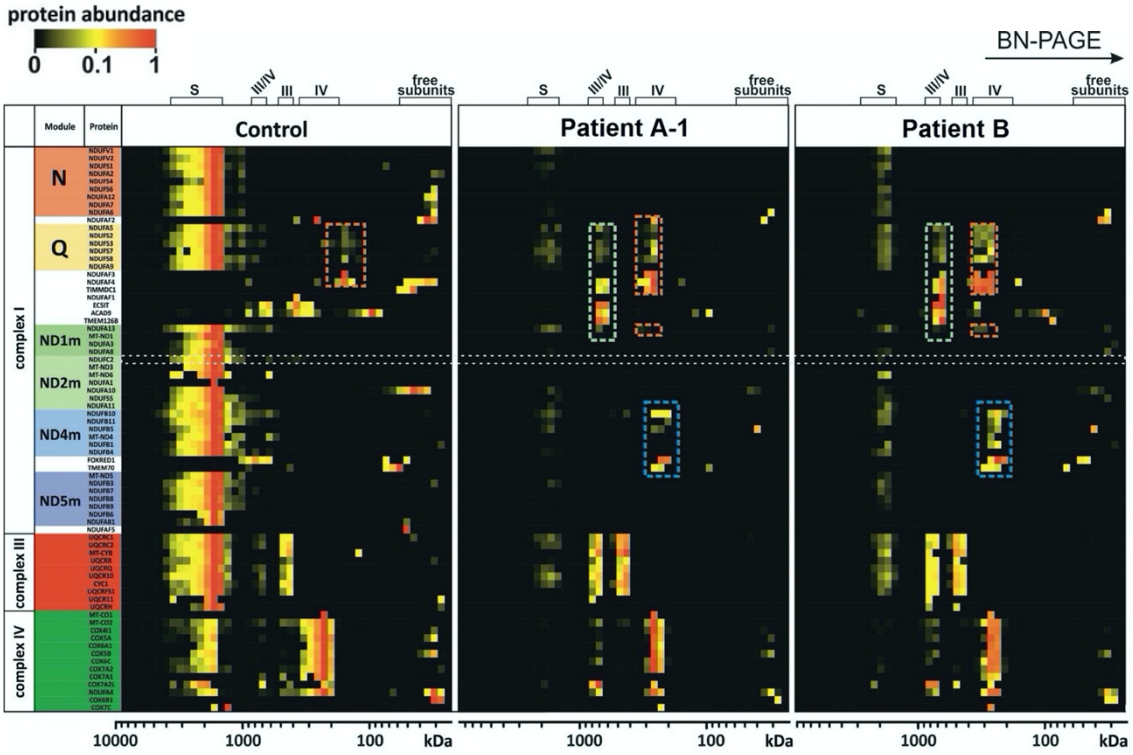

Figure 6.14 Complexome profiling of fibroblasts from patients A-1 and B confirm complex I deficiency

Complexome profiling identified assembly intermediates in patient cells with *NDUFC2* mutations. Complexes from mitochondrial membranes of Control, Patient A-1 and Patient B fibroblasts were separated by BN-PAGE (**Figure 6.11)** and analysed by complexome profiling. Assignment of complexes: III, complex III; IV, complex IV; III/IV, supercomplex containing dimer of complex III and 1-2 copies of complex IV; S, supercomplex containing complex I, dimer of complex III and 1-4 copies of complex IV. Assembly intermediates are highlighted in dashed boxes indicating stalled complex I assembly. In patient complexomes, various stalled complex I intermediates are assembled: ND4 module (blue dashed box); Q-TIMMDC1-NDUFA13 complex I intermediate (orange dashed box); and Q-TIMMDC1-NDUFA13-MCIA (green dashed box). In control complexome, the Q module (orange dashed box) is assembled without TIMMDC1 or NDUFA13. Complex I modules are denoted according to Stroud and colleagues (Stroud et al., 2016).

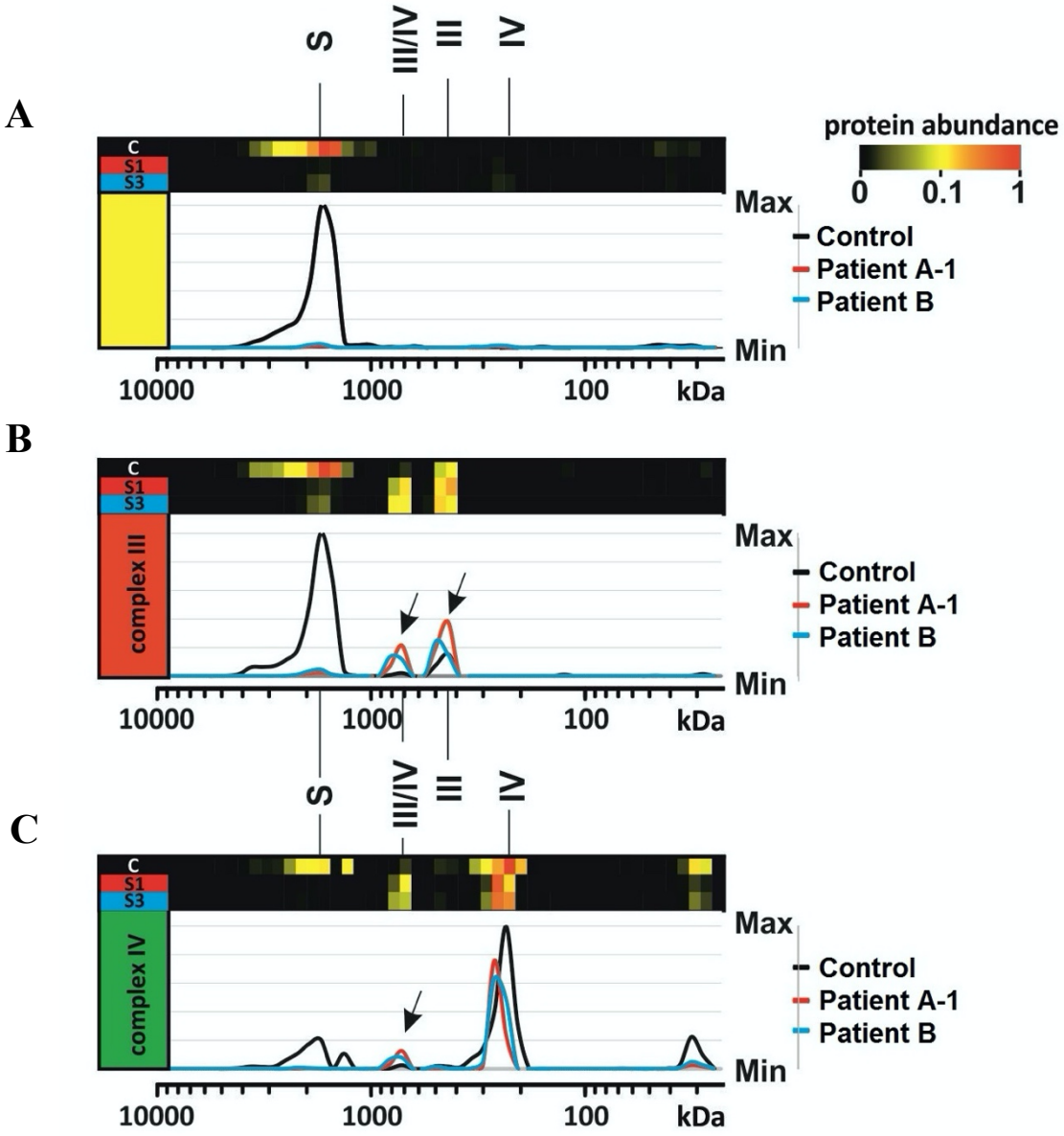

Figure 6.15 Complexome Profiling of Fibroblasts from Patients A-1 and B confirm deficiency in supercomplex formation.

A Abundance data for all the subunits of complex I were averaged to plot an abundance profile of complex I. Heatmap (upper panel) and profile plot (lower panel) compare complex I between control (black), Patient A-1 (red) and Patient B (blue).
B Profile plot of complex III (average of all subunits). Black arrows indicate shifted complex III to the position of the individual complex and small supercomplex (III/IV) in Patient A-1 and B.
C Profile plot of complex IV (average of all subunits) indicate less complex IV at the position of the supercomplexes for Patient A-1 and Patient B, but higher amounts of individual complex IV and small supercomplex (III/IV, black arrow).

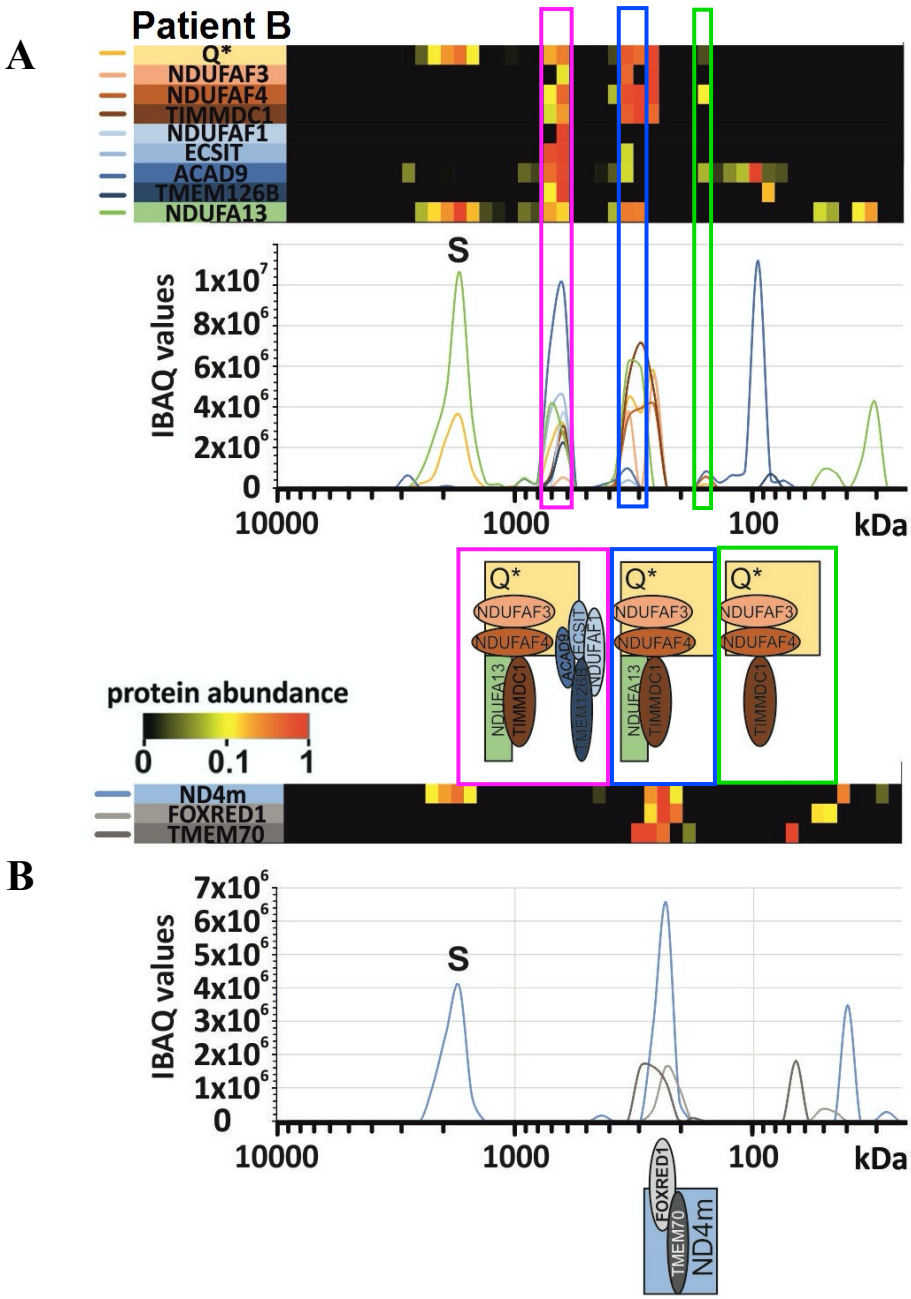

Figure 6.16 Complexome Profiling of Fibroblasts from Patient B demonstrate modular assembly of complex I.

A Details of Q module-containing assembly intermediates of Patient B. Intensity based absolute quantification (iBAQ) values of assembly factors, single subunit and averaged Q-module subunits were plotted to show abundance profiles. The cartoon (lower panel) indicates assembled intermediate complexes relative to coloured boxes in the plot.
B Details about ND4 module assembly intermediate of Patient B. Abundance profile of averaged iBAQ values of ND4 subunits and assembly factors show accumulation of a complex containing the ND4 module, FOXRED1 and TMEM70.

6.5 Discussion

Biochemical investigations assessing the functional effect of the confirmed *NDUFC2* variants showed similar findings in Patients A-1 and B even though one patient was homozygous for a loss-of-function variant and the other was homozygous for a missense variant that affects a highly conserved residue. No homozygous loss-of-function *NDUFC2* variants were reported in the gnomAD database and only two protein-coding variants were reported as homozygous in healthy controls: p.Leu46Val (n=4270 homozygotes; MAF=0.197) and p.Arg119His (n=1 homozygote; MAF=2.77×10^{-4}); neither substitution was predicted to change the biochemical properties of the affected residues (Lek *et al.*, 2016). Recent work including *NDUFC2*-knockout HEK293T cells showed a defect in the expression of ND2, ND5 and N module subunits, but ND4 module subunits were unaffected (Stroud *et al.*, 2016). In addition, ND1 module subunits were unaffected, however that is not the case in our *NDUFC2* patients where both had a defect in ND1 module assembly (or stability) and only the NDUFA13 subunit was detected (

Figure 6.14 **and Figure 6.16**). The observed loss of the ND2 module (where NDUFC2 is incorporated) in Patient B asserts that the conserved His58 residue plays an important role in the assembly or stability of the module (**Figure 6.16**).

The induction of wild-type NDUFC2 in Patient A-1 fibroblasts resulted in an increase in protein levels but it did not reach levels comparable to endogenous levels observed in controls. The induction also resulted in the partial rescue of steady-state levels of other complex I subunits and levels of fully assembled complex I (**Figure 6.12 and Figure 6.13**). In Patient B fibroblasts, induction resulted in NDUFC2 levels appearing similar to endogenous levels in controls, but steady-state levels of other complex I subunits and levels of fully assembled complex I did not reach control levels (**Figure 6.12 and Figure 6.13**). Assembly of complex I is suggested to require just 24 hours (Guerrero-Castillo *et al.*, 2017) meaning the 72 hours of doxycycline induction should have provided sufficient time for the expressed wild-type NDUFC2 to incorporate and assemble into complex I. Despite protein levels not reaching endogenous levels in rescued patient cell lines, results clearly demonstrate that the lentiviral expression of wild-type NDUFC2 ameliorates the biochemical phenotype, leading to observable increases in steady-state levels of complex I subunits, and more importantly the incorporation of the expressed wild-type NDUFC2 into complex I as observed in the increased levels of fully-assembled complex I.

It is worth noting that the patient cell populations were each transduced in single dishes, subjected to puromycin selection, and then propagated into multiple flasks for the uninduced and various induced concentrations tested. The cell lines were not grown up from single colonies of transduced fibroblasts as these were primary fibroblasts and growing enough cells for use in the experiments from a single transduced fibroblast cell was not possible due to the number of rounds of cell division required. Whilst the genetic integration will not have been in the same location in each cell, the wild-type *NDUFC2* should be as a single copy and is under the same inducible promoter in each cell so similar expression levels in each cell are expected. This is supported by the fact that multiple transductions were carried out independently and no noticeable difference is observed in NDUFC2 expression between each population of transduced cells. Some individual clones may well have had better expression than others if it were possible to use a clonal selection method, but this effect is expected to be relatively minor and producing reproducible data with multiple heterogeneous populations of transduced cells minimises the chance of observing off target effects from one specific clone. Overall, the results strongly support the pathogenicity of both *NDUFC2* variants identified in the patients.

Current work on complex I assembly states that the Q-intermediate binds to the ND1 module and the membrane spanning assembly factor TIMMDC1 forming complex I intermediate containing the Q module and ND1 module subunits (**Figure 6.17A**) (Guerrero-Castillo *et al.*, 2017; Formosa *et al.*, 2018; Signes and Fernandez-Vizarra, 2018). We identified an assembly intermediate in the *NDUFC2* patients consisting of the Q module and the assembly factors ACAD9, ECSIT, NDUFAF1 and TMEM126B, which comprise the MCIA, the assembly factor TIMMDC1 and NDUFA13 (**Figure 6.17C;**

Figure 6.14, Patient A-1 and Patient B, green dashed boxes). ND1 and NDUFA8 subunits were not detected despite being previously associated with this stage of assembly, but this may be due to the sensitivity of the assay. NDUFA13 is the only ND1 module subunit that was detected in a Q-intermediate in both patients (~300 kDa,

Figure 6.14, orange dashed boxes, **Figure 6.16A; Figure 6.17B**). A similar assembly intermediate, lacking the MCIA factors, was previously observed in cases harbouring pathogenic variants in *TMEM126B* (an MCIA factor) where control complexome data showed a Q module intermediate lacking the TIMMDC1 assembly factor, similar to the present control complexome (Alston *et al.*, 2016a). No other ND1 module subunits, or subunits from the neighbouring ND2 module, were detected in our *NDUFC2* patients.

The observed complex I assembly intermediates suggest the MCIA complex is involved in the incorporation and assembly of the ND2 module (Guerrero-Castillo *et al.*, 2017).

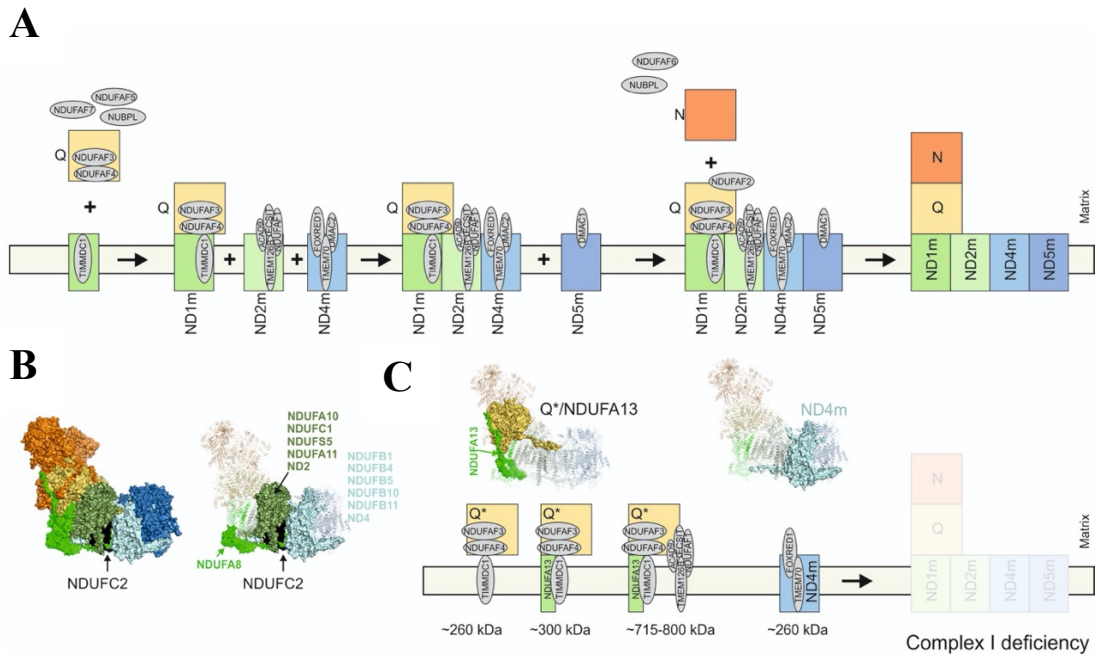

Figure 6.17 Molecular consequences of defects in NDUFC2 on complex I

A Assembly sequence of complex I modules according to current state of knowledge in human cells (Guerrero-Castillo *et al.*, 2017; Formosa *et al.*, 2018; Signes and Fernandez-Vizarra, 2018). The ND1 module (ND1m), ND2 module (ND2m), ND4 module (ND4m) and ND5 module (ND5m) are identified by these abbreviations.
B Left, structural modules of complex I highlighted in colours based on mouse cryo-EM structure (PDB: 6g2j) (Agip *et al.*, 2018). NDUFC2 is shown in black. Right, surface view indicates subunits interacting in a neighbourhood of less than 10 Å to NDUFC2. All other subunits not interacting on any part of the protein are in transparent cartoon view.
C Assembly intermediates/dead end assembly products in mitochondria from Subject 3 according to data from complexome profiling. Assembled subunits are highlighted in surface view within cryo-EM structure (PDB: 6g2j) (Agip *et al.*, 2018).

In the absence of NDUFC2, the ND2 module was not detected and an alternative complex I assembly intermediate was formed in the complexomes of the *NDUFC2* patients (~715-800 kDa,

Figure 6.14, Patient A-1 and Patient B, green dashed boxes; **Figure 6.15C**).

NDUFC2 is a complex I subunit assigned to the membrane bound ND2 module and molecular data obtained from collaborators at Goethe-Universität in Frankfurt, Germany, indicate NDUFC2 plays an important role in the assembly of the membrane arm of the complex (**Figure 6.17B**). NDUFC2 extends into the intermembrane space and has contact with 12 other subunits (**Figure 6.17B**, right panel) including NDUFA8 subunits of the ND1 module, neighbouring ND2 subunits (ND2, NDUFA10, NDUFA11, NDUFC1 and NDUFS5), and ND4 module subunits (ND4, NDUFB1, NDUFB5, NDUFB10 and NDUFB11) (Zhu *et al.*, 2016; Agip *et al.*, 2018). All these contact sites could be crucial for the assembly and stability of complex I. Complexome profiling of both *NDUFC2* patients showed a loss of ND1 and ND2 module subunits associated with it which is consistent with the suggested model.

The data also support the stalled complex I assembly following the formation of the Q module due to the failed formation of fully assembled ND1 in the inner mitochondrial membrane. The absence of ND1 and ND2 modules (and most of their subunits) in the complexome data of the patients indicates that the modules do not assemble independently and suggest that NDUFC2 might be important in the formation of the ND1 module.

By contrast, the ND4 module, which is comprised of ND4, NDUFB1, NDUFB5, NDUFB10 and NDUFB11 subunits along with its assembly factors FOXRED1 and TMEM70, was detected as a stable complex I intermediate in Patient B and less apparently in Patient A-1 (~260 kDa, Figure 6.14, Patient A-1 and Patient B, blue dashed boxes; **Figure 6.16B**; **Figure 6.17C**). This finding is consistent with previous models of complex I assembly and human complexome data show independent assembly of the membrane-bound module (Alston *et al.*, 2016b; Stroud *et al.*, 2016; Guerrero-Castillo *et al.*, 2017; Alston *et al.*, 2020). The N and ND5 modules were not detected in the complexome data of our *NDUFC2* patients suggesting that assembly intermediates of these distal modules are either unstable, they are governed by middle stage assembly, or they are turned over by mitochondrial proteases (Szczepanowska *et al.*, 2020).

A number of pathogenic variants in ND2 module subunits have been previously reported in *NDUFA1*, *NDUFA10* and *NDUFA11*. Although they all affect the same module, variable clinical presentations were reported in the patient, which is common observation in mitochondrial disease patients. Patients harbouring pathogenic variants in *NDUFA1* or *NDUFA10* mostly presented with Leigh syndrome or Leigh-like symptoms, while a single patient with an *NDUFA11* variant presented with early-onset fatal encephalocardiomyopathy (Fernandez-Moreira *et al.*, 2007; Berger *et al.*, 2008; Hoefs *et al.*, 2011; Minoia *et al.*, 2017). A variety of biochemical, molecular and functional investigations were performed in these cases, which revealed defects in complex I assembly (NDUFA1 and NDUFA10) and complex I enzyme deficiency (NDUFA1, NDUFA10 and NDUFA11). These reports support the association of pathogenic variants in ND2 module subunits with paediatric mitochondrial disease. Recently, an increasing number of complexome profiling data has been acquired from cell lines of cases with complex I deficiency due to bi-allelic mutations in *NDUFA6* encoding a complex I subunit, and in *TMEM126B* and *NDUFAF8* encoding complex I assembly factors; some cases presented with Leigh syndrome (Alston *et al.*, 2016a; Alston *et al.*, 2018; Alston *et al.*, 2020). This provided a means of assessing previously extrapolated steps of complex I assembly. These investigations of pathogenic variants in complex I structural subunits and assembly factors and their effects on complex I assembly revealed novel assembly intermediates indicating stalled assembly. To date, data from patient-derived functional investigations provide supporting evidence for the independent assembly of the Q and ND4 modules and have highlighted the important roles of novel assembly factors TMEM126B and NDUFAF8. In addition, they have described the functional consequence of pathogenic variants within structural complex I subunits (e.g., NDUFA6) and their effect on the assembly of complex I

Chapter 7. General discussion

The introduction of targeted NGS technologies has revolutionised the approach in diagnosing and understanding the aetiology of genetic disorders in the past decade. The employment of WES and WGS on cohorts of patients suspected of genetic disorders has resulted in the rapid diagnosis and discovery of novel candidate genes associated genetic disorders including mitochondrial disorders (Haack *et al.*, 2012; Saunders *et al.*, 2012; Lieber *et al.*, 2013; Yang *et al.*, 2013; Gilissen *et al.*, 2014; Soden *et al.*, 2014; Taylor *et al.*, 2014; Wortmann *et al.*, 2015; Pronicka *et al.*, 2016). Clinical heterogeneity and often weak genotype-phenotype correlations observed in mitochondrial disease patients pose a challenge in the pursuit of a diagnosis since mitochondrial functions are governed by proteins encoded in both mtDNA and nDNA. Of the 1,158 proteins purported to comprise the mitochondrial proteome (Calvo *et al.*, 2016), over 300 genes have been associated with mitochondrial disorders thus far with the continued discovery of novel candidate genes by utilising NGS technologies (Pagliarini *et al.*, 2008; Stenton and Prokisch, 2020). The foundation of my study is to apply unbiased WES to a well-characterised patient cohort from Kuwait to diagnose Mendelian mitochondrial disease, to improve diagnostic yield by utilising selection criteria, to expand clinical spectrums of disease and determine genetic architecture, to identify novel candidate genes and deepen our understanding of mitochondrial disease phenocopies.

7.1 The role of patient recruitment on the diagnostic rate

The high diagnostic yield in my study was heavily attributed to the recruitment process. Available clinical information and investigation results were first reviewed by Dr Buthaina Albash (a specialist in paediatric metabolic disorders at KMGC), then I reviewed the cases she referred and scored them based on a modified MDC scoring scheme that I developed (**Chapter 3**). Finally, the high scoring cases were reviewed by Professor Robert McFarland (a mitochondrial disease specialist and paediatric neurologist at the Wellcome Centre for Mitochondrial Research) for his input on which cases were likely suspected of mitochondrial disease as opposed to other neurological disorders. Furthermore, Professor McFarland was invited to KMGC in 2016 and 2018 to assess potential candidates for my study that were selected by Dr Albash. This multistep approach of reviewing referred cases ensured that cases were highly suspected of

mitochondrial disease involvement prior to being analysed using WES. Some factors and findings heavily influenced this recruitment process namely case referrals to KMGC, clinical information and investigation results available, and family participation which I will discuss below.

7.2 Limitations of recruiting candidate cases from Kuwait

The recruitment and selection of candidate patients and families from Kuwait exhibited numerous challenges including the limited referral of cases to KMGC, the lack of clinical information and investigations performed. From 2010 until 2016, patients referred to KMGC upon suspicion of mitochondrial disease involvement were genetically investigated by sequencing mtDNA for previously reported pathogenic mutations associated with disease. During that period, the lack of expertise in mitochondrial disease at KMGC resulted in a low diagnosis rate amongst the investigated patients. The arrival of Buthaina Albash at KMGC played a major role in the selection of candidate patients highly suspected of mitochondrial disease. However, the specialist reported many missing clinical details that needed to be obtained in order to review the case fully. This resulted in requesting missing clinical details from families and the referring clinicians in addition to requesting further investigations involving blood tests and radiological MRI scans in cases lacking such crucial information. Some families did not return calls, some families no longer reside in Kuwait, and some families opted not to participate in the study due to the frustration of pursuing a diagnosis for many years with no conclusive results from the hospitals or KMGC. Genetic counselling was provided to such families and clinicians explained the complexity reaching a diagnosis in genetic disorders, but the families had the final say in their consent and participation.

Referral of patients to KMGC from primary clinicians often came with limited referral clinical notes and investigations (should results be available). This resulted in many referred cases with insufficient information to assess their candidacy accurately. A thorough clinical history including family history was important in the recruitment process as it improved evaluation of patient candidacy and suspicion of mitochondrial disease in a highly consanguineous population where newborns with complications due to genetic diseases, including mitochondrial disease, are likely to go unreported after passing away. Such cases are often not investigated further, and families are consequently likely to go on to have multiple similarly affected siblings (Chaman *et al.*, 2014).

Of the clinical information available, radiological MRI findings suggestive of mitochondrial disease involvement greatly increased the candidacy of patients as it was heavily weighted in previously suggested MDC (Morava *et al.*, 2006; Joost *et al.*, 2012; Chi, 2015; Witters *et al.*, 2018) which led to it being included in the modified MDC I developed and used in the reviewing of cases (**Figure 3.3**). The mitochondrial disease criteria employed here and those previously suggested generally sacrifice sensitivity for specificity in relation to mitochondrial disease (Witters *et al.*, 2018). With both the 'Metabolic/Imaging' and 'Tissue Findings' categories having high max limits in the modified MDC employed, only the former could influence the candidacy of recruited patients since no tissue investigations have been performed in Kuwait.

7.3 WES as a first-tier genetic analysis technique

Of the available NGS tools, the gene agnostic approach of WES has proven to be a rapid and cost-effective approach in diagnosing genetic disorders, including mitochondrial disorders, in patients from the highly consanguineous Middle Eastern population with a diagnostic rate of 45% (Alahmad *et al.*, 2019). WES can help provide families with a rapid genetic diagnosis and genetic counselling thereafter to discuss possible options for future pregnancies. Therefore, WES was the tool of choice in my study to investigate and diagnose the recruited candidate families living in Kuwait.

The recruitment process is an important step in selecting a cohort of patients that were investigated upon suspicion of mitochondrial disease involvement based on clinical selection criteria. Using WES as a first-tier genetic analysis approach, I was able to achieve a genetic diagnosis in 14 of the 22 families recruited in my cohort (63.6% diagnosis rate) (**Chapter 4**). This diagnostic rate mirrors the rates achieved in previous studies investigating mitochondrial disease patients (Taylor *et al.*, 2014; Wortmann *et al.*, 2015; Pronicka *et al.*, 2016; Theunissen *et al.*, 2018). The bioinformatics filtering pipelines developed and used in the WES results were optimised for identifying variants in genes associated with mitochondrial function and disease. The filtering pipelines also included for identification of variants in genes associated with neurological disorders that were phenocopies of mitochondrial disease (*RNASEH2C*, *TREX1*, *VPS13B*, and *ATP8A2*). There remain 8 families without a diagnosis in my cohort, one reason for this could be that the reported clinical presentations were caused by trauma or environmental factors rather than genetic factors. On the other hand, genetic factors are suspected due to high rates of consanguinity in the recruited cohort, therefore it is possible that the

causative variants reside in non-coding regulatory regions of the genome or there could be copy number variations (CNVs) which are not well covered by WES analysis (Turner *et al.*, 2016; Shaikh, 2017; Burdick *et al.*, 2020). Although the alternative WGS can help overcome these obstacles, cost was a deciding factor in choosing WES which has already proven its high diagnostic rate when utilised as a first-tier genetic analysis test at the start of my study (Belkadi *et al.*, 2015).

7.4 Functional validation of segregated variants

KMGC does not currently have access to functional laboratory testing to validate candidate genetic variants and confirm their pathogenicity; this includes the absence of skin biopsy and tissue culture facilities. A large number of novel genetic variants in both mitochondrial and non-mitochondrial genes were identified in my study cohort, including missense and truncating variants that prompted further investigations to study their effect on protein expression and OXPHOS complex assembly. With family consent, I liaised with Dr Ahmad Alaqeel, a clinician at KMGC, to acquire patient skin biopsies from 4 recruited families with segregating novel variants (*MPC1*, *TTC19*, *NDUFA13* and *TREX1*). These biopsies were sent to Newcastle to establish fibroblast cell lines allowing the functional investigations of variant pathogenicity presented in my thesis (**Chapter 5**).

7.5 *LETM1* is a novel mitochondrial disease gene

As a novel mitochondrial disease gene, skin biopsies could have helped validate the pathogenicity of the *LETM1* variants identified in both families 1 (NM_012318.2; c.754_756delAAG; p.Lys252del) and family 6 (c.881G>A; p.Arg294Gln). Unfortunately, as all affected patients were deceased, no functional analysis was possible for either family. Due to a lack of available samples, the functional analysis required to confirm pathogenicity such as western blots, BN-PAGE and rescue experiments were not possible. The utilisation of functional investigation techniques to study the effect of novel variants and variants in novel candidate genes is a key step in validating the pathogenicity of the identified variants. These functional techniques were used to investigate and validate *NDUFC2* variants in 2 unrelated families which initiated a multicentre collaboration (**Chapter 6**).

7.6 GeneMatcher facilitated the *NDUFC2* collaboration

Dr Seham Alameer, a specialist in paediatric metabolic disorders, reported a patient homozygous for a *NDUFC2* deletion at their centre in Jeddah, Kingdom of Saudi Arabia.

GeneMatcher (https://genematcher.org/ (Sobreira *et al.*, 2015)) identified another patient homozygous for a missense *NDUFC2* variant reported by Professor Daniele Ghezzi, a mitochondrial disease specialist working in Milan, Italy. Both the Saudi Arabian and Italian groups had obtained skin biopsies from their genotyped patients and established fibroblast cell lines. I obtained these fibroblast cell lines and began functional analysis using western blotting and BN-PAGE and used these techniques to assess the effect of expressing wild-type NDUFC2 in patient cell lines using a lentiviral rescue experiment. Furthermore, patient cell lines were also sent to Professor Ilka Wittig for complexome profiling to assess how the *NDUFC2* variants affected complex I assembly. This multicentre collaboration began with a single matching of identified gene variants in GeneMatcher and the availability of patient cell lines from Saudi Arabia and Italy facilitated the functional investigations performed through extensive collaboration. This allowed the designation of different functional analyses to be performed simultaneously at different centres based on their specialisation and expertise. This led to a more rapid validation of pathogenicity and the comprehensive characterisation of the consequences due to the identified variants in a novel mitochondrial disease gene. NDUFC2 is a subunit of complex I's IMM embedded ND2 submodule that houses a proton pumping channel; its absence resulted in the stalling of complex I assembly and thus led to complex I deficiency, an established phenotype associated with mitochondrial disease.

7.7 Future approaches to diagnosing mitochondrial disease patients

When it comes to diagnosing mitochondrial disease in suspected patients, functional evidence was primarily used for clinical diagnosis; this requires invasive surgery to acquire a muscle biopsy. With the introduction of rapid NGS technologies that can extensively sequence the patients' exomes or genomes, a shift to "genetics first" approach was implemented to avoid the necessity of a muscle biopsy in all cases. The identification of novel variants and novel candidate genes was a key outcome of this approach that increased the rate of diagnoses. However, many cases remain undiagnosed such as the with the 8 undiagnosed patients in my study. These cases require further investigations that could lead to a diagnosis.

Worldwide, undiagnosed cases that have been investigated using NGS technologies are being followed up with a "multi-omics" approach that can help search for and identify the cause of disease in patients (Stenton *et al.*, 2020; Thompson *et al.*, 2020b). This includes sequencing RNA (transcriptomics), assessing protein levels (proteomics),

measuring metabolite levels (metabolomics) in patient cells. The source of the assessed cells is a challenge to overcome but this multi-disciplined approach is likely to lead to higher levels of diagnosis in patients primarily sequenced for genomic variants.

The 8 undiagnosed families in my study are difficult to investigate further using the aforementioned approach as biopsies and cell lines are not easily acquired in Kuwait. Further investigations might be implemented with WGS likely being the next stage of investigation prior to any investigations involving patient cells.

7.8 Future work

I plan to continue my work investigating genetic disease patients at KMGC and will advocate for the establishing of a core NGS facility to allow access to genetic analysis techniques with higher diagnostic rates and more rapid results. This includes WES, and possibly WGS, for patients highly suspected of a genetic disease involvement. A robust variant filtration pipeline also needs to be established to assist in the identification of candidate variants among the genotyped variants.

In addition to expanding the genetic analysis methods and techniques at KMGC, I will advocate for the expansion of the tissue culture laboratories to include facilities for functional analysis on patient tissues and cell lines. This includes performing techniques such as western blotting and BN-PAGE and later expanding with further techniques as deemed necessary. This will help validate the pathogenicity of novel variants which are likely to be identified in the highly consanguineous population as demonstrated in my study (12 out of 15 identified mutations were novel).

Should the establishment of an independent tissue culture facility be successful, I plan on establishing a cell line bank of patient fibroblast cell lines (parallel to the DNA bank at KMGC containing DNA samples) for future functional analysis should a diagnosis be reached or should functional analyses help narrow down the scope of candidate genes to investigate or interrogate in the WES results.

The clinical review of patients by specialists at KMGC can be improved by recommending diagnostic criteria to score and assess patient information such as the modified MDC I used in my study. Founder mutations identified in the population and in neighbouring populations should be prioritised when suspecting mitochondrial disease in Kuwait (Alahmad *et al.*, 2019). A database of founder mutations related to various genetic disorders in the population should also be organised with associated clinical presentations

and findings and the database should be routinely expanded as new founder mutations are discovered. This will help connect the clinical, genetic, and functional investigations at KMGC to better serve the local community through rapid and accurate genetic screening.

7.9 Concluding remarks

To summarise, patients from 22 families who were suspected of mitochondrial disease involvement were selected into my study cohort by reviewing patient phenotypes with the help of expertise from a paediatric specialist based in Kuwait, the scoring of referred patients using a developed MDC, and the review of the high scoring patient by a mitochondrial disease specialist based in Newcastle. WES performed on the patient cohort led to a genetic diagnosis in 14 of the families (63.6%) and functional analysis was carried out patient cell lines from 4 of these families to validate pathogenicity and functionally characterise the effect of the novel variants. A large collaboration involving research centres in Saudi Arabia, Italy and Germany led to the functional investigation of patients harbouring pathogenic variants in a novel mitochondrial disease gene (*NDUFC2*) which resulted in the validation of variant pathogenicity and added to the phenotypic diversity of mitochondrial disease. The methods of investigation implemented in my study can be used to expand the provided services at KMGC's diagnostic labs to help better serve patients and their families in Kuwait by providing more rapid genetic diagnoses and functional validation methods.

Appendix

Appendix A - Primers used to Sanger sequence genetic variants identified in patients using WES

Family	Gene	Ref	Exon/ Intron	DNA mutation	Protein residue	Primers	Product size	Annealing temp.	DMSO
1	*LETM1*	NM_012318	Exon 5	c.754_756del	p.252delLys	F- 5'-TGAGAGTCAGTGTGTTGTGAA-3' R- 5'-GGGTAAACTTTCAAGCGCCA-3'	385 bp	62°C	No
2	*SLC19A3*	NM_025243	Exon 3	c.175T>C	p.Trp59Arg	F- 5'-CCGGGGTTTATCTAAGTGTGTAC-3' R- 5'-CACTCCTTGGCCAAACAACA-3'	366 bp	62°C	No
3	*PDHX*	NM_003477	Exon 6	c.742C>T	p.Gln248Ter	F- 5'-ACATCTCACCTGCGTTTTCTG-3' R- 5'-ACTTAGAGAACACTACCACTGCA-3'	271 bp	58°C	Yes
4	*SURF1*	NM_003172	Exon 5	c.367_368delCT	p.Arg123fsTer4	F- 5'-GTTTTCCAGCCAAACCTTGC-3' R- 5'-GCTCCCACATGTCCTACTCA-3'	260 bp	62°C	No
5	*MPC1*	NM_016098	Exon 3	c.109C>T	p.Pro37Ser	F - 5'-GTAGGGACCTTGGGAAGCTG-3' R - 5'-CCTCCCAATTATCCAAATCTGCA-3'	383 bp	62°C	No
6	*LETM1*	NM_012318	Exon 6	c.881G>A	p.Arg294Gln	F - 5'-AGTGGTTTGAGTCCCTGAGG-3' R - 5'-CGATCGTTCAGCATCTTCCA-3'	429 bp	62°C	No
7	*TTC19*	NM_017775	Exon 8	c.779_780del	p.Try260Ter	F - 5'-TGTTCCCTAAGTGACATGTGG-3' R - 5'-TGAGGGTGCTGGTGATAAGAA-3'	407 bp	62°C	No
8	*NDUFA13*	NM_015965	Exon 1	c.22C>T	p.Gln8Ter	F - 5'-CTTCCGCCACACTCATCAT-3' R - 5'-CCCGGCGCAGAGTGATAC-3'	190 bp	62°C	No
9	*NDUFB9*	NM_005005	Exon 2	c.191T>C	p.Leu64Pro	F - 5'-CACTGCCCATCCAGAAGGTA-3' R - 5'-CCTTGAAGGGCAAGTGATTT-3'	390 bp	62°C	No
10	*RRM2B*	NM_015713	Exon 6	c.574G>A	p.Ala192Thr	F - 5'-CATGTGTGGTGCACACGTAA-3' R - 5'- ATGGAAAAGAAAAATAGATGAACATCA-3'	502 bp	62°C	No

Family	Gene	Ref	Exon/ Intron	DNA mutation	Protein residue	Primers	Product size	Annealing temp.	DMSO
11	*RNASEH2C*	NM_032193	Exon 2	c.202C>G	p.Leu68Val	F - 5'-TACCCGCCACACTGCATC-3' R - 5'-AGGGTGAAGCGGCTGAAG-3'	565 bp	58°C	Yes
12	*TREX1*	NM_033629	Exon 2	c.341G>A c.50dupT	p.Arg114His p.Asp18Argfs	F - 5'-CCCCATGCTCCTCTCCAG-3' R - 5'-ACAGAAGGCACCATCCAGAG-3'	500 bp	62°C	No
13	*VPS13B*	NM_015243	Exon 11	c.1512del	p.Glu505Lysfs	F - 5'-GGCAAAATAGTCAATGAAGGTGG-3' R - 5'-TCATACAATGTGTCCACCCAA-'3	357 bp	62°C	No
14	*ATP8A2*	NM_016529	Intron 3	c.321+1G>T	p.? retain intron 3?	F - 5'-CTTGAGGATGATTGCAGTGACT-3' R - 5'-AGCCCAATTTCCTGCCTTAA-3'	474 bp	58°C	No
Ch 6	*NDUFC2*	NM_004549	Exon 3	c.346_*7del	p.His116_Arg119delins21	F - 5'-ACATGAACATTCAGACCACAGC-3' R - 5'-CAAGGTGTCAACATACAGATTAGCA-3'	286 bp	62°C	No

DMSO: dimethylsulphoxide; Ref: Reference Sequence

Appendix B - Antibodies used in immunoblotting Western blot and BN-PAGE membranes

Protein	OXPHOS complex	Company	Catalogue number	Dilution	Predicted size/Observed size (kDa)	Mono/polyclonal	Secondary
NDUFV1	I	Proteintech	11238-1-AP	1:1000	51	Polyclonal	Rabbit
NDUFA9	I	abcam	ab14713	1:1000	35	Monoclonal	Mouse
NDUFB8	I	abcam	ab110242	1:1000	17	Monoclonal	Mouse
NDUFC2	I	abcam	ab192265	1:1000	14	Monoclonal	Rabbit
NDUFAF3	I AF	Sigma	HPA035377	1:1000	12	Polyclonal	Rabbit
NDUFA13	I	abcam	ab110240	1:1000	17	Monoclonal	Mouse
SDHA	II	abcam	ab14715	1:2000	73	Monoclonal	Mouse
UQCRC2 (CORE2)	III	abcam	ab14745	1:1000	48	Monoclonal	Mouse
UQCRFS1	III	abcam	ab14746	1:1000	25	Monoclonal	Mouse
MTCO1 (COX-1)	IV	abcam	ab14705	1:1000	40	Monoclonal	Mouse
MTCO2 (COX-2)	IV	abcam	ab110258	1:1000	21	Monoclonal	Mouse
ATP5A	V	abcam	ab14748	1:2000	53	Monoclonal	Mouse
TTC19	III AF	abcam	ab181191	1:1000	32	Monoclonal	Rabbit

Protein	OXPHOS complex	Company	Catalogue number	Dilution	Predicted size/Observed size (kDa)	Mono/polyclonal	Secondary
OXPHOS panel	I, II, III, IV, V	abcam	ab110411 [Antibody mixture: ab110242 (NDUFB8) ab14714 (SDHB) ab14745 (UQCRC2) ab110258 (MTCO2) ab14748 (ATP5A)]	1:1000	53 ATP5A (V) 48 UQCRC2 (III) 33 SDHB (II) 20 MTCO-2 (IV) 17 NDUFB8 (I)	Collection of monoclonal antibodies	Mouse
MPC1	IMM	Cell Signaling	14462	1:1000	12	Monoclonal	Rabbit
TREX1	Cytosol	Cell Signaling	12215	1:1000	33	Monoclonal	Rabbit
Beta actin	Cytosol	Cloud Clone	CAB340Hu22	1:10,000	42	Monoclonal	Mouse
Mouse secondary	-	DAKO	P0260	1:2000	-	-	-
Rabbit Secondary	-	DAKO	P0399	1:3000	-	-	-

I: complex I subunit; II complex II subunit; III complex III subunit; IMM: inner mitochondrial membrane; IV: complex IV subunit; V complex V subunit; I AF: complex I assembly factor; III AF: complex III assembly factor.

Appendix C - 299 genes amplified in custom gene panel in Italy*

ALKBH1	*COQ9*	*HSD17B10*	*MTCH2*	*NDUFS6*	*RARS2*	*TIMMDC1*
AARS2	*COX10*	*HSPA9*	*MTFMT*	*NDUFS7*	*RCC1L*	*TK2*
ABCB7	*COX14*	*HSPD1*	*MTO1*	*NDUFS8*	*RMND1*	*TMCO6*
ACAD9	*COX15*	*HSPE1*	*MTPAP*	*NDUFV1*	*RNASEH1*	*TMEM126A*
ACN9	*COX20*	*IARS*	*NARS2*	*NDUFV2*	*RPUSD4*	*TMEM126B*
ACO2	*COX4I1*	*IARS2*	*NAXE*	*NDUFV3*	*RRM2B*	*TMEM65*
ADCK3	*COX4I2*	*IBA57*	*NDUFA1*	*NFU1*	*RTN4IP1*	*TMEM70*
AFG3L2	*COX6B1*	*ISCA1*	*NDUFA10*	*NSUN3*	*SARS2*	*TOP2A*
AGK	*DARS*	*ISCA2*	*NDUFA11*	*NUBPL*	*SCO1*	*TOP2B*
AIFM1	*DARS2*	*ISCU*	*NDUFA12*	*OPA1*	*SCO2*	*TPK1*
APEX1	*DGUOK*	*KARS*	*NDUFA13*	*OPA3*	*SDHA*	*TRIAP1*
APOPT1	*DIAPH1*	*LARS2*	*NDUFA2*	*OXA1L*	*SDHAF1*	*TRMU*
APTX	*DLAT*	*LIAS*	*NDUFA3*	*PARS2*	*SDHAF2*	*TRNT1*
ARMCX1	*DLD*	*LIPT1*	*NDUFA4*	*PC*	*SDHB*	*TSFM*
ATAD3A	*DNA2*	*LIPT2*	*NDUFA5*	*PCK2*	*SDHC*	*TTC19*
ATP5A1	*DNAJC19*	*LRPPRC*	*NDUFA6*	*PDHA1*	*SDHD*	*TUFM*
ATP5D	*DNM1L*	*LYRM4*	*NDUFA7*	*PDHA2*	*SERAC1*	*TYMP*
ATP5E	*DPYD*	*LYRM7*	*NDUFA8*	*PDHB*	*SLC19A2*	*UQCRB*
ATP5ML	*E4F1*	*MARS2*	*NDUFA9*	*PDHX*	*SLC19A3*	*UQCRC1*
ATPAF2	*EARS2*	*MCUR1*	*NDUFAB1*	*PDK1*	*SLC25A1*	*UQCRC2*
AUH	*ECHS1*	*MDH2*	*NDUFAF1*	*PDK2*	*SLC25A19*	*UQCRFS1*
BCS1L	*ECSIT*	*MECR*	*NDUFAF2*	*PDK3*	*SLC25A21*	*UQCRQ*
BOLA3	*ELAC2*	*MFF*	*NDUFAF3*	*PDK4*	*SLC25A22*	*USMG5*
C10orf2	*ENDOG*	*MFN1*	*NDUFAF4*	*PDP1*	*SLC25A3*	*VARS2*
c12orf65	*ETFA*	*MFN2*	*NDUFAF5*	*PDP2*	*SLC25A4*	*WARS2*

C1QBP	*ETFB*	*MGME1*	*NDUFAF6*	*PDPR*	*SLC25A42*	*WFS1*
CAD	*ETFDH*	*MICU1*	*NDUFAF7*	*PDSS1*	*SLC25A46*	*YARS2*
CARS2	*ETHE1*	*MMAA*	*NDUFB1*	*PDSS2*	*SLC39A8*	*YBEY*
CHCHD10	*FARS2*	*MPC1*	*NDUFB10*	*PET100*	*SPART*	*YME1L1*
CHCHD4	*FASTKD2*	*MPC2*	*NDUFB11*	*PET117*	*SPATA5*	
CISD2	*FBXL4*	*MPV17*	*NDUFB2*	*PNKD*	*SPG7*	
CLPP	*FDXR*	*MPV17L*	*NDUFB3*	*PNPT1*	*SQSTM1*	
CLUH	*FGF21*	*MPV17L2*	*NDUFB4*	*POLG*	*SSBP1*	
COA5	*FLAD1*	*MRPL12*	*NDUFB5*	*POLG2*	*SUCLA2*	
COA6	*FOXRED1*	*MRPL23*	*NDUFB6*	*POLRMT*	*SUCLG1*	
COA7	*FTSJ2*	*MRPL24*	*NDUFB7*	*PPA2*	*SURF1*	
COASY	*GARS*	*MRPL3*	*NDUFB8*	*PREPL*	*TACO1*	
COQ10A	*GDAP1*	*MRPL44*	*NDUFB9*	*PRPS1*	*TANGO2*	
COQ10B	*GFER*	*MRPL50*	*NDUFC1*	*PRUNE*	*TARS2*	
COQ2	*GFM1*	*MRPS16*	*NDUFC2*	*PTCD1*	*TAZ*	
COQ3	*GLRX5*	*MRPS2*	*NDUFS1*	*PTCD2*	*TFAM*	
COQ4	*GTPBP3*	*MRPS22*	*NDUFS2*	*PTCD3*	*TFG*	
COQ5	*HARS2*	*MRPS34*	*NDUFS3*	*PUS1*	*THG1L*	
COQ6	*HCCS*	*MRPS7*	*NDUFS4*	*QRSL1*	*TIMM50*	
COQ7	*HSCB*	*MSTO1*	*NDUFS5*	*RANBP2*	*TIMM8A*	

*Genes in red have been previously associated with complex I deficiency.

References

Abdul-Rasoul, M., al-Qatan, H., Habeeb, H., al-Adwani, M., al-Bouloshi, M., Habeeb, Y. and Mousa, A. (2002) 'Leigh's disease in 3 sibs of a Kuwaiti family', *Med Princ Pract*, 11(1), pp. 46-9.

Adams, K.L. and Palmer, J.D. (2003) 'Evolution of mitochondrial gene content: gene loss and transfer to the nucleus', *Mol Phylogenet Evol*, 29(3), pp. 380-95.

Adang, L., Gavazzi, F., De Simone, M., Fazzi, E., Galli, J., Koh, J., Kramer-Golinkoff, J., De Giorgis, V., Orcesi, S., Peer, K., Ulrick, N., Woidill, S., Shults, J. and Vanderver, A. (2020) 'Developmental Outcomes of Aicardi Goutières Syndrome', *J Child Neurol*, 35(1), pp. 7-16.

Adzhubei, I.A., Schmidt, S., Peshkin, L., Ramensky, V.E., Gerasimova, A., Bork, P., Kondrashov, A.S. and Sunyaev, S.R. (2010) 'A method and server for predicting damaging missense mutations', *Nat Methods*, 7(4), pp. 248-9.

Agip, A.A., Blaza, J.N., Bridges, H.R., Viscomi, C., Rawson, S., Muench, S.P. and Hirst, J. (2018) 'Cryo-EM structures of complex I from mouse heart mitochondria in two biochemically defined states', *Nat Struct Mol Biol*, 25(7), pp. 548-556.

Agostino, A., Invernizzi, F., Tiveron, C., Fagiolari, G., Prelle, A., Lamantea, E., Giavazzi, A., Battaglia, G., Tatangelo, L., Tiranti, V. and Zeviani, M. (2003) 'Constitutive knockout of Surf1 is associated with high embryonic lethality, mitochondrial disease and cytochrome c oxidase deficiency in mice', *Human Molecular Genetics*, 12(4), pp. 399-413.

Ajioka, R.S., Phillips, J.D. and Kushner, J.P. (2006) 'Biosynthesis of heme in mammals', *Biochim Biophys Acta*, 1763(7), pp. 723-36.

Aken, B.L., Ayling, S., Barrell, D., Clarke, L., Curwen, V., Fairley, S., Fernandez Banet, J., Billis, K., Garcia Giron, C., Hourlier, T., Howe, K., Kahari, A., Kokocinski, F., Martin, F.J., Murphy, D.N., Nag, R., Ruffier, M., Schuster, M., Tang, Y.A., Vogel, J.H., White, S., Zadissa, A., Flicek, P. and Searle, S.M. (2016) 'The Ensembl gene annotation system', *Database (Oxford)*, 2016, p. baw093.

Al Aqeel, A.I., Rashid, M.S., Ruiter, J.P., Ijlst, L. and Wanders, R.J. (2003) 'A novel molecular defect of the carnitine acylcarnitine translocase gene in a Saudi patient', *Clin Genet*, 64(2), pp. 163-5.

Al-Hassnan, Z.N., Al-Dosary, M., Alfadhel, M., Faqeih, E.A., Alsagob, M., Kenana, R., Almass, R., Al-Harazi, O.S., Al-Hindi, H., Malibari, O.I., Almutari, F.B., Tulbah, S., Alhadeq, F., Al-Sheddi, T., Alamro, R., AlAsmari, A., Almuntashri, M., Alshaalan, H., Al-Mohanna, F.A., Colak, D. and Kaya, N. (2015) 'ISCA2 mutation causes infantile neurodegenerative mitochondrial disorder', *J Med Genet*, 52(3), pp. 186-94.

Al-Kandari, Y.Y. and Crews, D.E. (2011) 'The effect of consanguinity on congenital disabilities in the Kuwaiti population', *J Biosoc Sci*, 43(1), pp. 65-73.

Al-Awadi, S.A., Moussa, M.A., Naghuib, K.K., Farag, T.I., Teebi, A.S., El-Khalifa, M. and El-Dossary, L. (1985) 'Consanguinity among the Kuwaiti population', *Clinical Genetics*, 27(5), pp. 483-486.

Alahmad, A., Muhammad, H., Pyle, A., Albash, B., McFarland, R. and Taylor, R. (2019) 'Mitochondrial disorders in the Arab Middle East population: the impact of next generation sequencing on the genetic diagnosis', *Journal of Biochemical and Clinical Genetics*, pp. 54-64.

Alam, T.I., Kanki, T., Muta, T., Ukaji, K., Abe, Y., Nakayama, H., Takio, K., Hamasaki, N. and Kang, D. (2003) 'Human mitochondrial DNA is packaged with TFAM', *Nucleic Acids Research*, 31(6), pp. 1640-1645.

Alazami, A.M., Patel, N., Shamseldin, H.E., Anazi, S., Al-Dosari, M.S., Alzahrani, F., Hijazi, H., Alshammari, M., Aldahmesh, M.A., Salih, M.A., Faqeih, E., Alhashem, A., Bashiri, F.A., Al-Owain, M., Kentab, A.Y., Sogaty, S., Al Tala, S., Temsah, M.H., Tulbah, M., Aljelaify, R.F., Alshahwan, S.A., Seidahmed, M.Z., Alhadid, A.A., Aldhalaan, H., AlQallaf, F., Kurdi, W., Alfadhel, M., Babay, Z., Alsogheer, M., Kaya, N., Al-Hassnan, Z.N., Abdel-Salam, G.M., Al-Sannaa, N., Al Mutairi, F., El Khashab, H.Y., Bohlega, S., Jia, X., Nguyen, H.C., Hammami, R., Adly, N., Mohamed, J.Y., Abdulwahab, F., Ibrahim, N., Naim, E.A., Al-Younes, B., Meyer, B.F., Hashem, M., Shaheen, R., Xiong, Y., Abouelhoda, M., Aldeeri, A.A., Monies, D.M. and Alkuraya, F.S. (2015) 'Accelerating novel candidate gene discovery in neurogenetic disorders via whole-exome sequencing of prescreened multiplex consanguineous families', *Cell Rep*, 10(2), pp. 148-61.

Alcazar-Fabra, M., Navas, P. and Brea-Calvo, G. (2016) 'Coenzyme Q biosynthesis and its role in the respiratory chain structure', *Biochim Biophys Acta*, 1857(8), pp. 1073-1078.

Alconada, A., Kubrich, M., Moczko, M., Honlinger, A. and Pfanner, N. (1995) 'The mitochondrial receptor complex: the small subunit Mom8b/Isp6 supports association of receptors with the general insertion pore and transfer of preproteins', *Mol Cell Biol*, 15(11), pp. 6196-205.

Alfadhel, M. (2017) 'Early Infantile Leigh-like SLC19A3 Gene Defects Have a Poor Prognosis: Report and Review', *Journal of Central Nervous System Disease*, 9, p. 1179573517737521.

Alfadhel, M., Almuntashri, M., Jadah, R.H., Bashiri, F.A., Rifai, M.T.A., Shalaan, H.A., Balwi, M.A., Rumayan, A.A., Eyaid, W. and Al-Twaijri, W. (2013) 'Biotin-responsive basal ganglia disease should be renamed biotin-thiamine-responsive basal ganglia disease: a retrospective review of the clinical, radiological and molecular findings of 18 new cases', *Orphanet Journal of Rare Diseases*, 8(1), p. 83.

Alfadhel, M., Lillquist, Y.P., Waters, P.J., Sinclair, G., Struys, E., McFadden, D., Hendson, G., Hyams, L., Shoffner, J. and Vallance, H.D. (2011) 'Infantile cardioencephalopathy due to a COX15 gene defect: Report and review', *American Journal of Medical Genetics Part A*, 155(4), pp. 840-844.

Alfadhel, M., Nashabat, M., Alrifai, M.T., Alshaalan, H., Mutairi, F.A., Al-Shahrani, S.A., Plecko, B., Almass, R., Alsagob, M., Almutairi, F.B., Al-Rumayyan, A., Al-Twaijri, W., Al-Owain, M., Taylor, R.W. and Kaya, N. (2018) 'Further delineation of the phenotypic spectrum of ISCA2 defect: A report of ten new cases', *European Journal of Paediatric Neurology*, 22(1), pp. 46-55.

Alfadhel, M. and Tabarki, B. (2018) 'SLC19A3 Gene Defects Sorting the Phenotype and Acronyms: Review', *Neuropediatrics*, 49(2), pp. 83-92.

Alfares, A., Alfadhel, M., Wani, T., Alsahli, S., Alluhaydan, I., Al Mutairi, F., Alothaim, A., Albalwi, M., Al Subaie, L., Alturki, S., Al-Twaijri, W., Alrifai, M., Al-Rumayya, A., Alameer, S., Faqeeh, E., Alasmari, A., Alsamman, A., Tashkandia, S., Alghamdi, A., Alhashem, A., Tabarki, B., AlShahwan, S., Hundallah, K., Wali, S., Al-Hebbi, H., Babiker, A., Mohamed, S., Eyaid, W. and Zada, A.A.P. (2017) 'A multicenter clinical exome study in unselected cohorts from a consanguineous population of Saudi Arabia demonstrated a high diagnostic yield', *Mol Genet Metab*, 121(2), pp. 91-95.

Algahtani, H., Ghamdi, S., Shirah, B., Alharbi, B., Algahtani, R. and Bazaid, A. (2017) 'Biotin-thiamine-responsive basal ganglia disease: catastrophic consequences of delay in diagnosis and treatment', *Neurol Res*, 39(2), pp. 117-125.

Alipour, N., Salehpour, S., Tonekaboni, S.H., Rostami, M., Bahari, S., Yassaee, V., Miryounesi, M. and Ghafouri-Fard, S. (2020) 'Mutations in the VPS13B Gene in Iranian Patients with Different Phenotypes of Cohen Syndrome', *J Mol Neurosci*, 70(1), pp. 21-25.

Aljabri, M.F., Kamal, N.M., Arif, M., AlQaedi, A.M. and Santali, E.Y. (2016) 'A case report of biotin-thiamine-responsive basal ganglia disease in a Saudi child: Is extended genetic family study recommended?', *Medicine (Baltimore)*, 95(40), p. e4819.

Alkuraya, F.S. (2010) 'Homozygosity mapping: one more tool in the clinical geneticist's toolbox', *Genet Med*, 12(4), pp. 236-9.

Almannai, M., Alasmari, A., Alqasmi, A., Faqeih, E., Al Mutairi, F., Alotaibi, M., Samman, M.M., Eyaid, W., Aljadhai, Y.I., Shamseldin, H.E., Craigen, W. and Alkuraya, F.S. (2018a) 'Expanding the phenotype of SLC25A42-associated mitochondrial encephalomyopathy', *Clin Genet*, 93(5), pp. 1097-1102.

Almannai, M., Wang, J., Dai, H., El-Hattab, A.W., Faqeih, E.A., Saleh, M.A., Al Asmari, A., Alwadei, A.H., Aljadhai, Y.I., AlHashem, A., Tabarki, B., Lines, M.A., Grange, D.K., Benini, R., Alsaman, A.S., Mahmoud, A., Katsonis, P., Lichtarge, O. and Wong, L.C. (2018b) 'FARS2 deficiency; new cases, review of clinical, biochemical, and molecular spectra, and variants interpretation based on structural, functional, and evolutionary significance', *Mol Genet Metab*, 125(3), pp. 281-291.

Alsmadi, O., Thareja, G., Alkayal, F., Rajagopalan, R., John, S.E., Hebbar, P., Behbehani, K. and Thanaraj, T.A. (2013) 'Genetic substructure of Kuwaiti population reveals migration history', *PLoS One*, 8(9), p. e74913.

Alston, C.L., Compton, A.G., Formosa, L.E., Strecker, V., Olahova, M., Haack, T.B., Smet, J., Stouffs, K., Diakumis, P., Ciara, E., Cassiman, D., Romain, N., Yarham, J.W., He, L., De Paepe, B., Vanlander, A.V., Seneca, S., Feichtinger, R.G., Ploski, R., Rokicki, D., Pronicka, E., Haller, R.G., Van Hove, J.L., Bahlo, M., Mayr, J.A., Van Coster, R., Prokisch, H., Wittig, I., Ryan, M.T., Thorburn, D.R. and Taylor, R.W. (2016a) 'Biallelic Mutations in TMEM126B Cause Severe Complex I Deficiency with a Variable Clinical Phenotype', *Am J Hum Genet*, 99(1), pp. 217-27.

Alston, C.L., Heidler, J., Dibley, M.G., Kremer, L.S., Taylor, L.S., Fratter, C., French, C.E., Glasgow, R.I.C., Feichtinger, R.G., Delon, I., Pagnamenta, A.T., Dolling, H., Lemonde, H., Aiton, N., Bjornstad, A., Henneke, L., Gartner, J., Thiele, H., Tauchmannova, K., Quaghebeur, G., Houstek, J., Sperl, W., Raymond, F.L., Prokisch, H., Mayr, J.A., McFarland, R., Poulton, J., Ryan, M.T., Wittig, I., Henneke, M. and Taylor, R.W. (2018) 'Bi-allelic Mutations in NDUFA6 Establish Its Role in Early-Onset Isolated Mitochondrial Complex I Deficiency', *Am J Hum Genet*, 103(4), pp. 592-601.

Alston, C.L., Howard, C., Olahova, M., Hardy, S.A., He, L., Murray, P.G., O'Sullivan, S., Doherty, G., Shield, J.P., Hargreaves, I.P., Monavari, A.A., Knerr, I., McCarthy, P., Morris, A.A., Thorburn, D.R., Prokisch, H., Clayton, P.E., McFarland, R., Hughes, J., Crushell, E. and Taylor, R.W. (2016b) 'A recurrent mitochondrial p.Trp22Arg NDUFB3 variant causes a distinctive facial appearance, short stature and a mild biochemical and clinical phenotype', *J Med Genet*, 53(9), pp. 634-41.

Alston, C.L., Rocha, M.C., Lax, N.Z., Turnbull, D.M. and Taylor, R.W. (2017) 'The genetics and pathology of mitochondrial disease', *J Pathol*, 241(2), pp. 236-250.

Alston, C.L., Veling, M.T., Heidler, J., Taylor, L.S., Alaimo, J.T., Sung, A.Y., He, L., Hopton, S., Broomfield, A., Pavaine, J., Diaz, J., Leon, E., Wolf, P., McFarland, R., Prokisch, H., Wortmann, S.B., Bonnen, P.E., Wittig, I., Pagliarini, D.J. and Taylor, R.W. (2020) 'Pathogenic Bi-allelic Mutations in NDUFAF8 Cause Leigh Syndrome with an Isolated Complex I Deficiency', *Am J Hum Genet*, 106(1), pp. 92-101.

Amunts, A., Brown, A., Toots, J., Scheres, S.H.W. and Ramakrishnan, V. (2015) 'Ribosome. The structure of the human mitochondrial ribosome', *Science*, 348(6230), pp. 95-98.

Anand, R., Wai, T., Baker, M.J., Kladt, N., Schauss, A.C., Rugarli, E. and Langer, T. (2014) 'The i-AAA protease YME1L and OMA1 cleave OPA1 to balance mitochondrial fusion and fissionOPA1 processing balances mitochondrial dynamics', *The Journal of Cell Biology*, 204(6), pp. 919-929.

Anazi, S., Maddirevula, S., Faqeih, E., Alsedairy, H., Alzahrani, F., Shamseldin, H.E., Patel, N., Hashem, M., Ibrahim, N., Abdulwahab, F., Ewida, N., Alsaif, H.S., Al Sharif, H., Alamoudi, W., Kentab, A., Bashiri, F.A., Alnaser, M., AlWadei, A.H., Alfadhel, M., Eyaid, W., Hashem, A., Al Asmari, A., Saleh, M.M., AlSaman, A., Alhasan, K.A., Alsughayir, M., Al Shammari, M., Mahmoud, A., Al-Hassnan, Z.N., Al-Husain, M., Osama Khalil, R., Abd El Meguid, N., Masri, A., Ali, R., Ben-Omran, T., El Fishway, P., Hashish, A., Ercan Sencicek, A., State, M., Alazami, A.M., Salih, M.A., Altassan, N., Arold, S.T., Abouelhoda, M., Wakil, S.M., Monies, D., Shaheen, R. and Alkuraya, F.S. (2017) 'Clinical genomics expands the morbid genome of intellectual disability and offers a high diagnostic yield', *Mol Psychiatry*, 22(4), pp. 615-624.

Anderson, S., Bankier, A.T., Barrell, B.G., de Bruijn, M.H., Coulson, A.R., Drouin, J., Eperon, I.C., Nierlich, D.P., Roe, B.A., Sanger, F., Schreier, P.H., Smith, A.J., Staden, R. and Young, I.G. (1981) 'Sequence and organization of the human mitochondrial genome', *Nature*, 290(5806), pp. 457-65.

Angebault, C., Charif, M., Guegen, N., Piro-Megy, C., Mousson de Camaret, B., Procaccio, V., Guichet, P.O., Hebrard, M., Manes, G., Leboucq, N., Rivier, F., Hamel, C.P., Lenaers, G. and Roubertie, A. (2015) 'Mutation in NDUFA13/GRIM19 leads to early onset hypotonia, dyskinesia and sensorial deficiencies, and mitochondrial complex I instability', *Hum Mol Genet*, 24(14), pp. 3948-55.

Angell, J.E., Lindner, D.J., Shapiro, P.S., Hofmann, E.R. and Kalvakolanu, D.V. (2000) 'Identification of grim-19, a novel cell death regulatory gene induced by the interferon-beta and retinoic acid combination, using a genetic approch', *Journal of Biological Chemistry*, 275(43), pp. 33416-33426.

Anna, A. and Monika, G. (2018) 'Splicing mutations in human genetic disorders: examples, detection, and confirmation', *J Appl Genet*, 59(3), pp. 253-268.

Antonicka, H., Mattman, A., Carlson, C.G., Glerum, D.M., Hoffbuhr, K.C., Leary, S.C., Kennaway, N.G. and Shoubridge, E.A. (2003) 'Mutations in COX15 produce a defect in the mitochondrial heme biosynthetic pathway, causing early-onset fatal hypertrophic cardiomyopathy', *Am J Hum Genet*, 72(1), pp. 101-14.

Antonicka, H. and Shoubridge, E.A. (2015) 'Mitochondrial RNA Granules Are Centers for Posttranscriptional RNA Processing and Ribosome Biogenesis', *Cell Rep*, 10(6), pp. 920-932.

Antonny, B., Burd, C., Camilli, P.D., Chen, E., Daumke, O., Faelber, K., Ford, M., Frolov, V.A., Frost, A., Hinshaw, J.E., Kirchhausen, T., Kozlov, M.M., Lenz, M., Low, H.H., McMahon, H., Merrifield, C., Pollard, T.D., Robinson, P.J., Roux, A.

and Schmid, S. (2016) 'Membrane fission by dynamin: what we know and what we need to know', *The EMBO Journal*, 35(21), pp. 2270-2284.
Ardissone, A., Granata, T., Legati, A., Diodato, D., Melchionda, L., Lamantea, E., Garavaglia, B., Ghezzi, D. and Moroni, I. (2015) 'JIMD Reports, Volume 22', *JIMD reports*, 22, pp. 115-120.
Asano, K., Suzuki, T., Saito, A., Wei, F.Y., Ikeuchi, Y., Numata, T., Tanaka, R., Yamane, Y., Yamamoto, T., Goto, T., Kishita, Y., Murayama, K., Ohtake, A., Okazaki, Y., Tomizawa, K., Sakaguchi, Y. and Suzuki, T. (2018) 'Metabolic and chemical regulation of tRNA modification associated with taurine deficiency and human disease', *Nucleic Acids Res*, 46(4), pp. 1565-1583.
Ashe, P.C. and Berry, M.D. (2003) 'Apoptotic signaling cascades', *Prog Neuropsychopharmacol Biol Psychiatry*, 27(2), pp. 199-214.
Asin-Cayuela, J. and Gustafsson, C.M. (2007) 'Mitochondrial transcription and its regulation in mammalian cells', *Trends in Biochemical Sciences*, 32(3), pp. 111-117.
Atwal, P.S. (2014) 'Mutations in the Complex III Assembly Factor Tetratricopeptide 19 Gene TTC19 Are a Rare Cause of Leigh Syndrome', *JIMD Rep*, 14(6), pp. 43-5.
Baertling, F., Al-Murshedi, F., Sanchez-Caballero, L., Al-Senaidi, K., Joshi, N.P., Venselaar, H., van den Brand, M.A., Nijtmans, L.G. and Rodenburg, R.J. (2017a) 'Mutation in mitochondrial complex IV subunit COX5A causes pulmonary arterial hypertension, lactic acidemia, and failure to thrive', *Hum Mutat*, 38(6), pp. 692-703.
Baertling, F., Mayatepek, E. and Distelmaier, F. (2013) 'Hypertrichosis in presymptomatic mitochondrial disease', *J Inherit Metab Dis*, 36(6), pp. 1081-2.
Baertling, F., Sanchez-Caballero, L., Timal, S., van den Brand, M.A., Ngu, L.H., Distelmaier, F., Rodenburg, R.J. and Nijtmans, L.G. (2017b) 'Mutations in mitochondrial complex I assembly factor NDUFAF3 cause Leigh syndrome', *Mol Genet Metab*, 120(3), pp. 243-246.
Balsa, E., Marco, R., Perales-Clemente, E., Szklarczyk, R., Calvo, E., Landázuri, Manuel O. and Enríquez, José A. (2012) 'NDUFA4 Is a Subunit of Complex IV of the Mammalian Electron Transport Chain', *Cell Metabolism*, 16(3), pp. 378-386.
Bar-Yaacov, D., Frumkin, I., Yashiro, Y., Chujo, T., Ishigami, Y., Chemla, Y., Blumberg, A., Schlesinger, O., Bieri, P., Greber, B., Ban, N., Zarivach, R., Alfonta, L., Pilpel, Y., Suzuki, T. and Mishmar, D. (2016) 'Mitochondrial 16S rRNA Is Methylated by tRNA Methyltransferase TRMT61B in All Vertebrates', *PLOS Biology*, 14(9), p. e1002557.
Bareth, B., Dennerlein, S., Mick, D.U., Nikolov, M., Urlaub, H. and Rehling, P. (2013) 'The heme a synthase Cox15 associates with cytochrome c oxidase assembly intermediates during Cox1 maturation', *Mol Cell Biol*, 33(20), pp. 4128-37.
Barnerias, C., Saudubray, J.M., Touati, G., De Lonlay, P., Dulac, O., Ponsot, G., Marsac, C., Brivet, M. and Desguerre, I. (2010) 'Pyruvate dehydrogenase complex deficiency: four neurological phenotypes with differing pathogenesis', *Dev Med Child Neurol*, 52(2), pp. e1-9.
Bauerschmitt, H., Mick, D.U., Deckers, M., Vollmer, C., Funes, S., Kehrein, K., Ott, M., Rehling, P. and Herrmann, J.M. (2010) 'Ribosome-binding proteins Mdm38 and Mba1 display overlapping functions for regulation of mitochondrial translation', *Mol Biol Cell*, 21(12), pp. 1937-44.
Behbehani, R., Melhem, M., Alghanim, G., Behbehani, K. and Alsmadi, O. (2014) 'ND4L gene concurrent 10609T>C and 10663T>C mutations are associated with Leber's hereditary optic neuropathy in a large pedigree from Kuwait', *Br J Ophthalmol*, 98(6), pp. 826-31.

Belkadi, A., Bolze, A., Itan, Y., Cobat, A., Vincent, Q.B., Antipenko, A., Shang, L., Boisson, B., Casanova, J.-L. and Abel, L. (2015) 'Whole-genome sequencing is more powerful than whole-exome sequencing for detecting exome variants', *Proceedings of the National Academy of Sciences*, 112(17), pp. 5473-5478.

Ben-Rebeh, I., Hertecant, J.L., Al-Jasmi, F.A., Aburawi, H.E., Al-Yahyaee, S.A., Al-Gazali, L. and Ali, B.R. (2012) 'Identification of mutations underlying 20 inborn errors of metabolism in the United Arab Emirates population', *Genet Test Mol Biomarkers*, 16(5), pp. 366-71.

Bentinger, M., Tekle, M. and Dallner, G. (2010) 'Coenzyme Q--biosynthesis and functions', *Biochem Biophys Res Commun*, 396(1), pp. 74-9.

Berger, I., Hershkovitz, E., Shaag, A., Edvardson, S., Saada, A. and Elpeleg, O. (2008) 'Mitochondrial complex I deficiency caused by a deleterious NDUFA11 mutation', *Ann Neurol*, 63(3), pp. 405-8.

Berry, E.A., Guergova-Kuras, M., Huang, L.S. and Crofts, A.R. (2000) 'Structure and function of cytochrome bc complexes', *Annu Rev Biochem*, 69(1), pp. 1005-75.

Bezawork-Geleta, A., Rohlena, J., Dong, L., Pacak, K. and Neuzil, J. (2017) 'Mitochondrial Complex II: At the Crossroads', *Trends in Biochemical Sciences*, 42(4), pp. 312-325.

Bhargava, K., Templeton, P. and Spremulli, L.L. (2004) 'Expression and characterization of isoform 1 of human mitochondrial elongation factor G', *Protein Expr Purif*, 37(2), pp. 368-76.

Bianciardi, L., Imperatore, V., Fernandez-Vizarra, E., Lopomo, A., Falabella, M., Furini, S., Galluzzi, P., Grosso, S., Zeviani, M., Renieri, A., Mari, F. and Frullanti, E. (2016) 'Exome sequencing coupled with mRNA analysis identifies NDUFAF6 as a Leigh gene', *Molecular Genetics and Metabolism*, 119(3), pp. 214-222.

Boenzi, S. and Diodato, D. (2018) 'Biomarkers for mitochondrial energy metabolism diseases', *Essays Biochem*, 62(3), pp. 443-454.

Bogenhagen, D.F. (2012) 'Mitochondrial DNA nucleoid structure', *Biochim Biophys Acta*, 1819(9-10), pp. 914-20.

Boggan, R.M., Lim, A., Taylor, R.W., McFarland, R. and Pickett, S.J. (2019) 'Resolving complexity in mitochondrial disease: Towards precision medicine', *Mol Genet Metab*, 128(1-2), pp. 19-29.

Bolisetty, S. and Jaimes, E.A. (2013) 'Mitochondria and reactive oxygen species: physiology and pathophysiology', *Int J Mol Sci*, 14(3), pp. 6306-44.

Bolze, A., Byun, M., McDonald, D., Morgan, N.V., Abhyankar, A., Premkumar, L., Puel, A., Bacon, C.M., Rieux-Laucat, F., Pang, K., Britland, A., Abel, L., Cant, A., Maher, E.R., Riedl, S.J., Hambleton, S. and Casanova, J.L. (2010) 'Whole-exome-sequencing-based discovery of human FADD deficiency', *Am J Hum Genet*, 87(6), pp. 873-81.

Borowski, L.S., Dziembowski, A., Hejnowicz, M.S., Stepien, P.P. and Szczesny, R.J. (2013) 'Human mitochondrial RNA decay mediated by PNPase-hSuv3 complex takes place in distinct foci', *Nucleic Acids Res*, 41(2), pp. 1223-40.

Bottani, E., Cerutti, R., Harbour, M.E., Ravaglia, S., Dogan, S.A., Giordano, C., Fearnley, I.M., D'Amati, G., Viscomi, C., Fernandez-Vizarra, E. and Zeviani, M. (2017) 'TTC19 Plays a Husbandry Role on UQCRFS1 Turnover in the Biogenesis of Mitochondrial Respiratory Complex III', *Mol Cell*, 67(1), pp. 96-105 e4.

Bourdon, A., Minai, L., Serre, V., Jais, J.P., Sarzi, E., Aubert, S., Chretien, D., de Lonlay, P., Paquis-Flucklinger, V., Arakawa, H., Nakamura, Y., Munnich, A. and Rotig, A. (2007) 'Mutation of RRM2B, encoding p53-controlled ribonucleotide reductase

(p53R2), causes severe mitochondrial DNA depletion', *Nat Genet*, 39(6), pp. 776-80.

Bourgeron, T., Rustin, P., Chretien, D., Birch-Machin, M., Bourgeois, M., Viegas-Pequignot, E., Munnich, A. and Rotig, A. (1995) 'Mutation of a nuclear succinate dehydrogenase gene results in mitochondrial respiratory chain deficiency', *Nat Genet*, 11(2), pp. 144-9.

Bowmaker, M., Yang, M.Y., Yasukawa, T., Reyes, A., Jacobs, H.T., Huberman, J.A. and Holt, I.J. (2003) 'Mammalian mitochondrial DNA replicates bidirectionally from an initiation zone', *J Biol Chem*, 278(51), pp. 50961-9.

Boycott, K.M., Beaulieu, C.L., Kernohan, K.D., Gebril, O.H., Mhanni, A., Chudley, A.E., Redl, D., Qin, W., Hampson, S., Kury, S., Tetreault, M., Puffenberger, E.G., Scott, J.N., Bezieau, S., Reis, A., Uebe, S., Schumacher, J., Hegele, R.A., McLeod, D.R., Galvez-Peralta, M., Majewski, J., Ramaekers, V.T., Care4Rare Canada, C., Nebert, D.W., Innes, A.M., Parboosingh, J.S. and Abou Jamra, R. (2015) 'Autosomal-Recessive Intellectual Disability with Cerebellar Atrophy Syndrome Caused by Mutation of the Manganese and Zinc Transporter Gene SLC39A8', *Am J Hum Genet*, 97(6), pp. 886-93.

Bricker, D.K., Taylor, E.B., Schell, J.C., Orsak, T., Boutron, A., Chen, Y.C., Cox, J.E., Cardon, C.M., Van Vranken, J.G., Dephoure, N., Redin, C., Boudina, S., Gygi, S.P., Brivet, M., Thummel, C.S. and Rutter, J. (2012) 'A mitochondrial pyruvate carrier required for pyruvate uptake in yeast, Drosophila, and humans', *Science*, 337(6090), pp. 96-100.

Brivet, M., Garcia-Cazorla, A., Lyonnet, S., Dumez, Y., Nassogne, M.C., Slama, A., Boutron, A., Touati, G., Legrand, A. and Saudubray, J.M. (2003) 'Impaired mitochondrial pyruvate importation in a patient and a fetus at risk', *Molecular Genetics and Metabolism*, 78(3), pp. 186-192.

Brown, A., Amunts, A., Bai, X.C., Sugimoto, Y., Edwards, P.C., Murshudov, G., Scheres, S.H.W. and Ramakrishnan, V. (2014) 'Structure of the large ribosomal subunit from human mitochondria', *Science*, 346(6210), pp. 718-722.

Brown, R.M., Head, R.A., Boubriak, II, Leonard, J.V., Thomas, N.H. and Brown, G.K. (2004) 'Mutations in the gene for the E1beta subunit: a novel cause of pyruvate dehydrogenase deficiency', *Hum Genet*, 115(2), pp. 123-7.

Brown, R.M., Head, R.A., Morris, A.A., Raiman, J.A., Walter, J.H., Whitehouse, W.P. and Brown, G.K. (2006) 'Pyruvate dehydrogenase E3 binding protein (protein X) deficiency', *Dev Med Child Neurol*, 48(9), pp. 756-60.

Brzezniak, L.K., Bijata, M., Szczesny, R.J. and Stepien, P.P. (2011) 'Involvement of human ELAC2 gene product in 3' end processing of mitochondrial tRNAs', *RNA Biol*, 8(4), pp. 616-26.

Buermans, H.P. and den Dunnen, J.T. (2014) 'Next generation sequencing technology: Advances and applications', *Biochim Biophys Acta*, 1842(10), pp. 1932-1941.

Bugiani, M., Gyftodimou, Y., Tsimpouka, P., Lamantea, E., Katzaki, E., d'Adamo, P., Nakou, S., Georgoudi, N., Grigoriadou, M., Tsina, E., Kabolis, N., Milani, D., Pandelia, E., Kokotas, H., Gasparini, P., Giannoulia-Karantana, A., Renieri, A., Zeviani, M. and Petersen, M.B. (2008) 'Cohen syndrome resulting from a novel large intragenic COH1 deletion segregating in an isolated Greek island population', *Am J Med Genet A*, 146A(17), pp. 2221-6.

Bugiani, M., Invernizzi, F., Alberio, S., Briem, E., Lamantea, E., Carrara, F., Moroni, I., Farina, L., Spada, M., Donati, M.A., Uziel, G. and Zeviani, M. (2004) 'Clinical and molecular findings in children with complex I deficiency', *Biochim Biophys Acta*, 1659(2-3), pp. 136-47.

Bugiani, M., Tiranti, V., Farina, L., Uziel, G. and Zeviani, M. (2005) 'Novel mutations in COX15 in a long surviving Leigh syndrome patient with cytochrome c oxidase deficiency', *J Med Genet*, 42(5), p. e28.

Burdick, K.J., Cogan, J.D., Rives, L.C., Robertson, A.K., Koziura, M.E., Brokamp, E., Duncan, L., Hannig, V., Pfotenhauer, J., Vanzo, R., Paul, M.S., Bican, A., Morgan, T., Duis, J., Newman, J.H., Hamid, R., Phillips, J.A., 3rd and Undiagnosed Diseases, N. (2020) 'Limitations of exome sequencing in detecting rare and undiagnosed diseases', *Am J Med Genet A*, 182(6), pp. 1400-1406.

Byrnes, J. and Garcia-Diaz, M. (2014) 'Mitochondrial transcription', *Transcription*, 2(1), pp. 32-36.

Cacciagli, P., Haddad, M.R., Mignon-Ravix, C., El-Waly, B., Moncla, A., Missirian, C., Chabrol, B. and Villard, L. (2010) 'Disruption of the ATP8A2 gene in a patient with a t(10;13) de novo balanced translocation and a severe neurological phenotype', *Eur J Hum Genet*, 18(12), pp. 1360-3.

Cai, Y.C., Bullard, J.M., Thompson, N.L. and Spremulli, L.L. (2000) 'Interaction of mammalian mitochondrial elongation factor EF-Tu with guanine nucleotides', *Protein Sci*, 9(9), pp. 1791-800.

Calvo, S., Jain, M., Xie, X., Sheth, S.A., Chang, B., Goldberger, O.A., Spinazzola, A., Zeviani, M., Carr, S.A. and Mootha, V.K. (2006) 'Systematic identification of human mitochondrial disease genes through integrative genomics', *Nature Genetics*, 38(5), pp. 576-582.

Calvo, S.E., Clauser, K.R. and Mootha, V.K. (2016) 'MitoCarta2.0: an updated inventory of mammalian mitochondrial proteins', *Nucleic Acids Res*, 44(D1), pp. D1251-7.

Calvo, S.E., Compton, A.G., Hershman, S.G., Lim, S.C., Lieber, D.S., Tucker, E.J., Laskowski, A., Garone, C., Liu, S., Jaffe, D.B., Christodoulou, J., Fletcher, J.M., Bruno, D.L., Goldblatt, J., Dimauro, S., Thorburn, D.R. and Mootha, V.K. (2012) 'Molecular diagnosis of infantile mitochondrial disease with targeted next-generation sequencing', *Sci Transl Med*, 4(118), p. 118ra10.

Calvo, S.E. and Mootha, V.K. (2010) 'The mitochondrial proteome and human disease', *Annu Rev Genomics Hum Genet*, 11(1), pp. 25-44.

Carr, H.S. and Winge, D.R. (2003) 'Assembly of Cytochrome c Oxidase within the Mitochondrion', *Accounts of Chemical Research*, 36(5), pp. 309-316.

Carroll, J., Fearnley, I.M., Skehel, J.M., Shannon, R.J., Hirst, J. and Walker, J.E. (2006) 'Bovine Complex I Is a Complex of 45 Different Subunits', *Journal of Biological Chemistry*, 281(43), pp. 32724-32727.

Cecchini, G. (2003) 'Function and structure of complex II of the respiratory chain', *Annu Rev Biochem*, 72(1), pp. 77-109.

Central Bureau of Statistics, S.o.K. (2018). Available at: https://www.csb.gov.kw/.

Chaman, R., Gholami Taramsari, M., Khosravi, A., Amiri, M., Holakouie Naieni, K. and Yunesian, M. (2014) 'Consanguinity and neonatal death: a nested case-control study', *J Family Reprod Health*, 8(4), pp. 189-93.

Chen, H., Detmer, S.A., Ewald, A.J., Griffin, E.E., Fraser, S.E. and Chan, D.C. (2003) 'Mitofusins Mfn1 and Mfn2 coordinately regulate mitochondrial fusion and are essential for embryonic development', *J Cell Biol*, 160(2), pp. 189-200.

Chen, J.Y., Joyce, P.B., Wolfe, C.L., Steffen, M.C. and Martin, N.C. (1992) 'Cytoplasmic and mitochondrial tRNA nucleotidyltransferase activities are derived from the same gene in the yeast Saccharomyces cerevisiae', *J Biol Chem*, 267(21), pp. 14879-83.

Chertkova, R.V., Brazhe, N.A., Bryantseva, T.V., Nekrasov, A.N., Dolgikh, D.A., Yusipovich, A.I., Sosnovtseva, O., Maksimov, G.V., Rubin, A.B. and

Kirpichnikov, M.P. (2017) 'New insight into the mechanism of mitochondrial cytochrome c function', *PLOS ONE*, 12(5), p. e0178280.
Chi, C.S. (2015) 'Diagnostic approach in infants and children with mitochondrial diseases', *Pediatr Neonatol*, 56(1), pp. 7-18.
Chihara, T., Luginbuhl, D. and Luo, L. (2007) 'Cytoplasmic and mitochondrial protein translation in axonal and dendritic terminal arborization', *Nat Neurosci*, 10(7), pp. 828-37.
Chinnery, P.F., Thorburn, D.R., Samuels, D.C., White, S.L., Dahl, H.-H.M., Turnbull, D.M., Lightowlers, R.N. and Howell, N. (2000) 'The inheritance of mitochondrial DNA heteroplasmy: random drift, selection or both?', *Trends in Genetics*, 16(11), pp. 500-505.
Choi, M., Scholl, U.I., Ji, W., Liu, T., Tikhonova, I.R., Zumbo, P., Nayir, A., Bakkaloglu, A., Ozen, S., Sanjad, S., Nelson-Williams, C., Farhi, A., Mane, S. and Lifton, R.P. (2009) 'Genetic diagnosis by whole exome capture and massively parallel DNA sequencing', *Proc Natl Acad Sci U S A*, 106(45), pp. 19096-101.
Choi, Y. and Chan, A.P. (2015) 'PROVEAN web server: a tool to predict the functional effect of amino acid substitutions and indels', *Bioinformatics*, 31(16), pp. 2745-7.
Choi, Y., Sims, G.E., Murphy, S., Miller, J.R. and Chan, A.P. (2012) 'Predicting the functional effect of amino acid substitutions and indels', *PLoS One*, 7(10), p. e46688.
Ciesielski, G.L., Oliveira, M.T. and Kaguni, L.S. (2016) 'Chapter Eight Animal Mitochondrial DNA Replication', *The Enzymes*, 39, pp. 255-292.
Cizkova, A., Stranecky, V., Mayr, J.A., Tesarova, M., Havlickova, V., Paul, J., Ivanek, R., Kuss, A.W., Hansikova, H., Kaplanova, V., Vrbacky, M., Hartmannova, H., Noskova, L., Honzik, T., Drahota, Z., Magner, M., Hejzlarova, K., Sperl, W., Zeman, J., Houstek, J. and Kmoch, S. (2008) 'TMEM70 mutations cause isolated ATP synthase deficiency and neonatal mitochondrial encephalocardiomyopathy', *Nat Genet*, 40(11), pp. 1288-90.
Cogliati, S., Calvo, E., Loureiro, M., Guaras, A.M., Nieto-Arellano, R., Garcia-Poyatos, C., Ezkurdia, I., Mercader, N., Vazquez, J. and Enriquez, J.A. (2016) 'Mechanism of super-assembly of respiratory complexes III and IV', *Nature*, 539(7630), pp. 579-582.
Coleman, J.A., Kwok, M.C. and Molday, R.S. (2009) 'Localization, purification, and functional reconstitution of the P4-ATPase Atp8a2, a phosphatidylserine flippase in photoreceptor disc membranes', *J Biol Chem*, 284(47), pp. 32670-9.
Conboy, E., Selcen, D., Brodsky, M., Gavrilova, R. and Ho, M.L. (2018) 'Novel Homozygous Variant in TTC19 Causing Mitochondrial Complex III Deficiency with Recurrent Stroke-Like Episodes: Expanding the Phenotype', *Semin Pediatr Neurol*, 26, pp. 16-20.
Contreras, L., Drago, I., Zampese, E. and Pozzan, T. (2010) 'Mitochondria: the calcium connection', *Biochim Biophys Acta*, 1797(6-7), pp. 607-18.
Crofts, A.R., Rose, S.W., Burton, R.L., Desai, A.V., Kenis, P.J.A. and Dikanov, S.A. (2017) 'The Q-Cycle Mechanism of the bc 1 Complex: A Biologist's Perspective on Atomistic Studies', *The Journal of Physical Chemistry B*, 121(15), pp. 3701-3717.
Crow, Y.J., Chase, D.S., Lowenstein Schmidt, J., Szynkiewicz, M., Forte, G.M., Gornall, H.L., Oojageer, A., Anderson, B., Pizzino, A., Helman, G., Abdel-Hamid, M.S., Abdel-Salam, G.M., Ackroyd, S., Aeby, A., Agosta, G., Albin, C., Allon-Shalev, S., Arellano, M., Ariaudo, G., Aswani, V., Babul-Hirji, R., Baildam, E.M., Bahi-Buisson, N., Bailey, K.M., Barnerias, C., Barth, M., Battini, R., Beresford, M.W.,

Bernard, G., Bianchi, M., Billette de Villemeur, T., Blair, E.M., Bloom, M., Burlina, A.B., Carpanelli, M.L., Carvalho, D.R., Castro-Gago, M., Cavallini, A., Cereda, C., Chandler, K.E., Chitayat, D.A., Collins, A.E., Sierra Corcoles, C., Cordeiro, N.J., Crichiutti, G., Dabydeen, L., Dale, R.C., D'Arrigo, S., De Goede, C.G., De Laet, C., De Waele, L.M., Denzler, I., Desguerre, I., Devriendt, K., Di Rocco, M., Fahey, M.C., Fazzi, E., Ferrie, C.D., Figueiredo, A., Gener, B., Goizet, C., Gowrinathan, N.R., Gowrishankar, K., Hanrahan, D., Isidor, B., Kara, B., Khan, N., King, M.D., Kirk, E.P., Kumar, R., Lagae, L., Landrieu, P., Lauffer, H., Laugel, V., La Piana, R., Lim, M.J., Lin, J.P., Linnankivi, T., Mackay, M.T., Marom, D.R., Marques Lourenco, C., McKee, S.A., Moroni, I., Morton, J.E., Moutard, M.L., Murray, K., Nabbout, R., Nampoothiri, S., Nunez-Enamorado, N., Oades, P.J., Olivieri, I., Ostergaard, J.R., Perez-Duenas, B., Prendiville, J.S., Ramesh, V., Rasmussen, M., Regal, L., Ricci, F., Rio, M., Rodriguez, D., et al. (2015) 'Characterization of human disease phenotypes associated with mutations in TREX1, RNASEH2A, RNASEH2B, RNASEH2C, SAMHD1, ADAR, and IFIH1', *Am J Med Genet A*, 167A(2), pp. 296-312.

Crow, Y.J., Hayward, B.E., Parmar, R., Robins, P., Leitch, A., Ali, M., Black, D.N., Bokhoven, H.v., Brunner, H.G., Hamel, B.C., Corry, P.C., Cowan, F.M., Frints, S.G., Klepper, J., Livingston, J.H., Lynch, S.A., Massey, R.F., Meritet, J.F., Michaud, J.L., Ponsot, G., Voit, T., Lebon, P., Bonthron, D.T., Jackson, A.P., Barnes, D.E. and Lindahl, T. (2006a) 'Mutations in the gene encoding the 3′-5′ DNA exonuclease TREX1 cause Aicardi-Goutières syndrome at the AGS1 locus', *Nature Genetics*, 38(8), pp. 917-920.

Crow, Y.J., Leitch, A., Hayward, B.E., Garner, A., Parmar, R., Griffith, E., Ali, M., Semple, C., Aicardi, J., Babul-Hirji, R., Baumann, C., Baxter, P., Bertini, E., Chandler, K.E., Chitayat, D., Cau, D., Dery, C., Fazzi, E., Goizet, C., King, M.D., Klepper, J., Lacombe, D., Lanzi, G., Lyall, H., Martinez-Frias, M.L., Mathieu, M., McKeown, C., Monier, A., Oade, Y., Quarrell, O.W., Rittey, C.D., Rogers, R.C., Sanchis, A., Stephenson, J.B., Tacke, U., Till, M., Tolmie, J.L., Tomlin, P., Voit, T., Weschke, B., Woods, C.G., Lebon, P., Bonthron, D.T., Ponting, C.P. and Jackson, A.P. (2006b) 'Mutations in genes encoding ribonuclease H2 subunits cause Aicardi-Goutieres syndrome and mimic congenital viral brain infection', *Nat Genet*, 38(8), pp. 910-6.

D'Souza, A.R. and Minczuk, M. (2018) 'Mitochondrial transcription and translation: overview', *Essays Biochem*, 62(3), pp. 309-320.

Dahl, H.H. and Thorburn, D.R. (2001) 'Mitochondrial diseases: beyond the magic circle', *Am J Med Genet*, 106(1), pp. 1-3.

Danhauser, K., Herebian, D., Haack, T.B., Rodenburg, R.J., Strom, T.M., Meitinger, T., Klee, D., Mayatepek, E., Prokisch, H. and Distelmaier, F. (2016) 'Fatal neonatal encephalopathy and lactic acidosis caused by a homozygous loss-of-function variant in COQ9', *Eur J Hum Genet*, 24(3), pp. 450-4.

Davis, R.L., Liang, C., Edema-Hildebrand, F., Riley, C., Needham, M. and Sue, C.M. (2013) 'Fibroblast growth factor 21 is a sensitive biomarker of mitochondrial disease', *Neurology*, 81(21), pp. 1819-1826.

De Silva, D., Fontanesi, F. and Barrientos, A. (2013) 'The DEAD box protein Mrh4 functions in the assembly of the mitochondrial large ribosomal subunit', *Cell Metab*, 18(5), pp. 712-25.

Dell'Agnello, C., Leo, S., Agostino, A., Szabadkai, G., Tiveron, C., Zulian, A., Prelle, A., Roubertoux, P., Rizzuto, R. and Zeviani, M. (2007) 'Increased longevity and

refractoriness to Ca2+-dependent neurodegeneration in Surf1 knockout mice', *Human Molecular Genetics*, 16(4), pp. 431-444.
Dennerlein, S., Rozanska, A., Wydro, M., Chrzanowska-Lightowlers, Zofia M.A. and Lightowlers, Robert N. (2010) 'Human ERAL1 is a mitochondrial RNA chaperone involved in the assembly of the 28S small mitochondrial ribosomal subunit', *Biochemical Journal*, 430(3), pp. 551-558.
Depeint, F., Bruce, W.R., Shangari, N., Mehta, R. and O'Brien, P.J. (2006) 'Mitochondrial function and toxicity: role of the B vitamin family on mitochondrial energy metabolism', *Chem Biol Interact*, 163(1-2), pp. 94-112.
Dietmeier, K., Honlinger, A., Bomer, U., Dekker, P.J., Eckerskorn, C., Lottspeich, F., Kubrich, M. and Pfanner, N. (1997) 'Tom5 functionally links mitochondrial preprotein receptors to the general import pore', *Nature*, 388(6638), pp. 195-200.
DiFrancesco, J.C., Novara, F., Zuffardi, O., Forlino, A., Gioia, R., Cossu, F., Bolognesi, M., Andreoni, S., Saracchi, E., Frigeni, B., Stellato, T., Tolnay, M., Winkler, D.T., Remida, P., Isimbaldi, G. and Ferrarese, C. (2015) 'TREX1 C-terminal frameshift mutations in the systemic variant of retinal vasculopathy with cerebral leukodystrophy', *Neurological Sciences*, 36(2), pp. 323-330.
Diogo, L., Grazina, M., Garcia, P., Rebelo, O., Veiga, M.A., Cuevas, J., Vilarinho, L., de Almeida, I.T. and Oliveira, C.R. (2009) 'Pediatric mitochondrial respiratory chain disorders in the Centro region of Portugal', *Pediatr Neurol*, 40(5), pp. 351-6.
Dixon-Salazar, T.J., Silhavy, J.L., Udpa, N., Schroth, J., Bielas, S., Schaffer, A.E., Olvera, J., Bafna, V., Zaki, M.S., Abdel-Salam, G.H., Mansour, L.A., Selim, L., Abdel-Hadi, S., Marzouki, N., Ben-Omran, T., Al-Saana, N.A., Sonmez, F.M., Celep, F., Azam, M., Hill, K.J., Collazo, A., Fenstermaker, A.G., Novarino, G., Akizu, N., Garimella, K.V., Sougnez, C., Russ, C., Gabriel, S.B. and Gleeson, J.G. (2012) 'Exome Sequencing Can Improve Diagnosis and Alter Patient Management', *Science Translational Medicine*, 4(138), pp. 138ra78-138ra78.
Douzgou, S. and Petersen, M.B. (2011) 'Clinical variability of genetic isolates of Cohen syndrome', *Clin Genet*, 79(6), pp. 501-6.
Douzgou, S., Samples, J.R., Georgoudi, N. and Petersen, M.B. (2011) 'Ophthalmic findings in the Greek isolate of Cohen syndrome', *Am J Med Genet A*, 155A(3), pp. 534-9.
Duchen, M.R. (2000) 'Mitochondria and calcium: from cell signalling to cell death', *J Physiol*, 529 Pt 1(1), pp. 57-68.
Duplomb, L., Duvet, S., Picot, D., Jego, G., Chehadeh-Djebbar, S.E., Marle, N., Gigot, N., Aral, B., Carmignac, V., Thevenon, J., Lopez, E., Rivière, J.-B., Klein, A., Philippe, C., Droin, N., Blair, E., Girodon, F., Donadieu, J., Bellanné-Chantelot, C., Delva, L., Michalski, J.-C., Solary, E., Faivre, L., Foulquier, F. and Thauvin-Robinet, C. (2014) 'Cohen syndrome is associated with major glycosylation defects', *Human Molecular Genetics*, 23(9), pp. 2391-2399.
Dushay, J., Chui, P.C., Gopalakrishnan, G.S., Varela-Rey, M., Crawley, M., Fisher, F.M., Badman, M.K., Martinez-Chantar, M.L. and Maratos-Flier, E. (2010) 'Increased fibroblast growth factor 21 in obesity and nonalcoholic fatty liver disease', *Gastroenterology*, 139(2), pp. 456-63.
Dushay, J.R., Toschi, E., Mitten, E.K., Fisher, F.M., Herman, M.A. and Maratos-Flier, E. (2015) 'Fructose ingestion acutely stimulates circulating FGF21 levels in humans', *Mol Metab*, 4(1), pp. 51-7.
Echevarría, L., Clemente, P., Hernández-Sierra, R., Gallardo, María E., Fernández-Moreno, Miguel A. and Garesse, R. (2014) 'Glutamyl-tRNAGln amidotransferase

is essential for mammalian mitochondrial translation in vivo', *Biochemical Journal*, 460(1), pp. 91-101.
Egger, J., Lake, B.D. and Wilson, J. (1981) 'Mitochondrial cytopathy. A multisystem disorder with ragged red fibres on muscle biopsy', *Arch Dis Child*, 56(10), pp. 741-52.
El Chehadeh-Djebbar, S., Blair, E., Holder-Espinasse, M., Moncla, A., Frances, A.M., Rio, M., Debray, F.G., Rump, P., Masurel-Paulet, A., Gigot, N., Callier, P., Duplomb, L., Aral, B., Huet, F., Thauvin-Robinet, C. and Faivre, L. (2013) 'Changing facial phenotype in Cohen syndrome: towards clues for an earlier diagnosis', *Eur J Hum Genet*, 21(7), pp. 736-42.
Eldomery, M.K., Akdemir, Z.C., Vogtle, F.N., Charng, W.L., Mulica, P., Rosenfeld, J.A., Gambin, T., Gu, S., Burrage, L.C., Al Shamsi, A., Penney, S., Jhangiani, S.N., Zimmerman, H.H., Muzny, D.M., Wang, X., Tang, J., Medikonda, R., Ramachandran, P.V., Wong, L.J., Boerwinkle, E., Gibbs, R.A., Eng, C.M., Lalani, S.R., Hertecant, J., Rodenburg, R.J., Abdul-Rahman, O.A., Yang, Y., Xia, F., Wang, M.C., Lupski, J.R., Meisinger, C. and Sutton, V.R. (2016) 'MIPEP recessive variants cause a syndrome of left ventricular non-compaction, hypotonia, and infantile death', *Genome Med*, 8(1), p. 106.
Ellyard, J.I., Jerjen, R., Martin, J.L., Lee, A.Y.S., Field, M.A., Jiang, S.H., Cappello, J., Naumann, S.K., Andrews, T.D., Scott, H.S., Casarotto, M.G., Goodnow, C.C., Chaitow, J., Pascual, V., Hertzog, P., Alexander, S.I., Cook, M.C. and Vinuesa, C.G. (2014) 'Brief Report: Identification of a Pathogenic Variant in TREX1 in Early-Onset Cerebral Systemic Lupus Erythematosus by Whole-Exome Sequencing', *Arthritis & Rheumatology*, 66(12), pp. 3382-3386.
Elmore, S. (2007) 'Apoptosis: a review of programmed cell death', *Toxicol Pathol*, 35(4), pp. 495-516.
Endele, S., Fuhry, M., Pak, S.-J., Zabel, B.U. and Winterpacht, A. (1999) 'LETM1, A Novel Gene Encoding a Putative EF-Hand Ca2+-Binding Protein, Flanks the Wolf–Hirschhorn Syndrome (WHS) Critical Region and Is Deleted in Most WHS Patients', *Genomics*, 60(2), pp. 218-225.
Endo, H., Hasegawa, K., Narisawa, K., Tada, K., Kagawa, Y. and Ohta, S. (1989) 'Defective gene in lactic acidosis: abnormal pyruvate dehydrogenase E1 alpha-subunit caused by a frame shift', *Am J Hum Genet*, 44(3), pp. 358-64.
Fernandez-Moreira, D., Ugalde, C., Smeets, R., Rodenburg, R.J., Lopez-Laso, E., Ruiz-Falco, M.L., Briones, P., Martin, M.A., Smeitink, J.A. and Arenas, J. (2007) 'X-linked NDUFA1 gene mutations associated with mitochondrial encephalomyopathy', *Ann Neurol*, 61(1), pp. 73-83.
Fernández-Vizarra, E. and Zeviani, M. (2015) 'Nuclear gene mutations as the cause of mitochondrial complex III deficiency', *Frontiers in Genetics*, 6, p. 134.
Ferreira, C.R., Whitehead, M.T. and Leon, E. (2017) 'Biotin-thiamine responsive basal ganglia disease: Identification of a pyruvate peak on brain spectroscopy, novel mutation in SLC19A3, and calculation of prevalence based on allele frequencies from aggregated next-generation sequencing data', *Am J Med Genet A*, 173(6), pp. 1502-1513.
Fischer, A.H., Jacobson, K.A., Rose, J. and Zeller, R. (2008) 'Hematoxylin and eosin staining of tissue and cell sections', *CSH Protoc*, 2008(6), p. pdb prot4986.
Fisher, F.M. and Maratos-Flier, E. (2016) 'Understanding the Physiology of FGF21', *Annu Rev Physiol*, 78(1), pp. 223-41.
Fontanesi, F., Tigano, M., Fu, Y., Sfeir, A. and Barrientos, A. (2020) 'The Human Mitochondrial Genome', pp. 35-70.

Formosa, L.E., Dibley, M.G., Stroud, D.A. and Ryan, M.T. (2018) 'Building a complex complex: Assembly of mitochondrial respiratory chain complex I', *Semin Cell Dev Biol*, 76, pp. 154-162.

Formosa, L.E., Muellner-Wong, L., Reljic, B., Sharpe, A.J., Jackson, T.D., Beilharz, T.H., Stojanovski, D., Lazarou, M., Stroud, D.A. and Ryan, M.T. (2020) 'Dissecting the Roles of Mitochondrial Complex I Intermediate Assembly Complex Factors in the Biogenesis of Complex I', *Cell Rep*, 31(3), p. 107541.

Franco-Iborra, S., Cuadros, T., Parent, A., Romero-Gimenez, J., Vila, M. and Perier, C. (2018) 'Defective mitochondrial protein import contributes to complex I-induced mitochondrial dysfunction and neurodegeneration in Parkinson's disease', *Cell Death Dis*, 9(11), p. 1122.

Frazier, A.E., Thorburn, D.R. and Compton, A.G. (2019) 'Mitochondrial energy generation disorders: genes, mechanisms, and clues to pathology', *J Biol Chem*, 294(14), pp. 5386-5395.

Frazier, A.E., Vincent, A.E., Turnbull, D.M., Thorburn, D.R. and Taylor, R.W. (2020) 'Assessment of mitochondrial respiratory chain enzymes in cells and tissues', *Methods Cell Biol*, 155, pp. 121-156.

Friedman, J.R., Lackner, L.L., West, M., DiBenedetto, J.R., Nunnari, J. and Voeltz, G.K. (2011) 'ER tubules mark sites of mitochondrial division', *Science*, 334(6054), pp. 358-62.

Friedman, J.R. and Nunnari, J. (2014) 'Mitochondrial form and function', *Nature*, 505(7483), pp. 335-43.

Friedrich, T. (2014) 'On the mechanism of respiratory complex I', *J Bioenerg Biomembr*, 46(4), pp. 255-68.

Fuhrmann, D.C., Wittig, I., Drose, S., Schmid, T., Dehne, N. and Brune, B. (2018) 'Degradation of the mitochondrial complex I assembly factor TMEM126B under chronic hypoxia', *Cell Mol Life Sci*, 75(16), pp. 3051-3067.

Fukuhara, N., Tokiguchi, S., Shirakawa, K. and Tsubaki, T. (1980) 'Myoclonus epilepsy associated with ragged-red fibres (mitochondrial abnormalities): disease entity or a syndrome? Light-and electron-microscopic studies of two cases and review of literature', *J Neurol Sci*, 47(1), pp. 117-33.

Fusté, J.M., Wanrooij, S., Jemt, E., Granycome, C.E., Cluett, T.J., Shi, Y., Atanassova, N., Holt, I.J., Gustafsson, C.M. and Falkenberg, M. (2010) 'Mitochondrial RNA Polymerase Is Needed for Activation of the Origin of Light-Strand DNA Replication', *Molecular Cell*, 37(1), pp. 67-78.

Gakh, O., Cavadini, P. and Isaya, G. (2002) 'Mitochondrial processing peptidases', *Biochim Biophys Acta*, 1592(1), pp. 63-77.

Ganapathy, V., Smith, S.B. and Prasad, P.D. (2004) 'SLC19: the folate/thiamine transporter family', *Pflugers Arch*, 447(5), pp. 641-6.

Garrison, E. and Marth, G. (2012) 'Haplotype-based variant detection from short-read sequencing', *1207.3907*.

Genomes Project, C., Auton, A., Brooks, L.D., Durbin, R.M., Garrison, E.P., Kang, H.M., Korbel, J.O., Marchini, J.L., McCarthy, S., McVean, G.A. and Abecasis, G.R. (2015) 'A global reference for human genetic variation', *Nature*, 526(7571), pp. 68-74.

Gerber, S., Ding, M.G., Gerard, X., Zwicker, K., Zanlonghi, X., Rio, M., Serre, V., Hanein, S., Munnich, A., Rotig, A., Bianchi, L., Amati-Bonneau, P., Elpeleg, O., Kaplan, J., Brandt, U. and Rozet, J.M. (2017) 'Compound heterozygosity for severe and hypomorphic NDUFS2 mutations cause non-syndromic LHON-like optic neuropathy', *J Med Genet*, 54(5), pp. 346-356.

Germain, N., Dessein, A.-F., Vienne, J.-C., Dobbelaere, D., Mention, K., Joncquel, M., Dekiouk, S., Laine, W., Kluza, J. and Marchetti, P. (2019) 'First-line Screening of OXPHOS Deficiencies Using Microscale Oxygraphy in Human Skin Fibroblasts: A Preliminary Study', *International Journal of Medical Sciences*, 16(7), pp. 931-938.

Ghezzi, D., Arzuffi, P., Zordan, M., Da Re, C., Lamperti, C., Benna, C., D'Adamo, P., Diodato, D., Costa, R., Mariotti, C., Uziel, G., Smiderle, C. and Zeviani, M. (2011) 'Mutations in TTC19 cause mitochondrial complex III deficiency and neurological impairment in humans and flies', *Nat Genet*, 43(3), pp. 259-63.

Giacomello, M., Pyakurel, A., Glytsou, C. and Scorrano, L. (2020) 'The cell biology of mitochondrial membrane dynamics', *Nat Rev Mol Cell Biol*, 21(4), pp. 204-224.

Giese, H., Ackermann, J., Heide, H., Bleier, L., Drose, S., Wittig, I., Brandt, U. and Koch, I. (2015) 'NOVA: a software to analyze complexome profiling data', *Bioinformatics*, 31(3), pp. 440-1.

Gilissen, C., Hehir-Kwa, J.Y., Thung, D.T., van de Vorst, M., van Bon, B.W., Willemsen, M.H., Kwint, M., Janssen, I.M., Hoischen, A., Schenck, A., Leach, R., Klein, R., Tearle, R., Bo, T., Pfundt, R., Yntema, H.G., de Vries, B.B., Kleefstra, T., Brunner, H.G., Vissers, L.E. and Veltman, J.A. (2014) 'Genome sequencing identifies major causes of severe intellectual disability', *Nature*, 511(7509), pp. 344-7.

Glick, D., Barth, S. and Macleod, K.F. (2010) 'Autophagy: cellular and molecular mechanisms', *J Pathol*, 221(1), pp. 3-12.

Goldstein, J.C., Waterhouse, N.J., Juin, P., Evan, G.I. and Green, D.R. (2000) 'The coordinate release of cytochrome c during apoptosis is rapid, complete and kinetically invariant', *Nature Cell Biology*, 2(3), pp. 156-162.

Gomez-Suaga, P., Paillusson, S. and Miller, C.C.J. (2017) 'ER-mitochondria signaling regulates autophagy', *Autophagy*, 13(7), pp. 1250-1251.

Gonzalez-Quintana, A., Garcia-Consuegra, I., Belanger-Quintana, A., Serrano-Lorenzo, P., Lucia, A., Blazquez, A., Docampo, J., Ugalde, C., Moran, M., Arenas, J. and Martin, M.A. (2020) 'Novel NDUFA13 Mutations Associated with OXPHOS Deficiency and Leigh Syndrome: A Second Family Report', *Genes (Basel)*, 11(8), p. 855.

Gorman, G.S., Chinnery, P.F., DiMauro, S., Hirano, M., Koga, Y., McFarland, R., Suomalainen, A., Thorburn, D.R., Zeviani, M. and Turnbull, D.M. (2016) 'Mitochondrial diseases', *Nat Rev Dis Primers*, 2(1), p. 16080.

Gorman, G.S., Schaefer, A.M., Ng, Y., Gomez, N., Blakely, E.L., Alston, C.L., Feeney, C., Horvath, R., Yu-Wai-Man, P., Chinnery, P.F., Taylor, R.W., Turnbull, D.M. and McFarland, R. (2015) 'Prevalence of nuclear and mitochondrial DNA mutations related to adult mitochondrial disease', *Ann Neurol*, 77(5), pp. 753-9.

Goto, Y.-i., Nonaka, I. and Horai, S. (1990) 'A mutation in the tRNALeu(UUR) gene associated with the MELAS subgroup of mitochondrial encephalomyopathies', *Nature*, 348(6302), pp. 651-653.

Gotz, A., Tyynismaa, H., Euro, L., Ellonen, P., Hyotylainen, T., Ojala, T., Hamalainen, R.H., Tommiska, J., Raivio, T., Oresic, M., Karikoski, R., Tammela, O., Simola, K.O., Paetau, A., Tyni, T. and Suomalainen, A. (2011) 'Exome sequencing identifies mitochondrial alanyl-tRNA synthetase mutations in infantile mitochondrial cardiomyopathy', *Am J Hum Genet*, 88(5), pp. 635-42.

Grady, J.P., Pickett, S.J., Ng, Y.S., Alston, C.L., Blakely, E.L., Hardy, S.A., Feeney, C.L., Bright, A.A., Schaefer, A.M., Gorman, G.S., McNally, R.J., Taylor, R.W., Turnbull, D.M. and McFarland, R. (2018) 'mtDNA heteroplasmy level and copy

number indicate disease burden in m.3243A>G mitochondrial disease', *EMBO Mol Med*, 10(6), p. e8262.
Gray, M.W., Burger, G. and Lang, B.F. (1999) 'Mitochondrial Evolution', *Science*, 283(5407), pp. 1476-1481.
Greber, B.J., Bieri, P., Leibundgut, M., Leitner, A., Aebersold, R., Boehringer, D. and Ban, N. (2015) 'The complete structure of the 55S mammalian mitochondrial ribosome', *Science*, 348(6232), pp. 303-308.
Grosso, R., Fader, C.M. and Colombo, M.I. (2017) 'Autophagy: A necessary event during erythropoiesis', *Blood Reviews*, 31(5), pp. 300-305.
Grünewald, A., Lax, N.Z., Rocha, M.C., Reeve, A.K., Hepplewhite, P.D., Rygiel, K.A., Taylor, R.W. and Turnbull, D.M. (2014) 'Quantitative quadruple-label immunofluorescence of mitochondrial and cytoplasmic proteins in single neurons from human midbrain tissue', *Journal of Neuroscience Methods*, 232, pp. 143-149.
Guerrero-Castillo, S., Baertling, F., Kownatzki, D., Wessels, H.J., Arnold, S., Brandt, U. and Nijtmans, L. (2017) 'The Assembly Pathway of Mitochondrial Respiratory Chain Complex I', *Cell Metabolism*, 25(1), pp. 128-139.
Guo, R., Zong, S., Wu, M., Gu, J. and Yang, M. (2017) 'Architecture of Human Mitochondrial Respiratory Megacomplex I2III2IV2', *Cell*, 170(6), pp. 1247-1257.e12.
Haack, T.B., Danhauser, K., Haberberger, B., Hoser, J., Strecker, V., Boehm, D., Uziel, G., Lamantea, E., Invernizzi, F., Poulton, J., Rolinski, B., Iuso, A., Biskup, S., Schmidt, T., Mewes, H.-W., Wittig, I., Meitinger, T., Zeviani, M. and Prokisch, H. (2010) 'Exome sequencing identifies ACAD9 mutations as a cause of complex I deficiency', *Nature Genetics*, 42(12), pp. 1131-1134.
Haack, T.B., Haberberger, B., Frisch, E.-M., Wieland, T., Iuso, A., Gorza, M., Strecker, V., Graf, E., Mayr, J.A., Herberg, U., Hennermann, J.B., Klopstock, T., Kuhn, K.A., Ahting, U., Sperl, W., Wilichowski, E., Hoffmann, G.F., Tesarova, M., Hansikova, H., Zeman, J., Plecko, B., Zeviani, M., Wittig, I., Strom, T.M., Schuelke, M., Freisinger, P., Meitinger, T. and Prokisch, H. (2012) 'Molecular diagnosis in mitochondrial complex I deficiency using exome sequencing', *Journal of Medical Genetics*, 49(4), p. 277.
Haack, Tobias B., Kopajtich, R., Freisinger, P., Wieland, T., Rorbach, J., Nicholls, Thomas J., Baruffini, E., Walther, A., Danhauser, K., Zimmermann, Franz A., Husain, Ralf A., Schum, J., Mundy, H., Ferrero, I., Strom, Tim M., Meitinger, T., Taylor, Robert W., Minczuk, M., Mayr, Johannes A. and Prokisch, H. (2013) 'ELAC2 Mutations Cause a Mitochondrial RNA Processing Defect Associated with Hypertrophic Cardiomyopathy', *The American Journal of Human Genetics*, 93(2), pp. 211-223.
Haag, S., Sloan, K.E., Ranjan, N., Warda, A.S., Kretschmer, J., Blessing, C., Hübner, B., Seikowski, J., Dennerlein, S., Rehling, P., Rodnina, M.V., Höbartner, C. and Bohnsack, M.T. (2016) 'NSUN3 and ABH1 modify the wobble position of mt-tRNAMet to expand codon recognition in mitochondrial translation', *The EMBO Journal*, 35(19), pp. 2104-2119.
Habibzadeh, P., Inaloo, S., Silawi, M., Dastsooz, H., Fard, M.A.F., Sadeghipour, F., Faghihi, Z., Rezaeian, M., Yavarian, M., Böhm, J. and Faghihi, M.A. (2019) 'A Novel TTC19 Mutation in a Patient With Neurological, Psychological, and Gastrointestinal Impairment', *Frontiers in Neurology*, 10, p. 944.
Hagström, E., Held, C., Stewart, R.A.H., Aylward, P.E., Budaj, A., Cannon, C.P., Koenig, W., Krug-Gourley, S., Mohler, E.R., Steg, P.G., Tarka, E., Östlund, O., White, H.D., Siegbahn, A., Wallentin, L. and Investigators, S. (2017) 'Growth

Differentiation Factor 15 Predicts All-Cause Morbidity and Mortality in Stable Coronary Heart Disease', *Clinical Chemistry*, 63(1), pp. 325-333.
Hammans, S.R., Sweeney, M.G., Brockington, M., Morgan-Hughes, J.A. and Harding, A.E. (1991) 'Mitochondrial encephalopathies: molecular genetic diagnosis from blood samples', *The Lancet*, 337(8753), pp. 1311-1313.
Hamza, I. and Dailey, H.A. (2012) 'One ring to rule them all: Trafficking of heme and heme synthesis intermediates in the metazoans', *Biochimica et Biophysica Acta (BBA) - Molecular Cell Research*, 1823(9), pp. 1617-1632.
Han, H. (2018) 'Disease Gene Identification, Methods and Protocols', *Methods in molecular biology (Clifton, N.J.)*, 1706, pp. 293-302.
Hannappel, A., Bundschuh, F.A. and Ludwig, B. (2012) 'Role of Surf1 in heme recruitment for bacterial COX biogenesis', *Biochimica et Biophysica Acta (BBA) - Bioenergetics*, 1817(6), pp. 928-937.
Hart, L., Rauch, A., Carr, A.M., Vermeesch, J.R. and O'Driscoll, M. (2014) 'LETM1 haploinsufficiency causes mitochondrial defects in cells from humans with Wolf-Hirschhorn syndrome: implications for dissecting the underlying pathomechanisms in this condition', *Disease Models & Mechanisms*, 7(5), pp. 535-545.
Hartmann, B., Wai, T., Hu, H., MacVicar, T., Musante, L., Fischer-Zirnsak, B., Stenzel, W., Gräf, R., Heuvel, L.v.d., Ropers, H.-H., Wienker, T.F., Hübner, C., Langer, T. and Kaindl, A.M. (2016) 'Homozygous YME1L1 mutation causes mitochondriopathy with optic atrophy and mitochondrial network fragmentation', *eLife*, 5, p. e16078.
Hazkani-Covo, E., Sorek, R. and Graur, D. (2003) 'Evolutionary Dynamics of Large Numts in the Human Genome: Rarity of Independent Insertions and Abundance of Post-Insertion Duplications', *Journal of Molecular Evolution*, 56(2), pp. 169-174.
Heberle, L.C., Tawari, A.A.A., Ramadan, D.G. and Ibrahim, J.K. (2006) 'Ethylmalonic encephalopathy—report of two cases', *Brain and Development*, 28(5), pp. 329-331.
Heide, H., Bleier, L., Steger, M., Ackermann, J., Dröse, S., Schwamb, B., Zörnig, M., Reichert, Andreas S., Koch, I., Wittig, I. and Brandt, U. (2012) 'Complexome Profiling Identifies TMEM126B as a Component of the Mitochondrial Complex I Assembly Complex', *Cell Metabolism*, 16(4), pp. 538-549.
Hillen, H.S., Temiakov, D. and Cramer, P. (2018) 'Structural basis of mitochondrial transcription', *Nature Structural & Molecular Biology*, 25(9), pp. 754-765.
Hirschhorn, K., Cooper, H.L. and Firschein, I.L. (1965) 'Deletion of short arms of chromosome 4–5 in a child with defects of midline fusion', *Humangenetik*, 1(5), pp. 479-482.
Hoefs, S.J.G., Spronsen, F.J.v., Lenssen, E.W.H., Nijtmans, L.G., Rodenburg, R.J., Smeitink, J.A.M. and Heuvel, L.P.v.d. (2011) 'NDUFA10 mutations cause complex I deficiency in a patient with Leigh disease', *European Journal of Human Genetics*, 19(3), pp. 270-274.
Höhr, A.I.C., Straub, S.P., Warscheid, B., Becker, T. and Wiedemann, N. (2015) 'Assembly of β-barrel proteins in the mitochondrial outer membrane', *Biochimica et Biophysica Acta (BBA) - Molecular Cell Research*, 1853(1), pp. 74-88.
Holt, I.J., Harding, A.E. and Morgan-Hughes, J.A. (1988) 'Deletions of muscle mitochondrial DNA in patients with mitochondrial myopathies', *Nature*, 331(6158), pp. 717-719.
Holt, I.J., Harding, A.E., Petty, R.K. and Morgan-Hughes, J.A. (1990) 'A new mitochondrial disease associated with mitochondrial DNA heteroplasmy', *American journal of human genetics*, 46(3), pp. 428-33.

Holt, I.J., Lorimer, H.E. and Jacobs, H.T. (2000) 'Coupled Leading- and Lagging-Strand Synthesis of Mammalian Mitochondrial DNA', *Cell*, 100(5), pp. 515-524.
Holt, I.J. and Reyes, A. (2012) 'Human Mitochondrial DNA Replication', *Cold Spring Harbor Perspectives in Biology*, 4(12), p. a012971.
Höss, M., Robins, P., Naven, T.J.P., Pappin, D.J.C., Sgouros, J. and Lindahl, T. (1999) 'A human DNA editing enzyme homologous to the Escherichia coli DnaQ/MutD protein', *The EMBO Journal*, 18(13), pp. 3868-3875.
Houten, S.M., Violante, S., Ventura, F.V. and Wanders, R.J.A. (2016) 'The Biochemistry and Physiology of Mitochondrial Fatty Acid β-Oxidation and Its Genetic Disorders', *Annual Review of Physiology*, 78(1), pp. 1-22.
Hutchison, C.A., Newbold, J.E., Potter, S.S. and Edgell, M.H. (1974) 'Maternal inheritance of mammalian mitochondrial DNA', *Nature*, 251(5475), pp. 536-538.
Iborra, F.J., Kimura, H. and Cook, P.R. (2004) 'The functional organization of mitochondrial genomes in human cells', *BMC Biology*, 2(1), p. 9.
Invernizzi, F., D'Amato, I., Jensen, P.B., Ravaglia, S., Zeviani, M. and Tiranti, V. (2012) 'Microscale oxygraphy reveals OXPHOS impairment in MRC mutant cells', *Mitochondrion*, 12(2), pp. 328-335.
Ishiyama, A., Muramatsu, K., Uchino, S., Sakai, C., Matsushima, Y., Makioka, N., Ogata, T., Suzuki, E., Komaki, H., Sasaki, M., Mimaki, M., Goto, Y.I. and Nishino, I. (2018) 'NDUFAF3 variants that disrupt mitochondrial complex I assembly may associate with cavitating leukoencephalopathy', *Clinical Genetics*, 93(5), pp. 1103-1106.
Ismail, E.A., Seoudi, T.M., Morsi, E.A. and Ahmad, A.H. (2009) 'Ethylmalonic encephalopathy. Another patient from Kuwait', *Neurosciences (Riyadh, Saudi Arabia)*, 14(1), pp. 78-80.
Ivanov, I.S., Azmanov, D.N., Ivanova, M.B., Chamova, T., Pacheva, I.H., Panova, M.V., Song, S., Morar, B., Yordanova, R.V., Galabova, F.K., Sotkova, I.G., Linev, A.J., Bitchev, S., Shearwood, A.-M.J., Kancheva, D., Gabrikova, D., Karcagi, V., Guergueltcheva, V., Geneva, I.E., Bozhinova, V., Stoyanova, V.K., Kremensky, I., Jordanova, A., Savov, A., Horvath, R., Brown, M.A., Tournev, I., Filipovska, A. and Kalaydjieva, L. (2014) 'Founder p.Arg 446* mutation in the PDHX gene explains over half of cases with congenital lactic acidosis in Roma children', *Molecular Genetics and Metabolism*, 113(1-2), pp. 76-83.
Janer, A., Karnebeek, C.D.M.v., Sasarman, F., Antonicka, H., Ghamdi, M.A., Shyr, C., Dunbar, M., Stockler-Ispiroglu, S., Ross, C.J., Vallance, H., Dionne, J., Wasserman, W.W. and Shoubridge, E.A. (2015) 'RMND1 deficiency associated with neonatal lactic acidosis, infantile onset renal failure, deafness, and multiorgan involvement', *European Journal of Human Genetics*, 23(10), pp. 1301-1307.
Janer, A., Prudent, J., Paupe, V., Fahiminiya, S., Majewski, J., Sgarioto, N., Rosiers, C.D., Forest, A., Lin, Z.Y., Gingras, A.C., Mitchell, G., McBride, H.M. and Shoubridge, E.A. (2016) 'SLC25A46 is required for mitochondrial lipid homeostasis and cristae maintenance and is responsible for Leigh syndrome', *EMBO Molecular Medicine*, 8(9), pp. 1019-1038.
JeŠIna, P., TesaŘOvÁ, M., FornŮSkovÁ, D., VojtÍŠKovÁ, A., Pecina, P., KaplanovÁ, V., HansÍKovÁ, H., Zeman, J. and HouŠTĚK, J. (2004) 'Diminished synthesis of subunit a (ATP6) and altered function of ATP synthase and cytochrome c oxidase due to the mtDNA 2 bp microdeletion of TA at positions 9205 and 9206', *Biochemical Journal*, 383(3), pp. 561-571.

Jiang, Y., Li, Z., Liu, Z., Chen, D., Wu, W., Du, Y., Ji, L., Jin, Z.-B., Li, W. and Wu, J. (2017) 'mirDNMR: a gene-centered database of background de novo mutation rates in human', *Nucleic Acids Research*, 45(D1), pp. D796-D803.

Jobling, R.K., Assoum, M., Gakh, O., Blaser, S., Raiman, J.A., Mignot, C., Roze, E., Dürr, A., Brice, A., Lévy, N., Prasad, C., Paton, T., Paterson, A.D., Roslin, N.M., Marshall, C.R., Desvignes, J.-P., Roëckel-Trevisiol, N., Scherer, S.W., Rouleau, G.A., Mégarbané, A., Isaya, G., Delague, V. and Yoon, G. (2015) 'PMPCA mutations cause abnormal mitochondrial protein processing in patients with non-progressive cerebellar ataxia', *Brain*, 138(6), pp. 1505-1517.

Jonckheere, A.I., Smeitink, J.A.M. and Rodenburg, R.J.T. (2012) 'Mitochondrial ATP synthase: architecture, function and pathology', *Journal of Inherited Metabolic Disease*, 35(2), pp. 211-225.

Joost, K., Rodenburg, R.J., Piirsoo, A., Heuvel, L.v.d., Žordania, R., Põder, H., Talvik, I., Kilk, K., Soomets, U. and Õunap, K. (2012) 'A Diagnostic Algorithm for Mitochondrial Disorders in Estonian Children', *Molecular Syndromology*, 3(3), pp. 113-119.

Jourdain, A.A., Boehm, E., Maundrell, K. and Martinou, J.-C. (2016) 'Mitochondrial RNA granules: Compartmentalizing mitochondrial gene expressionRNA granules confine mitochondrial gene expression', *The Journal of Cell Biology*, 212(6), pp. 611-614.

Kadenbach, B. and Hüttemann, M. (2015) 'The subunit composition and function of mammalian cytochrome c oxidase', *Mitochondrion*, 24, pp. 64-76.

Kang, Y., Fielden, L.F. and Stojanovski, D. (2018) 'Mitochondrial protein transport in health and disease', *Seminars in Cell & Developmental Biology*, 76, pp. 142-153.

Kasamatsu, H. and Vinograd, J. (1974) 'Replication of Circular DNA in Eukaryotic Cells', *Annual Review of Biochemistry*, 43(1), pp. 695-719.

Kaushik, P., Mahajan, N., Girimaji, S.C. and Kumar, A. (2020) 'Whole Exome Sequencing Identifies a Novel Homozygous Duplication Mutation in the VPS13B Gene in an Indian Family with Cohen Syndrome', *Journal of Molecular Neuroscience*, 70(8), pp. 1225-1228.

Kearns, T.P. (1965) 'External Ophthalmoplegia, Pigmentary Degeneration of the Retina, and Cardiomyopathy: A Newly Recognized Syndrome', *Transactions of the American Ophthalmological Society*, 63, pp. 559-625.

Kearns, T.P. and Sayre, G.P. (1958) 'Retinitis Pigmentosa, External Ophthalmoplegia, and Complete Heart Block: Unusual Syndrome with Histologic Study in One of Two Cases', *A.M.A. Archives of Ophthalmology*, 60(2), pp. 280-289.

Kent, W.J., Sugnet, C.W., Furey, T.S., Roskin, K.M., Pringle, T.H., Zahler, A.M., Haussler and David (2002) 'The Human Genome Browser at UCSC', *Genome Research*, 12(6), pp. 996-1006.

Keshavan, N., Abdenur, J., Anderson, G., Assouline, Z., Barcia, G., Bouhikbar, L., Chakrapani, A., Cleary, M., Cohen, M.C., Feillet, F., Fratter, C., Hauser, N., Jacques, T., Lam, A., McCullagh, H., Phadke, R., Rötig, A., Sharrard, M., Simon, M., Smith, C., Sommerville, E.W., Taylor, R.W., Yue, W.W. and Rahman, S. (2020) 'The natural history of infantile mitochondrial DNA depletion syndrome due to RRM2B deficiency', *Genetics in Medicine*, 22(1), pp. 199-209.

Kilbride, S.M. and Prehn, J.H.M. (2013) 'Central roles of apoptotic proteins in mitochondrial function', *Oncogene*, 32(22), pp. 2703-2711.

Kim, H.-J. and Barrientos, A. (2018) 'MTG1 couples mitoribosome large subunit assembly with intersubunit bridge formation', *Nucleic Acids Research*, 46(16), pp. gky672-.

Kircher, M., Witten, D.M., Jain, P., O'Roak, B.J., Cooper, G.M. and Shendure, J. (2014) 'A general framework for estimating the relative pathogenicity of human genetic variants', *Nature Genetics*, 46(3), pp. 310-315.

Kivitie-Kallio, S. and Norio, R. (2001) 'Cohen Syndrome: Essential features, natural history, and heterogeneity', *American Journal of Medical Genetics*, 102(2), pp. 125-135.

Kleist-Retzow, J.-C.V.O.N., Yao, J., Taanman, J.-W., Chantrel, K., Chretien, D., Cormier-Daire, V., RÖTig, A., Munnich, A., Rustin, P. and Shoubridge, E.A. (2001) 'Mutations in SURF1 are not specifically associated with Leigh syndrome', *Journal of Medical Genetics*, 38(2), p. 109.

Koboldt, D.C., Zhang, Q., Larson, D.E., Shen, D., McLellan, M.D., Lin, L., Miller, C.A., Mardis, E.R., Ding, L. and Wilson, R.K. (2012) 'VarScan 2: Somatic mutation and copy number alteration discovery in cancer by exome sequencing', *Genome Research*, 22(3), pp. 568-576.

Koc, E.C. and Spremulli, L.L. (2002) 'Identification of Mammalian Mitochondrial Translational Initiation Factor 3 and Examination of Its Role in Initiation Complex Formation with Natural mRNAs', *Journal of Biological Chemistry*, 277(38), pp. 35541-35549.

Koch, J., Freisinger, P., Feichtinger, R.G., Zimmermann, F.A., Rauscher, C., Wagentristl, H.P., Konstantopoulou, V., Seidl, R., Haack, T.B., Prokisch, H., Ahting, U., Sperl, W., Mayr, J.A. and Maier, E.M. (2015) 'Mutations in TTC19: expanding the molecular, clinical and biochemical phenotype', *Orphanet Journal of Rare Diseases*, 10(1), p. 40.

Koene, S., Hendriks, J.C.M., Dirks, I., Boer, L., Vries, M.C., Janssen, M.C.H., Smuts, I., Fung, C.W., Wong, V.C.N., Coo, I.R.F.M., Vill, K., Stendel, C., Klopstock, T., Falk, M.J., McCormick, E.M., McFarland, R., Groot, I.J.M. and Smeitink, J.A.M. (2016) 'International Paediatric Mitochondrial Disease Scale', *Journal of Inherited Metabolic Disease*, 39(5), pp. 705-712.

Kolehmainen, J., Black, G.C.M., Saarinen, A., Chandler, K., Clayton-Smith, J., Träskelin, A.-L., Perveen, R., Kivitie-Kallio, S., Norio, R., Warburg, M., Fryns, J.-P., Chapelle, A.d.l. and Lehesjoki, A.-E. (2003) 'Cohen Syndrome Is Caused by Mutations in a Novel Gene, COH1, Encoding a Transmembrane Protein with a Presumed Role in Vesicle-Mediated Sorting and Intracellular Protein Transport', *The American Journal of Human Genetics*, 72(6), pp. 1359-1369.

Kolesnikov, A.A. (2016) 'The mitochondrial genome. The nucleoid', *Biochemistry (Moscow)*, 81(10), pp. 1057-1065.

Koressaar, T. and Remm, M. (2007) 'Enhancements and modifications of primer design program Primer3', *Bioinformatics*, 23(10), pp. 1289-1291.

Kropach, N., Shkalim-Zemer, V., Orenstein, N., Scheuerman, O. and Straussberg, R. (2017) 'Novel RRM2B Mutation and Severe Mitochondrial DNA Depletion: Report of 2 Cases and Review of the Literature', *Neuropediatrics*, 48(06), pp. 456-462.

Kruse, B., Narasimhan, N. and Attardi, G. (1989) 'Termination of transcription in human mitochondria: Identification and purification of a DNA binding protein factor that promotes termination', *Cell*, 58(2), pp. 391-397.

Kumar, P., Henikoff, S. and Ng, P.C. (2009) 'Predicting the effects of coding non-synonymous variants on protein function using the SIFT algorithm', *Nature Protocols*, 4(7), pp. 1073-1081.

Kunii, M., Doi, H., Higashiyama, Y., Kugimoto, C., Ueda, N., Hirata, J., Tomita-Katsumoto, A., Kashikura-Kojima, M., Kubota, S., Taniguchi, M., Murayama, K., Nakashima, M., Tsurusaki, Y., Miyake, N., Saitsu, H., Matsumoto, N. and Tanaka,

F. (2015) 'A Japanese case of cerebellar ataxia, spastic paraparesis and deep sensory impairment associated with a novel homozygous TTC19 mutation', *Journal of Human Genetics*, 60(4), pp. 187-191.

Lake, N.J., Bird, M.J., Isohanni, P. and Paetau, A. (2015) 'Leigh SyndromeNeuropathology and Pathogenesis', *Journal of Neuropathology & Experimental Neurology*, 74(6), pp. 482-492.

Lake, N.J., Compton, A.G., Rahman, S. and Thorburn, D.R. (2016) 'Leigh syndrome: One disorder, more than 75 monogenic causes', *Annals of Neurology*, 79(2), pp. 190-203.

Lake, N.J., Formosa, L.E., Stroud, D.A., Ryan, M.T., Calvo, S.E., Mootha, V.K., Morar, B., Procopis, P.G., Christodoulou, J., Compton, A.G. and Thorburn, D.R. (2019) 'A patient with homozygous nonsense variants in two Leigh syndrome disease genes: Distinguishing a dual diagnosis from a hypomorphic protein-truncating variant', *Human Mutation*, 40(7), pp. 893-898.

Lake, N.J., Webb, B.D., Stroud, D.A., Richman, T.R., Ruzzenente, B., Compton, A.G., Mountford, H.S., Pulman, J., Zangarelli, C., Rio, M., Boddaert, N., Assouline, Z., Sherpa, M.D., Schadt, E.E., Houten, S.M., Byrnes, J., McCormick, E.M., Zolkipli-Cunningham, Z., Haude, K., Zhang, Z., Retterer, K., Bai, R., Calvo, S.E., Mootha, V.K., Christodoulou, J., Rötig, A., Filipovska, A., Cristian, I., Falk, M.J., Metodiev, M.D. and Thorburn, D.R. (2017) 'Biallelic Mutations in MRPS34 Lead to Instability of the Small Mitoribosomal Subunit and Leigh Syndrome', *The American Journal of Human Genetics*, 101(2), pp. 239-254.

Lane, N. and Martin, W. (2010) 'The energetics of genome complexity', *Nature*, 467(7318), pp. 929-934.

Law, E.C., Wilman, H.R., Kelm, S., Shi, J. and Deane, C.M. (2016) 'Examining the Conservation of Kinks in Alpha Helices', *PLOS ONE*, 11(6), p. e0157553.

Leber, T. (1871) 'Ueber hereditäre und congenital-angelegte Sehnervenleiden', *Albrecht von Graefes Archiv für Ophthalmologie*, 17(2), pp. 249-291.

Lebigot, E., Gaignard, P., Dorboz, I., Slama, A., Rio, M., Lonlay, P.d., Héron, B., Sabourdy, F., Boespflug-Tanguy, O., Cardoso, A., Habarou, F., Ottolenghi, C., Thérond, P., Bouton, C., Golinelli-Cohen, M.P. and Boutron, A. (2017) 'Impact of mutations within the [Fe-S] cluster or the lipoic acid biosynthesis pathways on mitochondrial protein expression profiles in fibroblasts from patients', *Molecular Genetics and Metabolism*, 122(3), pp. 85-94.

Lee, H. and Yoon, Y. (2016) 'Mitochondrial fission and fusion', *Biochemical Society Transactions*, 44(6), pp. 1725-1735.

Lee, K.-W., Okot-Kotber, C., LaComb, J.F. and Bogenhagen, D.F. (2013) 'Mitochondrial Ribosomal RNA (rRNA) Methyltransferase Family Members Are Positioned to Modify Nascent rRNA in Foci near the Mitochondrial DNA Nucleoid', *Journal of Biological Chemistry*, 288(43), pp. 31386-31399.

Lee, S.-Y., Kang, M.-G., Shin, S., Kwak, C., Kwon, T., Seo, J.K., Kim, J.-S. and Rhee, H.-W. (2017) 'Architecture Mapping of the Inner Mitochondrial Membrane Proteome by Chemical Tools in Live Cells', *Journal of the American Chemical Society*, 139(10), pp. 3651-3662.

Lee-Kirsch, M.A., Gong, M., Chowdhury, D., Senenko, L., Engel, K., Lee, Y.-A., Silva, U.d., Bailey, S.L., Witte, T., Vyse, T.J., Kere, J., Pfeiffer, C., Harvey, S., Wong, A., Koskenmies, S., Hummel, O., Rohde, K., Schmidt, R.E., Dominiczak, A.F., Gahr, M., Hollis, T., Perrino, F.W., Lieberman, J. and Hübner, N. (2007) 'Mutations in the gene encoding the 3′-5′ DNA exonuclease TREX1 are associated with systemic lupus erythematosus', *Nature Genetics*, 39(9), pp. 1065-1067.

Legati, A., Reyes, A., Nasca, A., Invernizzi, F., Lamantea, E., Tiranti, V., Garavaglia, B., Lamperti, C., Ardissone, A., Moroni, I., Robinson, A., Ghezzi, D. and Zeviani, M. (2016) 'New genes and pathomechanisms in mitochondrial disorders unraveled by NGS technologies', *Biochimica et Biophysica Acta (BBA) - Bioenergetics*, 1857(8), pp. 1326-1335.

Lehtonen, J.M., Forsström, S., Bottani, E., Viscomi, C., Baris, O.R., Isoniemi, H., Höckerstedt, K., Österlund, P., Hurme, M., Jylhävä, J., Leppä, S., Markkula, R., Heliö, T., Mombelli, G., Uusimaa, J., Laaksonen, R., Laaksovirta, H., Auranen, M., Zeviani, M., Smeitink, J., Wiesner, R.J., Nakada, K., Isohanni, P. and Suomalainen, A. (2016) 'FGF21 is a biomarker for mitochondrial translation and mtDNA maintenance disorders', *Neurology*, 87(22), pp. 2290-2299.

Leigh, D. (1951) 'SUBACUTE NECROTIZING ENCEPHALOMYELOPATHY IN AN INFANT', *Journal of Neurology, Neurosurgery & Psychiatry*, 14(3), p. 216.

Lek, M., Karczewski, K.J., Minikel, E.V., Samocha, K.E., Banks, E., Fennell, T., O'Donnell-Luria, A.H., Ware, J.S., Hill, A.J., Cummings, B.B., Tukiainen, T., Birnbaum, D.P., Kosmicki, J.A., Duncan, L.E., Estrada, K., Zhao, F., Zou, J., Pierce-Hoffman, E., Berghout, J., Cooper, D.N., Deflaux, N., DePristo, M., Do, R., Flannick, J., Fromer, M., Gauthier, L., Goldstein, J., Gupta, N., Howrigan, D., Kiezun, A., Kurki, M.I., Moonshine, A.L., Natarajan, P., Orozco, L., Peloso, G.M., Poplin, R., Rivas, M.A., Ruano-Rubio, V., Rose, S.A., Ruderfer, D.M., Shakir, K., Stenson, P.D., Stevens, C., Thomas, B.P., Tiao, G., Tusie-Luna, M.T., Weisburd, B., Won, H.-H., Yu, D., Altshuler, D.M., Ardissino, D., Boehnke, M., Danesh, J., Donnelly, S., Elosua, R., Florez, J.C., Gabriel, S.B., Getz, G., Glatt, S.J., Hultman, C.M., Kathiresan, S., Laakso, M., McCarroll, S., McCarthy, M.I., McGovern, D., McPherson, R., Neale, B.M., Palotie, A., Purcell, S.M., Saleheen, D., Scharf, J.M., Sklar, P., Sullivan, P.F., Tuomilehto, J., Tsuang, M.T., Watkins, H.C., Wilson, J.G., Daly, M.J., MacArthur, D.G. and Consortium, E.A. (2016) 'Analysis of protein-coding genetic variation in 60,706 humans', *Nature*, 536(7616), pp. 285-291.

Lelieveld, S.H., Spielmann, M., Mundlos, S., Veltman, J.A. and Gilissen, C. (2015) 'Comparison of Exome and Genome Sequencing Technologies for the Complete Capture of Protein-Coding Regions', *Human Mutation*, 36(8), pp. 815-822.

Li, H. and Durbin, R. (2009) 'Fast and accurate short read alignment with Burrows–Wheeler transform', *Bioinformatics*, 25(14), pp. 1754-1760.

Li, H., Fang, Q., Gao, F., Fan, J., Zhou, J., Wang, X., Zhang, H., Pan, X., Bao, Y., Xiang, K., Xu, A. and Jia, W. (2010) 'Fibroblast growth factor 21 levels are increased in nonalcoholic fatty liver disease patients and are correlated with hepatic triglyceride', *Journal of Hepatology*, 53(5), pp. 934-940.

Li, X., Li, Y., Han, G., Li, X., Ji, Y., Fan, Z., Zhong, Y., Cao, J., Zhao, J., Mariusz, G., Zhang, M., Wen, J., Nesland, J.M. and Suo, Z. (2014) 'Establishment of mitochondrial pyruvate carrier 1 (MPC1) gene knockout mice with preliminary gene function analyses', *Oncotarget*, 5(0), pp. 79981-79994.

Lieber, D.S., Calvo, S.E., Shanahan, K., Slate, N.G., Liu, S., Hershman, S.G., Gold, N.B., Chapman, B.A., Thorburn, D.R., Berry, G.T., Schmahmann, J.D., Borowsky, M.L., Mueller, D.M., Sims, K.B. and Mootha, V.K. (2013) 'Targeted exome sequencing of suspected mitochondrial disorders', *Neurology*, 80(19), pp. 1762-1770.

Lightowlers, R.N., Taylor, R.W. and Turnbull, D.M. (2015) 'Mutations causing mitochondrial disease: What is new and what challenges remain?', *Science*, 349(6255), pp. 1494-1499.

Lill, R. (2009) 'Function and biogenesis of iron–sulphur proteins', *Nature*, 460(7257), pp. 831-838.

Lim, Sze C., Smith, Katherine R., Stroud, David A., Compton, Alison G., Tucker, Elena J., Dasvarma, A., Gandolfo, Luke C., Marum, Justine E., McKenzie, M., Peters, Heidi L., Mowat, D., Procopis, Peter G., Wilcken, B., Christodoulou, J., Brown, Garry K., Ryan, Michael T., Bahlo, M. and Thorburn, David R. (2014) 'A Founder Mutation in PET100 Causes Isolated Complex IV Deficiency in Lebanese Individuals with Leigh Syndrome', *The American Journal of Human Genetics*, 94(2), pp. 209-222.

Liu, T.C., Kim, H., Arizmendi, C., Kitano, A. and Patel, M.S. (1993) 'Identification of two missense mutations in a dihydrolipoamide dehydrogenase-deficient patient', *Proceedings of the National Academy of Sciences*, 90(11), pp. 5186-5190.

Livingston, J. and Crow, Y. (2016) 'Neurologic Phenotypes Associated with Mutations in TREX1, RNASEH2A, RNASEH2B, RNASEH2C, SAMHD1, ADAR1, and IFIH1: Aicardi–Goutières Syndrome and Beyond', *Neuropediatrics*, 47(06), pp. 355-360.

Lloyd, R.E. and McGeehan, J.E. (2013) 'Structural Analysis of Mitochondrial Mutations Reveals a Role for Bigenomic Protein Interactions in Human Disease', *PLoS ONE*, 8(7), p. e69003.

Lopez, M.F., Kristal, B.S., Chernokalskaya, E., Lazarev, A., Shestopalov, A.I., Bogdanova, A. and Robinson, M. (2000) 'High-throughput profiling of the mitochondrial proteome using affinity fractionation and automation', *ELECTROPHORESIS*, 21(16), pp. 3427-3440.

Lorenzoni, P.J., Scola, R.H., Kay, C.S.K., Silvado, C.E.S. and Werneck, L.C. (2014) 'When should MERRF (myoclonus epilepsy associated with ragged-red fibers) be the diagnosis?', *Arquivos de Neuro-Psiquiatria*, 72(10), pp. 803-811.

Lunsing, R.J., Strating, K., Koning, T.J.d. and Sijens, P.E. (2017) 'Diagnostic value of MRS-quantified brain tissue lactate level in identifying children with mitochondrial disorders', *European Radiology*, 27(3), pp. 976-984.

Lupski, J.R., Reid, J.G., Gonzaga-Jauregui, C., Deiros, D.R., Chen, D.C.Y., Nazareth, L., Bainbridge, M., Dinh, H., Jing, C., Wheeler, D.A., McGuire, A.L., Zhang, F., Stankiewicz, P., Halperin, J.J., Yang, C., Gehman, C., Guo, D., Irikat, R.K., Tom, W., Fantin, N.J., Muzny, D.M. and Gibbs, R.A. (2010) 'Whole-Genome Sequencing in a Patient with Charcot–Marie–Tooth Neuropathy', *The New England Journal of Medicine*, 362(13), pp. 1181-1191.

Maddirevula, S., Alzahrani, F., Al-Owain, M., Muhaizea, M.A.A., Kayyali, H.R., AlHashem, A., Rahbeeni, Z., Al-Otaibi, M., Alzaidan, H.I., Balobaid, A., Khashab, H.Y.E., Bubshait, D.K., Faden, M., Yamani, S.A., Dabbagh, O., Al-Mureikhi, M., Jasser, A.A., Alsaif, H.S., Alluhaydan, I., Seidahmed, M.Z., Alabbasi, B.H., Almogarri, I., Kurdi, W., Akleh, H., Qari, A., Tala, S.M.A., Alhomaidi, S., Kentab, A.Y., Salih, M.A., Chedrawi, A., Alameer, S., Tabarki, B., Shamseldin, H.E., Patel, N., Ibrahim, N., Abdulwahab, F., Samira, M., Goljan, E., Abouelhoda, M., Meyer, B.F., Hashem, M., Shaheen, R., AlShahwan, S., Alfadhel, M., Ben-Omran, T., Al-Qattan, M.M., Monies, D. and Alkuraya, F.S. (2019) 'Autozygome and high throughput confirmation of disease genes candidacy', *Genetics in Medicine*, 21(3), pp. 736-742.

Maiti, P., Kim, H.-J., Tu, Y.-T. and Barrientos, A. (2018) 'Human GTPBP10 is required for mitoribosome maturation', *Nucleic Acids Research*, pp. gky938-.

Malicdan, M.C.V., Vilboux, T., Ben-Zeev, B., Guo, J., Eliyahu, A., Pode-Shakked, B., Dori, A., Kakani, S., Chandrasekharappa, S.C., Ferreira, C.R., Shelestovich, N., Marek-Yagel, D., Pri-Chen, H., Blatt, I., Niederhuber, J.E., He, L., Toro, C., Taylor, R.W., Deeken, J., Yardeni, T., Wallace, D.C., Gahl, W.A. and Anikster, Y. (2018)

'A novel inborn error of the coenzyme Q10 biosynthesis pathway: cerebellar ataxia and static encephalomyopathy due to COQ5 C-methyltransferase deficiency', *Human Mutation*, 39(1), pp. 69-79.

Manor, U., Bartholomew, S., Golani, G., Christenson, E., Kozlov, M., Higgs, H., Spudich, J. and Lippincott-Schwartz, J. (2015) 'A mitochondria-anchored isoform of the actin-nucleating spire protein regulates mitochondrial division', *eLife*, 4, p. e08828.

Marchi, S., Patergnani, S., Missiroli, S., Morciano, G., Rimessi, A., Wieckowski, M.R., Giorgi, C. and Pinton, P. (2018) 'Mitochondrial and endoplasmic reticulum calcium homeostasis and cell death', *Cell Calcium*, 69, pp. 62-72.

Marchi, S., Patergnani, S. and Pinton, P. (2014) 'The endoplasmic reticulum–mitochondria connection: One touch, multiple functions', *Biochimica et Biophysica Acta (BBA) - Bioenergetics*, 1837(4), pp. 461-469.

Martin, J., Mahlke, K. and Pfanner, N. (1991) 'Role of an energized inner membrane in mitochondrial protein import: Delta Psi drives the movement of presequences', *J Biol Chem*, 266(27), pp. 18051-7.

Martínez-Reyes, I. and Chandel, N.S. (2020) 'Mitochondrial TCA cycle metabolites control physiology and disease', *Nature Communications*, 11(1), p. 102.

Martinou, J.-C. (1999) 'Key to the mitochondrial gate', *Nature*, 399(6735), pp. 411-412.

Máximo, V., Botelho, T., Capela, J., Soares, P., Lima, J., Taveira, A., Amaro, T., Barbosa, A.P., Preto, A., Harach, H.R., Williams, D. and Sobrinho-Simões, M. (2005) 'Somatic and germline mutation in GRIM-19, a dual function gene involved in mitochondrial metabolism and cell death, is linked to mitochondrion-rich (Hürthle cell) tumours of the thyroid', *British Journal of Cancer*, 92(10), pp. 1892-1898.

Mayr, Johannes A., Haack, Tobias B., Graf, E., Zimmermann, Franz A., Wieland, T., Haberberger, B., Superti-Furga, A., Kirschner, J., Steinmann, B., Baumgartner, Matthias R., Moroni, I., Lamantea, E., Zeviani, M., Rodenburg, Richard J., Smeitink, J., Strom, Tim M., Meitinger, T., Sperl, W. and Prokisch, H. (2012) 'Lack of the Mitochondrial Protein Acylglycerol Kinase Causes Sengers Syndrome', *The American Journal of Human Genetics*, 90(2), pp. 314-320.

McKinney, E.A. and Oliveira, M.T. (2013) 'Replicating animal mitochondrial DNA', *Genetics and Molecular Biology*, 36(3), pp. 308-315.

McLaren, W., Gil, L., Hunt, S.E., Riat, H.S., Ritchie, G.R.S., Thormann, A., Flicek, P. and Cunningham, F. (2016) 'The Ensembl Variant Effect Predictor', *Genome Biology*, 17(1), p. 122.

Melchionda, L., Damseh, N.S., Libdeh, B.Y.A., Nasca, A., Elpeleg, O., Zanolini, A. and Ghezzi, D. (2014) 'A novel mutation in TTC19 associated with isolated complex III deficiency, cerebellar hypoplasia, and bilateral basal ganglia lesions', *Frontiers in Genetics*, 5, p. 397.

Metodiev, M.D., Lesko, N., Park, C.B., Cámara, Y., Shi, Y., Wibom, R., Hultenby, K., Gustafsson, C.M. and Larsson, N.-G. (2009) 'Methylation of 12S rRNA Is Necessary for In Vivo Stability of the Small Subunit of the Mammalian Mitochondrial Ribosome', *Cell Metabolism*, 9(4), pp. 386-397.

Metodiev, M.D., Spåhr, H., Polosa, P.L., Meharg, C., Becker, C., Altmueller, J., Habermann, B., Larsson, N.-G. and Ruzzenente, B. (2014) 'NSUN4 Is a Dual Function Mitochondrial Protein Required for Both Methylation of 12S rRNA and Coordination of Mitoribosomal Assembly', *PLoS Genetics*, 10(2), p. e1004110.

Meyers, D.E., Basha, H.I. and Koenig, M.K. (2013) 'Mitochondrial cardiomyopathy: pathophysiology, diagnosis, and management. PMID - 24082366', *Texas Heart Institute journal*, 40(4), pp. 385-94.

Michel, H., Behr, J., Harrenga, A. and Kannt, A. (1998) 'CYTOCHROME C OXIDASE: Structure and Spectroscopy', *Annual Review of Biophysics and Biomolecular Structure*, 27(1), pp. 329-356.

Mihara, K. and Omura, T. (1996) 'Cytoplasmic chaperones in precursor targeting to mitochondria: the role of MSF and hsp 70', *Trends in Cell Biology*, 6(3), pp. 104-108.

Minczuk, M., He, J., Duch, A.M., Ettema, T.J., Chlebowski, A., Dzionek, K., Nijtmans, L.G.J., Huynen, M.A. and Holt, I.J. (2011) 'TEFM (c17orf42) is necessary for transcription of human mtDNA', *Nucleic Acids Research*, 39(10), pp. 4284-4299.

Miné, M., Chen, J.M., Brivet, M., Desguerre, I., Marchant, D., Lonlay, P.d., Bernard, A., Férec, C., Abitbol, M., Ricquier, D. and Marsac, C. (2007) 'A large genomic deletion in the PDHX gene caused by the retrotranspositional insertion of a full-length LINE-1 element', *Human Mutation*, 28(2), pp. 137-142.

Minoia, F., Bertamino, M., Picco, P., Severino, M., Rossi, A., Fiorillo, C., Minetti, C., Nesti, C., Santorelli, F.M. and Rocco, M.D. (2017) 'JIMD Reports, Volume 37', *JIMD reports*, pp. 37-43.

Miryounesi, M., Fardaei, M., Tabei, S.M. and Ghafouri-Fard, S. (2016) 'Leigh syndrome associated with a novel mutation in the COX15 gene', *Journal of Pediatric Endocrinology and Metabolism*, 29(6), pp. 741-744.

Modell, B. and Darr, A. (2002) 'Genetic counselling and customary consanguineous marriage', *Nature Reviews Genetics*, 3(3), pp. 225-229.

Molinari, F., Raas-Rothschild, A., Rio, M., Fiermonte, G., Encha-Razavi, F., Palmieri, L., Palmieri, F., Ben-Neriah, Z., Kadhom, N., Vekemans, M., Attié-Bitach, T., Munnich, A., Rustin, P. and Colleaux, L. (2005) 'Impaired Mitochondrial Glutamate Transport in Autosomal Recessive Neonatal Myoclonic Epilepsy', *The American Journal of Human Genetics*, 76(2), pp. 334-339.

Mollier, P., Hoffmann, B., Debast, C. and Small, I. (2002) 'The gene encoding Arabidopsis thaliana mitochondrial ribosomal protein S13 is a recent duplication of the gene encoding plastid S13', *Current Genetics*, 40(6), pp. 405-409.

Monies, D., Abouelhoda, M., AlSayed, M., Alhassnan, Z., Alotaibi, M., Kayyali, H., Al-Owain, M., Shah, A., Rahbeeni, Z., Al-Muhaizea, M.A., Alzaidan, H.I., Cupler, E., Bohlega, S., Faqeih, E., Faden, M., Alyounes, B., Jaroudi, D., Goljan, E., Elbardisy, H., Akilan, A., Albar, R., Aldhalaan, H., Gulab, S., Chedrawi, A., Saud, B.K.A., Kurdi, W., Makhseed, N., Alqasim, T., Khashab, H.Y.E., Al-Mousa, H., Alhashem, A., Kanaan, I., Algoufi, T., Alsaleem, K., Basha, T.A., Al-Murshedi, F., Khan, S., Al-Kindy, A., Alnemer, M., Al-Hajjar, S., Alyamani, S., Aldhekri, H., Al-Mehaidib, A., Arnaout, R., Dabbagh, O., Shagrani, M., Broering, D., Tulbah, M., Alqassmi, A., Almugbel, M., AlQuaiz, M., Alsaman, A., Al-Thihli, K., Sulaiman, R.A., Al-Dekhail, W., Alsaegh, A., Bashiri, F.A., Qari, A., Alhomadi, S., Alkuraya, H., Alsebayel, M., Hamad, M.H., Szonyi, L., Abaalkhail, F., Al-Mayouf, S.M., Almojalli, H., Alqadi, K.S., Elsiesy, H., Shuaib, T.M., Seidahmed, M.Z., Abosoudah, I., Akleh, H., AlGhonaium, A., Alkharfy, T.M., Mutairi, F.A., Eyaid, W., Alshanbary, A., Sheikh, F.R., Alsohaibani, F.I., Alsonbul, A., Tala, S.A., Balkhy, S., Bassiouni, R., Alenizi, A.S., Hussein, M.H., Hassan, S., Khalil, M., Tabarki, B., Alshahwan, S., Oshi, A., Sabr, Y., Alsaadoun, S., Salih, M.A., Mohamed, S., Sultana, H., Tamim, A., El-Haj, M., Alshahrani, S., Bubshait, D.K., Alfadhel, M., et al. (2017) 'The landscape of genetic diseases in Saudi Arabia based on the first 1000 diagnostic panels and exomes', *Human Genetics*, 136(8), pp. 921-939.

Montoya, J., Christianson, T., Levens, D., Rabinowitz, M. and Attardi, G. (1982) 'Identification of initiation sites for heavy-strand and light-strand transcription in human mitochondrial DNA', *Proceedings of the National Academy of Sciences*, 79(23), pp. 7195-7199.

Moraes, C.T., Ricci, E., Bonilla, E., DiMauro, S. and Schon, E.A. (1992) 'The mitochondrial tRNA(Leu(UUR)) mutation in mitochondrial encephalomyopathy, lactic acidosis, and strokelike episodes (MELAS): genetic, biochemical, and morphological correlations in skeletal muscle', *American journal of human genetics*, 50(5), pp. 934-49.

Morava, E., Heuvel, L.v.d., Hol, F., Vries, M.C.d., Hogeveen, M., Rodenburg, R.J. and Smeitink, J.A.M. (2006) 'Mitochondrial disease criteria', *Neurology*, 67(10), pp. 1823-1826.

Mordaunt, D.A., Jolley, A., Balasubramaniam, S., Thorburn, D.R., Mountford, H.S., Compton, A.G., Nicholl, J., Manton, N., Clark, D., Bratkovic, D., Friend, K. and Yu, S. (2015) 'Phenotypic variation of TTC19-deficient mitochondrial complex III deficiency: A case report and literature review', *American Journal of Medical Genetics Part A*, 167(6), pp. 1330-1336.

Morgan, J.E., Carr, I.M., Sheridan, E., Chu, C.E., Hayward, B., Camm, N., Lindsay, H.A., Mattocks, C.J., Markham, A.F., Bonthron, D.T. and Taylor, G.R. (2010) 'Genetic diagnosis of familial breast cancer using clonal sequencing', *Human Mutation*, 31(4), pp. 484-491.

Morino, H., Miyamoto, R., Ohnishi, S., Maruyama, H. and Kawakami, H. (2014) 'Exome sequencing reveals a novel TTC19 mutation in an autosomal recessive spinocerebellar ataxia patient', *BMC Neurology*, 14(1), p. 5.

Mourier, T., Hansen, A.J., Willerslev, E. and Arctander, P. (2001) 'The Human Genome Project Reveals a Continuous Transfer of Large Mitochondrial Fragments to the Nucleus', *Molecular Biology and Evolution*, 18(9), pp. 1833-1837.

Munnich, A., Rötig, A., Chretien, D., Cormier, V., Bourgeron, T., Bonnefont, J.P., Saudubray, J.M. and Rustin, P. (1996) 'Clinical presentation of mitochondrial disorders in childhood', *Journal of Inherited Metabolic Disease*, 19(4), pp. 521-527.

Murphy, M.E., Vin, C.D., Slough, M.M., Gombotz, W.R. and Kelley-Clarke, B. (2016) 'Design of a titering assay for lentiviral vectors utilizing direct extraction of DNA from transduced cells in microtiter plates', *Molecular Therapy - Methods & Clinical Development*, 3, p. 16005.

Murphy, Michael P. (2009) 'How mitochondria produce reactive oxygen species', *Biochemical Journal*, 417(1), pp. 1-13.

Musa, S., Eyaid, W., Kamer, K., Ali, R., Al-Mureikhi, M., Shahbeck, N., Mesaifri, F.A., Makhseed, N., Mohamed, Z., AlShehhi, W.A., Mootha, V.K., Juusola, J. and Ben-Omran, T. (2018) 'JIMD Reports, Volume 43', *JIMD reports*, pp. 79-83.

Nagaike, T., Suzuki, T., Tomari, Y., Takemoto-Hori, C., Negayama, F., Watanabe, K. and Ueda, T. (2001) 'Identification and Characterization of Mammalian Mitochondrial tRNA nucleotidyltransferases', *Journal of Biological Chemistry*, 276(43), pp. 40041-40049.

Nagao, A., Suzuki, T., Katoh, T., Sakaguchi, Y. and Suzuki, T. (2009) 'Biogenesis of glutaminyl-mt tRNAGln in human mitochondria', *Proceedings of the National Academy of Sciences*, 106(38), pp. 16209-16214.

Nair, V., Robinson-Cohen, C., Smith, M.R., Bellovich, K.A., Bhat, Z.Y., Bobadilla, M., Brosius, F., Boer, I.H.d., Essioux, L., Formentini, I., Gadegbeku, C.A., Gipson, D., Hawkins, J., Himmelfarb, J., Kestenbaum, B., Kretzler, M., Magnone, M.C.,

Perumal, K., Steigerwalt, S., Ju, W. and Bansal, N. (2017) 'Growth Differentiation Factor–15 and Risk of CKD Progression', *Journal of the American Society of Nephrology*, 28(7), pp. 2233-2240.

Nesbitt, V., Pitceathly, R.D.S., Turnbull, D.M., Taylor, R.W., Sweeney, M.G., Mudanohwo, E.E., Rahman, S., Hanna, M.G. and McFarland, R. (2013) 'The UK MRC Mitochondrial Disease Patient Cohort Study: clinical phenotypes associated with the m.3243A>G mutation—implications for diagnosis and management', *Journal of Neurology, Neurosurgery & Psychiatry*, 84(8), p. 936.

Neupert, W. and Herrmann, J.M. (2007) 'Translocation of Proteins into Mitochondria', *Annual Review of Biochemistry*, 76(1), pp. 723-749.

Ng, P.C. and Henikoff, S. (2001) 'Predicting Deleterious Amino Acid Substitutions', *Genome Research*, 11(5), pp. 863-874.

Ng, S.B., Buckingham, K.J., Lee, C., Bigham, A.W., Tabor, H.K., Dent, K.M., Huff, C.D., Shannon, P.T., Jabs, E.W., Nickerson, D.A., Shendure, J. and Bamshad, M.J. (2010) 'Exome sequencing identifies the cause of a mendelian disorder', *Nature Genetics*, 42(1), pp. 30-35.

Ni, H.-M., Williams, J.A. and Ding, W.-X. (2015) 'Mitochondrial dynamics and mitochondrial quality control', *Redox Biology*, 4, pp. 6-13.

Nogueira, C., Barros, J., Sá, M.J., Azevedo, L., Taipa, R., Torraco, A., Meschini, M.C., Verrigni, D., Nesti, C., Rizza, T., Teixeira, J., Carrozzo, R., Pires, M.M., Vilarinho, L. and Santorelli, F.M. (2013) 'Novel TTC19 mutation in a family with severe psychiatric manifestations and complex III deficiency', *neurogenetics*, 14(2), pp. 153-160.

Nowikovsky, K., Froschauer, E.M., Zsurka, G., Samaj, J., Reipert, S., Kolisek, M., Wiesenberger, G. and Schweyen, R.J. (2004) 'The LETM1/YOL027 Gene Family Encodes a Factor of the Mitochondrial K+ Homeostasis with a Potential Role in the Wolf-Hirschhorn Syndrome', *Journal of Biological Chemistry*, 279(29), pp. 30307-30315.

Nunnari, J. and Suomalainen, A. (2012) 'Mitochondria: In Sickness and in Health', *Cell*, 148(6), pp. 1145-1159.

O'Brien, T.W. (1971) 'The general occurrence of 55 S ribosomes in mammalian liver mitochondria', *The Journal of biological chemistry*, 246(10), pp. 3409-17.

O'Leary, N.A., Wright, M.W., Brister, J.R., Ciufo, S., Haddad, D., McVeigh, R., Rajput, B., Robbertse, B., Smith-White, B., Ako-Adjei, D., Astashyn, A., Badretdin, A., Bao, Y., Blinkova, O., Brover, V., Chetvernin, V., Choi, J., Cox, E., Ermolaeva, O., Farrell, C.M., Goldfarb, T., Gupta, T., Haft, D., Hatcher, E., Hlavina, W., Joardar, V.S., Kodali, V.K., Li, W., Maglott, D., Masterson, P., McGarvey, K.M., Murphy, M.R., O'Neill, K., Pujar, S., Rangwala, S.H., Rausch, D., Riddick, L.D., Schoch, C., Shkeda, A., Storz, S.S., Sun, H., Thibaud-Nissen, F., Tolstoy, I., Tully, R.E., Vatsan, A.R., Wallin, C., Webb, D., Wu, W., Landrum, M.J., Kimchi, A., Tatusova, T., DiCuccio, M., Kitts, P., Murphy, T.D. and Pruitt, K.D. (2016) 'Reference sequence (RefSeq) database at NCBI: current status, taxonomic expansion, and functional annotation', *Nucleic Acids Research*, 44(D1), pp. D733-D745.

O'Rourke, B. (2010) 'From Bioblasts to Mitochondria: Ever Expanding Roles of Mitochondria in Cell Physiology', *Frontiers in Physiology*, 1, p. 7.

Ojala, D., Montoya, J. and Attardi, G. (1981) 'tRNA punctuation model of RNA processing in human mitochondria', *Nature*, 290(5806), pp. 470-474.

Old, S.L. and Johnson, M.A. (1989) 'Methods of microphotometric assay of succinate dehydrogenase and cytochromec oxidase activities for use on human skeletal muscle', *The Histochemical Journal*, 21(9-10), pp. 545-555.

Olson, W., Engel, W.K., Walsh, G.O. and Einaugler, R. (1972) 'Oculocraniosomatic Neuromuscular Disease With Ragged-Red Fibers: Histochemical and Ultrastructural Changes in Limb Muscles of a Group of Patients With Idiopathic Progressive External Ophthalmoplegia', *Archives of Neurology*, 26(3), pp. 193-211.

Onat, O.E., Gulsuner, S., Bilguvar, K., Basak, A.N., Topaloglu, H., Tan, M., Tan, U., Gunel, M. and Ozcelik, T. (2013) 'Missense mutation in the ATPase, aminophospholipid transporter protein ATP8A2 is associated with cerebellar atrophy and quadrupedal locomotion', *European Journal of Human Genetics*, 21(3), pp. 281-285.

Oonthonpan, L., Rauckhorst, A.J., Gray, L.R., Boutron, A.C. and Taylor, E.B. (2019) 'Two human patient mitochondrial pyruvate carrier mutations reveal distinct molecular mechanisms of dysfunction', *JCI Insight*, 4(13).

Oquendo, C.E., Antonicka, H., Shoubridge, E.A., Reardon, W. and Brown, G.K. (2004) 'Functional and genetic studies demonstrate that mutation in the COX15 gene can cause Leigh syndrome', *Journal of Medical Genetics*, 41(7), p. 540.

Osellame, L.D., Singh, A.P., Stroud, D.A., Palmer, C.S., Stojanovski, D., Ramachandran, R. and Ryan, M.T. (2016) 'Cooperative and independent roles of the Drp1 adaptors Mff, MiD49 and MiD51 in mitochondrial fission', *J Cell Sci*, 129(11), pp. 2170-2181.

Østergaard, E., Bradinova, I., Ravn, S.H., Hansen, F.J., Simeonov, E., Christensen, E., Wibrand, F. and Schwartz, M. (2005) 'Hypertrichosis in patients with SURF1 mutations', *American Journal of Medical Genetics Part A*, 138A(4), pp. 384-388.

Ott, J., Wang, J. and Leal, S.M. (2015) 'Genetic linkage analysis in the age of whole-genome sequencing', *Nature Reviews Genetics*, 16(5), pp. 275-284.

Ow, Y.-L.P., Green, D.R., Hao, Z. and Mak, T.W. (2008) 'Cytochrome c: functions beyond respiration', *Nature Reviews Molecular Cell Biology*, 9(7), pp. 532-542.

Ozand, P.T., Gascon, G.G., Essa, M.A., Joshi, S., Jishi, E.A., Bakheet, S., Watban, J.A., Al-Kawi, M.Z. and Dabbagh, O. (1998) 'Biotin-responsive basal ganglia disease: a novel entity', *Brain*, 121(7), pp. 1267-1279.

Pagliarini, D.J., Calvo, S.E., Chang, B., Sheth, S.A., Vafai, S.B., Ong, S.-E., Walford, G.A., Sugiana, C., Boneh, A., Chen, W.K., Hill, D.E., Vidal, M., Evans, J.G., Thorburn, D.R., Carr, S.A. and Mootha, V.K. (2008) 'A Mitochondrial Protein Compendium Elucidates Complex I Disease Biology', *Cell*, 134(1), pp. 112-123.

Patel, M.S., Nemeria, N.S., Furey, W. and Jordan, F. (2014) 'The Pyruvate Dehydrogenase Complexes: Structure-based Function and Regulation', *Journal of Biological Chemistry*, 289(24), pp. 16615-16623.

Patergnani, S., Suski, J.M., Agnoletto, C., Bononi, A., Bonora, M., Marchi, E.D., Giorgi, C., Marchi, S., Missiroli, S., Poletti, F., Rimessi, A., Duszynski, J., Wieckowski, M.R. and Pinton, P. (2011) 'Calcium signaling around Mitochondria Associated Membranes (MAMs)', *Cell Communication and Signaling*, 9(1), p. 19.

Patton, J.R., Bykhovskaya, Y., Mengesha, E., Bertolotto, C. and Fischel-Ghodsian, N. (2005) 'Mitochondrial Myopathy and Sideroblastic Anemia (MLASA) MISSENSE MUTATION IN THE PSEUDOURIDINE SYNTHASE 1 (PUS1) GENE IS ASSOCIATED WITH THE LOSS OF tRNA PSEUDOURIDYLATION', *Journal of Biological Chemistry*, 280(20), pp. 19823-19828.

Pavlakis, S.G., Phillips, P.C., DiMauro, S., Vivo, D.C.D. and Rowland, L.P. (1984) 'Mitochondrial myopathy, encephalopathy, lactic acidosis, and strokelike episodes: A distinctive clinical syndrome', *Annals of Neurology*, 16(4), pp. 481-488.

Pearce, S.F., Rorbach, J., Haute, L.V., D'Souza, A.R., Rebelo-Guiomar, P., Powell, C.A., Brierley, I., Firth, A.E. and Minczuk, M. (2017) 'Maturation of selected human mitochondrial tRNAs requires deadenylation', *eLife*, 6, p. e27596.

Pesta, D. and Gnaiger, E. (2011) 'Mitochondrial Bioenergetics, Methods and Protocols', *Methods in molecular biology (Clifton, N.J.)*, 810, pp. 25-58.

Pfanner, N., Douglas, M.G., Endo, T., Hoogenraad, N.J., Jensen, R.E., Meijer, M., Neupert, W., Schatz, G., Schmitz, U.K. and Shore, G.C. (1996) 'Uniform nomenclature for the protein transport machinery of the mitochondrial membranes', *Trends in Biochemical Sciences*, 21(2), pp. 51-52.

Pfanner, N. and Meijer, M. (1997) 'Mitochondrial biogenesis: The Tom and Tim machine', *Current Biology*, 7(2), pp. R100-R103.

Phoenix, C., Schaefer, A.M., Elson, J.L., Morava, E., Bugiani, M., Uziel, G., Smeitink, J.A., Turnbull, D.M. and McFarland, R. (2006) 'A scale to monitor progression and treatment of mitochondrial disease in children', *Neuromuscular Disorders*, 16(12), pp. 814-820.

Piao, L., Li, Y., Kim, S.J., Byun, H.S., Huang, S.M., Hwang, S.-K., Yang, K.-J., Park, K.A., Won, M., Hong, J., Hur, G.M., Seok, J.H., Shong, M., Cho, M.-H., Brazil, D.P., Hemmings, B.A. and Park, J. (2009) 'Association of LETM1 and MRPL36 Contributes to the Regulation of Mitochondrial ATP Production and Necrotic Cell Death', *Cancer Research*, 69(8), pp. 3397-3404.

Pickett, S.J., Grady, J.P., Ng, Y.S., Gorman, G.S., Schaefer, A.M., Wilson, I.J., Cordell, H.J., Turnbull, D.M., Taylor, R.W. and McFarland, R. (2018) 'Phenotypic heterogeneity in m.3243A>G mitochondrial disease: The role of nuclear factors', *Annals of Clinical and Translational Neurology*, 5(3), pp. 333-345.

Pinto, M. and Màximo, V. (2018) 'NDUFA13 (NADH:ubiquinone oxidoreductase subunit A13)', *Atlas of Genetics and Cytogenetics in Oncology and Haematology*, (8).

Pitceathly, R.D.S., Smith, C., Fratter, C., Alston, C.L., He, L., Craig, K., Blakely, E.L., Evans, J.C., Taylor, J., Shabbir, Z., Deschauer, M., Pohl, U., Roberts, M.E., Jackson, M.C., Halfpenny, C.A., Turnpenny, P.D., Lunt, P.W., Hanna, M.G., Schaefer, A.M., McFarland, R., Horvath, R., Chinnery, P.F., Turnbull, D.M., Poulton, J., Taylor, R.W. and Gorman, G.S. (2012) 'Adults with RRM2B-related mitochondrial disease have distinct clinical and molecular characteristics', *Brain*, 135(11), pp. 3392-3403.

Plutino, M., Chaussenot, A., Rouzier, C., Ait-El-Mkadem, S., Fragaki, K., Paquis-Flucklinger, V. and Bannwarth, S. (2018) 'Targeted next generation sequencing with an extended gene panel does not impact variant detection in mitochondrial diseases', *BMC Medical Genetics*, 19(1), p. 57.

Popow, J., Alleaume, A.-M., Curk, T., Schwarzl, T., Sauer, S. and Hentze, M.W. (2015) 'FASTKD2 is an RNA-binding protein required for mitochondrial RNA processing and translation', *RNA*, 21(11), pp. 1873-1884.

Posse, V., Shahzad, S., Falkenberg, M., Hällberg, B.M. and Gustafsson, C.M. (2015) 'TEFM is a potent stimulator of mitochondrial transcription elongation in vitro', *Nucleic Acids Research*, 43(5), pp. 2615-2624.

Powell, Christopher A., Kopajtich, R., D'Souza, A.R., Rorbach, J., Kremer, Laura S., Husain, Ralf A., Dallabona, C., Donnini, C., Alston, Charlotte L., Griffin, H., Pyle, A., Chinnery, Patrick F., Strom, Tim M., Meitinger, T., Rodenburg, Richard J., Schottmann, G., Schuelke, M., Romain, N., Haller, Ronald G., Ferrero, I., Haack, Tobias B., Taylor, Robert W., Prokisch, H. and Minczuk, M. (2015) 'TRMT5 Mutations Cause a Defect in Post-transcriptional Modification of Mitochondrial

tRNA Associated with Multiple Respiratory-Chain Deficiencies', *The American Journal of Human Genetics*, 97(2), pp. 319-328.

Prasad, T.S.K., Goel, R., Kandasamy, K., Keerthikumar, S., Kumar, S., Mathivanan, S., Telikicherla, D., Raju, R., Shafreen, B., Venugopal, A., Balakrishnan, L., Marimuthu, A., Banerjee, S., Somanathan, D.S., Sebastian, A., Rani, S., Ray, S., Kishore, C.J.H., Kanth, S., Ahmed, M., Kashyap, M.K., Mohmood, R., Ramachandra, Y.L., Krishna, V., Rahiman, B.A., Mohan, S., Ranganathan, P., Ramabadran, S., Chaerkady, R. and Pandey, A. (2009) 'Human Protein Reference Database—2009 update', *Nucleic Acids Research*, 37(suppl_1), pp. D767-D772.

Prestele, M., Vogel, F., Reichert, A.S., Herrmann, J.M. and Ott, M. (2009) 'Mrpl36 Is Important for Generation of Assembly Competent Proteins during Mitochondrial Translation', *Molecular Biology of the Cell*, 20(10), pp. 2615-2625.

Pronicka, E., Piekutowska-Abramczuk, D., Ciara, E., Trubicka, J., Rokicki, D., Karkucińska-Więckowska, A., Pajdowska, M., Jurkiewicz, E., Halat, P., Kosińska, J., Pollak, A., Rydzanicz, M., Stawinski, P., Pronicki, M., Krajewska-Walasek, M. and Płoski, R. (2016) 'New perspective in diagnostics of mitochondrial disorders: two years' experience with whole-exome sequencing at a national paediatric centre', *Journal of Translational Medicine*, 14(1), p. 174.

Pronicki, M., Matyja, E., Piekutowska-Abramczuk, D., Szymańska-Dębińska, T., Karkucińska-Więckowska, A., Karczmarewicz, E., Grajkowska, W., Kmieć, T., Popowska, E. and Sykut-Cegielska, J. (2008) 'Light and electron microscopy characteristics of the muscle of patients with SURF1 gene mutations associated with Leigh disease', *Journal of Clinical Pathology*, 61(4), pp. 460-466.

Puusepp, S., Reinson, K., Pajusalu, S., Murumets, Ü., Õiglane-Shlik, E., Rein, R., Talvik, I., Rodenburg, R.J. and Õunap, K. (2018) 'Effectiveness of whole exome sequencing in unsolved patients with a clinical suspicion of a mitochondrial disorder in Estonia', *Molecular Genetics and Metabolism Reports*, 15, pp. 80-89.

Quinlan, A.R. and Hall, I.M. (2010) 'BEDTools: a flexible suite of utilities for comparing genomic features', *Bioinformatics*, 26(6), pp. 841-842.

Radovanovic, Z., Shah, N. and Behbehani, J. (1999) 'Prevalence and Social Correlates of Consanguinity in Kuwait', *Annals of Saudi Medicine*, 19(3), pp. 206-210.

Rafiq, M.A., Leblond, C.S., Saqib, M.A.N., Vincent, A.K., Ambalavanan, A., Khan, F.S., Ayaz, M., Shaheen, N., Spiegelman, D., Ali, G., Amin-ud-din, M., Laurent, S., Mahmood, H., Christian, M., Ali, N., Fennell, A., Nanjiani, Z., Egger, G., Caron, C., Waqas, A., Ayub, M., Rasheed, S., d'Arc, B.F., Johnson, A., So, J., Brohi, M.Q., Mottron, L., Ansar, M., Vincent, J.B. and Xiong, L. (2015) 'Novel VPS13B Mutations in Three Large Pakistani Cohen Syndrome Families Suggests a Baloch Variant with Autistic-Like Features', *BMC Medical Genetics*, 16(1), p. 41.

Rahman, J., Noronha, A., Thiele, I. and Rahman, S. (2017) 'Leigh map: A novel computational diagnostic resource for mitochondrial disease', *Annals of Neurology*, 81(1), pp. 9-16.

Rahman, S., Blok, R.B., Dahl, H.H.M., Danks, D.M., Kirby, D.M., Chow, C.W., Christodoulou, J. and Thorburn, D.R. (1996) 'Leigh syndrome: Clinical features and biochemical and DNA abnormalities', *Annals of Neurology*, 39(3), pp. 343-351.

Rahman, S., Brown, R.M., Chong, W.K., Wilson, C.J. and Brown, G.K. (2001) 'A SURF1 gene mutation presenting as isolated leukodystrophy', *Annals of Neurology*, 49(6), pp. 797-800.

Rajgopal, A., Edmondnson, A., Goldman, I.D. and Zhao, R. (2001) 'SLC19A3 encodes a second thiamine transporter ThTr2', *Biochimica et Biophysica Acta (BBA) - Molecular Basis of Disease*, 1537(3), pp. 175-178.

Ramadan, D.G., Head, R.A., Al-Tawari, A., Habeeb, Y., Zaki, M., Al-Ruqum, F., Besley, G.T.N., Wraith, J.E., Brown, R.M. and Brown, G.K. (2004) 'Lactic acidosis and developmental delay due to deficiency of E3 binding protein (protein X) of the pyruvate dehydrogenase complex', *Journal of Inherited Metabolic Disease*, 27(4), pp. 477-485.

Ray, P.D., Huang, B.-W. and Tsuji, Y. (2012) 'Reactive oxygen species (ROS) homeostasis and redox regulation in cellular signaling', *Cellular Signalling*, 24(5), pp. 981-990.

Raymond, F.L., Horvath, R. and Chinnery, P.F. (2018) 'First-line genomic diagnosis of mitochondrial disorders', *Nature Reviews Genetics*, 19(7), pp. 399-400.

Reid, R.A. and Leech, R.M. (1980) 'Biochemistry and Structure of Cell Organelles'.

Reidling, J.C., Lambrecht, N., Kassir, M. and Said, H.M. (2010) 'Impaired Intestinal Vitamin B1 (Thiamin) Uptake in Thiamin Transporter-2–Deficient Mice', *Gastroenterology*, 138(5), pp. 1802-1809.

Rentzsch, P., Witten, D., Cooper, G.M., Shendure, J. and Kircher, M. (2018) 'CADD: predicting the deleteriousness of variants throughout the human genome', *Nucleic Acids Research*, 47(D1), pp. D886-D894.

Repp, B.M., Mastantuono, E., Alston, C.L., Schiff, M., Haack, T.B., Rötig, A., Ardissone, A., Lombès, A., Catarino, C.B., Diodato, D., Schottmann, G., Poulton, J., Burlina, A., Jonckheere, A., Munnich, A., Rolinski, B., Ghezzi, D., Rokicki, D., Wellesley, D., Martinelli, D., Wenhong, D., Lamantea, E., Ostergaard, E., Pronicka, E., Pierre, G., Smeets, H.J.M., Wittig, I., Scurr, I., Coo, I.F.M.d., Moroni, I., Smet, J., Mayr, J.A., Dai, L., Meirleir, L.d., Schuelke, M., Zeviani, M., Morscher, R.J., McFarland, R., Seneca, S., Klopstock, T., Meitinger, T., Wieland, T., Strom, T.M., Herberg, U., Ahting, U., Sperl, W., Nassogne, M.-C., Ling, H., Fang, F., Freisinger, P., Coster, R.V., Strecker, V., Taylor, R.W., Häberle, J., Vockley, J., Prokisch, H. and Wortmann, S. (2018) 'Clinical, biochemical and genetic spectrum of 70 patients with ACAD9 deficiency: is riboflavin supplementation effective?', *Orphanet Journal of Rare Diseases*, 13(1), p. 120.

Reyes, A., Kazak, L., Wood, S.R., Yasukawa, T., Jacobs, H.T. and Holt, I.J. (2013) 'Mitochondrial DNA replication proceeds via a 'bootlace' mechanism involving the incorporation of processed transcripts', *Nucleic Acids Research*, 41(11), pp. 5837-5850.

Rice, G., Newman, W.G., Dean, J., Patrick, T., Parmar, R., Flintoff, K., Robins, P., Harvey, S., Hollis, T., O'Hara, A., Herrick, A.L., Bowden, A.P., Perrino, F.W., Lindahl, T., Barnes, D.E. and Crow, Y.J. (2007a) 'Heterozygous Mutations in TREX1 Cause Familial Chilblain Lupus and Dominant Aicardi-Goutières Syndrome', *The American Journal of Human Genetics*, 80(4), pp. 811-815.

Rice, G., Patrick, T., Parmar, R., Taylor, C.F., Aeby, A., Aicardi, J., Artuch, R., Montalto, S.A., Bacino, C.A., Barroso, B., Baxter, P., Benko, W.S., Bergmann, C., Bertini, E., Biancheri, R., Blair, E.M., Blau, N., Bonthron, D.T., Briggs, T., Brueton, L.A., Brunner, H.G., Burke, C.J., Carr, I.M., Carvalho, D.R., Chandler, K.E., Christen, H.-J., Corry, P.C., Cowan, F.M., Cox, H., D'Arrigo, S., Dean, J., Laet, C.D., Praeter, C.D., Déry, C., Ferrie, C.D., Flintoff, K., Frints, S.G.M., Garcia-Cazorla, A., Gener, B., Goizet, C., Goutières, F., Green, A.J., Guët, A., Hamel, B.C.J., Hayward, B.E., Heiberg, A., Hennekam, R.C., Husson, M., Jackson, A.P., Jayatunga, R., Jiang, Y.-H., Kant, S.G., Kao, A., King, M.D., Kingston, H.M., Klepper, J., Knaap, M.S.v.d., Kornberg, A.J., Kotzot, D., Kratzer, W., Lacombe, D., Lagae, L., Landrieu, P.G., Lanzi, G., Leitch, A., Lim, M.J., Livingston, J.H., Lourenco, C.M., Lyall, E.G.H., Lynch, S.A., Lyons, M.J., Marom, D., McClure,

J.P., McWilliam, R., Melancon, S.B., Mewasingh, L.D., Moutard, M.-L., Nischal, K.K., Østergaard, J.R., Prendiville, J., Rasmussen, M., Rogers, R.C., Roland, D., Rosser, E.M., Rostasy, K., Roubertie, A., Sanchis, A., Schiffmann, R., Scholl-Bürgi, S., Seal, S., Shalev, S.A., Corcoles, C.S., Sinha, G.P., Soler, D., Spiegel, R., Stephenson, J.B.P., Tacke, U., Tan, T.Y., Till, M., Tolmie, J.L., et al. (2007b) 'Clinical and Molecular Phenotype of Aicardi-Goutières Syndrome', *The American Journal of Human Genetics*, 81(4), pp. 713-725.

Richards, A., van den Maagdenberg, A.M.J.M., Jen, J.C., Kavanagh, D., Bertram, P., Spitzer, D., Liszewski, M.K., Barilla-LaBarca, M.-L., Terwindt, G.M., Kasai, Y., McLellan, M., Grand, M.G., Vanmolkot, K.R.J., de Vries, B., Wan, J., Kane, M.J., Mamsa, H., Schäfer, R., Stam, A.H., Haan, J., de Jong, P.T.V.M., Storimans, C.W., van Schooneveld, M.J., Oosterhuis, J.A., Gschwendter, A., Dichgans, M., Kotschet, K.E., Hodgkinson, S., Hardy, T.A., Delatycki, M.B., Hajj-Ali, R.A., Kothari, P.H., Nelson, S.F., Frants, R.R., Baloh, R.W., Ferrari, M.D. and Atkinson, J.P. (2007) 'C-terminal truncations in human 3′-5′ DNA exonuclease TREX1 cause autosomal dominant retinal vasculopathy with cerebral leukodystrophy', *Nature Genetics*, 39(9), pp. 1068-1070.

Richards, S., Aziz, N., Bale, S., Bick, D., Das, S., Gastier-Foster, J., Grody, W.W., Hegde, M., Lyon, E., Spector, E., Voelkerding, K., Rehm, H.L. and Committee, A.L.Q.A. (2015) 'Standards and guidelines for the interpretation of sequence variants: a joint consensus recommendation of the American College of Medical Genetics and Genomics and the Association for Molecular Pathology', *Genetics in Medicine*, 17(5), pp. 405-423.

Richter, U., Lahtinen, T., Marttinen, P., Myöhänen, M., Greco, D., Cannino, G., Jacobs, Howard T., Lietzén, N., Nyman, Tuula A. and Battersby, Brendan J. (2013) 'A Mitochondrial Ribosomal and RNA Decay Pathway Blocks Cell Proliferation', *Current Biology*, 23(6), pp. 535-541.

Riley, L.G., Cowley, M.J., Gayevskiy, V., Roscioli, T., Thorburn, D.R., Prelog, K., Bahlo, M., Sue, C.M., Balasubramaniam, S. and Christodoulou, J. (2017) 'A SLC39A8 variant causes manganese deficiency, and glycosylation and mitochondrial disorders', *Journal of Inherited Metabolic Disease*, 40(2), pp. 261-269.

Robberson, D.L., Kasamatsu, H. and Vinograd, J. (1972) 'Replication of Mitochondrial DNA. Circular Replicative Intermediates in Mouse L Cells', *Proceedings of the National Academy of Sciences*, 69(3), pp. 737-741.

Roberti, M., Polosa, P.L., Bruni, F., Manzari, C., Deceglie, S., Gadaleta, M.N. and Cantatore, P. (2009) 'The MTERF family proteins: Mitochondrial transcription regulators and beyond', *Biochimica et Biophysica Acta (BBA) - Bioenergetics*, 1787(5), pp. 303-311.

Robinson, B.H. (2006) 'Lactic acidemia and mitochondrial disease', *Molecular Genetics and Metabolism*, 89(1-2), pp. 3-13.

Rocha, M.C., Grady, J.P., Grünewald, A., Vincent, A., Dobson, P.F., Taylor, R.W., Turnbull, D.M. and Rygiel, K.A. (2015) 'A novel immunofluorescent assay to investigate oxidative phosphorylation deficiency in mitochondrial myopathy: understanding mechanisms and improving diagnosis', *Scientific Reports*, 5(1), p. 15037.

Roos, S., Sofou, K., Hedberg-Oldfors, C., Kollberg, G., Lindgren, U., Thomsen, C., Tulinius, M. and Oldfors, A. (2019) 'Mitochondrial complex IV deficiency caused by a novel frameshift variant in MT-CO2 associated with myopathy and perturbed acylcarnitine profile', *European Journal of Human Genetics*, 27(2), pp. 331-335.

Rorbach, J., Boesch, P., Gammage, P.A., Nicholls, T.J.J., Pearce, S.F., Patel, D., Hauser, A., Perocchi, F. and Minczuk, M. (2014) 'MRM2 and MRM3 are involved in biogenesis of the large subunit of the mitochondrial ribosome', *Molecular Biology of the Cell*, 25(17), pp. 2542-2555.

Rorbach, J., Richter, R., Wessels, H.J., Wydro, M., Pekalski, M., Farhoud, M., Kühl, I., Gaisne, M., Bonnefoy, N., Smeitink, J.A., Lightowlers, R.N. and Chrzanowska-Lightowlers, Z.M.A. (2008) 'The human mitochondrial ribosome recycling factor is essential for cell viability', *Nucleic Acids Research*, 36(18), pp. 5787-5799.

Rosenbloom, K.R., Armstrong, J., Barber, G.P., Casper, J., Clawson, H., Diekhans, M., Dreszer, T.R., Fujita, P.A., Guruvadoo, L., Haeussler, M., Harte, R.A., Heitner, S., Hickey, G., Hinrichs, A.S., Hubley, R., Karolchik, D., Learned, K., Lee, B.T., Li, C.H., Miga, K.H., Nguyen, N., Paten, B., Raney, B.J., Smit, A.F.A., Speir, M.L., Zweig, A.S., Haussler, D., Kuhn, R.M. and Kent, W.J. (2015) 'The UCSC Genome Browser database: 2015 update', *Nucleic Acids Research*, 43(D1), pp. D670-D681.

Rossignol, R., Faustin, B., Rocher, C., Malgat, M., Mazat, J.-P. and Letellier, T. (2003) 'Mitochondrial threshold effects', *Biochemical Journal*, 370(3), pp. 751-762.

Rouzier, C., Chaussenot, A., Fragaki, K., Serre, V., Ait-El-Mkadem, S., Richelme, C., Paquis-Flucklinger, V. and Bannwarth, S. (2019) 'NDUFS6 related Leigh syndrome: a case report and review of the literature', *Journal of Human Genetics*, 64(7), pp. 637-645.

Rutter, J., Winge, D.R. and Schiffman, J.D. (2010) 'Succinate dehydrogenase – Assembly, regulation and role in human disease', *Mitochondrion*, 10(4), pp. 393-401.

Ruzzenente, B., Metodiev, M.D., Wredenberg, A., Bratic, A., Park, C.B., Cámara, Y., Milenkovic, D., Zickermann, V., Wibom, R., Hultenby, K., Erdjument-Bromage, H., Tempst, P., Brandt, U., Stewart, J.B., Gustafsson, C.M. and Larsson, N.G. (2012) 'LRPPRC is necessary for polyadenylation and coordination of translation of mitochondrial mRNAs', *The EMBO Journal*, 31(2), pp. 443-456.

Saada, A., Shaag, A., Mandel, H., Nevo, Y., Eriksson, S. and Elpeleg, O. (2001) 'Mutant mitochondrial thymidine kinase in mitochondrial DNA depletion myopathy', *Nature Genetics*, 29(3), pp. 342-344.

Saada, A., Vogel, R.O., Hoefs, S.J., Brand, M.A.v.d., Wessels, H.J., Willems, P.H., Venselaar, H., Shaag, A., Barghuti, F., Reish, O., Shohat, M., Huynen, M.A., Smeitink, J.A.M., Heuvel, L.P.v.d. and Nijtmans, L.G. (2009) 'Mutations in NDUFAF3 (C3ORF60), Encoding an NDUFAF4 (C6ORF66)-Interacting Complex I Assembly Protein, Cause Fatal Neonatal Mitochondrial Disease', *The American Journal of Human Genetics*, 84(6), pp. 718-727.

Saito, T. and Sadoshima, J. (2015) 'Molecular Mechanisms of Mitochondrial Autophagy/Mitophagy in the Heart', *Circulation Research*, 116(8), pp. 1477-1490.

Sanchez, M.I.G.L., Mercer, T.R., Davies, S.M.K., Shearwood, A.-M.J., Nygård, K.K.A., Richman, T.R., Mattick, J.S., Rackham, O. and Filipovska, A. (2011) 'RNA processing in human mitochondria', *Cell Cycle*, 10(17), pp. 2904-2916.

Sánchez-Caballero, L., Guerrero-Castillo, S. and Nijtmans, L. (2016) 'Unraveling the complexity of mitochondrial complex I assembly: A dynamic process', *Biochimica et Biophysica Acta (BBA) - Bioenergetics*, 1857(7), pp. 980-990.

Saoura, M., Powell, C.A., Kopajtich, R., Alahmad, A., Al-Balool, H.H., Albash, B., Alfadhel, M., Alston, C.L., Bertini, E., Bonnen, P.E., Bratkovic, D., Carrozzo, R., Donati, M.A., Nottia, M.D., Ghezzi, D., Goldstein, A., Haan, E., Horvath, R., Hughes, J., Invernizzi, F., Lamantea, E., Lucas, B., Pinnock, K.G., Pujantell, M., Rahman, S., Rebelo-Guiomar, P., Santra, S., Verrigni, D., McFarland, R., Prokisch,

H., Taylor, R.W., Levinger, L. and Minczuk, M. (2019) 'Mutations in ELAC2 associated with hypertrophic cardiomyopathy impair mitochondrial tRNA 3′-end processing', *Human Mutation*, 40(10), pp. 1731-1748.

Sasarman, F., Brunel-Guitton, C., Antonicka, H., Wai, T., Shoubridge, E.A. and Consortium, L. (2010) 'LRPPRC and SLIRP Interact in a Ribonucleoprotein Complex That Regulates Posttranscriptional Gene Expression in Mitochondria', *Molecular Biology of the Cell*, 21(8), pp. 1315-1323.

Sato, M. and Sato, K. (2013) 'Maternal inheritance of mitochondrial DNA by diverse mechanisms to eliminate paternal mitochondrial DNA', *Biochimica et Biophysica Acta (BBA) - Molecular Cell Research*, 1833(8), pp. 1979-1984.

Saunders, C.J., Miller, N.A., Soden, S.E., Dinwiddie, D.L., Noll, A., Alnadi, N.A., Andraws, N., Patterson, M.L., Krivohlavek, L.A., Fellis, J., Humphray, S., Saffrey, P., Kingsbury, Z., Weir, J.C., Betley, J., Grocock, R.J., Margulies, E.H., Farrow, E.G., Artman, M., Safina, N.P., Petrikin, J.E., Hall, K.P. and Kingsmore, S.F. (2012) 'Rapid Whole-Genome Sequencing for Genetic Disease Diagnosis in Neonatal Intensive Care Units', *Science Translational Medicine*, 4(154), pp. 154ra135-154ra135.

Schaefer, A.M., Phoenix, C., Elson, J.L., McFarland, R., Chinnery, P.F. and Turnbull, D.M. (2006) 'Mitochondrial disease in adults: A scale to monitor progression and treatment', *Neurology*, 66(12), pp. 1932-1934.

Schaefer, A.M., Taylor, R.W., Turnbull, D.M. and Chinnery, P.F. (2004) 'The epidemiology of mitochondrial disorders—past, present and future', *Biochimica et Biophysica Acta (BBA) - Bioenergetics*, 1659(2-3), pp. 115-120.

Schägger, H. (2006) 'Tricine–SDS-PAGE', *Nature Protocols*, 1(1), pp. 16-22.

Schneider, H.C., Westermann, B., Neupert, W. and Brunner, M. (1996) 'The nucleotide exchange factor MGE exerts a key function in the ATP-dependent cycle of mt-Hsp70-Tim44 interaction driving mitochondrial protein import', *The EMBO Journal*, 15(21), pp. 5796-5803.

Scholle, L.M., Lehmann, D., Deschauer, M., Kraya, T. and Zierz, S. (2018) 'FGF-21 as a Potential Biomarker for Mitochondrial Diseases', *Current Medicinal Chemistry*, 25(18), pp. 2070-2081.

Schon, E.A., DiMauro, S. and Hirano, M. (2012) 'Human mitochondrial DNA: roles of inherited and somatic mutations', *Nature Reviews Genetics*, 13(12), pp. 878-890.

Schwarz, J.M., Cooper, D.N., Schuelke, M. and Seelow, D. (2014) 'MutationTaster2: mutation prediction for the deep-sequencing age', *Nature Methods*, 11(4), pp. 361-362.

Sciacco, M. and Bonilla, E. (1996) '[43]Cytochemistry and immunocytochemistry of mitochondria in tissue sections', *Methods in Enzymology*, 264, pp. 509-521.

Seaby, E.G., Pengelly, R.J. and Ennis, S. (2015) 'Exome sequencing explained: a practical guide to its clinical application', *Briefings in Functional Genomics*, 15(5), pp. 374-384.

Seifert, W., Holder-Espinasse, M., Kühnisch, J., Kahrizi, K., Tzschach, A., Garshasbi, M., Najmabadi, H., Kuss, A.W., Kress, W., Laureys, G., Loeys, B., Brilstra, E., Mancini, G.M.S., Dollfus, H., Dahan, K., Apse, K., Hennies, H.C. and Horn, D. (2009) 'Expanded mutational spectrum in Cohen syndrome, tissue expression, and transcript variants of COH1', *Human Mutation*, 30(2), pp. E404-E420.

Seifert, W., Kühnisch, J., Maritzen, T., Horn, D., Haucke, V. and Hennies, H.C. (2011) 'Cohen Syndrome-associated Protein, COH1, Is a Novel, Giant Golgi Matrix Protein Required for Golgi Integrity', *Journal of Biological Chemistry*, 286(43), pp. 37665-37675.

Seifert, W., Kühnisch, J., Maritzen, T., Lommatzsch, S., Hennies, H.C., Bachmann, S., Horn, D. and Haucke, V. (2015) 'Cohen Syndrome-associated Protein COH1 Physically and Functionally Interacts with the Small GTPase RAB6 at the Golgi Complex and Directs Neurite Outgrowth', *Journal of Biological Chemistry*, 290(6), pp. 3349-3358.

Shaham, O., Slate, N.G., Goldberger, O., Xu, Q., Ramanathan, A., Souza, A.L., Clish, C.B., Sims, K.B. and Mootha, V.K. (2010) 'A plasma signature of human mitochondrial disease revealed through metabolic profiling of spent media from cultured muscle cells', *Proceedings of the National Academy of Sciences*, 107(4), pp. 1571-1575.

Shaikh, T.H. (2017) 'Copy Number Variation Disorders', *Current Genetic Medicine Reports*, 5(4), pp. 183-190.

Shamseldin, H.E., Alasmari, A., Salih, M.A., Samman, M.M., Mian, S.A., Alshidi, T., Ibrahim, N., Hashem, M., Faqeih, E., Al-Mohanna, F. and Alkuraya, F.S. (2017) 'A null mutation in MICU2 causes abnormal mitochondrial calcium homeostasis and a severe neurodevelopmental disorder', *Brain*, 140(11), pp. 2806-2813.

Shamseldin, H.E., Alshammari, M., Al-Sheddi, T., Salih, M.A., Alkhalidi, H., Kentab, A., Repetto, G.M., Hashem, M. and Alkuraya, F.S. (2012) 'Genomic analysis of mitochondrial diseases in a consanguineous population reveals novel candidate disease genes', *Journal of Medical Genetics*, 49(4), p. 234.

Shamseldin, H.E., Smith, L.L., Kentab, A., Alkhalidi, H., Summers, B., Alsedairy, H., Xiong, Y., Gupta, V.A. and Alkuraya, F.S. (2016) 'Mutation of the mitochondrial carrier SLC25A42 causes a novel form of mitochondrial myopathy in humans', *Human Genetics*, 135(1), pp. 21-30.

Shao, J., Fu, Z., Ji, Y., Guan, X., Guo, S., Ding, Z., Yang, X., Cong, Y. and Shen, Y. (2016) 'Leucine zipper-EF-hand containing transmembrane protein 1 (LETM1) forms a Ca2+/H+ antiporter', *Scientific Reports*, 6(1), p. 34174.

Shawky, R.M., Elsayed, S.M., Zaki, M.E., El-Din, S.M.N. and Kamal, F.M. (2013) 'Consanguinity and its relevance to clinical genetics', *Egyptian Journal of Medical Human Genetics*, 14(2), pp. 157-164.

Sheftel, A.D., Wilbrecht, C., Stehling, O., Niggemeyer, B., Elsässer, H.-P., Mühlenhoff, U. and Lill, R. (2012) 'The human mitochondrial ISCA1, ISCA2, and IBA57 proteins are required for [4Fe-4S] protein maturation', *Molecular Biology of the Cell*, 23(7), pp. 1157-1166.

Shendure, J. and Ji, H. (2008) 'Next-generation DNA sequencing', *Nature Biotechnology*, 26(10), pp. 1135-1145.

Sheppard, S., Biswas, S., Li, M.H., Jayaraman, V., Slack, I., Romasko, E.J., Sasson, A., Brunton, J., Rajagopalan, R., Sarmady, M., Abrudan, J.L., Jairam, S., DeChene, E.T., Ying, X., Choi, J., Wilkens, A., Raible, S.E., Scarano, M.I., Santani, A., Pennington, J.W., Luo, M., Conlin, L.K., Devkota, B., Dulik, M.C., Spinner, N.B. and Krantz, I.D. (2018) 'Utility and limitations of exome sequencing as a genetic diagnostic tool for children with hearing loss', *Genetics in Medicine*, 20(12), pp. 1663-1676.

Shinwari, Z.M.A., Almesned, A., Alakhfash, A., Al-Rashdan, A.M., Faqeih, E., Al-Humaidi, Z., Alomrani, A., Alghamdi, M., Colak, D., Alwadai, A., Rababh, M., Al-Fayyadh, M. and Al-Hassnan, Z.N. (2017) 'The Phenotype and Outcome of Infantile Cardiomyopathy Caused by a Homozygous ELAC2 Mutation', *Cardiology*, 137(3), pp. 188-192.

Shoffner, J.M., Lott, M.T., Lezza, A.M.S., Seibel, P., Ballinger, S.W. and Wallace, D.C. (1990) 'Myoclonic epilepsy and ragged-red fiber disease (MERRF) is associated with a mitochondrial DNA tRNALys mutation', *Cell*, 61(6), pp. 931-937.

Signes, A. and Fernandez-Vizarra, E. (2018) 'Assembly of mammalian oxidative phosphorylation complexes I–V and supercomplexes', *Essays In Biochemistry*, 62(3), pp. 255-270.

Silva, U.d., Choudhury, S., Bailey, S.L., Harvey, S., Perrino, F.W. and Hollis, T. (2007) 'The Crystal Structure of TREX1 Explains the 3′ Nucleotide Specificity and Reveals a Polyproline II Helix for Protein Partnering', *Journal of Biological Chemistry*, 282(14), pp. 10537-10543.

Sims, D., Sudbery, I., Ilott, N.E., Heger, A. and Ponting, C.P. (2014) 'Sequencing depth and coverage: key considerations in genomic analyses', *Nature Reviews Genetics*, 15(2), pp. 121-132.

Sissler, M., González-Serrano, L.E. and Westhof, E. (2017) 'Recent Advances in Mitochondrial Aminoacyl-tRNA Synthetases and Disease', *Trends in Molecular Medicine*, 23(8), pp. 693-708.

Skladal, D., Halliday, J. and Thorburn, D.R. (2003) 'Minimum birth prevalence of mitochondrial respiratory chain disorders in children', *Brain*, 126(8), pp. 1905-1912.

Slomovic, S., Laufer, D., Geiger, D. and Schuster, G. (2005) 'Polyadenylation and Degradation of Human Mitochondrial RNA: the Prokaryotic Past Leaves Its Mark†', *Molecular and Cellular Biology*, 25(15), pp. 6427-6435.

Slone, J., Gui, B. and Huang, T. (2018) 'The current landscape for the treatment of mitochondrial disorders', *Journal of Genetics and Genomics*, 45(2), pp. 71-77.

Smirnova, E., Griparic, L., Shurland, D.-L. and Bliek, A.M.v.d. (2001) 'Dynamin-related Protein Drp1 Is Required for Mitochondrial Division in Mammalian Cells', *Molecular Biology of the Cell*, 12(8), pp. 2245-2256.

Smits, P., Smeitink, J. and Heuvel, L.v.d. (2010) 'Mitochondrial Translation and Beyond: Processes Implicated in Combined Oxidative Phosphorylation Deficiencies', *Journal of Biomedicine and Biotechnology*, 2010, p. 737385.

SNPCheck3 *SNPCheck3*. Available at: https://genetools.org/SNPCheck/snpcheck.htm.

Sobreira, N., Schiettecatte, F., Valle, D. and Hamosh, A. (2015) 'GeneMatcher: A Matching Tool for Connecting Investigators with an Interest in the Same Gene', *Human Mutation*, 36(10), pp. 928-930.

Soden, S.E., Saunders, C.J., Willig, L.K., Farrow, E.G., Smith, L.D., Petrikin, J.E., LePichon, J.-B., Miller, N.A., Thiffault, I., Dinwiddie, D.L., Twist, G., Noll, A., Heese, B.A., Zellmer, L., Atherton, A.M., Abdelmoity, A.T., Safina, N., Nyp, S.S., Zuccarelli, B., Larson, I.A., Modrcin, A., Herd, S., Creed, M., Ye, Z., Yuan, X., Brodsky, R.A. and Kingsmore, S.F. (2014) 'Effectiveness of exome and genome sequencing guided by acuity of illness for diagnosis of neurodevelopmental disorders', *Science Translational Medicine*, 6(265), pp. 265ra168-265ra168.

Soleimanpour-Lichaei, H.R., Kühl, I., Gaisne, M., Passos, J.F., Wydro, M., Rorbach, J., Temperley, R., Bonnefoy, N., Tate, W., Lightowlers, R. and Chrzanowska-Lightowlers, Z. (2007) 'mtRF1a Is a Human Mitochondrial Translation Release Factor Decoding the Major Termination Codons UAA and UAG', *Molecular Cell*, 27(5), pp. 745-757.

Sommerville, E.W., Ng, Y.S., Alston, C.L., Dallabona, C., Gilberti, M., He, L., Knowles, C., Chin, S.L., Schaefer, A.M., Falkous, G., Murdoch, D., Longman, C., Visser, M.d., Bindoff, L.A., Rawles, J.M., Dean, J.C.S., Petty, R.K., Farrugia, M.E., Haack, T.B., Prokisch, H., McFarland, R., Turnbull, D.M., Donnini, C., Taylor, R.W. and

Gorman, G.S. (2017) 'Clinical Features, Molecular Heterogeneity, and Prognostic Implications in YARS2-Related Mitochondrial Myopathy', *JAMA Neurology*, 74(6), p. 686.

Spinazzola, A., Santer, R., Akman, O.H., Tsiakas, K., Schaefer, H., Ding, X., Karadimas, C.L., Shanske, S., Ganesh, J., Mauro, S.D. and Zeviani, M. (2008) 'Hepatocerebral Form of Mitochondrial DNA Depletion Syndrome: Novel MPV17 Mutations', *Archives of Neurology*, 65(8), pp. 1108-1113.

Stehling, O. and Lill, R. (2013) 'The Role of Mitochondria in Cellular Iron–Sulfur Protein Biogenesis: Mechanisms, Connected Processes, and Diseases', *Cold Spring Harbor Perspectives in Biology*, 5(8), p. a011312.

Stehling, O., Wilbrecht, C. and Lill, R. (2014) 'Mitochondrial iron–sulfur protein biogenesis and human disease', *Biochimie*, 100, pp. 61-77.

Stenton, S.L., Kremer, L.S., Kopajtich, R., Ludwig, C. and Prokisch, H. (2020) 'The diagnosis of inborn errors of metabolism by an integrative "multi-omics" approach: A perspective encompassing genomics, transcriptomics, and proteomics', *Journal of Inherited Metabolic Disease*, 43(1), pp. 25-35.

Stenton, S.L. and Prokisch, H. (2020) 'Genetics of mitochondrial diseases: Identifying mutations to help diagnosis', *EBioMedicine*, 56, p. 102784.

Straub, S.P., Stiller, S.B., Wiedemann, N. and Pfanner, N. (2016) 'Dynamic organization of the mitochondrial protein import machinery', *Biological Chemistry*, 397(11), pp. 1097-1114.

Stroud, D.A., Surgenor, E.E., Formosa, L.E., Reljic, B., Frazier, A.E., Dibley, M.G., Osellame, L.D., Stait, T., Beilharz, T.H., Thorburn, D.R., Salim, A. and Ryan, M.T. (2016) 'Accessory subunits are integral for assembly and function of human mitochondrial complex I', *Nature*, 538(7623), pp. 123-126.

Swenson, S., Cannon, A., Harris, N.J., Taylor, N.G., Fox, J.L. and Khalimonchuk, O. (2016) 'Analysis of Oligomerization Properties of Heme a Synthase Provides Insights into Its Function in Eukaryotes', *Journal of Biological Chemistry*, 291(19), pp. 10411-10425.

Szczepanowska, K., Senft, K., Heidler, J., Herholz, M., Kukat, A., Höhne, M.N., Hofsetz, E., Becker, C., Kaspar, S., Giese, H., Zwicker, K., Guerrero-Castillo, S., Baumann, L., Kauppila, J., Rumyantseva, A., Müller, S., Frese, C.K., Brandt, U., Riemer, J., Wittig, I. and Trifunovic, A. (2020) 'A salvage pathway maintains highly functional respiratory complex I', *Nature Communications*, 11(1), p. 1643.

Tadmouri, G.O., Nair, P., Obeid, T., Ali, M.T.A., Khaja, N.A. and Hamamy, H.A. (2009) 'Consanguinity and reproductive health among Arabs', *Reproductive Health*, 6(1), p. 17.

Tajir, M., Arnoux, J.B., Boutron, A., Elalaoui, S.C., Lonlay, P.D., Sefiani, A. and Brivet, M. (2012) 'Pyruvate dehydrogenase deficiency caused by a new mutation of PDHX gene in two Moroccan patients', *European Journal of Medical Genetics*, 55(10), pp. 535-540.

Tamai, S., Iida, H., Yokota, S., Sayano, T., Kiguchiya, S., Ishihara, N., Hayashi, J.-I., Mihara, K. and Oka, T. (2008) 'Characterization of the mitochondrial protein LETM1, which maintains the mitochondrial tubular shapes and interacts with the AAA-ATPase BCS1L', *Journal of Cell Science*, 121(15), pp. 2588-2600.

Taylor, R.W., Pyle, A., Griffin, H., Blakely, E.L., Duff, J., He, L., Smertenko, T., Alston, C.L., Neeve, V.C., Best, A., Yarham, J.W., Kirschner, J., Schara, U., Talim, B., Topaloglu, H., Baric, I., Holinski-Feder, E., Abicht, A., Czermin, B., Kleinle, S., Morris, A.A.M., Vassallo, G., Gorman, G.S., Ramesh, V., Turnbull, D.M., Santibanez-Koref, M., McFarland, R., Horvath, R. and Chinnery, P.F. (2014) 'Use

of Whole-Exome Sequencing to Determine the Genetic Basis of Multiple Mitochondrial Respiratory Chain Complex Deficiencies', *JAMA*, 312(1), pp. 68-77.
Team, S.G.P. (2015) 'The Saudi Human Genome Program: An oasis in the desert of Arab medicine is providing clues to genetic disease', *IEEE Pulse*, 6(6), pp. 22-26.
The UniProt Consortium (2017) 'UniProt: the universal protein knowledgebase', *Nucleic Acids Research*, 45(D1), pp. D158-D169.
Theunissen, T.E.J., Nguyen, M., Kamps, R., Hendrickx, A.T., Sallevelt, S.C.E.H., Gottschalk, R.W.H., Calis, C.M., Stassen, A.P.M., Koning, B.d., Hartog, E.N.M.M.-D., Schoonderwoerd, K., Fuchs, S.A., Hilhorst-Hofstee, Y., Visser, M.d., Vanoevelen, J., Szklarczyk, R., Gerards, M., Coo, I.F.M.d., Hellebrekers, D.M.E.I. and Smeets, H.J.M. (2018) 'Whole Exome Sequencing Is the Preferred Strategy to Identify the Genetic Defect in Patients With a Probable or Possible Mitochondrial Cause', *Frontiers in Genetics*, 9, p. 400.
Thompson, K., Collier, J.J., Glasgow, R.I.C., Robertson, F.M., Pyle, A., Blakely, E.L., Alston, C.L., Oláhová, M., McFarland, R. and Taylor, R.W. (2020a) 'Recent advances in understanding the molecular genetic basis of mitochondrial disease', *Journal of Inherited Metabolic Disease*, 43(1), pp. 36-50.
Thompson, K., Majd, H., Dallabona, C., Reinson, K., King, M.S., Alston, C.L., He, L., Lodi, T., Jones, S.A., Fattal-Valevski, A., Fraenkel, N.D., Saada, A., Haham, A., Isohanni, P., Vara, R., Barbosa, I.A., Simpson, M.A., Deshpande, C., Puusepp, S., Bonnen, P.E., Rodenburg, R.J., Suomalainen, A., Õunap, K., Elpeleg, O., Ferrero, I., McFarland, R., Kunji, E.R.S. and Taylor, R.W. (2016) 'Recurrent De Novo Dominant Mutations in SLC25A4 Cause Severe Early-Onset Mitochondrial Disease and Loss of Mitochondrial DNA Copy Number', *The American Journal of Human Genetics*, 99(4), pp. 860-876.
Thompson, R., Spendiff, S., Roos, A., Bourque, P.R., Warman Chardon, J., Kirschner, J., Horvath, R. and Lochmüller, H. (2020b) 'Advances in the diagnosis of inherited neuromuscular diseases and implications for therapy development', *The Lancet Neurology*, 19(6), pp. 522-532.
Tiranti, V., Hoertnagel, K., Carrozzo, R., Galimberti, C., Munaro, M., Granatiero, M., Zelante, L., Gasparini, P., Marzella, R., Rocchi, M., Bayona-Bafaluy, M.P., Enriquez, J.-A., Uziel, G., Bertini, E., Dionisi-Vici, C., Franco, B., Meitinger, T. and Zeviani, M. (1998) 'Mutations of SURF-1 in Leigh Disease Associated with Cytochrome c Oxidase Deficiency', *The American Journal of Human Genetics*, 63(6), pp. 1609-1621.
Tolkunova, E., Park, H., Xia, J., King, M.P. and Davidson, E. (2000) 'The human lysyl-tRNA synthetase gene encodes both the cytoplasmic and mitochondrial enzymes by means of an unusual alternative splicing of the primary transcript', *Journal of Biological Chemistry*, 275(45), pp. 35063-35069.
Trumpower, B.L. and Gennis, R.B. (1994) 'Energy Transduction by Cytochrome Complexes in Mitochondrial and Bacterial Respiration: The Enzymology of Coupling Electron Transfer Reactions to Transmembrane Proton Translocation', *Annual Review of Biochemistry*, 63(1), pp. 675-716.
Tsuboi, M., Morita, H., Nozaki, Y., Akama, K., Ueda, T., Ito, K., Nierhaus, K.H. and Takeuchi, N. (2009) 'EF-G2mt Is an Exclusive Recycling Factor in Mammalian Mitochondrial Protein Synthesis', *Molecular Cell*, 35(4), pp. 502-510.
Tucker, Elena J., Hershman, Steven G., Köhrer, C., Belcher-Timme, Casey A., Patel, J., Goldberger, Olga A., Christodoulou, J., Silberstein, Jonathon M., McKenzie, M., Ryan, Michael T., Compton, Alison G., Jaffe, Jacob D., Carr, Steven A., Calvo, Sarah E., RajBhandary, Uttam L., Thorburn, David R. and Mootha, Vamsi K.

(2011) 'Mutations in MTFMT Underlie a Human Disorder of Formylation Causing Impaired Mitochondrial Translation', *Cell Metabolism*, 14(3), pp. 428-434.

Turner, Tychele N., Hormozdiari, F., Duyzend, Michael H., McClymont, Sarah A., Hook, Paul W., Iossifov, I., Raja, A., Baker, C., Hoekzema, K., Stessman, Holly A., Zody, Michael C., Nelson, Bradley J., Huddleston, J., Sandstrom, R., Smith, Joshua D., Hanna, D., Swanson, James M., Faustman, Elaine M., Bamshad, Michael J., Stamatoyannopoulos, J., Nickerson, Deborah A., McCallion, Andrew S., Darnell, R. and Eichler, Evan E. (2016) 'Genome Sequencing of Autism-Affected Families Reveals Disruption of Putative Noncoding Regulatory DNA', *The American Journal of Human Genetics*, 98(1), pp. 58-74.

Vakifahmetoglu-Norberg, H., Ouchida, A.T. and Norberg, E. (2017) 'The role of mitochondria in metabolism and cell death', *Biochemical and Biophysical Research Communications*, 482(3), pp. 426-431.

van der Bliek, A.M., Shen, Q. and Kawajiri, S. (2013) 'Mechanisms of mitochondrial fission and fusion', *Cold Spring Harb Perspect Biol*, 5(6), p. a011072.

Vanderperre, B., Bender, T., Kunji, E.R.S. and Martinou, J.-C. (2015) 'Mitochondrial pyruvate import and its effects on homeostasis', *Current Opinion in Cell Biology*, 33, pp. 35-41.

Vemaps (2019) *Multicolor Map of Kuwait with Governorates*. Available at: https://vemaps.com/kuwait/kw-07 (Accessed: 12/12/2020).

Vernau, K., Napoli, E., Wong, S., Ross-Inta, C., Cameron, J., Bannasch, D., Bollen, A., Dickinson, P. and Giulivi, C. (2015) 'Thiamine Deficiency-Mediated Brain Mitochondrial Pathology in Alaskan Huskies with Mutation in SLC19A3.1', *Brain Pathology*, 25(4), pp. 441-453.

Vernau, K.M., Runstadler, J.A., Brown, E.A., Cameron, J.M., Huson, H.J., Higgins, R.J., Ackerley, C., Sturges, B.K., Dickinson, P.J., Puschner, B., Giulivi, C., Shelton, G.D., Robinson, B.H., DiMauro, S., Bollen, A.W. and Bannasch, D.L. (2013) 'Genome-Wide Association Analysis Identifies a Mutation in the Thiamine Transporter 2 (SLC19A3) Gene Associated with Alaskan Husky Encephalopathy', *PLoS ONE*, 8(3), p. e57195.

Vinothkumar, K.R., Zhu, J. and Hirst, J. (2014) 'Architecture of mammalian respiratory complex I', *Nature*, 515(7525), pp. 80-84.

Viscomi, C., Burlina, A.B., Dweikat, I., Savoiardo, M., Lamperti, C., Hildebrandt, T., Tiranti, V. and Zeviani, M. (2010) 'Combined treatment with oral metronidazole and N-acetylcysteine is effective in ethylmalonic encephalopathy', *Nature Medicine*, 16(8), pp. 869-871.

Vizcaíno, J.A., Côté, R.G., Csordas, A., Dianes, J.A., Fabregat, A., Foster, J.M., Griss, J., Alpi, E., Birim, M., Contell, J., O'Kelly, G., Schoenegger, A., Ovelleiro, D., Pérez-Riverol, Y., Reisinger, F., Ríos, D., Wang, R. and Hermjakob, H. (2013) 'The Proteomics Identifications (PRIDE) database and associated tools: status in 2013', *Nucleic Acids Research*, 41(D1), pp. D1063-D1069.

Wadapurkar, R.M. and Vyas, R. (2018) 'Computational analysis of next generation sequencing data and its applications in clinical oncology', *Informatics in Medicine Unlocked*, 11, pp. 75-82.

Waite, A., Somer, M., O'Driscoll, M., Millen, K., Manson, F.D.C. and Chandler, K.E. (2010) 'Cerebellar hypoplasia and Cohen syndrome: A confirmed association', *American Journal of Medical Genetics Part A*, 152A(9), pp. 2390-2393.

Walberg, M.W. and Clayton, D.A. (1981) 'Sequence and properties of the human KB cell and mouse L cell D-loop regions of mitochondrial DNA', *Nucleic Acids Research*, 9(20), pp. 5411-5421.

Wallace, D.C., Singh, G., Lott, M.T., Hodge, J.A., Schurr, T.G., Lezza, A.M., Elsas, L.J. and Nikoskelainen, E.K. (1988) 'Mitochondrial DNA mutation associated with Leber's hereditary optic neuropathy', *Science*, 242(4884), pp. 1427-1430.

Wang, K., Li, M. and Hakonarson, H. (2010) 'ANNOVAR: functional annotation of genetic variants from high-throughput sequencing data', *Nucleic Acids Research*, 38(16), pp. e164-e164.

Wanrooij, P.H., Uhler, J.P., Simonsson, T., Falkenberg, M. and Gustafsson, C.M. (2010) 'G-quadruplex structures in RNA stimulate mitochondrial transcription termination and primer formation', *Proceedings of the National Academy of Sciences*, 107(37), pp. 16072-16077.

Wedatilake, Y., Brown, R.M., McFarland, R., Yaplito-Lee, J., Morris, A.A.M., Champion, M., Jardine, P.E., Clarke, A., Thorburn, D.R., Taylor, R.W., Land, J.M., Forrest, K., Dobbie, A., Simmons, L., Aasheim, E.T., Ketteridge, D., Hanrahan, D., Chakrapani, A., Brown, G.K. and Rahman, S. (2013) 'SURF1 deficiency: a multi-centre natural history study', *Orphanet Journal of Rare Diseases*, 8(1), p. 96.

White, S.L., Collins, V.R., Wolfe, R., Cleary, M.A., Shanske, S., DiMauro, S., Dahl, H.-H.M. and Thorburn, D.R. (1999) 'Genetic Counseling and Prenatal Diagnosis for the Mitochondrial DNA Mutations at Nucleotide 8993', *The American Journal of Human Genetics*, 65(2), pp. 474-482.

Wiedemann, N. and Pfanner, N. (2017) 'Mitochondrial Machineries for Protein Import and Assembly', *Annual Review of Biochemistry*, 86(1), pp. 1-30.

Wirth, C., Brandt, U., Hunte, C. and Zickermann, V. (2016) 'Structure and function of mitochondrial complex I', *Biochimica et Biophysica Acta (BBA) - Bioenergetics*, 1857(7), pp. 902-914.

Witters, P., Saada, A., Honzik, T., Tesarova, M., Kleinle, S., Horvath, R., Goldstein, A. and Morava, E. (2018) 'Revisiting mitochondrial diagnostic criteria in the new era of genomics', *Genetics in Medicine*, 20(4), pp. 444-451.

Wittig, I., Braun, H.-P. and Schägger, H. (2006) 'Blue native PAGE', *Nature Protocols*, 1(1), pp. 418-428.

Wolf, N.I. and Smeitink, J.A.M. (2002) 'Mitochondrial disorders', *Neurology*, 59(9), pp. 1402-1405.

Wolf, U., Reinwein, H., Porsch, R., Schröter, R. and Baitsch, H. (1965) '[Deficiency on the short arms of a chromosome No. 4]', *Humangenetik*, 1(5), pp. 397-413.

Wong, M.L. and Medrano, J.F. (2005) 'Real-time PCR for mRNA quantitation', *BioTechniques*, 39(1), pp. 75-85.

Wortmann, S., Mayr, J., Nuoffer, J., Prokisch, H. and Sperl, W. (2017) 'A Guideline for the Diagnosis of Pediatric Mitochondrial Disease: The Value of Muscle and Skin Biopsies in the Genetics Era', *Neuropediatrics*, 48(04), pp. 309-314.

Wortmann, S.B., Koolen, D.A., Smeitink, J.A., Heuvel, L. and Rodenburg, R.J. (2015) 'Whole exome sequencing of suspected mitochondrial patients in clinical practice', *Journal of Inherited Metabolic Disease*, 38(3), pp. 437-443.

Wu, M., Gu, J., Guo, R., Huang, Y. and Yang, M. (2016a) 'Structure of Mammalian Respiratory Supercomplex I1III2IV1', *Cell*, 167(6), pp. 1598-1609.e10.

Wu, Y., Wei, F.-Y., Kawarada, L., Suzuki, T., Araki, K., Komohara, Y., Fujimura, A., Kaitsuka, T., Takeya, M., Oike, Y., Suzuki, T. and Tomizawa, K. (2016b) 'Mtu1-Mediated Thiouridine Formation of Mitochondrial tRNAs Is Required for Mitochondrial Translation and Is Involved in Reversible Infantile Liver Injury', *PLOS Genetics*, 12(9), p. e1006355.

Xu, H., Luo, X., Qian, J., Pang, X., Song, J., Qian, G., Chen, J. and Chen, S. (2012) 'FastUniq: A Fast De Novo Duplicates Removal Tool for Paired Short Reads', *PLoS ONE*, 7(12), p. e52249.

Yang, M.Y., Bowmaker, M., Reyes, A., Vergani, L., Angeli, P., Gringeri, E., Jacobs, H.T. and Holt, I.J. (2002) 'Biased Incorporation of Ribonucleotides on the Mitochondrial L-Strand Accounts for Apparent Strand-Asymmetric DNA Replication', *Cell*, 111(4), pp. 495-505.

Yang, Y., Muzny, D.M., Reid, J.G., Bainbridge, M.N., Willis, A., Ward, P.A., Braxton, A., Beuten, J., Xia, F., Niu, Z., Hardison, M., Person, R., Bekheirnia, M.R., Leduc, M.S., Kirby, A., Pham, P., Scull, J., Wang, M., Ding, Y., Plon, S.E., Lupski, J.R., Beaudet, A.L., Gibbs, R.A. and Eng, C.M. (2013) 'Clinical Whole-Exome Sequencing for the Diagnosis of Mendelian Disorders', *The New England Journal of Medicine*, 369(16), pp. 1502-1511.

Yarham, J.W., Lamichhane, T.N., Pyle, A., Mattijssen, S., Baruffini, E., Bruni, F., Donnini, C., Vassilev, A., He, L., Blakely, E.L., Griffin, H., Santibanez-Koref, M., Bindoff, L.A., Ferrero, I., Chinnery, P.F., McFarland, R., Maraia, R.J. and Taylor, R.W. (2014) 'Defective i6A37 Modification of Mitochondrial and Cytosolic tRNAs Results from Pathogenic Mutations in TRIT1 and Its Substrate tRNA', *PLoS Genetics*, 10(6), p. e1004424.

Yasukawa, T., Reyes, A., Cluett, T.J., Yang, M.Y., Bowmaker, M., Jacobs, H.T. and Holt, I.J. (2006) 'Replication of vertebrate mitochondrial DNA entails transient ribonucleotide incorporation throughout the lagging strand', *The EMBO Journal*, 25(22), pp. 5358-5371.

Yatsuga, S., Fujita, Y., Ishii, A., Fukumoto, Y., Arahata, H., Kakuma, T., Kojima, T., Ito, M., Tanaka, M., Saiki, R. and Koga, Y. (2015) 'Growth differentiation factor 15 as a useful biomarker for mitochondrial disorders', *Annals of Neurology*, 78(5), pp. 814-823.

Yatsuga, S. and Suomalainen, A. (2012) 'Effect of bezafibrate treatment on late-onset mitochondrial myopathy in mice', *Human Molecular Genetics*, 21(3), pp. 526-535.

Yavarna, T., Al-Dewik, N., Al-Mureikhi, M., Ali, R., Al-Mesaifri, F., Mahmoud, L., Shahbeck, N., Lakhani, S., AlMulla, M., Nawaz, Z., Vitazka, P., Alkuraya, F.S. and Ben-Omran, T. (2015) 'High diagnostic yield of clinical exome sequencing in Middle Eastern patients with Mendelian disorders', *Human Genetics*, 134(9), pp. 967-980.

Yavuz, H., Bertoli-Avella, A.M., Alfadhel, M., Al-Sannaa, N., Kandaswamy, K.K., Al-Tuwaijri, W., Rolfs, A., Brandau, O. and Bauer, P. (2018) 'A founder nonsense variant in NUDT2 causes a recessive neurodevelopmental disorder in Saudi Arab children', *Clinical Genetics*, 94(3-4), pp. 393-395.

Yoneda, M., Tanno, Y., Horai, S., Ozawa, T., Miyatake, T. and Tsuji, S. (1990) 'A common mitochondrial DNA mutation in the t-RNA(Lys) of patients with myoclonus epilepsy associated with ragged-red fibers', *Biochemistry international*, 21(5), pp. 789-96.

Yu, Z., O'Farrell, P.H., Yakubovich, N. and DeLuca, S.Z. (2017) 'The Mitochondrial DNA Polymerase Promotes Elimination of Paternal Mitochondrial Genomes', *Current Biology*, 27(7), pp. 1033-1039.

Yu-Wai-Man, P., Turnbull, D.M. and Chinnery, P.F. (2002) 'Leber hereditary optic neuropathy', *Journal of Medical Genetics*, 39(3), p. 162.

Yüksel, A., Seven, M., Cetincelik, Ü., Yeşil, G. and Köksal, V. (2006) 'Facial Dysmorphism in Leigh Syndrome With SURF-1 Mutation and COX Deficiency', *Pediatric Neurology*, 34(6), pp. 486-489.

Zafeiriou, D.I., Koletzko, B., Mueller-Felber, W., Paetzke, I., Kueffer, G. and Jensen, M. (1995) 'Deficiency in complex IV (cytochrome c oxidase) of the respiratory chain, presenting as a leukodystrophy in two siblings with Leigh syndrome', *Brain and Development*, 17(2), pp. 117-121.

Zaganelli, S., Rebelo-Guiomar, P., Maundrell, K., Rozanska, A., Pierredon, S., Powell, C.A., Jourdain, A.A., Hulo, N., Lightowlers, R.N., Chrzanowska-Lightowlers, Z.M., Minczuk, M. and Martinou, J.-C. (2017) 'The Pseudouridine Synthase RPUSD4 Is an Essential Component of Mitochondrial RNA Granules', *Journal of Biological Chemistry*, 292(11), pp. 4519-4532.

Zayed, H. (2016) 'The Qatar genome project: translation of whole-genome sequencing into clinical practice', *International Journal of Clinical Practice*, 70(10), pp. 832-834.

Zeng, W.-Q., Al-Yamani, E., Acierno, J.S., Slaugenhaupt, S., Gillis, T., MacDonald, M.E., Ozand, P.T. and Gusella, J.F. (2005) 'Biotin-Responsive Basal Ganglia Disease Maps to 2q36.3 and Is Due to Mutations in SLC19A3', *The American Journal of Human Genetics*, 77(1), pp. 16-26.

Zhao, S., Luo, Z., Xiao, Z., Li, L., Zhao, R., Yang, Y. and Zhong, Y. (2019) 'Case report: two novel VPS13B mutations in a Chinese family with Cohen syndrome and hyperlinear palms', *BMC Medical Genetics*, 20(1), p. 187.

Zhou, R., Yazdi, A.S., Menu, P. and Tschopp, J. (2011) 'A role for mitochondria in NLRP3 inflammasome activation', *Nature*, 469(7329), pp. 221-225.

Zhu, J., Vinothkumar, K.R. and Hirst, J. (2016) 'Structure of mammalian respiratory complex I', *Nature*, 536(7616), pp. 354-358.

Zhu, Z., Yao, J., Johns, T., Fu, K., Bie, I.D., Macmillan, C., Cuthbert, A.P., Newbold, R.F., Wang, J.-c., Chevrette, M., Brown, G.K., Brown, R.M. and Shoubridge, E.A. (1998) 'SURF1, encoding a factor involved in the biogenesis of cytochrome c oxidase, is mutated in Leigh syndrome', *Nature Genetics*, 20(4), pp. 337-343.

Zinovkina, L.A. (2019) 'DNA Replication in Human Mitochondria', *Biochemistry (Moscow)*, 84(8), pp. 884-895.